INTERWELL CONNECTIVITY EVALUATION FROM WELLRATE FLUCTUATIONS: A WATERFLOODING MANAGEMENT TOOL

A Dissertation

by

DANIAL KAVIANI

Submitted to the Office of Graduate Studies of
Texas A&M University
in partial fulfillment of the requirements for the degree of

DOCTOR OF PHILOSOPHY

December 2009

Major Subject: Petroleum Engineering

INTERWELL CONNECTIVITY EVALUATION FROM WELLRATE FLUCTUATIONS: A WATERFLOODING MANAGEMENT TOOL

A Dissertation

by

DANIAL KAVIANI

Submitted to the Office of Graduate Studies of
Texas A&M University
in partial fulfillment of the requirements for the degree of

DOCTOR OF PHILOSOPHY

Approved by:

Co-Chairs of Committee,	Peter P. Valkó
	Jerry L. Jensen
Committee Members,	Thomas A. Blasingame
	Walter B. Ayers
	Yuefeng Sun
Head of Department,	Stephen A. Holditch

December 2009

Major Subject: Petroleum Engineering

ABSTRACT

Interwell Connectivity Evaluation from Wellrate

Fluctuations: A Waterflooding Management Tool. (December 2009)

Danial Kaviani, B.S.; M.S. Amirkabir University of Technology (Tehran Polytechnic)

Co-Chairs of Advisory Committee: Dr. Peter P. Valkó
Dr. Jerry L. Jensen

Using injection and production data, we can evaluate the connectivity between injector and producer well pairs to characterize their interwell regions and provide a tool for waterflood management. The capacitance model (CM) has been suggested as a phenomenological method to analyze the injection and production data for these purposes. Early studies involving reservoir simulation have shown CM to be a valuable tool but also have revealed several shortcomings. Many of these deficiencies have become more transparent in analyzing field data. This work consists of two parts: in the first part, we investigate some of the shortcomings of the CM and attempt to overcome them by modifying the algorithms. In the second part, we relate the problem of interwell connectivity to the rigorous concept of Multiwell Productivity Index (MPI) and provide a semi analytical approach.

We have developed two modifications on the CM: the segmented CM that can be used where bottomhole pressures (BHP) are unknown and may change during the analysis interval, and the compensated CM that overcomes the requirement to rerun the model after adding a new producer or shutting in an existing producer. If both BHP changes and shut-in periods occur, the segmented and compensated CMs can be used simultaneously to construct a single model for a period of data. We show several hypothetical cases and a field case where these modifications generate a more reliable evaluation of interwell connectivity and increase the R^2 of the model up to 15%.

On the other hand, the MPI-based approach can predict the reservoir performance analytically for homogeneous cases under specific conditions. In the heterogeneous cases, this approach provides a robust connectivity parameter, which solely represents the reservoir heterogeneity and possible anisotropy and hence allows improved information exchange with the geologist. In addition, this connectivity parameter is insensitive to possible variations of skin factor and changes in number of wells. A further advantage of the new method is the flexibility to incorporate additional information, such as injector BHP, into the analysis process. We applied this approach on several hypothetical cases and observed excellent evaluation of both reservoir performance and connectivity.

DEDICATION

This dissertation is dedicated to the memory of Dr. Mohammad Mossadegh, the architect of nationalization of the Iranian oil industry.

ACKNOWLEDGEMENTS

I would like to thank my committee co-chairs, Dr. Jerry Jensen and Dr. Peter Valkó, and my committee members, Dr. Thomas Blasingame, Dr. Walter Ayers, and Dr. Yuefeng Sun, for their guidance and support throughout the course of this research. Dr. Jensen supervised me for a major part of this research and another independent project and provided some financial support for my research. Dr. Valkó directed me to a new aspect of this topic and provided partial financial support for my research. I would also like to thank Dr. Blasingame for providing the opportunity to study at Texas A&M University. Special thanks also go to Dr. Ayers for giving me my first opportunity to be a teaching assistant and for providing partial financial assistance for my research. My appreciation is extended to Dr. Larry Lake from the University of Texas at Austin for his help, useful comments, and ideas on this research.

Thanks also go to my friends and colleagues and the department faculty and staff, specifically Ayse Nazli Demiroren and Iranian students for making my time at Texas A&M University a great experience. I would like to thank to Dr. Morteza Sayarpour from Chevron Co. and Dr. Behnam Jafarpour for useful discussions. I would also like to thank Ms. D.J. Weatherford for her advice on making the dissertation more organized. Thanks also go the National Iranian Oil Company (NIOC) for providing the financial support for a major part of my PhD studies.

Finally, thanks to my mother and father for their encouragement and help and most importantly to my wife for her patience, support, and love.

TABLE OF CONTENTS

Page

Page

Page

LIST OF FIGURES

Page

Page

Page

Page

Page

Page

Page

Page

LIST OF TABLES

Page

1. INTRODUCTION: THE IMPORTANCE OF RESEARCH

1.1 Interwell Connectivity

To put it in simple words, interwell connectivity evaluation is the attempt to understand how effectively two wells are connected to each other. In homogeneous systems the interwell connectivity is a function of location of the wells and reservoir geometry. In heterogeneous systems the properties of the interwell region also affect the connectivity. Thus, connectivity evaluation provides a tool to characterize the reservoir. For instance, low connectivity between two adjacent wells could indicate existence of a low permeability zone or barrier in their interwell region, and high connectivity could be evidence of a high permeability zone or a flow channel (**Fig. 1.1**). Evaluating the interwell connectivity assists in optimizing field management: for example in waterflooding, we can predict how the changes in the injection rates affect the production rate. A model that can predict the production rates based on the injection rates enables us to determine the optimum injection rates to maximize the objective function (for example net present value) under various technical constraints.

Despite the simple definition of connectivity, no unique criteria exist to define the connectivity level of two wells. In fact, depending on the evaluation method of connectivity, we may define several types of connectivity parameters between the well pairs. In general there are two broad approaches to evaluate the connectivity: static and dynamic. This terminology is adopted from heterogeneity measurement classifications by Lake and Jensen (1991). In the static methods, the connectivity evaluation is based on the geological data. In this manner, a number of connectivity parameters have been defined. Some of these definitions are directly related to the individual well pair connectivity, like the Li et al. (2009) definition of probability of well connectivity. Other definitions are not specifically related to the connectivity between well pairs; instead they assign a connectivity index for a specific layer or gridblock. For example, Wang et al. (2008) defined two connectivity parameters for sand layers based on existence of the sand in the adjacent wells, and Hird and Dubrule (1998) defined two parameters to evaluate connectivity for each gridblock. In the dynamic evaluation of connectivity, we use reservoir engineering data (such as injection and production data) or specific test data [e.g. tracer testing (Du and Guan 2005) and interference and pulse testing (Lee et al. 2003)] to evaluate the connectivity. In the dynamic approaches we also distinguish well pair connectivity evaluation and the region connectivity evaluation.

1.2 Connectivity Evaluation Based on Injection and Production Data

Injection and production data are the most available and abundant data in any waterflood project. Using these data we are able to evaluate the connectivity between the injector and producer wells.

This dissertation follows the style of *SPE Journal.*

Analysis of injection and production data to infer the interwell connectivity becomes more crucial in cases where the reservoir is heterogeneous or we do not have enough information about the reservoir characteristics. Although we have several other sources of connectivity evaluation such as tracer tests or more detailed geological studies, applying a method based on only wellrate fluctuations has specific advantages. It needs no extra field tests and uses already available data. Integrating the analysis of injection and production rates with other data leads to an enhanced view of the reservoir.

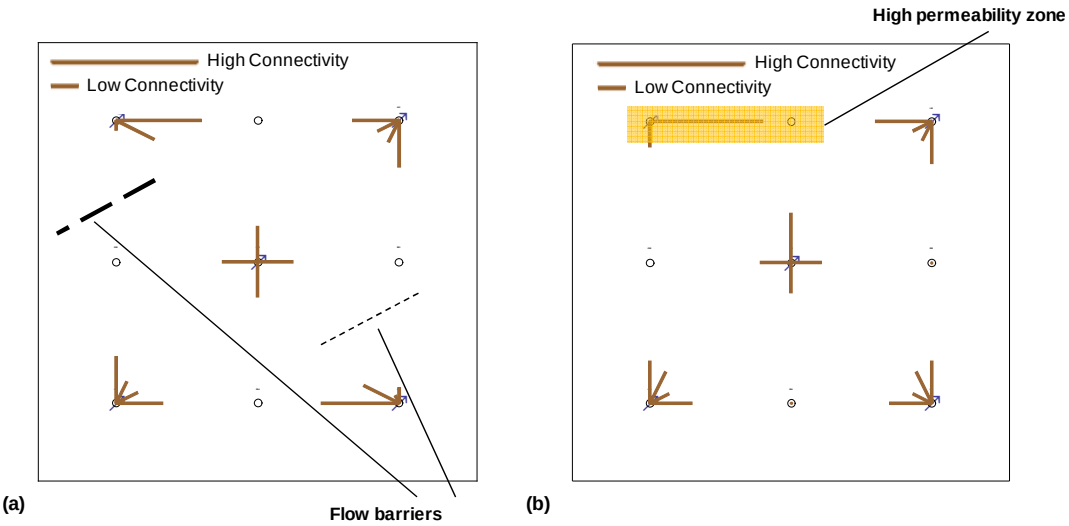

Fig. 1.1—Interwell connectivity evaluations, using vector maps to indicate directions and connectivity levels, supply information about barriers and conduits in the reservoir. The length of the vector from each injector to each producer shows the connectivity level between them. (a) Low connectivity could be an indicator of a fault or low permeability zone and (b) high connectivity could be evidence of a fracture or other high-permeability zone.

Ideally, we expect to estimate a connectivity parameter that reveals the heterogeneity of the interwell region. However, besides the interwell heterogeneity, the apparent degree of connectivity of a well pair is a function of well locations, reservoir extents, wellbore skin factor, existence of other wells, injection rates of other injectors, and bottomhole pressure (BHP) of all the wells. We expect a robust connectivity index to be able to decouple these effects from the apparent connectivity and merely represent the reservoir heterogeneity. For instance, looking at a set of injection and production data, probably the simplest evidence of connectivity between an injector/producer pair is a high correlation coefficient between their rates. However, the effect of existence of other injectors may lead to estimation of a small “apparent connectivity” (**Fig. 1.2**). Thus the correlation coefficient may not be a robust connectivity estimator.

Besides the application of the connectivity parameter as an index to understand the heterogeneity, we may need another type of connectivity parameter that describes the effect of change in rate or BHP of each

well on the other wells. Such a connectivity index will not be the same as the heterogeneity indicator because for this one, we do not need to decouple the effect of location and existence of the other wells from the connectivity parameter. In general, if a connectivity parameter decouples the effect of the location and number of the wells from the apparent connectivity we call it a “first-type” connectivity parameter; however, if it does not decouple these effects, we call it the “second-type” connectivity parameter (**Fig. 1.3**). For example, in a homogeneous system, a first-type connectivity parameter for all wells is expected to be zero. However, considering the second type of connectivity parameters and depending on the location of the wells, different values can be assigned to the connectivity of the well pairs (**Fig. 1.4**).

Fig. 1.2—Considering only the correlation coefficient of a well pair may show no connectivity for a highly-connected pair. In this case, the effect of other injectors leads to a poor apparent connectivity. Data are from I01 and P01 from Case 3-3-0.

Some models have been developed to predict the reservoir performance based on the information obtained from connectivity evaluation. By adopting a watercut predictor to the model, we may also estimate the oil production. Compared to reservoir simulators, these models have the advantage of predicting the production rates much faster.

1.3 Improving the Connectivity Evaluation

In this work, at first we try to overcome the problems associated with estimation of connectivity parameters using the current available methods. One of the problems that decrease the accuracy of connectivity evaluation in field cases is the lack of information on the producers’ BHP. We show that this may lead to incorrect connectivity evaluation. We introduce a method that can effectively decouple the

effect of a limited number of producer BHP changes from the data. Another problem with the current methods is their sensitivity to changing the number of the producers. In fact, since the connectivity parameter is from the second-type, we need to re-evaluate the connectivity parameters after a change in the number of producers. In this work we provide a modification that relates the connectivity parameters before and after the change in the number of producers. Applying this modification gives a better understanding of the connectivity and reduces the data requirement.

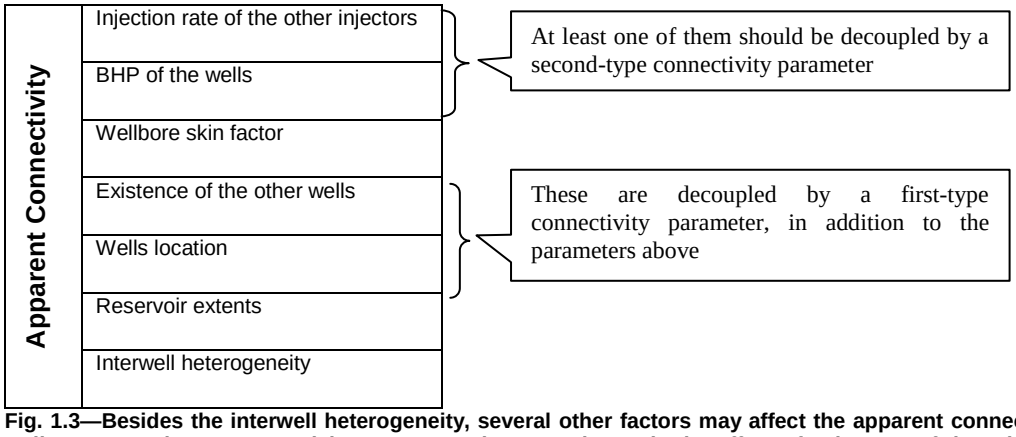

Fig. 1.3—Besides the interwell heterogeneity, several other factors may affect the apparent connectivity of two wells. A second-type connectivity parameter does not decouple the effect of existence of the other wells and well locations from the apparent connectivity; however, a first-type connectivity parameter decouples these effects.

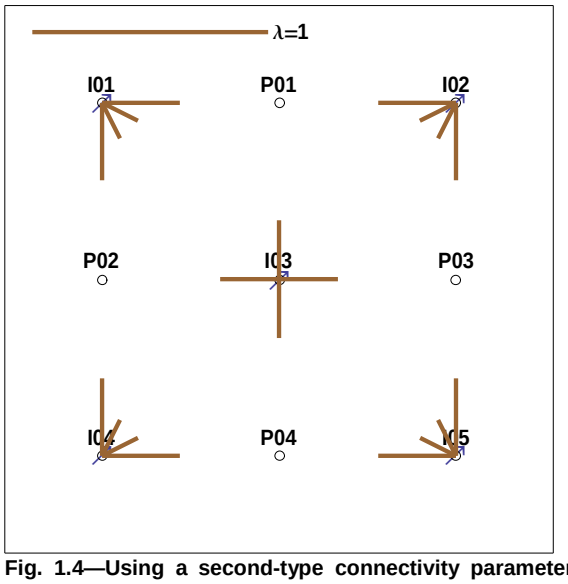

Fig. 1.4—Using a second-type connectivity parameter, in a homogeneous case, the connectivity parameter depends on the well location and reservoir shape (λ is a connectivity parameter from the capacitance model that will be explained in Section 3.1). Using a first-type connectivity parameter, the connectivity parameters for all these well pairs are zero.

In the second part of this work, we develop an approach to evaluate the connectivity based on the multiwell productivity index (MPI). Using this method, we can analytically predict the reservoir performance in homogeneous reservoirs under specific conditions. For heterogeneous formations, this method provides a first-type connectivity parameter. This model is not sensitive to frequent shut-in of the producers. In addition, in case injector BHPs are available the model can evaluate the injectors' connectivity.

2. LITERATURE REVIEW

Despite the importance and abundance of injection and production data, only a limited number of studies have specifically considered these data. Some of the studies only considered them qualitatively along with other available data and did not provide a specific connectivity index between the well pairs. However, a few quantitative studies and some phenomenological procedures have been developed using the intuitive concepts of well-pair connectivity, time-shift, and characteristics in frequency domain. We divide connectivity evaluation approaches into four general groups that we describe in the following sections.

2.1 Correlation Coefficient Based Methods and Exploratory Data Analysis

Heffer et al. (1997) used the Spearman rank correlation rates of well rates between injector/producer well pairs as an indicator of the connectivity of well pairs. They found good agreement between the correlation coefficients of well pairs and the direction of the mean maximum horizontal stress. By projecting the correlation coefficient between the well pairs they also produced a connectivity map. Based on their results in the calculation of correlation, no time lag between the injector and producer signal is required. Refunjol and Lake (1999) applied a similar method, this time by considering a time lag that maximizes the rank correlation. They explained this time lag as the effect of compressibility of the reservoir fluids.

Jansen and Kelkar (1996) applied a number of exploratory data analysis methods on the injection and production data, including analysis of rate and pressure versus time and spatial location. For example, by comparing the map of median oil rates from primary production and secondary recovery, they evaluate the field waterflood response. They also used the cross-correlation between the well rates (injector/producer, injector/injector, and producer/producer pairs) and found that determining the correlation coefficient in a selected time window may provide a better indicator of connectivity. Finally, by combining this global and local connectivity information, they ranked the field areas for improvement of waterflood efficiency. In a later work (Jansen and Kelkar 1997a), they used kriging of the cross-correlation between the well rates to map the connectivity.

To overcome the problem of nonstationary treatment of well rates, Jansen and Kelkar (1997b) suggested a wavelet based approach that generates a time-dependent cross-correlation of frequency components of the well rates.

All the studies above mentioned the interaction of the injection rates as a limitation for the cross-correlation method. To overcome this problem, Soeriawinata and Kelkar (1999) developed a procedure to account for the superposition effect of multiple injection wells on a producing well. In this method, the cross-correlation of summation of the rates of the selected injectors (these injectors are selected in a multistage procedure) with the target producer is calculated.

2.2 Linear Regression Related Methods

Albertoni and Lake (2003) developed a multivariate linear regression (MLR)-based approach (in this dissertation the AL model) to analyze the injection and production data. In this model, the injection rates are the explanatory variables and the production rates (total fluid) are the response variables. They found that the weighting coefficient of the injection rates in the regression is independent of injection/production rates and depends only on geology and relative position between the wells. Based on the discussion in Section 1.2, this weighting coefficient, λ, is a second-type connectivity parameter. To consider the time lag between the injection and production rates, they applied a diffusivity filter to the injection rates. The most important advantage of this model over the previous ones is its ability to predict the future production rate. They applied their model on a number of synthetic and field cases and showed that their method can properly determine the connectivity and predict the liquid rate. However, they mentioned some limitations for their approach, including its constant number of producers and injectors, constant gas/oil ratio (GOR), constant BHP, constant well productivity, no new completions, constant non-waterflooding production, and constant effective permeability.

Jensen et al. (2004) defined a connectivity parameter based on the ratio of the number of streamlines from an injector to a producer over the total number of streamlines ending at the producer. They found that λ may disagree with this connectivity index, because the streamline ratio shows the steady-state hydraulic connectivity, while λ shows the injection perturbation effect on the production rate.

Gentil (2005) described the λ as the fraction of injected water from an injector that flows to a producer if all the other injectors are shut-in. He also found that the λ is equivalent to the relative average transmissibility between an injector/producer pair divided by the summation of transmissibilities of this injector and all producers. He tested this for several cases and found that the estimated λs from his definition and the AL method are generally in good agreement.

Dinh and Tiab (2008a) developed a model based on the AL model with the BHPs of injectors and producers as the input and output instead of the rates. The data for this model should be measured under a multiwell pressure test similar to an interference test. Similar to λ, the connectivity parameter obtained using this method is a second-type connectivity parameter that relates pressures instead of rates; however, its values are different than λs. In addition to the assumptions for the AL method (besides the constant BHP), they added assumptions including constant flow rate at the producers, constant total injection rate, and no use of artificial lift in the producers. In a later work, Dinh and Tiab (2008b) presented a modified model that does not have the assumption of constant number of wells. In this work they introduced a more robust connectivity parameter, called relative interwell permeability (it is different from relative permeability), that is independent of the position and distance of the wells.

2.3 Capacitance Model

Yousef et al. (2006) used a nonlinear signal processing model, called a capacitance model (CM), to evaluate interwell connectivity. Similar to the AL method, the CM is based on MLR. However, the time shift in this model is performed using a time constant coefficient between well pairs that could be determined from the well rates. Furthermore, this method can incorporate the producers' BHP data in case BHP fluctuates. The other advantage of this method over the AL method is the insensitivity of the model parameters to injector shut-in. It also considers the effect of the primary production of the reservoir. However, it has the other restrictions of the AL method. The CM provides three different connectivity coefficients: λ is the indicator of connectivity between an injector and a producer (equivalent to the λ in the AL method), τ is the time constant of the drainage volume, and ν is the coefficient of the BHP term. We will describe this model in detail in Section 3.1.

Later, Yousef et al. (2009) showed the application of the CM as a diagnostic tool to detect the permeability trends and enhance the geological features. They found that combination of λ and τ values can extract more geological information than using them individually. They showed that using a log-log plot of τ-λ and an F-C plot (combination of λ and τ using the idea of the Lorenz plot) can identify if the injector/producer connectivity is through a fracture, a high permeability zone, or a partially completed zone. They applied these approaches on a field case and showed that the CM results are consistent with the geological information from other studies.

By adapting a power-law watercut prediction model to the CM, Liang et al. (2007) described a method to estimate the oil production rate. They used this model to optimize injection rates to maximize the NPV in a synthetic field. Using a similar method, Sayarpour et al. (2007) optimized the injection rates in a field case. They also defined some improved versions of the CM (they called it CRM as the capacitance-resistive model) in terms of free parameters based on the number of time constants of the model. Sayarpour et al. (2008) applied the CM to a CO_2 flooding case and found the CM was a reliable tool in predicting the reservoir performance for both waterflood and CO_2 flooding. Webber et al. (2009) discussed the possible issues of applying the CM in large field cases and provided some suggestions to use the method in a more reliable manner. Although adopting the watercut model enables the CM to have an estimation of the oil rate after breakthrough, none of the above studies could provide a satisfactory oil rate prediction during the period before breakthrough period for individual producers in the studied synthetic cases.

2.4 Other Approaches

By superimposing the map of watercut of the producers and the fault map, Honarpour and Tomutsa (1990) related the water advancement to the heterogeneity of the reservoir. They also used the slope of the Hall plot of the injectors as a diagnostic tool for evaluation of the waterflood importance.

Panda and Chopra (1998) applied an artificial neural network (ANN) to estimate the connectivity. They used the injection rates (from a time window), permeability, and thickness as the input of the network and the oil and water rates as the output of the model. They determined the relative influence of each injector on the producer by taking the partial derivative of oil production with respect to the injection rate. Demiryurek et al. (2008) applied sensitivity analysis models to infer the injector/producer connectivity from the trained network and used that to rank the injectors.

Based on the analogy between the resistance/capacitance (RC) network and a reservoir, Demiroren (2007) analyzed the injection and production data in frequency domain to provide an estimation of connectivity between well pairs. However, she found that this analogy is applicable only for simple reservoirs under specific conditions.

Liu and Mendel (2007) presented a method using an extended Kalman filter to evaluate the interwell connectivity. They evaluated a connectivity parameter, called injector/producer relation, that may vary over time as production conditions change. However, they provided no explanation of the physical meaning of their connectivity parameters. In a later work, Zhai et al. (2009) fixed some of the problems of this model, such as its negative connectivity parameters. By normalizing the injector/producer relation for each injector, they also provided a more robust connectivity parameter which they interpreted as the percentage of the total water allocated to an injector flowing to a specific producer.

Table 2.1 summarizes some of the most important approaches we described here.

Table 2.1—Approaches to interwell connectivity evaluation based on injector and producer data

Approach	Input Data	Rate Prediction Model	Interwell Connectivity parameter	Confirmed with heterogeneous hypothetical case	Field Case Example	Major Reported Limitations
Exploratory data analysis	Rate and pressure	No	No	No	Yes	Not mentioned
Correlation coefficient	Rate	No	Yes	No	Yes	Effect of other injectors decreases the performance
Albertoni and Lake	Rate	Yes	Yes	Yes	Yes	Fluctuating BHP and changing the number of wells may lead to incorrect results.
Capacitance Model	Rate and pressure	Yes	Yes	Yes	Yes	Unreported fluctuating BHP and changing the number of producers may lead to incorrect results.
Extended Kalman Filter	Rate	Yes	Yes	No	Yes	Not mentioned
Neural Network	Rate and some reservoir properties	Yes	Yes	Yes (only one)	Yes	Very long period of data is required.
Dinh and Tiab	Pressure	No	Yes	Yes	No	Additional test is required.

3. CAPACITANCE MODEL

3.1 Introduction

As we discussed in the Section 2.3, the CM provides a robust tool to analyze injection and production data in a waterflood. In Section 3.2 we describe the CM and discuss some modifications to its original formula. We will show how to determine the coefficients in a more efficient way to overcome some of the difficulties we had in the original approach. At the end, we discuss some of the limitations of the CM using numerical simulation examples. In Sections 4.2 and 5.2 , we will show two CM modifications to overcome the problem of lack of BHP data and the effects of shut-in periods.

3.2 Capacitance Model

In a waterflood based on the material balance and the definition of productivity index for a system of a single producer and injector, the total liquid production rate of a well is (Yousef et al., 2006):

$$\hat{q}(t) = q(t_0)e^{-\frac{(t-t_0)}{\tau}} + \frac{e^{-\frac{t}{\tau}}}{\tau}\int_{\xi=t_0}^{\xi=t} e^{\frac{\xi}{\tau}} w(\xi)\,d\xi + J\left[p_{wf}(t_0)e^{\frac{-(t-t_0)}{\tau}} - p_{wf}(t) + \frac{e^{\frac{-t}{\tau}}}{\tau}\int_{\xi=t_0}^{\xi=t} e^{\frac{-\xi}{\tau}} p_{wf}(\xi)\,d\xi \right], \quad \text{..... (3.1)}$$

where $\hat{q}(t)$ is the total (sum of all fluid in reservoir volumes/time) estimated production rate at time $t \geq t_0$, t_0 is the time production begins, w is the injection rate, p_{wf} is the BHP of the producer and ξ is a variable of integration. τ is the time constant of the drainage volume and controls the time shift of the injection rate signal. τ may be defined as $\tau = (c_t V_p)/J$, where c_t is the total compressibility, V_p is the pore volume and J is the productivity index of the producer. Appendix A shows the detailed derivation of this equation.

Eq. 3.1 consists of three components. The first component is the production rate caused by fluid and rock expansion which decreases with time. The rate of this decline is controlled by τ. The second term is the effect of injection, where the injection rates of the current and previous time steps affect the production rate. The last term accounts for changes of the producer's BHP.

By generalizing the CM for multiple injectors and discretizing the integrals, we obtain:

$$\hat{q}_j(t) = \lambda_{pj} q_j(t_0) e^{-\frac{(t-t_0)}{\tau_{pj}}} + \sum_{i=1}^{i=I} \lambda_{ij} w'_{ij}(t) + \sum_{k=1}^{k=K} \nu_{kj}\left[p_{wf_j}(t_0)e^{\frac{-(t-t_0)}{\tau_{kj}}} - p_{wf_k}(t) + p'_{wf_{kj}}(t) \right], \quad \text{..... (3.2)}$$

where λ_{pj} is the effect of primary production on well j, λ_{ij} is the interwell connectivity coefficient between an injector/producer well pair, ν_{kj} is the coefficient of the producers' BHP term, I is the number of injectors, and K is the number of producers. w'_{ij} is the shifted (convolved) injection rate of injector i with respect to producer j. Assuming a stepwise change of injection rate in each time step t_1, t_2,…, t, w'_{ij} can be found using Eq. 3.3:

$$w'_{ij}(t) = \sum_{m=1}^{n} \left[e^{\frac{(t_m - t)}{\tau_{ij}}} - e^{\frac{(t_{m-1} - t)}{\tau_{ij}}} \right] w_j(t_m) \quad \text{..... (3.3)}$$

or in the convolution form,

$$w'_{ij} = \alpha_{ij} * w_{ij}, \quad \text{..... (3.4)}$$

where * denotes convolution and α is the impulse response and equal to

$$\alpha_{ij_m} = \left[e^{\frac{(t_0 - t_{m-1})}{\tau_{ij}}} - e^{\frac{(t_0 - t_m)}{\tau_{ij}}} \right] \quad \text{..... (3.5)}$$

$p'_{wf_{kj}}(t)$ is the shifted BHP of producer *k* with respect to producer *j* (assuming a stepwise change of BHP in each time interval)

$$p'_{wf_{kj}}(t) = \sum_{m=1}^{n} \left[e^{\frac{(t_m - t)}{\tau_{kj}}} - e^{\frac{(t_{m-1} - t)}{\tau_{kj}}} \right] p_{wf_k}(t_m) \quad \text{..... (3.6)}$$

or in the convolution form,

$$p'_{wf_{kj}} = \beta_{kj} * p_{wf_{kj}}, \quad \text{..... (3.7)}$$

where β equals to:

$$\beta_{kj_m} = \left[e^{\frac{(t_0 - t_{m-1})}{\tau_{kj}}} - e^{\frac{(t_0 - t_m)}{\tau_{kj}}} \right] \quad \text{..... (3.8)}$$

Eqs. 3.3 and 3.6 differ slightly from the formulas derived by Yousef (2006). In fact, these equations are equivalent to Yousef's "normalized" relations. For details refer to Appendix A.

λ reflects the connectivity between the injector/producer well pairs. The values of λs are independent of injection and production rates and producer BHPs (if we have the BHP data). However, if we change the production conditions (such as adding a new producer or shutting-in an active producer, changing the skin factor of the wells, and making recompleting in new zones), they will change. Values of λs are between zero and one and, based on material balance, for each injector $\sum_{j=1}^{K} \lambda_{ij} = 1$ for $1 \le j \le K$.

ν, the coefficient of the BHP term, reflects the connectivity of the producers. ν indicates how the change in BHP of a producer affects its own and other wells, production rates, and it has the dimension of the productivity index. Yousef (2006) reported that $\sum_{k=1}^{K} \nu_{jk} = 0$ for $1 \le j \le K$.

Ideally, we assign a time constant (τ) for each injector/producer pair because V_p and J and maybe c_t can change from one well pair to another. For example, in a homogeneous reservoir the pore volume of the interwell region of two close wells is much smaller than the one between two distant wells. However, because of the limitations in the number of data, we may prefer to have fewer time constants. In this case, we may have one time constant for each producer. In Sayarpour's (2008) detail discussion of the number of time constants, he suggested an additional type of time constant, where dividing the interwell region into a number of blocks applies a time shift block by block. He suggested that this modification gives a better estimation of production rate especially for the cases where the time constants are very large. In this dissertation, we either apply one time constant for each well pair or one time constant for each producer. Similar to the λs, the τs are independent of the injection and production rates and producer BHPs; however, if the λs change, the τs will also change. In addition, if the total compressibility changes within the domain being modeled (e.g., if saturation changes), then τ will change. If this change is small over the time of analysis, the error in CM prediction will be negligible. However, if this change is large (as in case of variable GOR), then τ will change over time and the performance of the CM will decrease.

If the producer BHPs are constant during the analyzing period, Eq. 3.2 reduces to:

$$\hat{q}_j(t) = \lambda_{pj} q_j(t_0) e^{-\frac{(t-t_0)}{\tau_p}} + \sum_{i=1}^{i=I} \lambda_{ij} w'_{ij}(t) \cdot \quad \text{..... (3.9)}$$

In this case, the production rate is simply a linear combination of the shifted injection rates and the primary production effect. In addition, when the BHP data are not available, we have to ignore the BHP term. In this dissertation we call this form of the CM (Eq. 3.9) the *simple CM* and in case we include the BHP term (Eq. 3.2) we call it the *full CM*.

When the total injection rate of the system is close to the total production rate, the system is balanced and the model is called the *balanced CM*. In cases where the total injection rate of the system is considerably different from the total production rate, Eqs. 3.2 and 3.5 must be modified by adding a term representing the size of the imbalance, q_{0j}. Strictly speaking, q_{0j} should be a function of pressure. Yousef et al. (2006), however, assumed q_0 is constant and called the resulting modification the *unbalanced CM*. In this case, $\sum_{j=1}^{K} \lambda_{ij} \leq 1$.

3.3 Estimation of the Model Parameters

To estimate the model parameters, we need to determine the τs and λs (and νs in case of full CM and q_{0j}s in case of unbalanced CM) that minimize the error in total liquid production rate of the system based on the injection and production data. Yousef et al. (2006) used a combined iterative and MLR (Jensen et al. 2003) algorithm. In their method (**Fig. 3.1**), we initialize the τs and, using the MLR, we determine the

other parameters. Then, using an optimization algorithm, we update the τs and recalculate the other parameters. We repeat this procedure until the error is minimized. For most of the simulation cases and with reasonable estimates for the τs, this procedure works perfectly and we obtain λs that are in the acceptable range. However, if we get farther from the ideal conditions, we may get nonphysical λs (i.e. $\lambda<0$ or $\lambda>1$). To avoid this problem, we need to add limits to the λs. To apply this limitation, it is easier to use a different solution method. We jointly initialize both τs and λs and minimize the error.

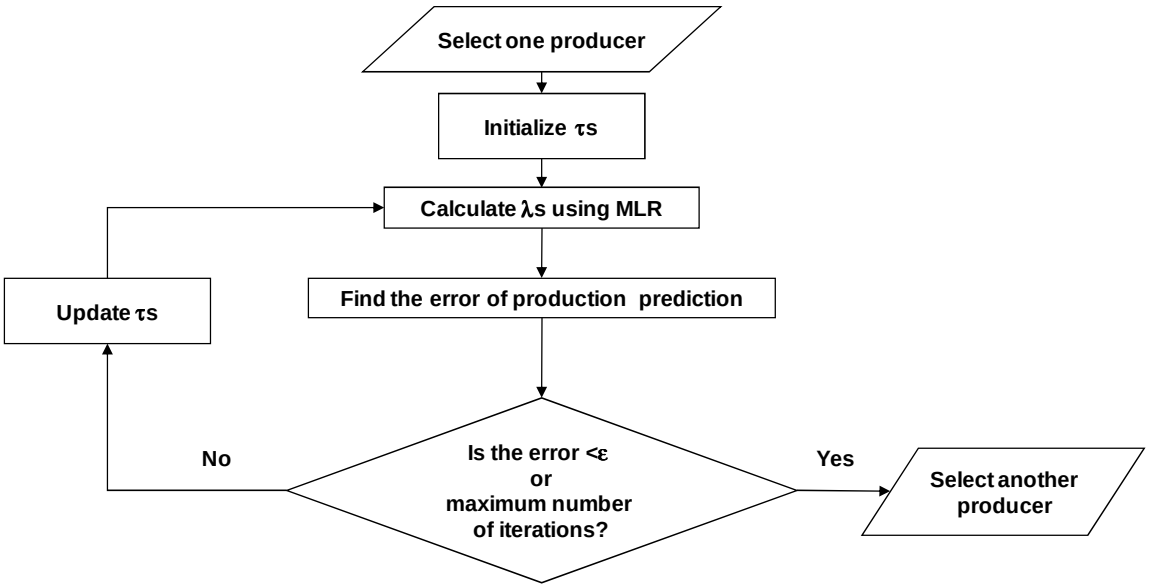

Fig. 3.1—Estimation of model parameters based on Yousef's Algorithm. In this method τs are estimated in an iterative procedure using a solver and λs are determined using MLR.

We can estimate the model parameters for each well separately or estimate them all at the same time. In other words, we can set the objective function as prediction error of a single producer,

$$L_j = \sum_{t=1}^{n} \left[\hat{q}_j(t) - q_j(t) \right]^2 , \quad \text{..... (3.10)}$$

and determine the corresponding model parameters well by well, or we can set the objective function as the prediction error of all individual wells,

$$L = \sum_{j=1}^{K} \sum_{t=1}^{n} \left[\hat{q}_j(t) - q_j(t) \right]^2 , \quad \text{..... (3.11)}$$

and estimate the model parameters all in the same optimization problem. Ideally, the results of applying either of these objective functions will be the same. However, as we observed, the results of these methods may differ. For example, when the objective function is the production rate of a single well, we cannot

apply the $\sum_{i=1}^{I}\lambda_{ij}\le 1$ condition. Thus the second objective function is more reliable because it guarantees this constraint on λs and the material balance. The only problem with this "batch" optimization is the large number of parameters in the model, which increases the computation time dramatically. Determining *I.K* parameters simultaneously will take much more time than calculating *I* parameters for *K* problems at the same size. If we determine the gradient for each variable analytically, the optimization procedure becomes much faster. With these gradients, the algorithm does not need to calculate them numerically and this decreases the number of function evaluations, thereby reducing the computation time. The gradient of the objective function for each variable can be determined easily using the chain rule. For the simple CM (Eq. 3.9) and objective function (Eq. 3.11) we have:

$$\frac{\partial L}{\partial x}=\sum_{j=1}^{K}\frac{\partial L}{\partial \hat{q}_j}\frac{\partial \hat{q}_j}{\partial x}=\sum_{j=1}^{K}\sum_{t=1}^{n}2\left[\hat{q}_j(t)-q_j(t)\right]\frac{\partial q_j}{\partial x}, \quad \text{..... (3.12)}$$

where *x* denotes the model parameter. The gradients of the model parameters for the simple CM are listed in **Table 3.1**.

Table 3.1— Gradient of the objective function (Eq. 3.11) on the variables for the simple CM

Variable	Gradient
τ_{ij}	$\lambda_{ij}\sum_{m=1}^{n}\left[\frac{(t_{m-1}-t)e^{\frac{(t_{m-1}-t)}{\tau_{ij}}}-(t_m-t)e^{\frac{(t_m-t)}{\tau_{ij}}}}{\tau_{ij}^2}\right]w_i(t_m)$
τ_{pj}	$\frac{\lambda_{pj}q_j(t_0)(t-t_0)e^{-\frac{(t-t_0)}{\tau_{pj}}}}{\tau_{pj}^2}$
λ_{ij}	w'_{ij}
λ_{pj}	$q_j(t_0)e^{-\frac{(t-t_0)}{\tau_{pj}}}$
λ_{0j}	1

These gradients also show the effect of each model parameter on the production rate. Depending on the strength of the shifted injection signal, λ affects the production rate. If the injection rate of an injector is small, this sensitivity will be smaller and the estimated λs for that well may be less accurate because they have less effect on the objective function. However, in cases of high injection rates, they become more important. Small errors in τ may have less effect in the prediction compared to the error in λ. The inverse squared term in the denominator of the derivative with respect to τ makes the sensitivity of the production

rate to τ changes small. However, if sharp changes exist in the injection rate signal, this parameter may become more important. We suggest performing a more detailed sensitivity analysis of the CM parameters for different cases with various diffusivity constants, injection rates, and number of available data.

Here, we show some simple examples of determining the CM coefficients and interpretation of its results.

Case 3-1. This case is a 5x4 (5 injectors and 4 producers) system (**Fig. 3.2**). The general reservoir and fluid properties are shown in **Table 3.2**. The producer BHPs change twice during the analysis period (**Fig. 3.3**) and injection rates are set as in **Fig. 3.4**. Using a numerical reservoir simulator (Eclipse 100), we predict the reservoir performance. Applying the full CM (Eq. 3.2), we determined the model parameters and confirmed that the model estimates the production rates accurately (**Table 3.3**). We also modeled the data using Eq. 3.9 and, as expected, the accuracy of the model decreased (Table 3.3), because the producers' BHP changes are not included in the model. We ran another case with constant BHP and confirmed that Eq. 3.9 was able to estimate the model parameters and production rate accurately (Table 3.3). **Fig. 3.5** shows the map of λs. In the λ map, we draw a vector from each injector to the producer so that the length of this vector shows the connectivity between the well pairs. In this case, since the system is homogeneous and isotropic, the λ map is symmetric. If we plot the λ map from the results obtained for the case of changing BHP excluding the BHP data (**Fig. 3.6**), we can see the results are misleading and wrong conclusions may be obtained. For example, based on this map the λ between I01 and P04 is almost equal to the one between I01 and P02, where in fact there is considerably less communication between I01 and P04. The other problem with this inaccurate estimation of the model parameters is the decreasing prediction ability of the model. In this situation, the model parameters may perform properly only for these specific injection rates. For example, using these two sets of connectivity coefficients, we applied the CM to predict the production rates for 50 more months using a different set of injection rates and observed more than 5% percent difference between the results. Comparing these results with the one from the reservoir simulator, we observed that the R^2 of the model considering the BHP data is 0.999; however, the one of the model ignoring the BHP data is 0.728. This confirms that ignoring the fluctuating BHP data may lead to incorrect connectivity evaluation and poor prediction. We will show another example for this problem in Section 3.4.

Case 3-2. Similar to Case 3-1, this case is a 5x4 system and the general reservoir properties are identical. However, in this case, a barrier exists between Wells I03 and P04 (**Fig. 3.7**). Applying the simple CM and mapping the λs, we see how a barrier affects the λs (**Fig. 3.8**): the λ between well pairs (I03, P04) decreases and the ones for (I03, P01) and (I04, P04) and (I05, P04) increase. This barrier, by blocking the interwell region between I03 and P04 (that resulted in smaller λ), directs flow in the well pairs with increased λ.

Yousef (2006) presented more examples of λ maps and showed how to interpret the results.

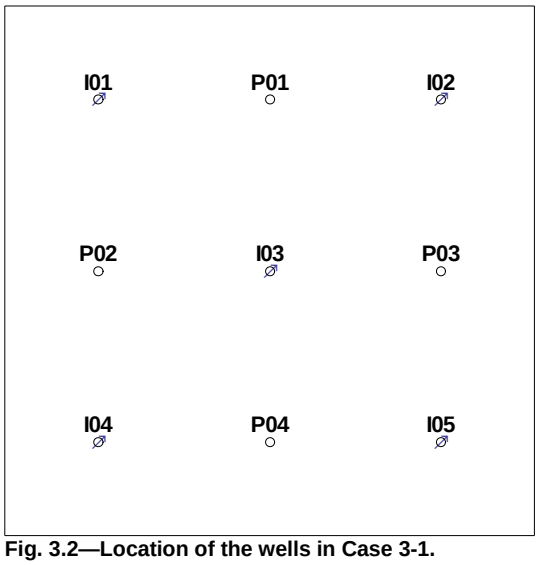

Fig. 3.2—Location of the wells in Case 3-1.

Table 3.2— General reservoir properties of Cases 3-1 and 3-2.

Reservoir dimensions				
	x	=	2480	ft
	y	=	2480	ft
	h	=	60	ft
Porosity	ϕ	=	0.18	
Permeability				
	Absolute	=	40	md
	Oil end point	=	36	md
	Water end point	=	9	md
Viscosity				
	Oil	=	0.5	cp
	Water	=	2	cp
Formation Volume Factor				
	Oil	=	1.07	
	Water	=	1.01	
Initial Reservoir Pressure	p_i	=	1470	psi
Compressibility				
	Oil	=	5×10^{-6}	psi^{-1}
	Water	=	1×10^{-6}	psi^{-1}
	Rock	=	1×10^{-6}	psi^{-1}

Table 3.3— Accuracy of the production rates prediction using the CM for different cases.

Case	BHP	Algorithm	Abs error, %	R^2
2-1	Variable	Full CM	0.1694	0.9999
2-1	Variable	Simple CM	1.9046	0.9879
2-1	Constant	Simple CM	0.1628	0.9999
2-2	Constant	Simple CM	0.1637	0.9997

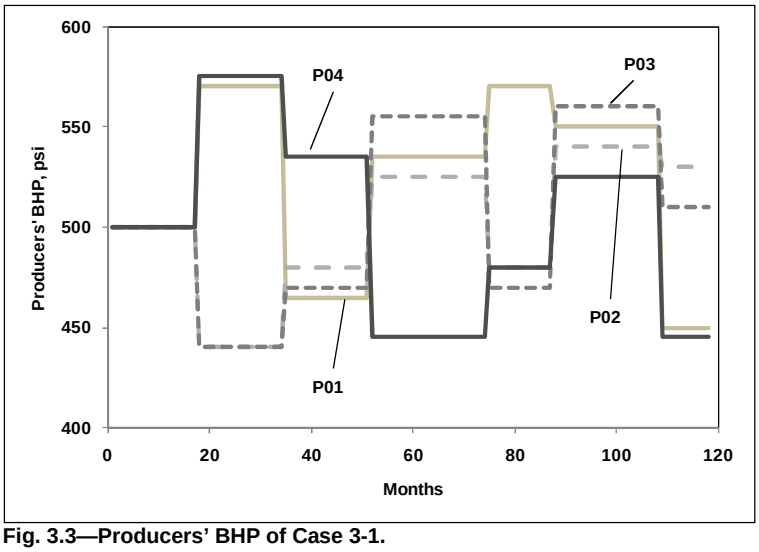

Fig. 3.3—Producers' BHP of Case 3-1.

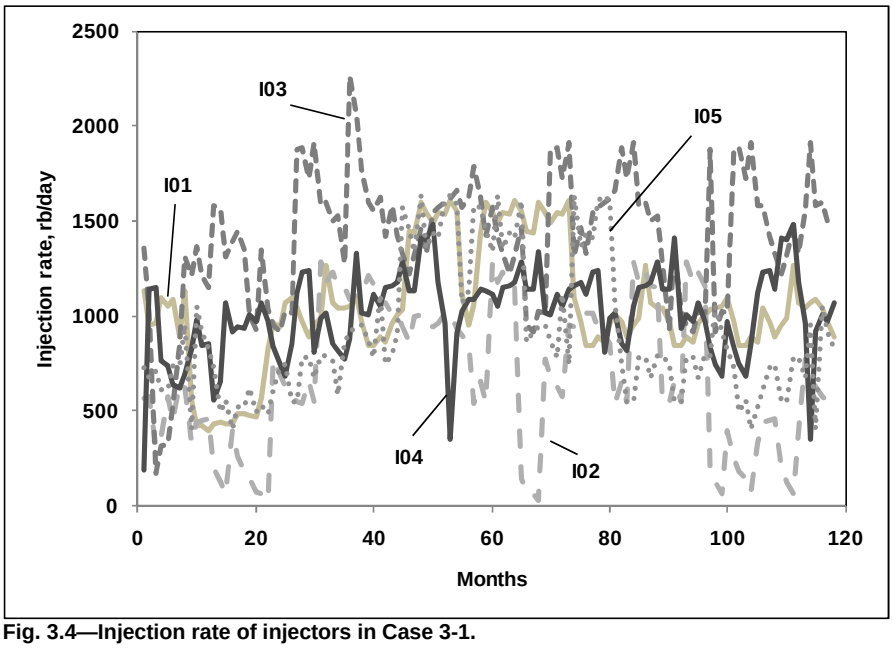

Fig. 3.4—Injection rate of injectors in Case 3-1.

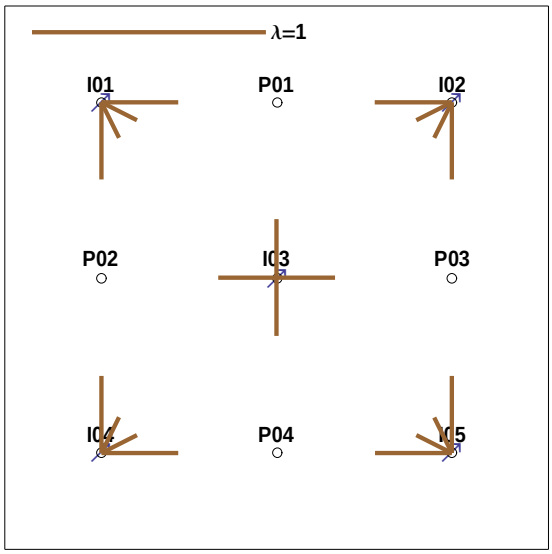

Fig. 3.5—λ map of Case 3-1. As we expected since this case is homogeneous and isotropic, the λ map is perfectly symmetric, and since the system is closed, the summation of λs for each injector is 1.

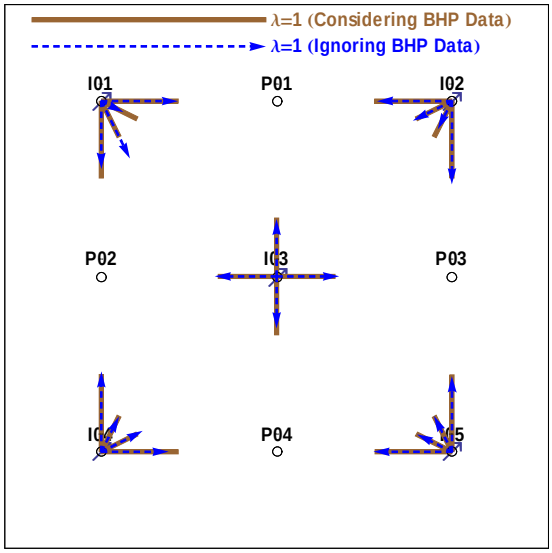

Fig. 3.6—λ map of Case 3-1 with variable BHP disregarding BHP data. For this simple case, the results are slightly misleading, specifically for wells I01, I02, and I03; that implies some heterogeneity in the interwell region.

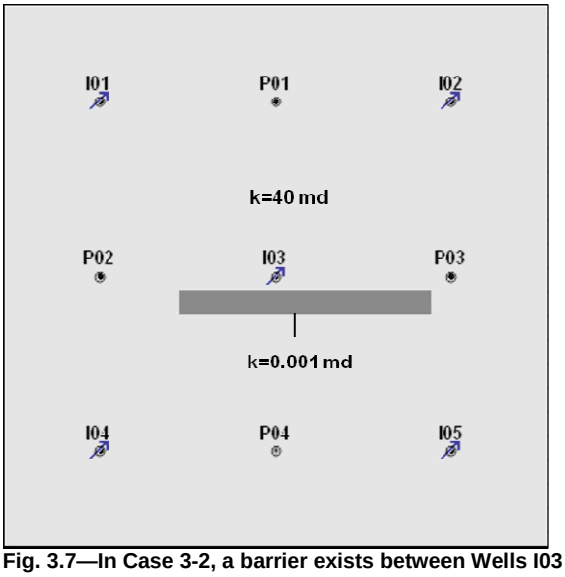

Fig. 3.7—In Case 3-2, a barrier exists between Wells I03 and P04.

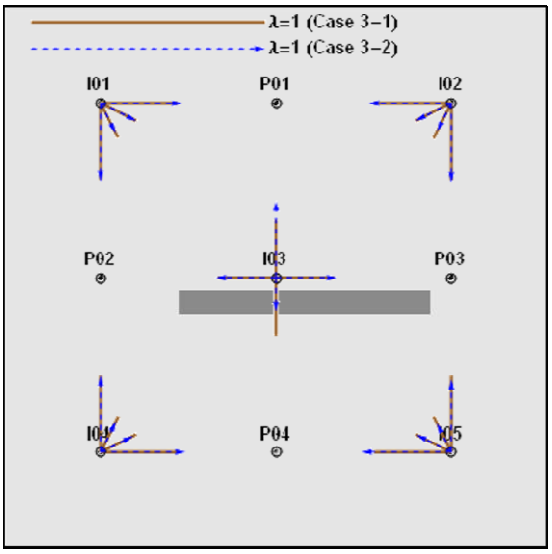

Fig. 3.8—λ map of Case 3-2. λ between I03 and P04 is much less than the homogenous case. In addition, λs between P04 and I04 and I05 and between I03 and P01 are larger than the ones for the homogeneous case.

3.4 Limitations of the CM

In the derivations of the CM (Eqs. 3.1 and 3.2), we require several assumptions. Among them, the most important ones are:

- Constant number of producers; i.e. no shut-in period or new production wells
- Availability of BHP data (Eq. 3.2) or constant and similar BHP (Eq. 3.9)

- Constant reservoir and well conditions
    - No new perforations in other zones
    - Constant productivity index
- Long period of data
- Negligible change in gas saturation
- Accurate measurements
- Uncorrelated injection rates

Violation of these assumptions may lead to low performance and unstable or questionable results. By unstable results, we mean obtaining significantly different model parameters after each run. Since the objective function is not convex, we may have several local minima for the same set of data. When we violate the CM assumptions, since there is no true answer and no perfect minimum for the problem, the chance of ending in these local minima becomes higher and we will have more unstable results. In cases where the CM assumptions are correct, we observed that the chance of obtaining unstable results is much smaller. By questionable results we mean obtaining a set of model parameters that are not consistent with the geological model, such as showing large connectivity for distant wells. In this research we directly address the first three tasks, and we indirectly reduce the minimum required data. Yousef (2006) performed an analysis on the effect of data quality and injection rate history, and we did not repeat them in this project.

Here we show an example of how violating the listed assumptions by adding a new well, lack of BHP data, and well stimulation (varying productivity index) decrease the accuracy of modeling the data using the CM.

Example 3-1. In this example we consider a 5x2 configuration (**Fig. 3.9)**. The reservoir is homogeneous and its properties are similar to Case 3-1. To determine the correct connectivity coefficients we ran a case (**Case 3-3-0**) with 216 data, constant BHP, and none of the other assumptions of the CM violated. Since the field is homogeneous and isotropic, the λs for the well pairs with equal distance [such as (I02, P02) and (I04, P01)] are identical (**Fig. 3.10),** and the CM models the data accurately (**Table 3.4**). We also ran three other cases:

Case 3-3-1. The producers' BHPs are constant but they have different values.

Case 3-3-2. Both producers' BHPs change one time.

Case 3-3-3. Well P02 is shut in at the middle of the analysis period.

Case 3-3-4. The skin factor of well P02 changes to -2.

As we expected, applying simple CM (ignoring the BHP data) for all these cases, the CM predicts the results poorly (**Table 3.4 and Fig. 3.11**). For Case 3-3-1, although the prediction accuracy is acceptable, the λs are far from correct. If we include the BHP data, the accuracy of the CM increases for Cases 3-3-1

to 3-3-3 (see Sections 4-5 and 5-3 for further details). For Case 3-3-4, since the BHPs are constant and equal and the source of the error is not the BHP data, including BHP data does not change the results. We will see how to overcome these problems in Sections 4.2 and 5.2.

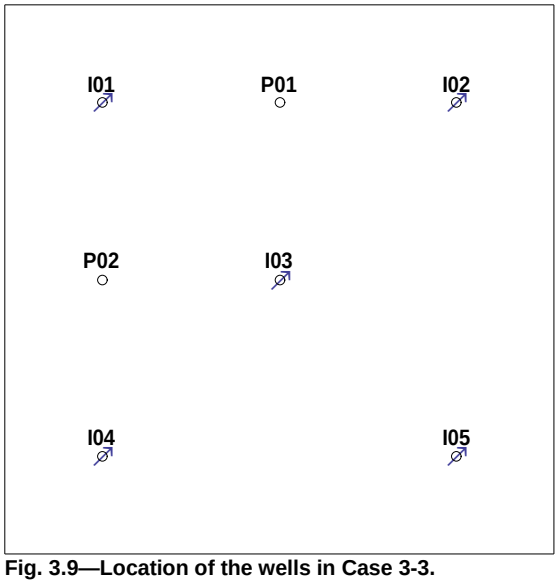

Fig. 3.9—Location of the wells in Case 3-3.

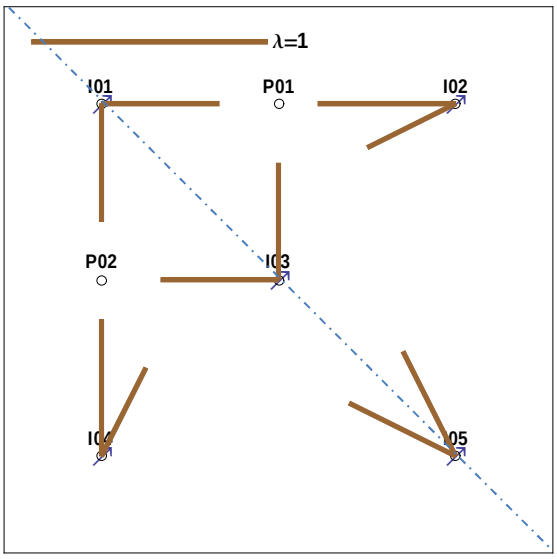

Fig. 3.10—λ map of Case 3-3-0. As we expected, similar to Case 3-1, since this case is homogeneous and isotropic the λ map is perfectly symmetric (with respect to the diagonal line).

Table 3.4—Violating the CM assumptions, the performance of the CM may decrease and the estimated connectivity coefficients may be different from the true ones.

Case	Abs. error in production rate, %	R^2	Abs. error in estimation of λ, %
3-3-0	0.3658	0.9980	-
3-3-1	1.5660	0.9834	23.69
3-3-2	4.6850	0.9018	17.20
3-3-3	66.3814	0.2040	92.57
3-3-4	5.9510	0.8473	25.95

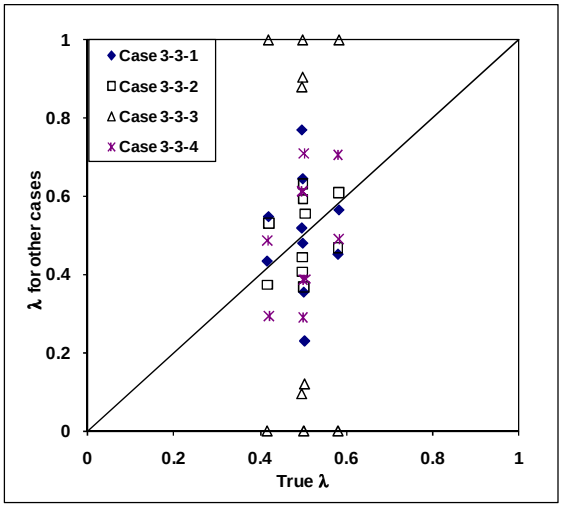

Fig. 3.11—Violating the CM assumptions not only decreases the accuracy of the flow rate predictions, but also may produce inaccurate connectivity coefficients.

Another source of error in the CM predictions that is little discussed in the literature is the effects of a small diffusivity constant ($k/\phi\mu c_t$) and, more generally, having large τs. This violates the assumption of constant productivity index during the analysis period because of the longer transient region in small diffusivity constants and long distances that require variable productivity indices. In this case, the CM is unable to predict the production rate accurately. For example, if we rerun Case 3-1 with k=4 md, the absolute error will be 0.986% (for k=40 md it was 0.169%) and the λs will be slightly different from the true ones (**Fig. 3.12**). To investigate the effect of increasing the diffusivity constant on the results, we ran Case 4-1 (See Section 4-2) with different permeabilities. Applying the CM, we observed that decreasing permeability increases the prediction error (**Fig. 3.13**). We also tested another case where only water exists in the reservoir. As we expected, similar to the previous case, the performance of the CM decreases when permeability decreases (**Fig. 3.14**) although the error is smaller because in this case the permeability is higher (there is no relative permeability), eliminating the error due to the change in total compressibility.

We also tested this problem by changing fluid viscosity and, as expected, saw that increasing viscosity has exactly the same effect as decreasing permeability on the accuracy of the CM. In a similar way, increasing c_t decreases the performance of the CM (**Fig. 3.15**). However, its trend is not exactly the same as factors like k and μ. k and μ affect both J and τ, but c_t and V_p only influence τ. Since in the CM we do not consider the effect of the transient region, we cannot use it to model these effects. However, when we calculate the model parameters, we may get slightly different parameters from the true ones that somehow approximate the effect of this region.

3.5 Conclusions

Under specific conditions, the CM is able to predict the production rate and reveal the interwell characteristics in a waterflood. In the case of fluctuating BHP, we need to use the full CM to determine the CM parameters correctly. We also observed that in the cases of stimulation and changing the number of the producers, the calculated parameters using the CM may be different from the true ones. Inaccurate estimation of the CM parameters not only may lead to incorrect interpretation of the interwell characteristics, but also will result in poor production rate prediction. Since the CM is based on the pseudosteady-state productivity index, it cannot estimate the effects of the transient region, and decreasing the diffusivity constant decreases the accuracy of the model.

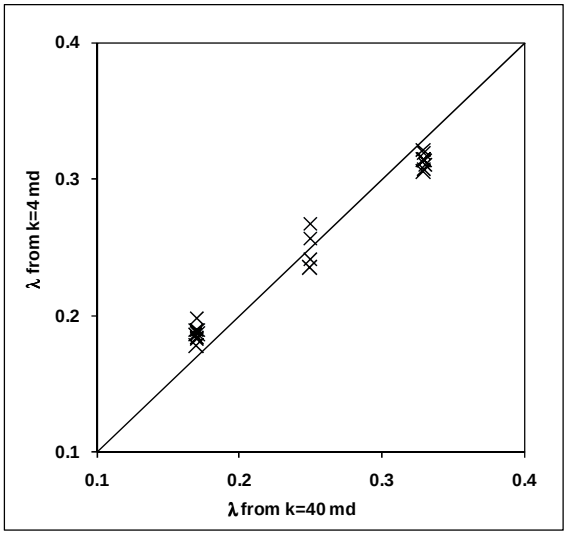

Fig. 3.12—In case of lower permeability, the connectivity coefficients may be slightly different from those of higher permeabilities.

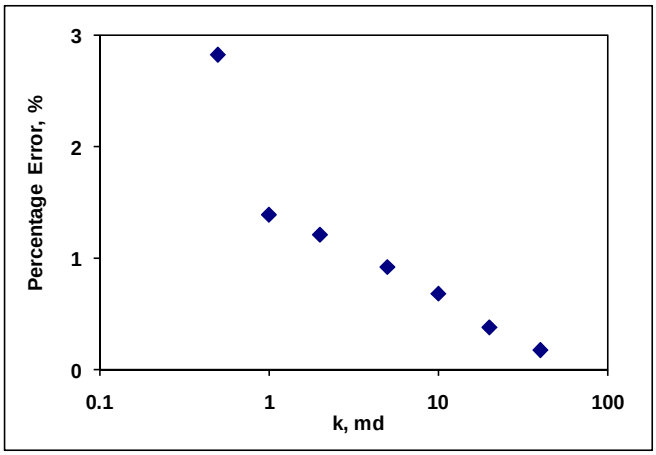

Fig. 3.13—When both oil and water exist, the accuracy of the CM decreases by decreasing the permeability. Data are from Case 3-1.

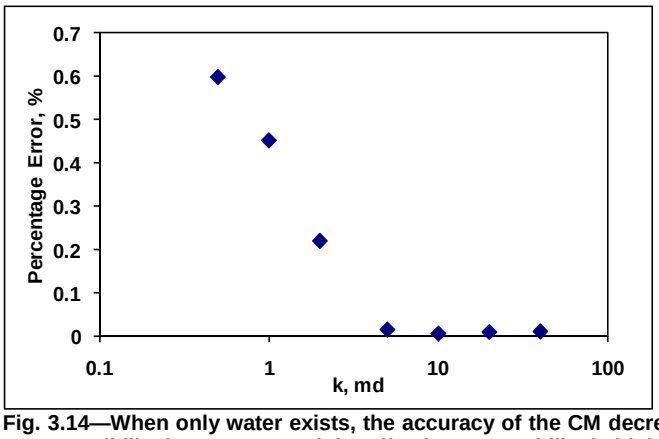

Fig. 3.14—When only water exists, the accuracy of the CM decreases by decreasing the permeability. Since the compressibility is constant and the effective permeability is higher, the overall accuracy is much higher than the case with both oil and water. Data are from Case 3-1.

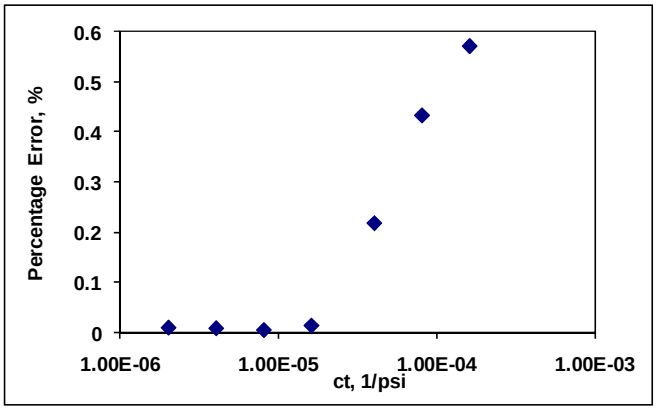

Fig. 3.15—Increasing the total compressibility increases the accuracy of the CM. Increasing total compressibility and decreasing permeability decreases the CM accuracy. However, their effect in decreasing the permeability is not exact the same.

4. SEGMENTED CM

4.1 Introduction

The underlying idea of the full CM is that connectivity can be determined by analyzing the effect of injection rate fluctuations upon production rates when the flow rates and BHPs are known. Changing producer BHPs affects production rates and can therefore influence the injection/production connectivity determination. The full CM considers this effect through the third term in Eq. 3.1, which contains all the information regarding pressure changes and, in effect, "decouples" the effect of changing producer BHPs from the injection-related component. In field situations, however, it is common for producer BHPs to be infrequently measured or entirely unavailable, even though the wells may experience BHP changes through events such as choke changes and workover operations. In these situations, we must use the simple CM instead of the full CM, but the connectivity evaluation is degraded because we lack pressure information. Here, we propose a modification of the simple CM that mitigates the need for pressure information required by the full CM.

4.2 Segmented CM

As we observed in Example 3-1, if the producers' BHPs are not constant and equal, then applying the simple CM (ignoring the BHP data) may result in misleading λs and the predicted production rate may be inaccurate. We observed that changing the BHP of a producer will shift the production rate of this well and its surrounding wells. Recalling Eq. 3.1, if the producers' BHPs are different from each other, we cannot predict the correct production rate based only on the injection rates, and the effect of the producers' BHPs shifts the production profile. We observed that the amount of this shift stays almost constant within the periods the BHPs do not change. In other words, for a specific set of producer BHPs, we just need to shift the expected production rate with a constant. So for producer j we can rewrite the full CM (Eq. 3.2) as

$$\hat{q}_j(t) = \lambda_{pj} q_j(t_0) e^{-\frac{(t-t_0)}{\tau_{pj}}} + \sum_{i=1}^{i=I} \lambda_{ij} w'_{ij}(t) + \lambda'_{0j}(s) \quad , \qquad (4.1)$$

where $\lambda'_{0j}(s)$ is the required shift for the specific set of producer BHPs for producer j within the time interval s, where $t_s - t_{s-1}$ is the duration of the interval s, $s \le S$, $t_S = t_{max}$, and $t_{s-1} < t \le t_s$. All connectivity coefficients, λ_{ij}, will be constant for all intervals. The t_s are the *segmentation times* and represent the times at which one or more of the producer BHPs change. If the producers' BHPs are all equal, even though different from the original BHP, the $\lambda'_{0j}(s)$ will be zero and Eq. 3.13 will be the same as Eq. 3.9. Incorporating the effect of BHP changes based on adding a constant $\lambda'_{0j}(s)$ between the segmentation times instead of using the BHP term is called the *segmented CM*.

The segmented CM can be explained using Eq.3.2. For the full CM, Yousef (2006) reported that the time constant between producer pairs is, in general, a very large value, so that he simplified the BHP term as

$$\text{BHP term}=\sum_{k=1}^{k=K} v_{kj}\left[p_{wf_j}(t_0)e^{\frac{-(t-t_0)}{\tau_{kj}}} - p_{wf_k}(t)+p'_{wf_{kj}}(t)\right]=\sum_{k=1}^{k=K} v_{kj}\left[p_{wf_j}(t_0)-p_{wf_k}(t)\right], \quad \text{..... (4.2)}$$

Based on this equation, if the producers' BHPs are constant through whole the analysis period, the BHP term becomes zero. If they are equal to each other but different from the initial one, this term will be zero again. Because

$$\text{BHP term}=\sum_{k=1}^{k=K} v_{kj}\left[p_{wf_j}(t_0)-p_{wf_k}(t)\right]=\left[p_{wf_j}(t_0)-p_{wf_j}(t)\right]\sum_{k=1}^{k=K} v_{kj} \quad \text{..... (4.3)}$$

and since $\sum_{k=1}^{k=K} v_{kj}=0$, the BHP term will be zero for this case. In general, for each interval between the segmentation times, the summation of the BHP terms for each well will be a constant number; this is equivalent to the $\lambda'_{0j}(s)$ in the segmented CM.

Fig. 4.1 illustrates a simple example of the segmented CM concept in a system similar to Case 3-3, where $\lambda'_{0j}(s)$ for each producer changes at the segmentation times. Based on the BHP profile, the segmentation times are at 32, 63, 90, 130, and 180 months. At the time interval 1 to32 months (when the BHPs of the producers are equal to each other), the $\lambda'_{0j}(1)$ for both wells is zero. So the production rates over this interval can be modeled using only the pre-analysis production term and the injection rates. At the time interval of 33 to 63 months, where BHP of P01 is larger than P02, the production rate of P01 decreases. This decrease will be modeled by a negative $\lambda'_{0j}(2)$ for P01 at this period and a positive one for well P02. At time 64, although only the BHP of P02 increases and BHP of P01 is still constant, the $\lambda'_{0j}(2)$ of both wells changes. At interval 64 to 90, since the BHP of P01 is still higher than P02, $\lambda'_{01}(3)$ is negative and $\lambda'_{02}(3)$ is positive; however, their absolute values are less than those of the previous interval. At time 91, BHP of P01 becomes smaller than P02. Consequently, $\lambda'_{01}(4)$ turns positive and $\lambda'_{02}(4)$ becomes negative. After the other segmentation times, we observe a similar pattern as previous intervals. At time 181, the BHPs of both wells become equal and $\lambda'_{0j}(7)$ for both becomes zero.

In the segmented CM, it may appear that we require *S* new parameters to model each well (*S* values of λ'_{0j}). In fact, we need to add a new $\lambda'_{0j}(s)$ only at the segmentation times and not at every time step. If we have frequent BHP changes, the segmented CM requires several $\lambda'_{0j}(s)$s, and this may lead to overfitting of the data and become less reliable. However, if we have a limited number of BHP changes, the segmented CM performs well.

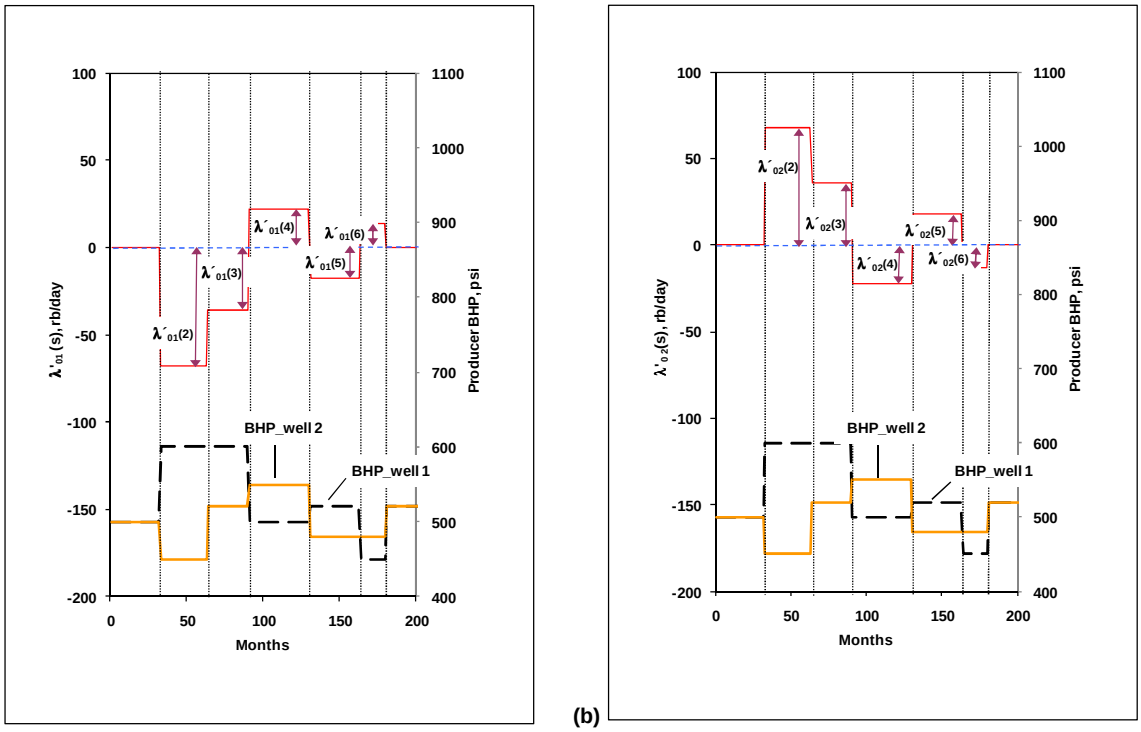

Fig. 4.1—In the segmented CM, a constant, $\lambda'_{0j}(s)$, is added to the model. The $\lambda'_{0j}(s)$ will change at the segmentation points, and it could be negative or positive, depending on the BHPs. If the BHPs of the producers are equal, $\lambda'_{0j}(s)$ will be zero as in this example where, in the first and last interval (<32 and >180 months), the BHPs are equal. a) Producer 1 and b) Producer 2.

In summary, in the segmented CM, we estimate the effect of BHP changes with $\lambda'_{0j}(s)$, which replaces the pressure term of the full CM. The value of $\lambda'_{0j}(s)$ is valid for all times that the producers' BHPs do not change. In other words, if the producer BHPs are constant (i.e. within two successive segmentation times):

- If they are equal to each other (even different from the initial pressure), $\lambda'_{0j}(s)$ for all the wells are zero and Eq. 4.1 will be equivalent to the simple CM (Eq. 3.9).
- If they are different from each other, we have a $\lambda'_{0j}(s)$ for each producer that stays constant during this interval.

To determine the model coefficients, similar to the simple CM, we need to find the set of coefficients that minimizes the sum of squared error (SSE) between the actual and predicted production rates of all the producers (Eq. 3.11). After initializing all the coefficients (λs, $\lambda'_{0j}(s)$s, and τs) and setting the constraints (e.g. $0<\lambda<1$ and $\sum_{i=1}^{I} \lambda_{ij} \leq 1$, and $t_s \geq t_{s-1}$), we can do this optimization using an appropriate nonlinear optimizer. If the system is balanced (the total injection rate of the system is close to the total production

rate), we expect to have $\sum_{j=1}^{K} \lambda'_{0j}(s) = 0$ because of mass balance. If the system is unbalanced, however, such a constraint does not exist.

Here, we show the application of the segmented CM using a simple example.

Case 4-1. This case is very similar to Case 3-1; the only difference is the injection rates and producer BHPs (**Fig. 4.2**) are different from Case 3-1. Applying simple CM, since the BHPs are not constant as we observed in Case 3-1 with its fluctuating BHP, the predicted production is not accurate (**Table 4.1**) and the connectivity coefficients are on average 15% different from the true ones (**Fig. 4.3**). Similar to Case 3-1, as we expected, using the full CM yields accurate results. Applying the segmented CM, we observed prediction error as low as the full CM (Table 4.1) and accurate interwell connectivity coefficients (**Fig. 4.3**). By plotting the BHP terms from both Eqs. 3.2 and 4.2 and the segmented CM, we observe that all the methods (**Fig. 4.4**) correctly approximate the effect of the BHP term. However, the segmented CM approximates this effect without using the BHP data.

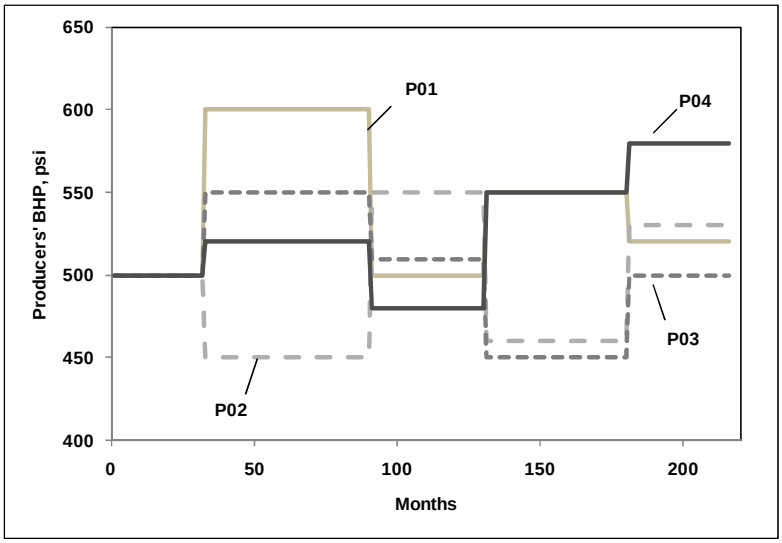

Fig. 4.2—Producer BHPs for Case 4-1, requiring four segmentation times at 32, 90, 130, and 180 months.

Table 4.1— Accuracy of the production rates using different CM algorithms for Case 4-1

Algorithm		P01	P02	P03	P04
Simple CM	R^2	0.9358	0.8590	0.9548	0.9301
	Abs. Error, %	4.7274	4.7206	3.3465	3.5897
Full CM	R^2	0.9997	0.9995	0.9997	0.9996
	Abs. Error, %	0.1856	0.1766	0.1766	0.1746
Segmented CM	R^2	0.9997	0.9995	0.9996	0.9995
	Abs. Error, %	0.1947	0.1753	0.1799	0.1794

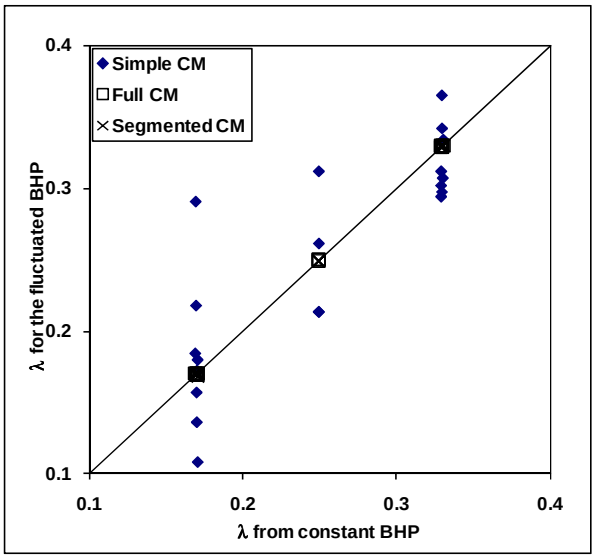

Fig. 4.3—Both the full CM and segmented CM determine the true λs that are independent of the BHP fluctuations. However, the λs obtained using the simple CM differ from the true ones. The true λs are calculated when the producers' BHPs are constant.

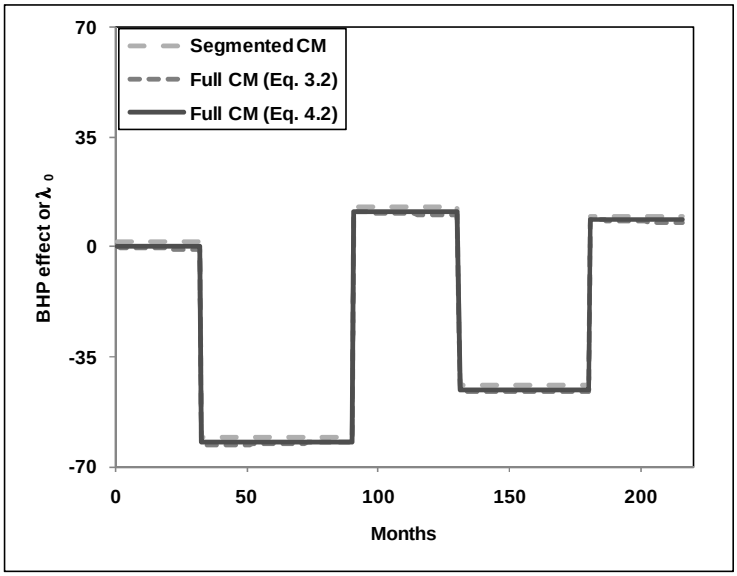

Fig. 4.4—The BHP term of the full CM for well P01 (both Eqs. 3.2 and 4.2) and the λ'_{0j}(s) from the segmented CM are in good agreement for Case 4-1.

We also applied the segmented CM on Case 3-1, where we have 6 segmentation times in 118 months, and, as we expected, the segmented CM generates the true connectivity coefficients (**Fig. 4.5**).

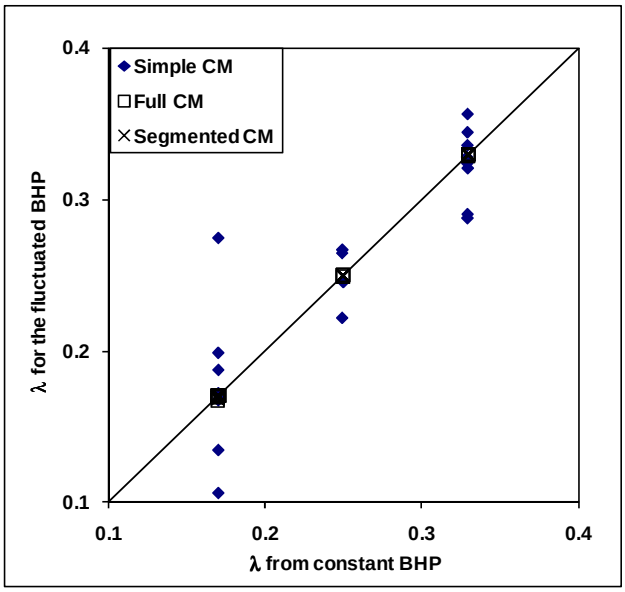

Fig. 4.5—Similar to Case 4-1, for Case 3-1 the segmented CM determines the coefficients as accurately as the full CM.

4.3 Estimation of the Segmentation Times

The segmented CM infers the connectivity properly provided that we know the segmentation times; however, this information might not be available. One possible solution to determine the proper segmentation times is to select the sudden changes in the production profiles as the segmentation times. **Fig. 4.6** shows a synthetic case where the major changes in the production profile correspond to the correct segmentation times. In fact, in this case the production rate caused by the BHP change is larger than the rates made by the injection rate fluctuations. In general, however, it may be difficult to determine the segmentation times, based only on the production rates. Specifically, if this sharp change is from injection rate fluctuations and not from changing the producers' BHPs, the segmented CM may provide incorrect results. For example, looking at the production profile of Well P01 (Case 4-1), it is almost impossible to select the correct segmentation times based only on the production profile (**Fig. 4.7**). In this case, the effect of injection rate fluctuations is much larger than the effect of producer BHP changes. Therefore, we need to determine the segmentation times independently of changes in the injection rates. For this purpose, we just need to find the optimum segmentation times that provide the largest decrease in the sum of the squared error (SSE) of the predicted production rates. Since the effect of injection rates fluctuations is mainly explained by applying the segmented CM on each stage of the algorithm above, the chance decreases that sharp injection rates will be selected as segmentation times. Determining these optimum segmentation times could be done in a simple, multistep algorithm:

1. In the data series select the second time-step as an apparent segmentation time.

2. Apply the segmented CM considering all the segmentation times determined earlier (if available) and the apparent segmentation time, and calculate the prediction error.

3. Ignore the current apparent segmentation time and select the next time-step as an apparent segmentation time.

4. Repeat Steps 2 and 3 for all the other points.

5. Select the time step that gives the lowest error as a segmentation time.

6. If more than one segmentation time has been selected, go to Step 7; otherwise repeat Steps 1-5.

7. If the error is almost the same for two successive steps (if there is no major decrease in error by including the segmentation times determined in two following steps), ignore the last two selected segmentation times and stop the algorithm. Otherwise consider all the selected points up to this step as the segmentation times and go to Step 1.

We tested this procedure on Case 4-1, assuming that the segmentation times are unknown. At the first step, we assumed a segmentation time exists at the second month, and based on that we determined the prediction error of the model using Eq. 3.11. In the same way, we assumed all the other months one by one as a segmentation time, and we determined the error for each of them. At this point, we could determine the segmentation time of the first step, which is at the 90^{th} month (Stage 1, **Fig. 4.8**). Considering this segmentation time, we repeated the same algorithm to determine the second segmentation time, which is found at the 130^{th} month (Stage 2, Fig. 4.8). At this step, we see that the Stage 2 error at 90^{th} month is one of the largest errors. This is because adding a segmentation time at the same month as Step 1 has no effect on the model performance. Also, we see some local maxima (for example, at 70^{th} month) in the Stage 2 curve that have values higher than the error at 90^{th} month. The main reason for this behavior is non-uniqueness of the CM results, specifically in case of unavailable fluctuating BHP, as we discussed in Section 3-4. This may lead to obtaining a large SSE for a correct segmentation time, and as a result selecting another time as a segmentation one. To overcome this problem, it is better to rerun the model several times for each segmentation time candidate to decrease the chance of losing a proper segmentation time. We continued the algorithm considering the obtained segmentation times, and 130^{th}, 32^{nd}, 180^{th}, 10^{th}, and 9^{th} months were determined as the times that minimize the error at the next steps, respectively. However, by plotting the error reduction at different steps, we can see only that 4 segmentation times is enough, and there is no need to consider the last two segmentation times (**Fig. 4.9**). In this example, we can see all the segmentation times at the first stage and we do not need to run the other stages. In general, however, finding all the segmentation times at the first stage is not guaranteed.

The above algorithm is not the only way to determine the segmentation times; we may use some optimization methods such as pattern search (Jensen et al., 2007) to determine several segmentation times simultaneously; however, these algorithms may take a very long time to determine the segmentation times, particularly if we have a large number of wells.

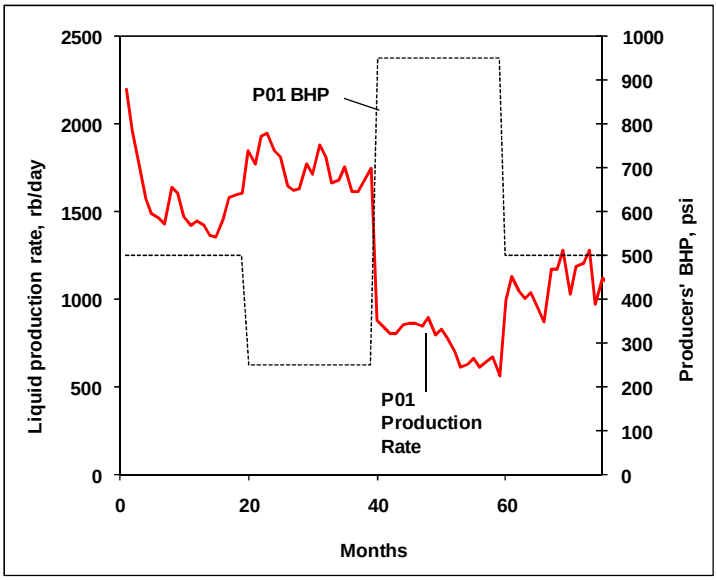

Fig. 4.6—If the BHP changes are large, we may be able to recognize the segmentation times by looking at the production profile.

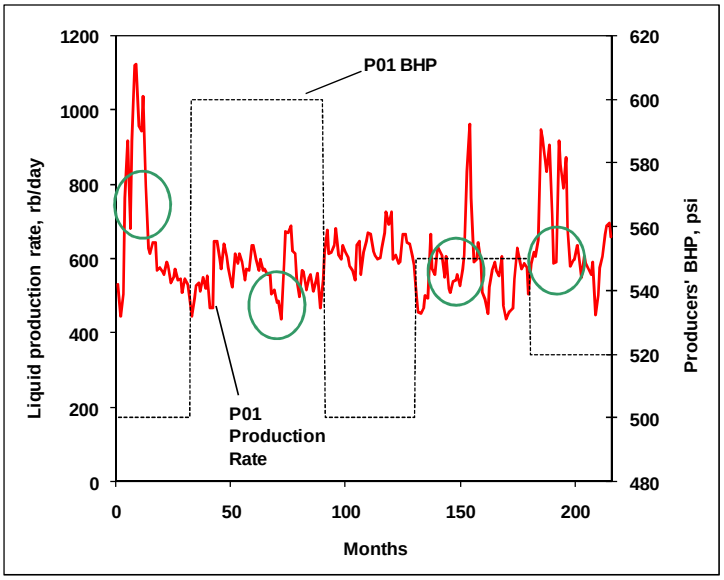

Fig. 4.7—If the BHP changes are smaller than the injection rate fluctuations determining the segmentation times only based on the production profile might be misleading. For example in this case, looking at the production profile we may select the green circled areas as the segmentation times.

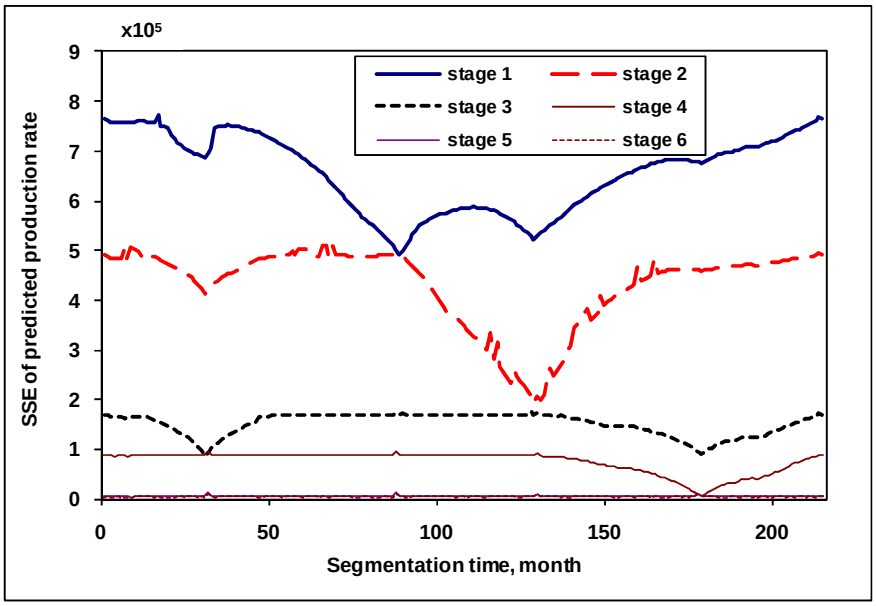

Fig. 4.8—The optimal segmentation point at each stage is the one that provides the greatest decrease in the sum of squared errors (SSE) of the predicted production rates for all the producers. In this simple case, all the segmentation times appear as local minima at the first stage. In general, we must run several stages to recognize all the required segmentation points.

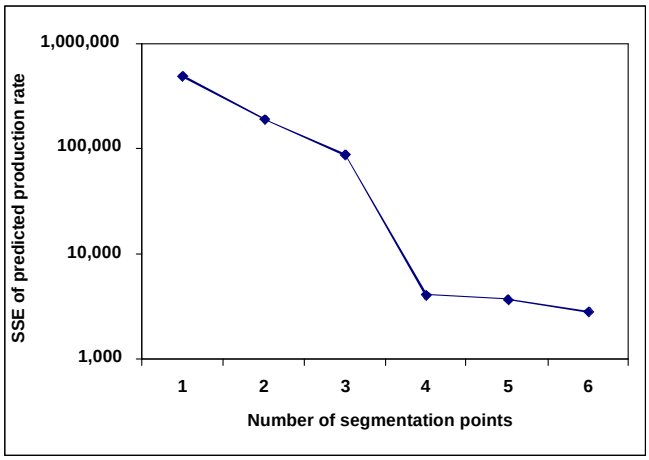

Fig. 4.9—Adding more than 4 segmentation points does not decrease the prediction error significantly for Case 4-1. This number of required segmentation points is in agreement with the number of imposed BHP changes in the time period of analysis.

4.4 Segmented CM for Stimulated Wells

Besides BHP fluctuations, one of the other common problems involved with applying the CM in field cases is well stimulations, which violates the CM assumption of constant well conditions (by changing the

productivity index) during the period of analysis. Theoretically, we cannot use the segmented CM for these cases; because, after stimulation, the interwell connectivity parameters may change and this cannot be accommodated in the model by only adding a constant term. As we will see in Section 9-4, the λs will change after stimulation. If the changes of the λs are not large, the segmented CM or even the simple CM may be used to model the system. In general, however, it is better to divide the data into pre- and post-stimulation intervals and determine the interwell connectivity coefficients for each case separately. In the case where there is only a short time period of data available, however, the segmented CM could be the better choice because, if we model the data separately, the models may be overfitted to the data and the resulting connectivity coefficients will be unrepresentative. Here, Case 4-2 addresses a possible application of the segmented CM on a simple stimulation case.

Case 4-2. The reservoir properties and well locations are similar to Case 3-3. The simulation was run for 216 months. In Month 108, producer 1 has been stimulated and its skin factor reduced from 0 to -2. Running the CM on pre- and post-stimulation intervals separately, we obtain different values of interwell connectivity coefficients (**Fig. 4.10**). If we apply the simple CM on the whole 216-month interval, the performance of the model, as reflected in the R^2 and absolute error percentage, is poor (**Table 4.2**) and the connectivity coefficients differ from the true ones (Fig. 4.10). Applying the segmented CM, however, gives better performance than the simple CM. We also observe that the coefficient values for the segmented CM for almost all the wells are between the pre- and post-stimulation values (Fig. 4.10).

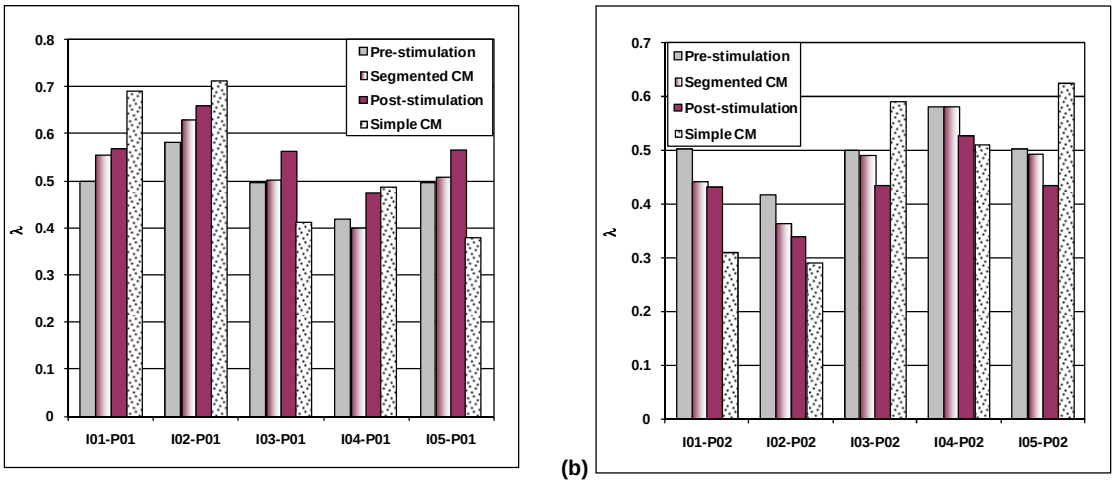

Fig. 4.10—The λs obtained using segmented CM are between the pre and post-stimulation ones: (a) Well P01, (b) Well P02. The λs provided by the simple CM, however, may differ significantly (for this example up to 40%) from both pre- and post-stimulation values.

Table 4.2—Performance of the simple and segmented CM on Case 4-2. The segmented CM predicts the production rate with an acceptable accuracy.

Algorithm		P01	P02
Simple CM	**R^2**	0.8682	0.8486
	Abs. Error, %	5.0604	5.8090
Segmented CM	**R^2**	0.9923	0.9959
	Abs. Error, %	0.8998	0.6903

4.5 Conclusions

If the BHP of the producers changes a limited number of times and the BHP data are unavailable, applying the segmented CM we can approximate the effect of the BHP changes on the production rate. In a hypothetical case we observed that the estimated BHP effect from the full CM is in excellent agreement with the BHP-related parameter from the segmented CM. In addition, the estimated λs using the segmented CM for the fluctuating BHP case is identical to the true λs obtained from the case with constant BHP. On the hand, for this case, the average R^2 of the predicted production rate using the segmented CM is 8% more than the one using the simple CM. In case the segmentation times are unknown, we can use the algorithm developed in Section 4.3 to determine the segmentation times. In a hypothetical case, after determining the segmentation times, we calculated the connectivity coefficients using the segmented CM that are as accurate as the results of the full CM. In cases of well stimulation, it is more accurate to calculate the model parameters after and before stimulation separately. However, if we do not have enough data, the segmented CM models the data in a single model with a much higher accuracy than the simple CM.

5. COMPENSATED CM

5.1 Introduction

If the number of producing wells changes (for example, a producer is shut in or a new producer is added) during the analysis period, we typically cannot use the CM to analyze all the data using a single model. The full CM would be able to model the data only with the BHP values of the shut-in well. Practically, by shutting in or adding a well, we need to divide the data into different periods in a way that the number of producers stays constant in each period. In this case, we cannot use the segmented CM on the whole interval because we need to have a limited number of BHP changes; changing the number of producers causes the BHP of the shut-in producer to change at every time step (**Fig. 5.1**). Thus, we would need to have segmentation times at all data points, making the model overfit the data. To solve this problem, we exploit the CMs insensitivity to the number of injectors (Yousef et al., 2006) to produce the compensated CM. Here, we derive the basic equations of the method and show its application on some synthetic cases and a field case.

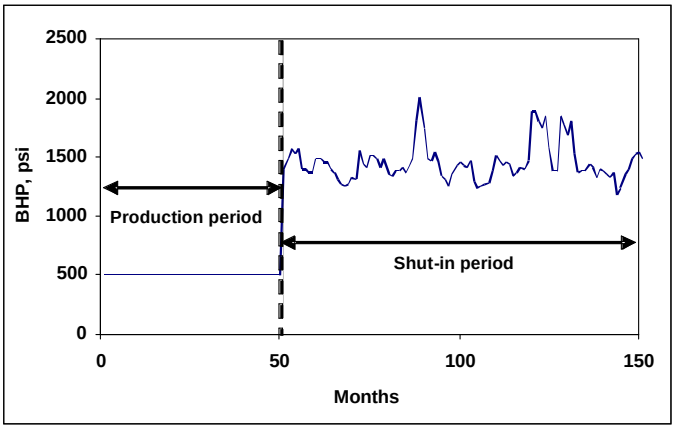

Fig. 5.1—The BHP of a shut-in well changes with time.

5.2 Compensated CM

As we discussed in Section 3.4 changing the number of producers will change the CM parameters. However, change in the number of injectors has no effect on the model parameters. Mathematically, since the injection rate is an explanatory variable of the model, changing it (even setting to zero) has not effect on the CM parameters. We will discuss it in Section 9.4. On the other hand, for producers this is not true because they are response variables that depend on each other; i.e. changing one of them affects the other

ones. Thus, assigning a specific rate (and not necessarily shutting-in) for a producer leads to a different set of model parameters.

By superposition, a shut-in producer may be treated as an open producer with all the produced fluid re-injected from a virtual injector at the same location (**Fig. 5.2**). By shutting in a producer, the reservoir pressure distribution changes and the fluids will be redirected to the other active producers; the virtual injector allows us to consider this effect without shutting in a producer. The injection rate of this virtual injector is equal to the amount of production that would be produced from the shut-in well if the well were not shut in. Since adding a "virtual" injector will not violate the CM assumptions, we can analyze the injection and production data without separating the dataset into before- and after-shut-in periods. The new parameter added to the model is the connectivity of the virtual injector with the other producers. From Eq. 3.9, after shutting in the producer *x*, we have

$$\hat{q}_j^{(x)}(t) = \lambda_{pj} q_j(t_0) e^{-\frac{(t-t_0)}{\tau_p}} + \sum_{i=1}^{n} \lambda_{ij}^{(x)} w_{ij}'^{(x)}(t), \quad \text{..... (5.1)}$$

where $\hat{q}_j^{(x)}$ is the predicted production rate of producer *j* when producer *x* is shut in, $\lambda_{ij}^{(x)}$ is the new interwell connectivity coefficient after shutting in the producer *x* and $w'^{(x)}_{ij}$ is the shifted injection rate of injector *i* with respect to producer *j* when producer *x* is shut in. Thus, the shut-in producer is replaced by a pair of wells, the original producer and a virtual injector. The new production rate of any producer is the summation of the regular production rate (before shutting in producer well *x*) and a portion of the virtual well's injection at the location of producer *x*. In other words,

$$\hat{q}_j^{(x)}(t) = \hat{q}_j(t) + \beta_{xj} \hat{q}_x(t), \quad \text{..... (5.2)}$$

where $\hat{q}_x$ is the virtual production (injection) rate of shut-in producer *x* and β_{xj} is the interwell connectivity coefficient between the virtual injector at producer *x* and producer *j*; in other words, the effect of shutting-in producer *x* on producer *j*. In general, we need to include the time lag between the pair of producers:

$$\hat{q}_j^{(x)}(t) = \hat{q}_j(t) + \beta_{xj} \hat{q}'_{xj}(t), \quad \text{..... (5.3)}$$

where $\hat{q}'_{xj}(t)$ is the shifted virtual production rate of producer *x* with respect to the time delayed interaction between wells *x* and *j*. Recalling Eq. 3.9, $\hat{q}_x(t)$ can be written in terms of injection rates

$$\hat{q}_x(t) = \lambda_{px} \hat{q}_x(t_0) e^{-\frac{(t-t_0)}{\tau_{px}}} + \sum_{i=1}^{I} \lambda_{ix} w'_{ix}(t) \quad \text{..... (5.4)}$$

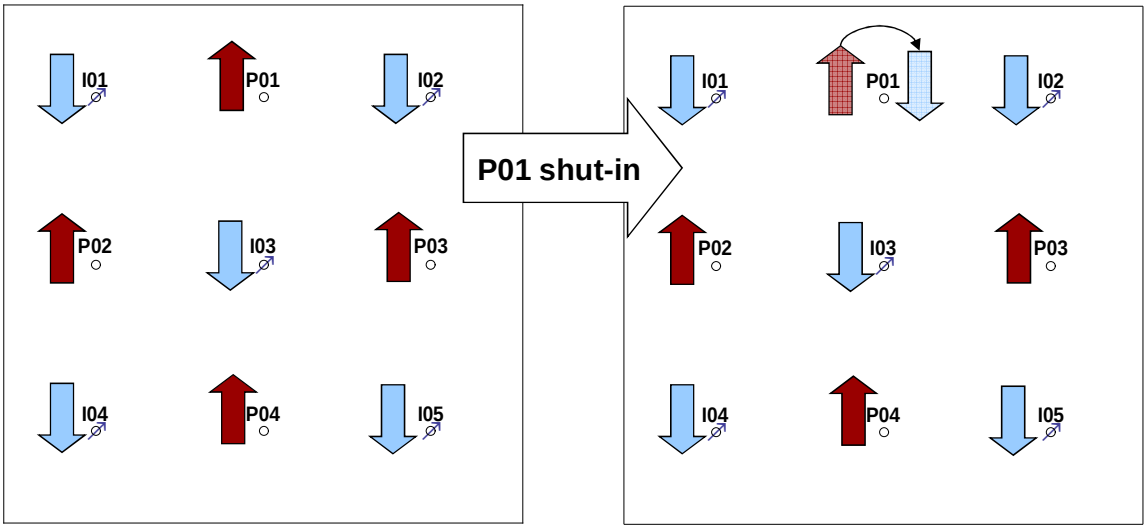

Fig. 5.2—The compensated CM assumes that the fluid that was supposed to be produced from the shut-in well (P01) is re-injected into the reservoir from an injector at the same location of the shut-in producer.

and the shifted rate of virtual production rate of producer *x* with respect to producer *j* will be

$$\hat{q}'_{xj}(t)=\left[\lambda_{px}\hat{q}_x(t_0)e^{-\frac{(t-t_0)}{\tau_{px}}}\right]'+\sum_{i=1}^{I}\lambda_{ix}w'^{(x)}_{ij}(t), \quad \text{..... (5.5)}$$

where $w'^{(x)}_{ij}$ is the shifted injection rate of injector *i* with respect to producer *j* when producer *x* is shut in. In fact, w'_{ix} is replaced by $w'^{(x)}_{ij}$, because here we consider the shift from injector *i* to producer *j*. The proper shift in the primary production rate could be performed by replacing τ_{px} with τ'_{px}

$$\hat{q}'_{xj}(t)=\lambda_{px}\hat{q}_x(t_0)e^{-\frac{(t-t_0)}{\tau'_{px}}}+\sum_{i=1}^{I}\lambda_{ix}w'^{(x)}_{ij}(t). \quad \text{..... (5.6)}$$

Substituting Eqs. 3.9 and 5.6 in Eq. 5.3 we obtain

$$\hat{q}^{(x)}_j(t)=\lambda_{pj}\hat{q}_j(t_0)e^{-\frac{(t-t_0)}{\tau_p}}+\beta_{xj}\lambda_{px}\hat{q}_x(t_0)e^{-\frac{(t-t_0)}{\tau'_{px}}}+\sum_{i=1}^{n}\lambda_{ij}w'^{(x)}_{ij}(t)+\beta_{xj}\sum_{i=1}^{n}\lambda_{ix}w'^{(x)}_{ij}(t) \quad \text{..... (5.7)}$$

or

$$\hat{q}^{(x)}_j(t)=\lambda_{pj}\hat{q}_j(t_0)e^{-\frac{(t-t_0)}{\tau_p}}+\beta_{xj}\lambda_{px}\hat{q}_x(t_0)e^{-\frac{(t-t_0)}{\tau'_{px}}}+\sum_{i=1}^{n}\left(\lambda_{ij}+\beta_{xj}\lambda_{ix}\right)w'^{(x)}_{ij}(t). \quad \text{..... (5.8)}$$

We call Eq. 5.8 the compensated CM.

Since the primary production effect may be small in mature waterfloods, and in Eq. 5.8 it also multiplied with β_{xj} which is smaller than 1, this term could be neglected and Eq. 5.8 becomes:

$$\hat{q}_j^{(x)}(t) = \lambda_{pj}\hat{q}_j(t_0)e^{-\frac{(t-t_0)}{\tau_p}} + \sum_{i=1}^{n}\left(\lambda_{ij} + \beta_{xj}\lambda_{ix}\right)w_{ij}'^{(x)}(t), \quad \text{..... (5.9)}$$

Comparing Eqs. 5.1 and 5.9, we conclude:

$$\lambda_{ij}^{(x)} = \lambda_{ij} + \beta_{xj}\lambda_{ix}, \quad \text{..... (5.10)}$$

where $\lambda_{ij}^{(x)}$ is the updated λ_{ij} after shutting-in well *x*.

Based on Eq. 5.10:

- If a well is shut in during the production period, we do not need to determine all the interwell connectivity coefficients again with the compensated CM as we would have to do when using the simple CM. Instead of reevaluating all the λs, we just need to determine the βs. For example, using the simple CM and assuming one shut-in well, we need to determine 2.*I*.*K* new parameters (*I* is the number of injectors and *K* is the number of producers): *I*.*K* new λs and *I*.*K* new τs are required. Using the compensated CM, only *K*.(*I*+*1*) new parameters are required: *I*.*K* new τs and *K* new βs. In the case of using a single value for τ for all injectors, the simple CM after shutting-in a well requires *K*.(*I*+1) new parameters (*I*.*K* new λs and *K* new τs) while the compensated CM requires only 2.*K* new parameters: *K* βs and *K* τs. This reduction in the number of parameters could be very important for many fields, where we may have a problem of a short analysis interval.
- If a new producer is added to the system, we can estimate new interwell connectivity coefficients, by estimating many fewer new parameters compared to the simple CM.
- We can predict the interwell connectivity coefficients if a producer converts to injector. Based on the definition of β, the producer/producer interaction is equivalent to λ, if the producer is replaced by an injector. The only requirement to calculate this coefficient is having the data for a few months of shut in (at least two sample periods) to estimate β.

Similar to the segmented CM, after initializing all the coefficients and setting the constraints, we can determine the model coefficients using an appropriate numerical solver. It should be mentioned that, in this method, the λs for producers that are active throughout the analysis period are constant. By having βs we can estimate the $\lambda^{(x)}$s for the cases where some of the producers are shut in. To get robust and reasonable results, we need to estimate all the λs and βs at the same time, because their values will be estimated based on both before and after shut-in data and not only one of these periods. Also we will have a greater number of data in the estimation. It may seem that the βs are independent of the non-shut-in period. However, since the $\lambda^{(x)}$s depend directly on both βs and λs, inaccurate estimation of βs, biases the λs to get more accurate values of $\lambda^{(x)}$s, and similarly inaccurate estimation of λs affects βs. Here we apply the compensated CM to two simple synthetic examples.

Case 5-1. The reservoir properties and well locations are identical to Case 3-1. The simulation was run for 216 months. The producer BHPs are constant throughout this period. At Month 116, Well P01 is shut in. Applying the compensated CM, we predicted the production rate over the whole production period accurately (average R^2 of 0.9996 for all the producers). We also applied the simple CM to each of the before- and after-shut-in periods. By updating the λs using Eq. 5.10 and using the compensated CM, we obtain the correct λs when Well P01 is shut in (**Fig. 5.3a**). We also ran a case with 6 injectors and 3 producers where the new injector is located at the position of the shut-in producer. As expected, we observed that the βs obtained for Well P01 are very close to the λs of the new injector (**Fig. 5.3b**). Plotting βs and λs in the same map (**Fig. 5.4**), we observe that the compensated CM, having a limited number of shut-in periods of producers, enhances our knowledge of the reservoir connectivity through evaluating the level of producer/producer interaction. In fact, without compensated CM we have no information about the producer connectivity. If we have the BHP of P01 (the shut-in producer) we can analyze the data using the full CM and the results will be very similar to the true connectivity map (**Fig. 5.5**); however, we obtain the same type of information using the compensated CM without using these data.

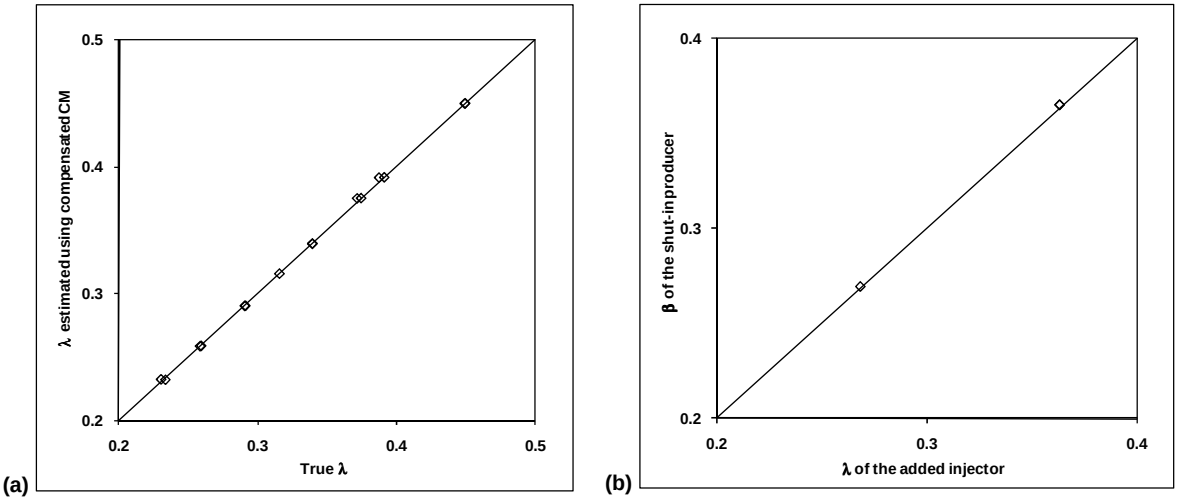

Fig. 5.3—The compensated CM can determine the connectivity coefficients correctly for Case 5.1: (a) calculated λ using compensated CM based on Eq. 5.10 for the period that well P01 is shut in is very close to the true λ, (b) β of the shut-in producer is very close to the λ of the added injector at the same location of the shut-in well.

Case 5-2. The reservoir includes a low permeability zone in the system similar to Case 3-2. Simulation was run for 94 months, where Producer 4 is added in Month 63. Also, the producers' BHPs change with time (**Fig. 5.6**). To analyze this system, we need to apply both the segmented CM and the compensated CM simultaneously, that predicts the production rates with very good accuracy (average R^2 of 0.9998). To

obtain the true λs, we also ran simulation cases with a longer period of data with a constant BHP for different cases: 5x3, 5x4 and 6x3 (including an injector instead of the added producer) and we observed that the segmented/compensated results accurately determine the connectivity coefficients (**Fig. 5.7**). In the λ–map for this case (**Fig. 5.8**) we observed, by including βs, that the effect of the barrier is more enhanced comparing to the map based on Case 3-2.

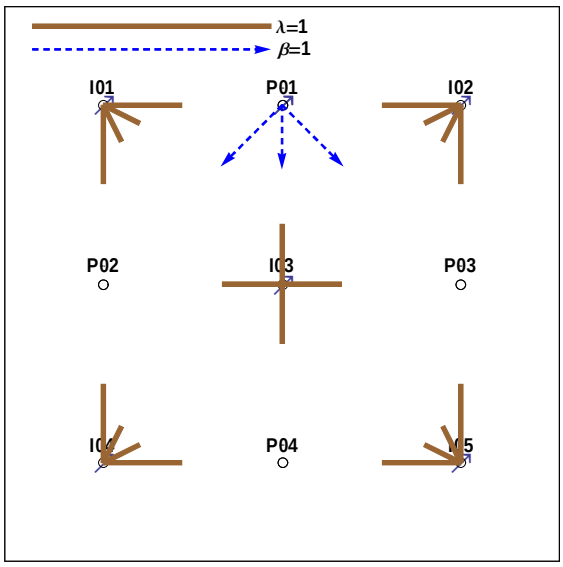

Fig. 5.4—The connectivity map including both λs and βs gives more detail of the reservoir connectivity.

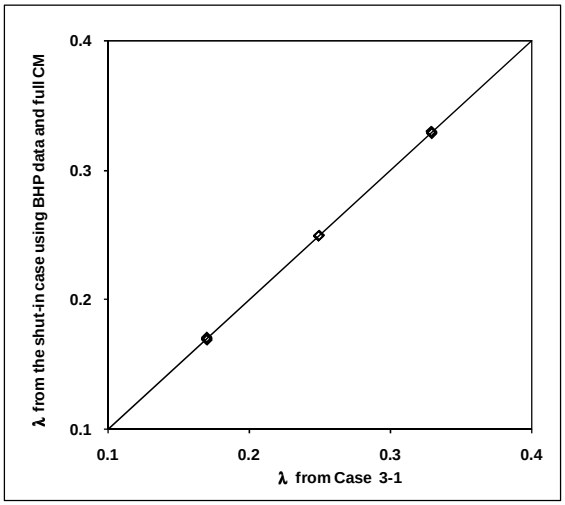

Fig. 5.5—If the BHP data of the shut-in producer is available we can estimate the λs accurately.

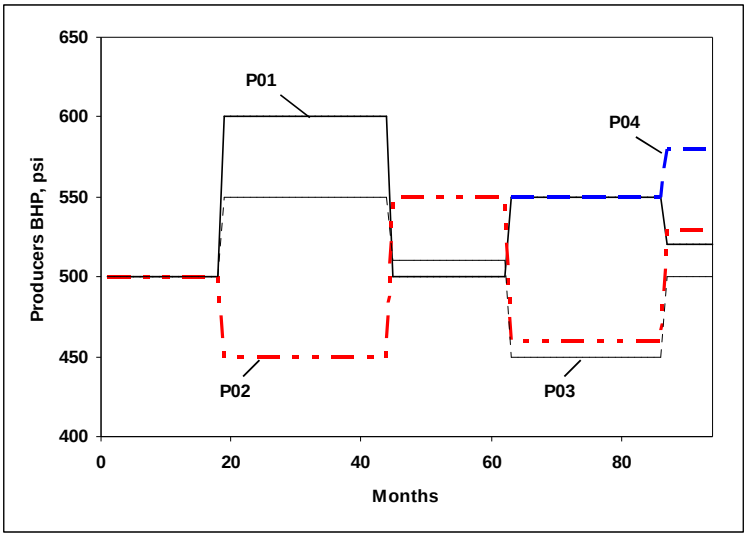

Fig. 5.6—BHP changes of producers in Case 5-2. Producer P04 started production in Month 63.

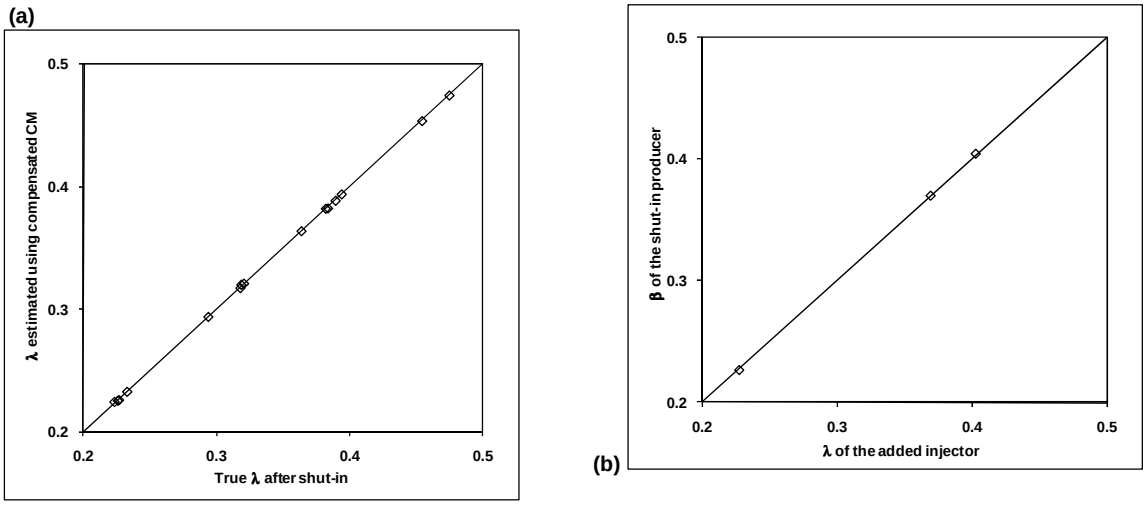

Fig. 5.7—The combination of the compensated CM and segmented CM predicts the interwell connectivity coefficients accurately for Case 5-2: (a) predicted λ using compensated CM vs. true ones, (b) β estimated using compensated CM vs. the λ of the added injector.

5.3 Field Case Example

The synthetic cases suggest that the segmented and compensated CMs perform well. Now, we apply these methods to a set of field data to demonstrate what can be achieved in practice. The application constitutes a validation of the method.

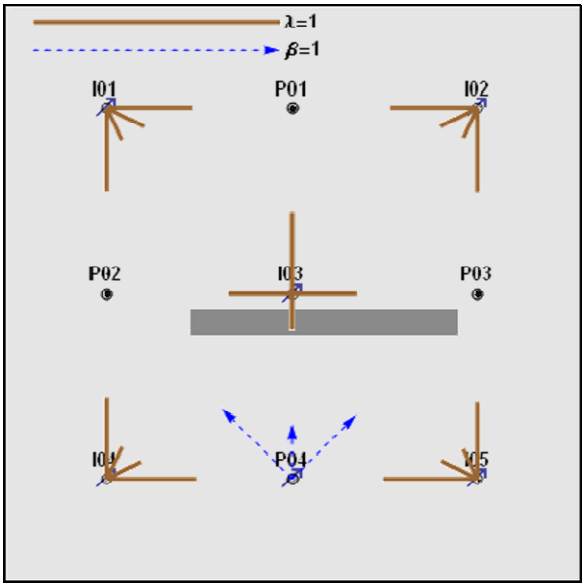

Fig. 5.8—Including βs in the connectivity map enhances the barrier.

The field, located in the Williston basin and discovered in the 1960s, was under primary depletion until the 1970s, and then waterflooding was implemented on a piecemeal basis. To date, over 20 wells have been drilled into the pool. This light-oil, carbonate reservoir has a median permeability of 5 md and median porosity of 15% based on routine core analysis. A 3D seismic survey shows no evidence of faults or other tectonic features that might affect connectivity. The wells are not artificially lifted. We evaluated the interwell connectivity for an 84-month period, during which time 13 wells were under production and water was injected from 7 wells. Well P08 was added to the reservoir in the 44th month.

After investigating all the available data for the wells, we ignored some data from each producer. The main reason for ignoring data was partially shut-in intervals in the producers within a month. If a well worked for less than 28 days a month, the liquid rate was checked, and if it was significantly different from its previous and later time steps, we ignored the data point for that producer. To reduce the number of parameters, we omitted wells with very low total liquid production rate (less than 3 bbl/day). We also eliminated one well with relatively low liquid production rate (10 bbl/day) and high fluctuating GOR. Finally, we used 7 injectors and 7 producers in the model.

Since the BHP data are not available and based on the production profiles some BHP changes (or producer stimulation) occurred in this period (**Fig. 5.9**), we need to use the segmented CM. On the other hand, since P08 is added at the 44th month, we have two choices to analyze the data: dividing the data into two intervals and applying the segmented CM at each one applying the segmented and compensated CM simultaneously. The main problem with dividing the data into parts is the small number of remaining data in each period. Thus we decided to use second choice. Ideally, the segmentation times of all the wells are

at the same time; if BHP changes for one well, we should consider this segmentation time for all the other wells. In practice, if we use the segmentation times of each well for all the other wells, we will have a very large number of segmentation times. This gives a situation where we can have as many or more unknowns as equations. Consequently, we used a separate set of segmentation times for each producer that we identified, using the algorithm described earlier, but this time with the objective function being the SSE of the production rate of each producer instead of a summation of rates for all the producers.

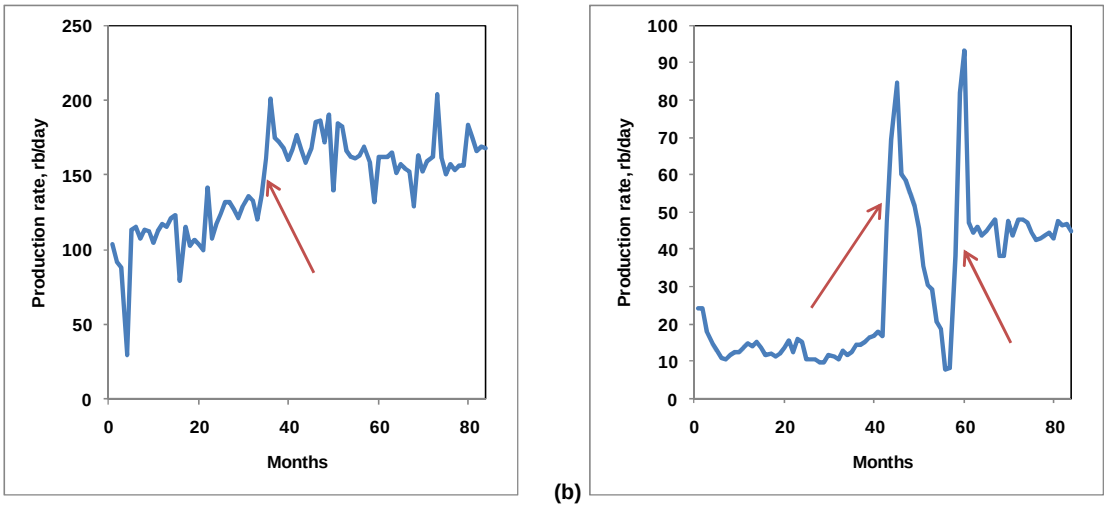

Fig. 5.9—Production profiles suggest that some BHP change/well stimulation occurred for most of the wells. Fig. 5.9a suggests a possible workover at time 37 for P03. Fig. 5.9b shows at least two major changes in the production rate trend of Well P06.

After determining the segmentation times, we ran the segmented and compensated CMs. Mapping the results, we observed some questionable λs, where some distant wells [e.g. (I08, P05) and (I08, P09)[show high connectivity (**Fig. 5.10**). The main reason for this problem is high correlation of the injection rates in some periods (**Fig. 5.11**). The other reason for these questionable λs is low injection rates of these wells that make the model less sensitive to λ changes and may lead to unrepresentative connectivity coefficients. To overcome this problem we assumed no connectivity between I08 and P03, P05, P06, P08, and P09 where the injector is very far from the other wells and its rate is highly correlated with the other injectors' rate. After several runs (with different initializations) we selected the most plausible one based on the root mean square of the estimate production rates, where the R^2 of the prediction is 0.95. The results are in acceptable agreement with the seismic impedance map (**Fig. 5.12a**).

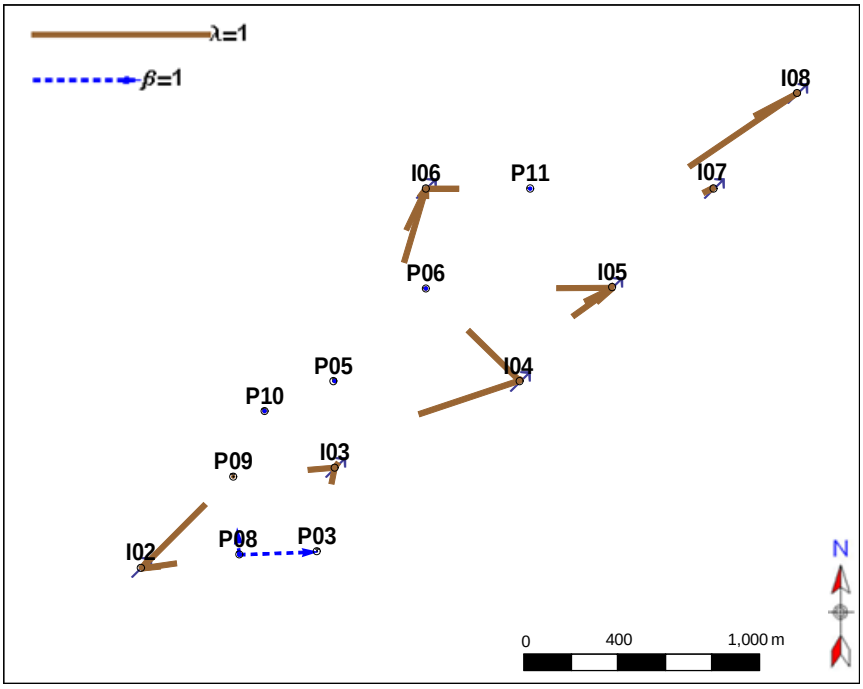

Fig. 5.10—High λs between some distant wells [e.g. (I08,P09) and (I08, P08)] seem suspicious.

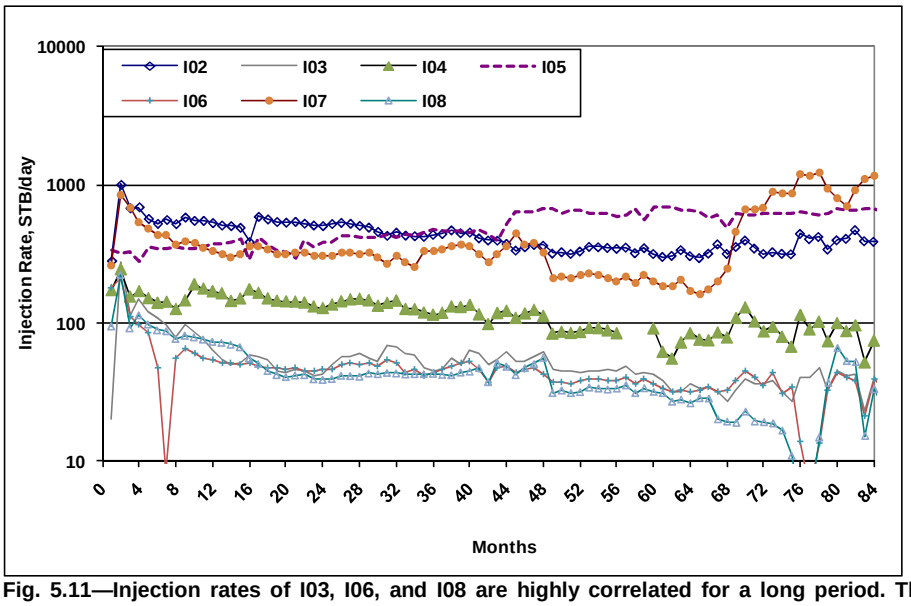

Fig. 5.11—Injection rates of I03, I06, and I08 are highly correlated for a long period. This may lead to wrong evaluation of λs for these wells.

To confirm our findings we used the seismic-impedance map of the field. Based on other studies (e.g. Abbaszadeh et al., 2004), seismic impedance may correlate with permeability. For this field we observed the same behavior (**Fig. 5.13**). This correlation may be caused by changes in porosity, lithology, or other

factors. However, in this study we did not investigate which mechanisms may be present nor their impact for field permeability. Nonetheless, we use this relationship to compare the impedance map with the calculated connectivities.

By overlaying the CM results, on the seismic impedance map (**Fig. 5.12a**) we observed:

1. The wells with the best communication are in the southwest, where the permeability is large (acoustic impedance small).

2. Communication is poorer (e.g. between I07 and P11) in the northeast and the permeability is smaller (acoustic impedance large)

3. Northeast-southwest communications are very poor (I04 and I06 to P11 and I07 to all the southwest wells), in agreement with the high impedance region laying between the northeast and southwest regions.

4. The good connectivities of most of the southwest wells agrees with the impedance continuity displayed on the seismic map. In particular, the good impedance continuity between wells P08 and P09 agrees with the large value $\beta = 0.43$ obtained from the compensated CM analysis.

We also applied the simple CM to these data (**Fig. 5.12b**) and obtained good, but somewhat poorer results, with $R^2 = 0.81$ and larger error in predicted production rate, particularly for the wells with small production. Comparison of Figs. 5.12a and 5.12b shows a weaker correspondence with the impedance for the simple CM and several questionable λs obtained using the model: several injectors are mainly connected to only one producer, e.g. I06 to P05 and I05 and I04 to P03.

Better results interpretation requires some criteria to determine the reliability of connectivity coefficients. The current practice, as we did in this field case, is to confirm the results with geological information. A well-established criterion can help build greater confidence in the CM results. A comprehensive sensitivity analysis of the CM parameters (as suggested in Section 3.4) can help us to develop such a criterion.

Using the synthetic cases and the field case, we showed that if some production wells are shut in, the simple CM may not be capable of evaluating the connectivity of the before- and after- shut-in data together. If we have the BHP of the producer when it is shut in (such as Fig. 5.5), the full CM evaluates the connectivity correctly. Such data, however, may not be available, and using the simple CM does not provide accurate results. In the large field cases, because of the large number of parameters, shutting in or stimulating individual wells may have only a small effect on the total performance (such as total production rate) and we may use the full (or simple) CM to evaluate the field performance (e.g. Sayarpour et al. 2008). In these cases, we may also exclude the shut-in period from the data and reinitialize the model after reopening the well (e.g. Weber et al. 2009). However, in general, to evaluate the connectivity of the wells and performance of individual wells in case of producer(s) shut in, the compensated CM is the best choice that can also give us producer/producer connectivities for some wells. In fact for the data with shut-in period, compensated CM provides more accurate results than the simple CM if we run the simple CM

for whole period, and it requires fewer parameters than the simple CM when we run the simple CM for before- and after-shut-in separately.

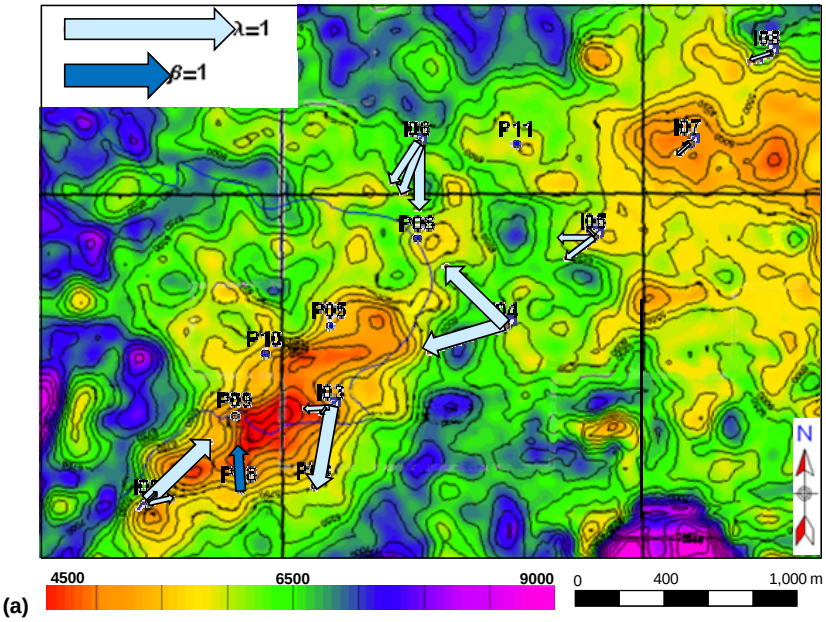

(a)

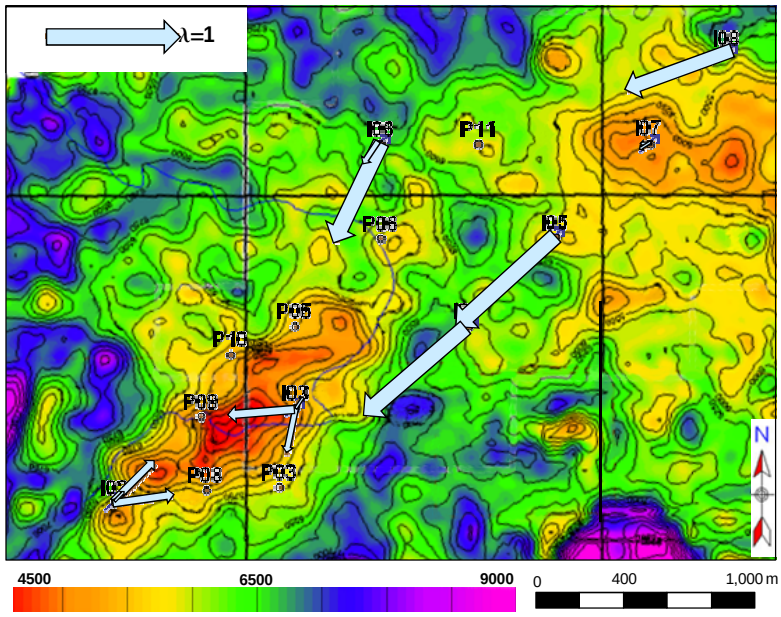

(b)

Fig. 5.12—Overlay of the seismic impedance with CM vector maps using a) segmented and compensated CM and b) simple CM. The smaller impedance values correlate with high permeability. Since there was only one new well (P08) we obtained the βs only between this well and the other producers. The connectivity between P08 and P09 can only be obtained using compensated CM (a); the simple CM (without BHP data) does not give us important information about the producers' connectivity in this region of the field (b).

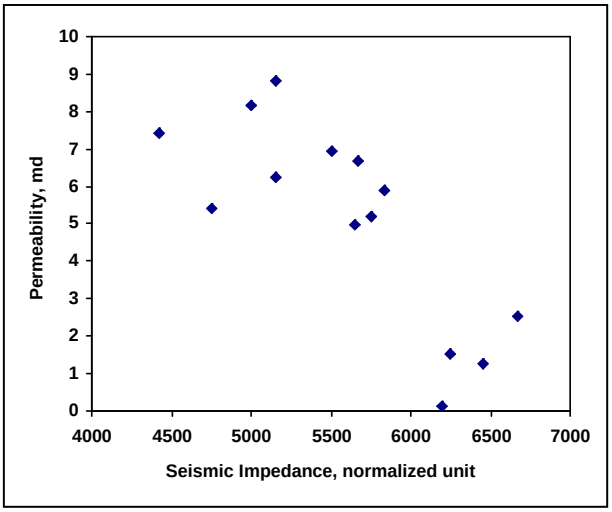

Fig. 5.13—Correlation between seismic impedance (normalized units), measured at cored wells, and permeability, obtained by averaging core measurements. Correlation coefficient is -0.79.

5.4 Conclusions

If the number of producers changes, (shutting in or adding a producer), the CM parameters will change, and we need to re-model the data. By defining the relationship between the λs before and after this change, the compensated CM allows us to model the data with a much smaller number of parameters. The producer/producer connectivity term defined in this approach also helps us to get a clearer representation of the interwell region characteristics. In testing hypothetical cases, this method successfully estimated the connectivity for before and after shut-in intervals using a single model. By combining the segmented and the compensated CM, we estimated the model parameters of a hypothetical case and the results were in excellent agreement with the true connectivity coefficients. We also applied the segmented and compensated CM on a field case where the results had 14% higher R^2 than the simple CM and the connectivity map was in better correspondence with the seismic impedance.

6. APPLICATION OF MULTIWELL PRODUCTIVITY INDEX IN PREDICTION OF WATERFLOOD PERFORMANCE

6.1 Introduction

In a single-well system, under pseudosteady-state conditions, the single phase reservoir performance can be calculated easily using the productivity index. This productivity index will stay constant as long as pseudosteady-state continues. It can be calculated analytically for homogeneous cases. In cases of several wells, by considering only the single well productivity indices we cannot predict the reservoir performance unless we know the individual drainage areas a priori. Valkó et al. (2000) developed and discussed the MPI concept as a generalization of pseudosteady-state productivity index of a single well [It was also developed independently by Umnuayponwiwat and Ozkan (2000)]. This concept is based on the superposition in space of the effect of single wells. It relates the vector of production rates and pressure drawdowns at well locations. In a homogeneous rectangular system, we can easily calculate the MPI matrix analytically and apply it to predict the production rates as well as pressure at any point of the reservoir. The effect of well skin factor can be also considered in this matrix. Here, we will derive the required formula to predict the liquid rate and pressure in a waterflood using MPI. We also discuss the application of this method for approximate description of transient behavior.

6.2 Influence Matrix

In the classical reservoir engineering for a single-well system, under the pseudosteady-state regime, we can estimate the liquid (single phase) production rate of the well using

$$q=J\Delta p, \quad \text{.....} \quad (6.1)$$

where q is the production rate, J is the productivity index, and Δp is the pressure drawdown at a well location where drawdown is defined as difference from volumetric average. In a rectangular homogeneous reservoir, we can calculate the productivity index using the influence factor and rock and fluid properties. In a similar way, based on the definition of multiwell productivity index (Valkó et al. 2000), we can predict the production rate from several wells using

$$\vec{q} = [\mathbf{J}]\Delta\vec{p}\,, \quad \text{.....} \quad (6.2)$$

where $\vec{q}$ is the vector of total liquid (water and oil) production rates, [**J**] is the multiwell productivity index matrix, and $\Delta\vec{p}$ is the vector of pressure drawdown at the wellbore locations. The multiwell productivity index matrix is simply obtained from inverse of the influence matrix and the rock and fluid properties

$$[\mathbf{J}] = \kappa\times[\mathbf{A}]^{-1}, \quad \text{.....} \quad (6.3)$$

where [**A**] is the influence matrix and κ is the rock/fluid factor (See Appendix B). Replacing Eq. 6.3 into Eq. 6.2 and rearranging we obtain

$$\Delta\vec{p} = \frac{1}{\kappa}[\mathbf{A}]\vec{q}\,. \quad \text{..... (6.4)}$$

In the influence matrix, the influence factor between each well pair shows us how changing the rate in one well affects the other ones. This effect is independent of the existence and location of the other wells. In fact, this is the main advantage of using [**A**] instead of [**J**] in our formulation because adding/shutting in a well will add or eliminate only a column and row in this matrix, or stimulating any of the wells will change just a diagonal element of [**A**]; however, any of these changes will affect all the elements of [**J**].

In cases of damaged or stimulated wells, we just need to add the diagonal matrix of the skin factors to the influence matrix. In this case Eq. 6.4 becomes

$$\Delta\vec{p} = \frac{1}{\kappa}\left([\mathbf{A}]+[\mathbf{D}_s]\right)\vec{q}\,, \quad \text{..... (6.5)}$$

where [$\mathbf{D}_s$] is the diagonal matrix of the skin factors. (See Appendix B)

In a homogeneous reservoir with constant production rates and zero skin factor, the pressure drawdown at the well locations or at any point of the reservoir (considering as wells with zero production) depends on the location of the wells, rock/fluid factor, and reservoir extents. In other words, the influence matrix has all this information. By mapping the influence factor of each well, we can see how that well affects the pressure geometric drawdown at any point of the reservoir (the rock/fluid factor is constant for all the points in the reservoir). **Fig. 6.1** shows an example of the influence function map for a single well system. The contours show the value of the influence function at the other points of the reservoir with respect to a specific producer. The influence function may have a negative or positive value. The points that have negative influence functions have higher pressure than the average reservoir pressure, and the ones with positive influence functions have lower pressure than the average reservoir pressure. As we move farther from the well location, the value of the influence function decreases. Thus we have the minimum value of the influence function at the distant boundaries of the system and the maximum value of that at the radius of the well. This maximum value indicates the inverse of the single-well dimensionless productivity index. Raghavan (1993) shows how to calculate the Dietz shape factor for rectangular cases from the influence function. The diagonal elements of the influence matrix consist of the single-well inverse productivity indices, and their values are independent of the existence and location of the other wells.

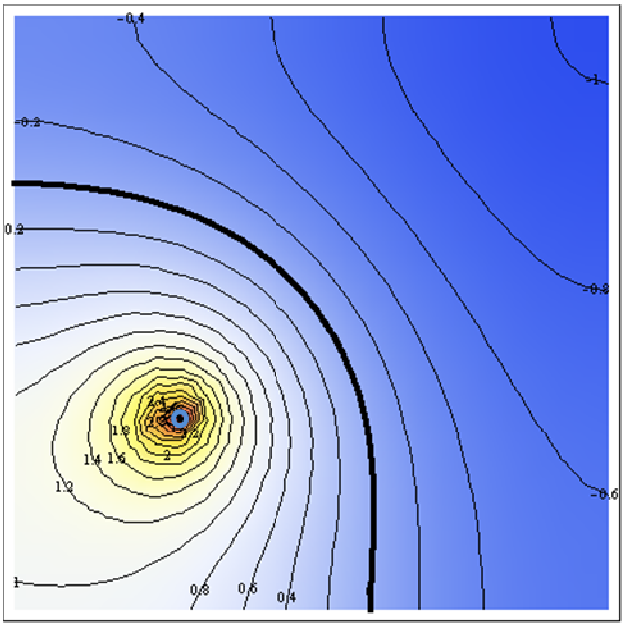

Fig. 6.1— An example of the influence function map. The influence function reaches a maximum in the area around the well location, and its minimum value is at the farthest corner. At the locations with positive influence factor, the pressure will be higher than the average reservoir pressure, and at the points with negative influence factor, the pressure will be higher than the average reservoir pressure.

We know that the influence function is constant only if we are in the pseudosteady region. In fact, if the flow is still under transient effects, the influence function will change with time. Thus, we need to know when this assumption is correct. For a single-well system, the dimensionless time based on the drainage area is (Raghavan, 1993)

$$t_{AD} = \frac{kt}{\phi \mu c_t A}. \quad \text{.....(6.6)}$$

Depending on location of the well and reservoir geometry (shape factor in classical reservoir engineering), we can use the pseudosteady-state regime when t_{AD} is larger than a specific value. For a well located at the center of the square reservoir, this value is 0.1. Considering the reservoir dimensions and properties, we can estimate the required time to remain in the pseudosteady-state regime. For a multiwell system depending on the number and location of the wells, this value will be different. In fact, ideally if the drainage areas of all the wells are equal, the dimensionless time of the system to reach the pseudosteady-state will be divided by the number of the wells. In general, this dimensionless time will not be more than the calculated one for any of the wells.

Practically, for a multiwell system in field applications of waterflooding using monthly data, the pseudosteady-state assumption is reasonable. We will discuss that in Section 6.4.

6.3 Waterflooding Performance Prediction Using MPI

By including the pressure and rates of both injectors and producers, we can apply the MPI concept for a system of injectors and producers. Since oil and water may have different formation volume factors (*B*), reservoir volumes are preferable to standard conditions. In this case, we need to neglect the formation volume factor in the rock/fluid factor, κ (See Eq. B.2). Then we can include the injection rates in the $\vec{q}_t$ with negative production rates

$$\vec{q}_t = \begin{bmatrix} \vec{w} & \vec{q} \end{bmatrix}^T = \begin{bmatrix} w_1 & \cdots & w_I & q_1 & \cdots & q_K \end{bmatrix}^T, \quad \text{..... (6.7)}$$

where $\vec{w}$ is the vector of both injection and production rates, $\vec{q}_t$ is the vector of injection rates, *I* is the number of injectors, and *K* is the number of producers. *T* denotes the transpose matrix. In the same way, we define the $\Delta\vec{p}$ vector as the pressure drop at both injectors and producers

$$\begin{aligned} \Delta\vec{p} &= \begin{bmatrix} \Delta p_{i1} & \cdots & \Delta p_{iI} & \Delta p_{q1} & \cdots & \Delta p_{qK} \end{bmatrix}^T = \begin{bmatrix} \overline{p} - p_{i1} & \cdots & \overline{p} - p_{iI} & \overline{p} - p_{q1} & \cdots & \overline{p} - p_{qK} \end{bmatrix}^T \\ &= \begin{bmatrix} \overline{p} - \vec{p}_{i*} & \overline{p} - \vec{p}_{q*} \end{bmatrix}^T \end{aligned}, \quad \text{..... (6.8)}$$

where $\overline{p}$ is the average reservoir pressure, $\vec{p}_{i*}$ is the vector of injector BHPs, and $\vec{p}_{q*}$ is the vector of producer BHPs. The influence matrix in this case will be simply the one for all the injectors and producers

$$[\mathbf{A}] = \left[\begin{array}{ccc|ccc} & a_{i_1 i_1} & \cdots & a_{i_1 i_I} & a_{i_1 q_1} & \cdots & a_{i_1 q_K} \\ \mathbf{A_{inj}} = & \vdots & \ddots & \vdots & \mathbf{A_{con}} = \vdots & \ddots & \vdots \\ & a_{i_I i_1} & \cdots & a_{i_I i_I} & a_{i_I q_1} & \cdots & a_{i_I q_K} \\ \hline & a_{i_1 q_1} & \cdots & a_{i_I q_1} & a_{q_1 q_1} & \cdots & a_{q_1 q_K} \\ \mathbf{A_{con}^T} = & \vdots & \ddots & \vdots & \mathbf{A_{prod}} = \vdots & \ddots & \vdots \\ & a_{i_1 q_K} & \cdots & a_{i_I q_K} & a_{q_1 q_K} & \cdots & a_{q_K q_K} \end{array}\right], \quad \text{..... (6.9)}$$

where [$\mathbf{A_{inj}}$] is the influence matrix of the injectors, [$\mathbf{A_{con}}$] is the influence matrix between the injector and producer well pairs, and [$\mathbf{A_{prod}}$] is the influence matrix of the producers. By rewriting Eq. 6.4 in terms of Eqs. 6.7, 6.8, and 6.9, we obtain

$$\begin{bmatrix} \overline{p} - \vec{p}_{i*} \\ \overline{p} - \vec{p}_{q*} \end{bmatrix} = \frac{1}{\kappa} \begin{bmatrix} \mathbf{A_{inj}} & \mathbf{A_{con}} \\ \mathbf{A_{con}^T} & \mathbf{A_{prod}} \end{bmatrix} \begin{bmatrix} \vec{w} \\ \vec{q} \end{bmatrix}. \quad \text{..... (6.10)}$$

To predict the performance of the waterflood, we generally need to have the producer BHPs and either injection rates or injector BHPs. Then we have *I*+*K* equations and *I*+*K*+*1* unknowns: producer production rates, injector BHPs or injection rates, and average reservoir pressure. Therefore, we need an additional equation to determine the unknowns. Here, we implement the simple material balance equation in a closed waterflooding system

$$c_t V_p \frac{d\bar{p}}{dt} = -\sum \vec{w} - \sum \vec{q}\,, \quad (6.11)$$

where c_t is the total compressibility and V_p is the reservoir pore volume. Now we can solve Eq. 6.10 along with Eq. 6.11 for the unknowns, using any numerical solvers. Determining the unknowns in this way, however, is very time-consuming. In evaluating the connectivity, as we see in Section 7.4 we may need to repeat these calculations thousands of times; thus, using numerical solvers becomes impractical. To overcome this problem we solved these equations analytically with block matrix techniques. In case of having injection rates and producer BHPs, combining Eqs. 6.10 and 6.11 and solving for $\bar{p}$ leads to (see Appendix C)

$$\bar{p} = \frac{c_2}{c_1} + \left(\bar{p}_i - \frac{c_2}{c_1} \right) \exp\left(\frac{-c_1}{c_t V_p} t \right), \quad (6.12)$$

where t is the time passed after changing injection rate or producer BHPs from the previous state (here we define a new state after the change of the control parameters including injection rate, producer BHPs and well skin factor), $\bar{p}_i$ is the average reservoir pressure in the previous state, and

$$c_1 = \kappa \sum \sum \left[\mathbf{A}_{\mathbf{prod}} \right]^{-1} \quad (6.13)$$

and

$$c_2 = -\sum \vec{w} + \sum \left[\mathbf{A}_{\mathbf{prod}} \right]^{-1} \left[\mathbf{A}_{\mathbf{con}} \right]^T \vec{w} + \kappa \sum \left[\mathbf{A}_{\mathbf{prod}} \right]^{-1} \vec{p}_{q^*}\,. \quad (6.14)$$

Solving Eq. 6.10 for $\vec{q}$ we get

$$\vec{q} = \kappa \left[\mathbf{A}_{\mathbf{prod}} \right]^{-1} \left[\bar{p} - \vec{p}_{q^*} \right] - \left[\mathbf{A}_{\mathbf{prod}} \right]^{-1} \left[\mathbf{A}_{\mathbf{con}} \right]^T \vec{w}\,. \quad (6.15)$$

Also the injector BHPs ($\vec{p}_{i^*}$) will be

$$\vec{p}_i = \bar{p}.[\mathbf{1}]_{Ix1} - \frac{1}{\kappa} \left[\mathbf{A}_{\mathbf{inj}} \quad \mathbf{A}_{\mathbf{con}} \right] \begin{bmatrix} \vec{w} \\ \vec{q} \end{bmatrix}, \quad (6.16)$$

where $[\mathbf{1}]_{Ix1}$ is a Ix1 matrix with elements of 1. Using these formulas, we can calculate the reservoir performance several orders of magnitude faster than using a general, nonlinear solver.

If instead of injection rates, we have injector BHPs, we will have (see appendix C)

$$\bar{p} = \frac{\sum [\mathbf{A}]^{-1} \left[\vec{p}_{i^*} \quad \vec{p}_{q^*} \right]^T}{\sum \sum [\mathbf{A}]^{-1}} + \left(\bar{p}_i - \frac{\sum [\mathbf{A}]^{-1} \left[\vec{p}_{i^*} \quad \vec{p}_{q^*} \right]^T}{\sum \sum [\mathbf{A}]^{-1}} \right) \exp\left(\frac{\kappa \sum \sum [\mathbf{A}]^{-1}}{c_t V_p} t \right) \quad (6.17)$$

and

$$\begin{bmatrix} \vec{w} \\ \vec{q} \end{bmatrix} = \kappa \left[\mathbf{A}\right]^{-1} \begin{bmatrix} \bar{p} - \vec{p}_{i*} \\ \bar{p} - \vec{p}_{q*} \end{bmatrix} . \quad \text{..... (6.18)}$$

Since we mostly deal with the first set of data where injection rate and producer BHPs are available, we continue with this assumption.

To have a better understanding of the relationship between the influence matrix and the production rate, we replace Eq. 6.12 in Eq. 6.15 and rearrange to obtain (see Appendix C)

$$\vec{q} = \left\{ \left(\frac{1 - \exp\left(- \frac{\left[\mathbf{1}\right]_{1xK} \left[\mathbf{A}_{\mathbf{prod}}\right]^{-1} \left[\mathbf{1}\right]_{Kx1} \kappa t}{c_t V_p} \right)}{\left[\mathbf{1}\right]_{1xK} \left[\mathbf{A}_{\mathbf{prod}}\right]^{-1} \left[\mathbf{1}\right]_{Kx1}} \right) \left[\mathbf{A}_{\mathbf{prod}}\right]^{-1} \left(\left[\mathbf{1}\right]_{KxK} \left[\mathbf{A}_{\mathbf{prod}}\right]^{-1} \left[\mathbf{A}_{\mathbf{con}}\right]^{T} - \left[\mathbf{1}\right]_{KxI} \right) - \left[\mathbf{A}_{\mathbf{prod}}\right]^{-1} \left[\mathbf{A}_{\mathbf{con}}\right]^{T} \right\} \vec{w} +$$

$$\kappa \left[\mathbf{A}_{\mathbf{prod}}\right]^{-1} \left\{ \left[\frac{\left[\mathbf{1}\right]_{1xK} \left[\mathbf{A}_{\mathbf{prod}}\right]^{-1} \vec{p}_{q*}}{\left[\mathbf{1}\right]_{1xK} \left[\mathbf{A}_{\mathbf{prod}}\right]^{-1} \left[\mathbf{1}\right]_{Kx1}} + \left(\bar{p}_i - \frac{\left[\mathbf{1}\right]_{1xK} \left[\mathbf{A}_{\mathbf{prod}}\right]^{-1} \vec{p}_{q*}}{\left[\mathbf{1}\right]_{1xK} \left[\mathbf{A}_{\mathbf{prod}}\right]^{-1} \left[\mathbf{1}\right]_{Kx1}} \right) \exp\left(- \frac{\left[\mathbf{1}\right]_{1xK} \left[\mathbf{A}_{\mathbf{prod}}\right]^{-1} \left[\mathbf{1}\right]_{Kx1} \kappa t}{c_t V_p} \right) \right] \left[\mathbf{1}\right]_{Kx1} - \vec{p}_{q*} \right\}$$

. ..... (6.19)

In this equation, the first term summarizes the effect of injection rate and the second term accounts for the effect of producer BHPs and average reservoir pressure at the previous state. $\frac{\left[\mathbf{1}\right]_{1xK} \left[\mathbf{A}_{\mathbf{prod}}\right]^{-1} \vec{p}_{q*}}{\left[\mathbf{1}\right]_{1xK} \left[\mathbf{A}_{\mathbf{prod}}\right]^{-1} \left[\mathbf{1}\right]_{Kx1}}$ is simply a weighted average of producer BHPs based on the sum of the correspondence row of the $[\mathbf{A}_{\mathbf{prod}}]^{-1}$ matrix for each producer. The $\exp\left(- \frac{\left[\mathbf{1}\right]_{1xK} \left[\mathbf{A}_{\mathbf{prod}}\right]^{-1} \left[\mathbf{1}\right]_{Kx1} \kappa t}{c_t V_p} \right)$ term is the coefficient of $\bar{p}_i$ that transfers the previous state of the system to the current state, and we call it the *delay term*. Basically, with small c_t, small V_p, large k, large h, small μ, and long time after establishing the pseudosteady-state regime (t), the delay term decays to zero. The other term in the delay term is $[1]_{1xK}[\mathbf{A}_{\mathbf{prod}}]^{-1}[1]_{Kx1}$, which is related to the number and location of the wells. We will discuss the delay term more in Section 6.4.

In deriving the MPI predictor, we used several assumptions. The most important assumptions are:

- Pseudosteady-state regime: Since the MPI predictor is based on the pseudosteady-state regime, it does not consider the effect of the transient flow regime. In fact, in the MPI-based method we assume in each period, we record the data at a late enough time after introducing any abrupt change. We will discuss this issue more in Section 6.4.
- Constant total compressibility: If oil and water have different compressibilities, the total compressibility will change as saturations vary. In this case, if both water and oil flow in the system, the total compressibility will change with time, and we do not consider this change in the

MPI predictor. If we have an estimation of oil production, we can estimate oil and water saturation in the reservoir, and this error will be decreased.

- Unit mobility ratio: In the MPI predictor we assume that water and oil have the same mobility. If the mobility ratio is significantly different from one, we will have large prediction error.
- Negligible gas production: Eq. 6.4 is based on liquid production. If we have high gas production, this equation is not valid anymore.

Here we show the application of the MPI in prediction of the reservoir performance in some synthetic homogeneous cases, and we compare its results with the results of a commercial numerical reservoir simulator (Eclipse 100).

Case 6-1. This case is a system of two injectors and two producers (2x2). The location of the wells is shown in **Fig. 6.2,** and the reservoir properties and dimensions are similar to what we had in Case 3-1. Based on the reservoir dimensions and location of the wells, the influence matrix is:

$$[\mathbf{A}] = \begin{bmatrix} 7.7832 & -0.7278 & -0.4375 & -0.0414 \\ -0.7278 & 8.9155 & 0.1224 & 0.0900 \\ -0.4375 & 0.1224 & 8.2208 & -0.4519 \\ -0.0414 & 0.0900 & -0.4519 & 7.8256 \end{bmatrix}$$

Setting the injection rates as in **Fig. 6.3** and producer BHPs as in **Fig. 6.4** we calculated the average reservoir pressure, liquid production rate, and injector BHPs using Eqs. 6.12 to 6.16. For this case, we observed good agreement between the results using MPI and the reservoir simulator (**Fig. 6.5** and **Table 6.1**). The main reason for the small difference between the results is inconsistency of the total compressibility with time because of varying oil saturation. To eliminate this effect, we considered another case, where only residual oil exists and water is the only flowing phase in the system. For this case, we observed that the results of the MPI predictor get closer to the simulator **(**Table 6.1).

Case 6-2. This case is a 5x4 system similar to Case 4-1. Similar to Case 6-2, the MPI predictor is in an excellent agreement with the numerical simulator **(**Table 6.1). In case only water exists, we have much higher accuracy than the case where both oil and water flow. The main reason for this higher accuracy is the constant total compressibility. The second reason is the higher permeability than in the previous case because in this case the permeability is the absolute one. We also ran this case for a lower permeability (k=8 md) when both oil and water exist. In this case, although the accuracy of the method is lower, the results are still acceptable. We will further discuss the effect of permeability on the performance of the MPI predictor in the next section.

Table 6.1—Accuracy of the prediction of production rates and injector BHPs using the MPI-based method. Having one flowing phase and high permeability increases the accuracy of the method. Also, the performance of the method for the cases with non-unit mobility ratios is poor.

					Production rate		Injectors' BHP	
Well Pattern	k, md	Mobility Ratio	Phase	Flowing phase	Abs error, %	R^2	Abs error, %	R^2
2x2	40	1	Oil and water	Oil and water	0.3663	0.9981	0.1601	0.9997
2x2	40	1	Oil and water	Water	0.3061	0.9990	0.1437	0.9998
5x4	40	1	Oil and water	Oil and water	0.1694	0.9999	0.0970	1.0000
5x4	8	1	Oil and water	Oil and water	0.9446	0.9968	0.5558	0.9993
5x4	40	1	Water	Water	0.0062	1.0000	0.0129	1.0000
5x4	40	3	Oil and water	Oil and water	1.8637	0.9763	17.3222	0.4523
5x4	40	1/3	Oil and water	Oil and water	2.2702	0.9748	54.31	-2.426
5x4-with skin factor	40	1	Oil and water	Oil and water	0.1922	0.9999	0.1034	1.0000
8x8	40	1	Oil and water	Oil and water	0.4831	0.9998	0.1308	0.9999

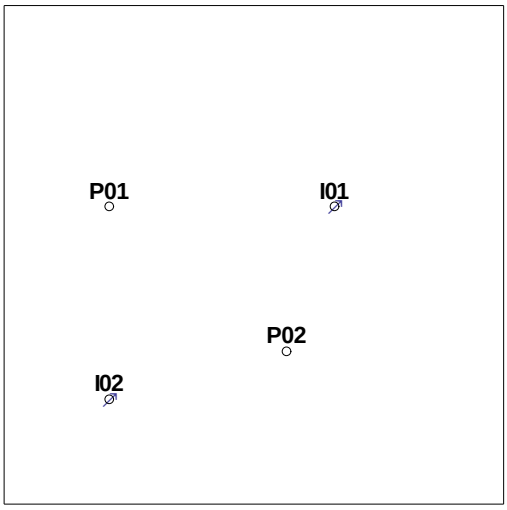

Fig. 6.2—Location of the wells in Case 6-1.

Case 6-3. This case is similar to the previous one; the only difference is that we set the skin factor of Well P01 to -2. After we modified the influence matrix with Eq. 6.5, the MPI predictor calculated the reservoir performance accurately (Table 6.1).

Case 6-4. This case is very similar to Case 6-2; the only difference is that in this case the mobility ratio is 3. Applying the MPI predictor we observed higher error in calculation of injector BHPs and a slightly increased error in predicting production rates (Table 6.1). The reason for smaller increased error for production rates than for injector BHPs is the fact the mass balance moves the summation of the production rates (considering the delay term) very close to the summation of the injection rates. This forces the estimated production rates to be within a range. However, this property does not affect the

injector BHPs and it leads to a larger error for estimation. We observed the same error for a mobility ratio of 1/3 (Table 6.1).

Case 6-5. This case is a larger reservoir with 8 injectors and 8 producers (**Fig. 6.6**). Some of the wells were converted from producer to injector and some of them were shut in at different times (**Fig. 6.7**). As expected, the MPI results are in good agreement with the simulator results (Table 6.1).

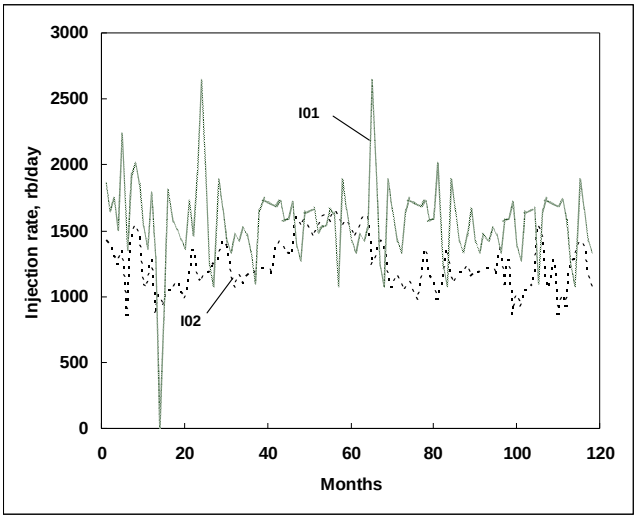

Fig. 6.3—Injection rates of injectors for Case 6-1.

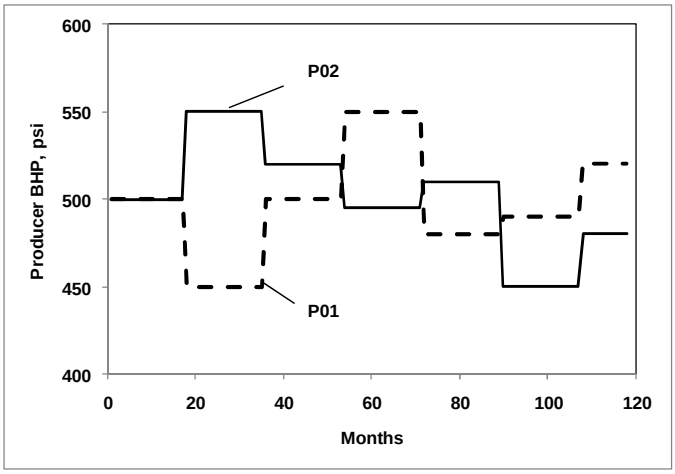

Fig. 6.4—Producer BHPs for Case 6-1.

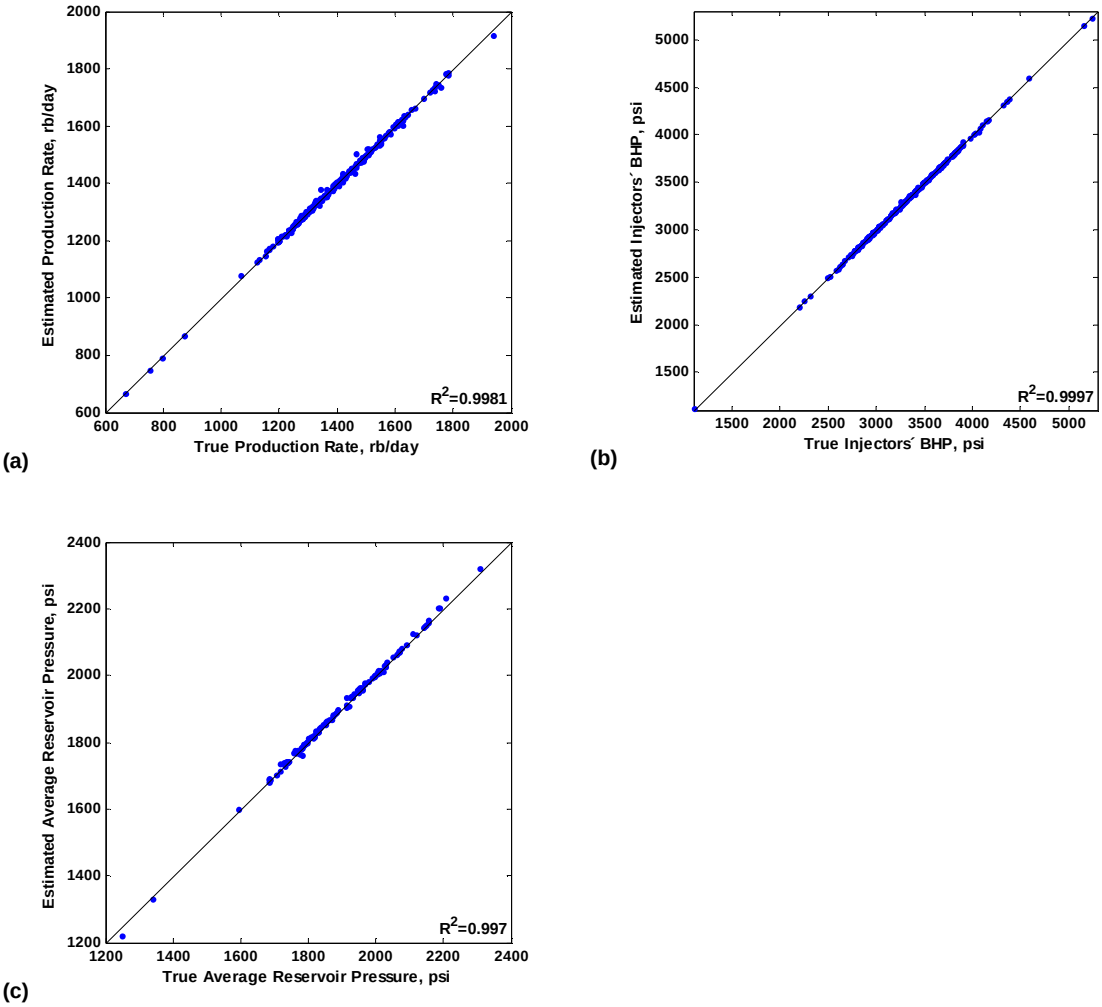

Fig. 6.5—Comparison of true and predicted reservoir performance using MPI for a 2x2 reservoir (water injection and oil production): (a) production rates, (b) injector BHPs and (c) average reservoir pressure.

6.4 MPI for Longer Delay Terms

As discussed earlier, to use the MPI method properly we need to make sure that the transient effects are negligible. The delay term we have in Eq. 6.16 is very similar to the dimensionless time based on the drainage area, as we show in Eq. 6.20

$$t_{AD} = \frac{kt}{\phi\mu c_t A} = \frac{\frac{kh}{\mu}t}{\phi\mu c_t Ah} = \frac{1}{2\pi}\cdot\frac{\kappa t}{c_t V_p} \quad \text{..... (6.20)}$$

or

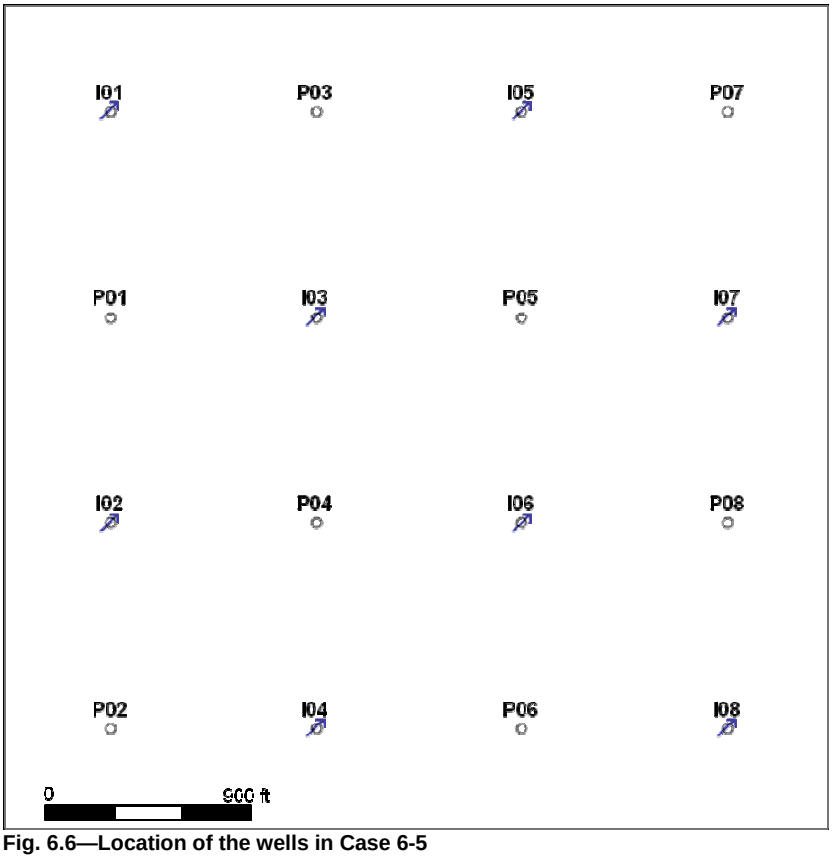

Fig. 6.6—Location of the wells in Case 6-5

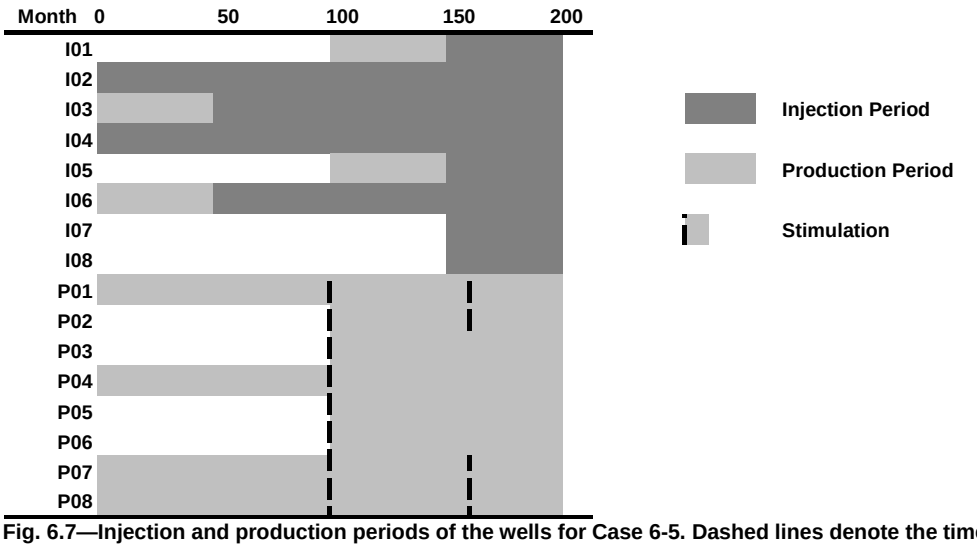

Fig. 6.7—Injection and production periods of the wells for Case 6-5. Dashed lines denote the time of stimulation.

$$\text{Delay term} = \exp\left(-\frac{[\mathbf{1}]_{1xK}\left[\mathbf{A}_{\mathbf{prod}}\right]^{-1}[\mathbf{1}]_{Kx1}}{2\pi}\cdot t_{AD}\right). \quad \text{..... (6.21)}$$

In fact, the main difference between the delay term and the dimensionless time is the $[\mathbf{1}]_{1xK}[\mathbf{A}_{\mathbf{prod}}]^{-1}[\mathbf{1}]_{Kx1}$ that accounts for the effect of multiple wells on the length of the transient region.

To see the effect of longer delay terms in the accuracy of the MPI predictor we looked at Cases 6-1 and 6-2 with different delay terms. To eliminate the effect of varying compressibility, we assumed that only water existed in the reservoir. In this case, the effective and absolute permeability are the same. To have different delay terms, we changed only the permeability. As expected, increasing the delay term, deceased accuracy of the MPI predictor for both cases (**Figs. 6.8 and 6.9**). Although the percentage error increases for almost all permeabilities, its trend is not the same at all permeabilities and its rate of change is different. As expected, we observed similar results by changing the viscosity. Since the total compressibility and pore volume have no effect on the productivity index, changing them has slightly different effects on the MPI results (**Fig. 6.10**). However, as expected, increasing them decreases the accuracy of the MPI predictor. These estimated errors are for a specific set of injection rates and well locations. However, we expect to have a similar behavior of percentage error for other injection rates and well locations.

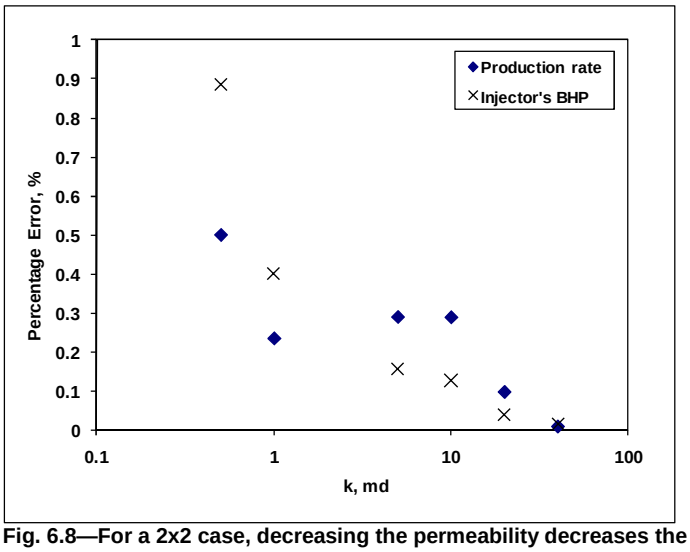

Fig. 6.8—For a 2x2 case, decreasing the permeability decreases the accuracy of the MPI predictor.

If we estimate the influence matrix for low permeability cases based on the data (we will discuss how to estimate this matrix in the Section 7.2), we may see that the optimized influence matrix is slightly

different from the original one obtained analytically. In other words, we may find a different influence matrix that gives us a lower prediction error than the "true" influence matrix. For Case 6-1 at k=5 md, we estimated the influence matrix as:

$$[\mathbf{A}_1] = \begin{bmatrix} 7.7423 & -0.6620 & -0.2317 & 0.1193 \\ -0.6620 & 9.0358 & 0.4093 & 0.3313 \\ -0.2317 & 0.4093 & 8.6668 & -0.0675 \\ 0.1193 & 0.3313 & -0.0675 & 8.1788 \end{bmatrix}$$

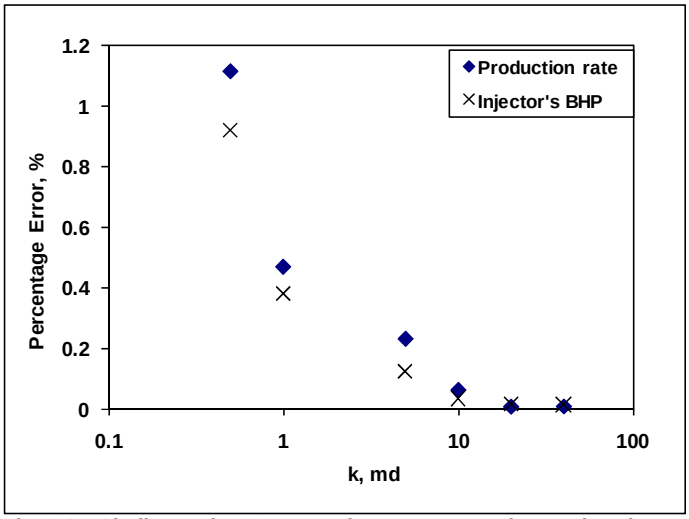

Fig. 6.9—Similar to the 2x2 case, for a 5x4 case, decreasing the permeability decreases the accuracy of the MPI predictor.

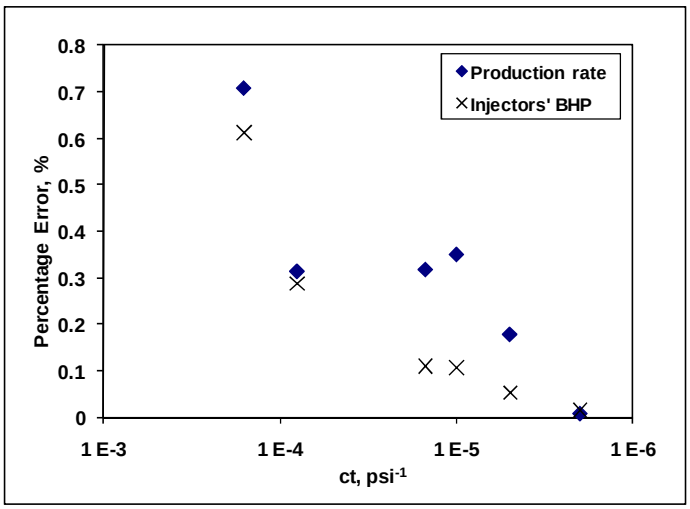

Fig. 6.10—For a 2x2 case, increasing the total compressibility decreases the accuracy of the MPI predictor. However, the trend of this decrease is slightly different from the case of permeability decreases.

We see that the influence function is slightly different from the true one (from analytical method). We also estimated the influence function in a similar way for a different set of injection rates, and we obtained the influence matrix as:

$$[\mathbf{A}_2] = \begin{bmatrix} 7.7959 & -0.5912 & -0.1790 & 0.1758 \\ -0.5912 & 9.1504 & 0.4923 & 0.4173 \\ -0.1790 & 0.4923 & 8.7204 & -0.001 \\ 0.1758 & 0.4173 & -0.001 & 8.2062 \end{bmatrix}$$

As we see, [$\mathbf{A_2}$] is slightly different from [$\mathbf{A_1}$]. In fact, these differences stem from the fact that when we ignored the transient effects, the estimated influence matrix somehow approximated this transient effect and, therefore, has less clear physical meaning. In fact, based on the injection and production rates, the estimated matrix might be different. In Section 7.2 we will show how we can interpret the influence matrices to get the true connectivity.

6.5 Conclusions

In a rectangular homogeneous multiwell reservoir, under the pseudosteady-state regime we can predict the liquid production rate and injector BHPs analytically using the MPI. We can also predict the pressure at any point of the reservoir quickly. The MPI is the multiplication of the rock/fluid factor by the inverse of the influence matrix, which includes the connectivity information of the wells from the reservoir extents and the well locations. Changing the number of producers and injectors and the skin factors of the wells has no effect on the performance of the method. However, if the mobility ratio is nonunique and the total compressibility of the system changes dramatically, the accuracy of the method decreases. In cases of long delay terms, the accuracy of the method using monthly data decreases.

7. CONNECTIVITY EVALUATION USING MPI

7.1 Introduction

In Section 6.3, we showed how we could determine the production rate and injector BHPs in a waterflood in a homogeneous reservoir using an influence matrix. In a heterogeneous reservoir, however, no general analytical formula is available to determine the influence matrix. One possible solution to obtain the influence matrix for heterogeneous cases is to estimate it from the injection and production history. In this approach, we estimate the influence matrix that minimizes the error in prediction of production rates, injector BHPs and other available pressure data (such as pressure at shut-in wells or average reservoir pressure). We define the heterogeneity matrix as the difference between this optimized influence matrix and the influence matrix for the homogeneous case with similar well layout. This matrix contains the heterogeneity related connectivity information of the reservoir. In fact, it decouples all the injection rate, producer BHPs, skin factor, well location, and reservoir dimensions components of the connectivity from the data, and this index solely shows the heterogeneity of the reservoir.

7.2 Heterogeneity Matrix

The analytical formula for the influence matrix is valid only for a homogenous reservoir. For a heterogeneous reservoir, we need to estimate this matrix from reservoir performance. In fact, the homogeneous influence matrix has all the information of well locations, reservoir dimensions, and general rock/fluid factor (such as average mobility). The deviation of the estimated influence matrix from the analytical one reveals the heterogeneity components of interwell connectivity. We call this deviation the *heterogeneity matrix* ([**Δ**]), and we have

$$[\mathbf{\Delta}]=[\mathbf{A}^{(\mathbf{H})}]-[\mathbf{A}], \quad \text{..... (7.1)}$$

where $[\mathbf{A}^{(\mathbf{H})}]$ is the estimated influence matrix for the heterogeneous case. Similar to the homogeneous influence matrix, this matrix is symmetric, and for simplicity we can decompose this matrix into four matrices as we have in Eq. 7.2

$$[\mathbf{\Delta}]=\left[\begin{array}{ccc|ccc} & \delta_{i_1 i_1} & \cdots & \delta_{i_1 i_I} & \delta_{i_1 q_1} & \cdots & \delta_{i_1 q_K} \\ \mathbf{\Delta_{inj}}= & \vdots & \ddots & \vdots & \mathbf{\Delta_{con}}= \vdots & \ddots & \vdots \\ & \delta_{i_1 i_I} & \cdots & \delta_{i_I i_I} & \delta_{i_I q_1} & \cdots & \delta_{i_I q_K} \\ \hline & \delta_{i_1 q_1} & \cdots & \delta_{i_I q_1} & \delta_{q_1 q_1} & \cdots & \delta_{q_1 q_K} \\ \mathbf{\Delta}_{\mathbf{con}}^{T}= & \vdots & \ddots & \vdots & \mathbf{\Delta_{prod}}= \vdots & \ddots & \vdots \\ & \delta_{i_1 q_K} & \cdots & \delta_{i_I q_K} & \delta_{q_1 q_K} & \cdots & \delta_{q_K q_K} \end{array}\right]. \quad \text{..... (7.2)}$$

In addition, to add (or shut in) a well, we just need to add (or eliminate) a row and column to the matrix, and the other elements stay constant. As we discussed in Section 6.2 for homogeneous reservoirs, the

diagonal elements of the influence matrix show the inverse of the single-well dimensionless productivity index of each individual well. For the heterogeneous case, similarly, the diagonal elements of the estimated influence matrix approximate the inverse of the single-well productivity index. In addition, similar to the homogeneous case we had in Eq. 6.5, we may add the skin factor matrix to this matrix. The off-diagonal elements of the heterogeneity matrix represent the heterogeneity in the interwell region, and we call each off-diagonal term the *connectivity index* between the corresponding wells defined by row and column. In homogeneous cases, the influence factor for closer wells is higher and that of further ones is smaller. In the heterogeneity matrix, however, this factor is mainly related to the permeability (and thickness): a positive connectivity index is a sign of a high-permeability zone, and a negative connectivity index is an evidence of a low-permeability zone in the interwell region. Recalling the classification of connectivity parameters in Section 2.1, this is a first-type connectivity parameter.

As we discussed above, the heterogeneity information of a system is contained in both diagonal and off-diagonal elements of the heterogeneity matrix. We can obtain a more robust indicator of the heterogeneous interwell connectivity (we will see why this is more robust later in this section) by including the heterogeneity information of the diagonal term in the connectivity indices. This can be done easily using Eq. 7.3

$$\delta'_{ij} = \begin{cases} \delta_{ij} - \dfrac{\delta_{ii} + \delta_{jj}}{2} & \text{if } i \neq j\,, \\ 0 & \text{if } i = j \end{cases} \qquad \text{..... (7.3)}$$

where δ'_{ij} is the i,j-th element of the *modified heterogeneity matrix* ([**Δ´**]) and δ_{ij} is the i,j-th element of the heterogeneity matrix. So the [**Δ´**] will be simply:

$$[\mathbf{\Delta'}] = \left[\begin{array}{ccc|ccc} & 0 & & & \delta'_{i_1 i_I} & \\ \mathbf{\Delta'_{inj}} = & \vdots & \ddots & \vdots & \mathbf{\Delta'_{con}} = & \vdots & \ddots & \vdots \\ & \delta'_{i_I i_1} & & 0 & & \delta'_{i_I q_1} & & \delta'_{i_I q_K} \\ \hline & \delta'_{i_1 q_1} & & \delta'_{i_1 q_K} & & 0 & & \delta'_{q_1 q_K} \\ \mathbf{\Delta'^{T}_{con}} = & \vdots & \ddots & \vdots & \mathbf{\Delta'_{prod}} = & \vdots & \ddots & \vdots \\ & \delta'_{i_1 q_K} & & \delta'_{i_I q_K} & & \delta'_{q_1 q_K} & & 0 \end{array}\right]$$

$$= \begin{bmatrix} 0 & \cdots & \delta_{i_1 i_I} - \dfrac{\delta_{i_1 i_1} + \delta_{i_I i_I}}{2} & \delta_{i_1 q_1} - \dfrac{\delta_{i_1 i_1} + \delta_{q_1 q_1}}{2} & \cdots & \delta_{i_1 q_K} - \dfrac{\delta_{i_1 i_1} + \delta_{q_K q_K}}{2} \\ \vdots & \ddots & \vdots & \vdots & \ddots & \vdots \\ \delta_{i_I i_1} - \dfrac{\delta_{i_1 i_1} + \delta_{i_I i_I}}{2} & \cdots & 0 & \delta_{i_I q_1} - \dfrac{\delta_{i_I i_I} + \delta_{q_1 q_1}}{2} & \cdots & \delta_{i_I q_K} - \dfrac{\delta_{i_I i_I} + \delta_{q_K q_K}}{2} \\ \delta_{i_1 q_1} - \dfrac{\delta_{i_1 i_1} + \delta_{q_1 q_1}}{2} & \cdots & \delta_{i_I q_1} - \dfrac{\delta_{i_I i_I} + \delta_{q_1 q_1}}{2} & 0 & \cdots & \delta_{q_1 q_K} - \dfrac{\delta_{q_1 q_1} + \delta_{q_K q_K}}{2} \\ \vdots & \ddots & \vdots & \vdots & \ddots & \vdots \\ \delta_{i_1 q_K} - \dfrac{\delta_{i_1 i_1} + \delta_{q_K q_K}}{2} & \cdots & \delta_{i_I q_K} - \dfrac{\delta_{i_I i_I} + \delta_{q_K q_K}}{2} & \delta_{q_1 q_K} - \dfrac{\delta_{q_1 q_1} + \delta_{q_K q_K}}{2} & \cdots & 0 \end{bmatrix}. \qquad \text{..... (7.4)}$$

Applying this modification, the heterogeneity component of the diagonal elements will be zero, and all the heterogeneity information will be transferred into the modified connectivity indices. This equation will be discussed more in Section 7.3. The important point here is that a negative diagonal element (equivalent to negative skin) in the heterogeneity matrix increases the modified connectivity index between the well pairs, and a positive one (equivalent to positive skin) decreases the modified connectivity index. Because of the effect of the diagonal elements, applying this modification may reveal a negative or positive modified connectivity index between two wells where no barrier or channel exists. Thus, besides the interwell heterogeneity, the heterogeneity around wells (made by geological features and different from the skin factor) affects the modified connectivity index, and we need to consider it in interpretation of the results.

In Section 6.4 we observed that for different permeabilities, a different optimum influence matrix is obtained. Based on the definition of the heterogeneity matrix, we expect that the difference between this matrix and the analytical influence matrix will show the heterogeneity. Recalling the estimated influence matrix for that example, the heterogeneity matrices are

$$[\boldsymbol{\Delta}_1]=\begin{bmatrix} -0.0410 & 0.0658 & 0.2059 & 0.1608 \\ 0.0658 & 0.1203 & 0.2869 & 0.2412 \\ 0.2059 & 0.2869 & 0.4459 & 0.3844 \\ 0.1608 & 0.2412 & 0.3844 & 0.3532 \end{bmatrix}$$

and

$$[\boldsymbol{\Delta}_2]=\begin{bmatrix} 0.0127 & 0.1367 & 0.2585 & 0.2172 \\ 0.1367 & 0.2349 & 0.3699 & 0.3273 \\ 0.2585 & 0.3699 & 0.4995 & 0.4512 \\ 0.2172 & 0.3273 & 0.4512 & 0.4143 \end{bmatrix}.$$

However, we know that both these cases are for a homogeneous case and no heterogeneity exists in the system. For these cases, the modified heterogeneity matrices are

$$[\boldsymbol{\Delta}_1']=\begin{bmatrix} 0 & 0.0262 & 0.0034 & 0.0047 \\ 0.0262 & 0 & 0.0038 & 0.0045 \\ 0.0034 & 0.0038 & 0 & -0.0151 \\ 0.0047 & 0.0045 & -0.0151 & 0 \end{bmatrix}$$

and

$$[\boldsymbol{\Delta}_2']=\begin{bmatrix} 0 & 0.0129 & 0.0024 & 0.0037 \\ 0.0129 & 0 & 0.0026 & 0.0027 \\ 0.0024 & 0.0026 & 0 & -0.0058 \\ 0.0037 & 0.0027 & -0.0058 & 0 \end{bmatrix}.$$

We see that these are very close to the zero matrix and indicate homogeneous reservoirs. This simple example confirms that the modified heterogeneity matrix is a more robust estimator of reservoir heterogeneity. We will show an example of a heterogeneous reservoir in Case 7-1.

In the CM, to show the connectivity we map the λs by drawing an arrow between the injection/production well pairs, where the length of the arrow is related to the value of λ. For the modified heterogeneity matrix, we do the same: we draw an arrow between the well pairs where the length of the arrow is related to the absolute value of modified connectivity index between the well pairs. To distinguish the positive and negative connectivity indices, we use different colors and line patterns. For simplicity, for $[\mathbf{\Delta'_{con}}]$, we draw an arrow from only injectors to the producers, and for $[\mathbf{\Delta'_{inj}}]$ and $[\mathbf{\Delta'_{prod}}]$, we draw the arrow from both wells.

Fig. 7.1 shows some synthetic cases and their corresponding connectivity maps, where the modified heterogeneity matrix describes the heterogeneity very well. **Fig. 7.1a** illustrates a barrier with k=1 md in the reservoir. This barrier mainly decreases the connectivity indices of (I01, I02), (I01, P02), and (P01, P02) and has less effect on the modified connectivity index of the three other well pairs (**Fig. 7.1b)**. For the case shown in **Fig. 7.1c**, the barrier has a lower permeability. We see the effect of this lower permeability in the form of smaller modified connectivity indices between the well pairs than in the previous case (**Fig. 7.1d)**.

In **Fig. 7.1e** a channel exists in the system. This channel increases the connectivity between the well pairs (I01, I02), (I01, P02), and (P01, P02), and does not affect the other ones significantly (**Fig. 7.1f)**. For the case where the channel has a higher permeability (**Fig. 7.1g),** these connectivity indices (**Fig. 7.1h)** increase compared to the ones of the previous case (**Fig. 7.1f)**.

7.3 Properties of the Heterogeneity Matrix

In general, if we have the general reservoir properties and injector and producer rates and BHPs, we can determine the optimized heterogeneity matrix that minimizes the prediction error of production rates and injector BHPs using an appropriate numerical optimization software. However, this matrix may not properly represent the reservoir heterogeneity. In fact, it is common to have more than one matrix that minimizes this prediction error. To select the best and most plausible heterogeneity matrix, we need to know the properties of the heterogeneity matrix and also include some other sources of data (such as geological data) if available. Here, we discuss some of the most important properties of the MPI matrix that helps us to limit the possible solutions for the heterogeneity matrix. Of course, several other properties for this matrix may exist that we could not find and considering them, we may further improve these results.

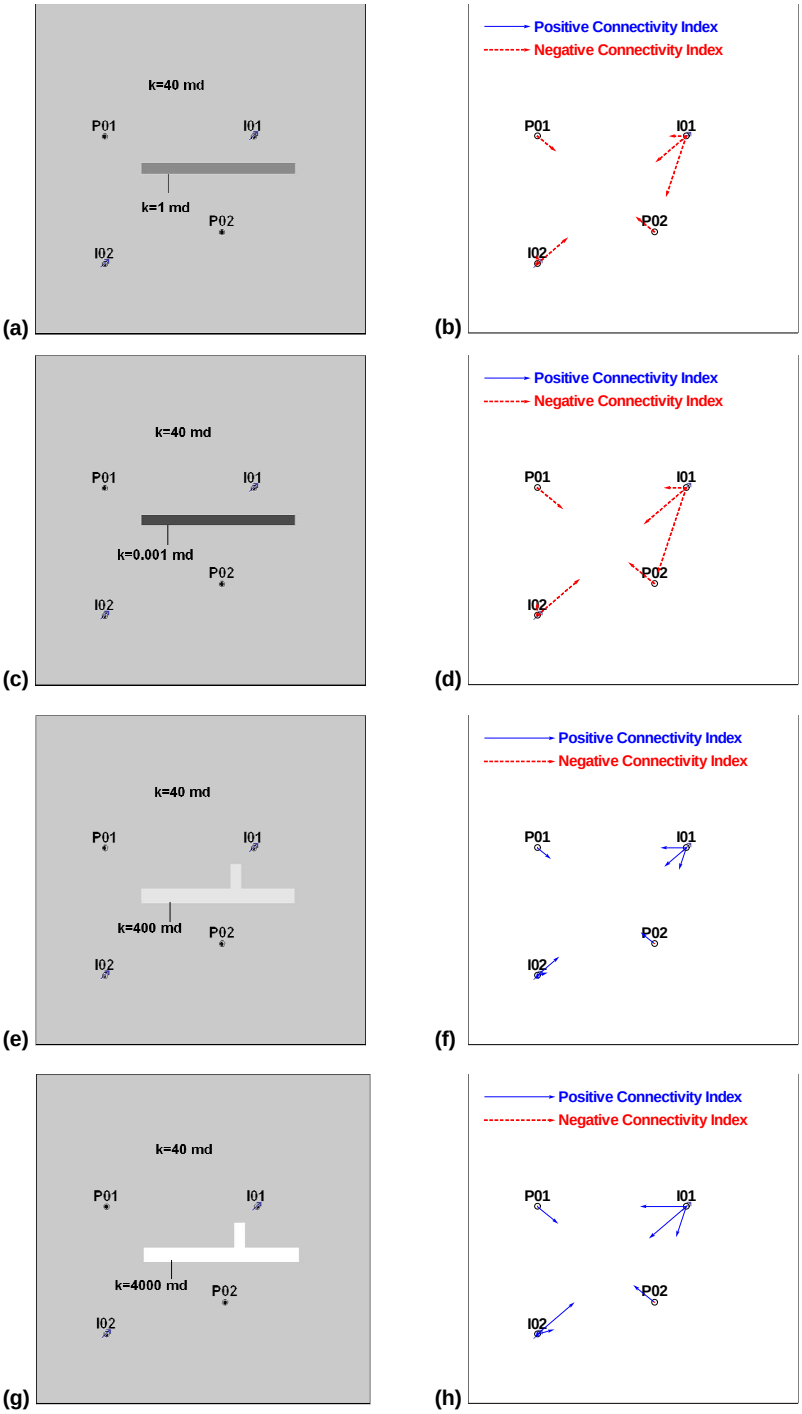

Fig. 7.1—Connectivity map for some synthetic heterogeneous cases. As expected we have negative connectivity indices for the cases with barriers and positive connectivity indices for the cases with channels. Also we can see that the strength of the heterogeneity affects the connectivity index. For example, the connectivity indices of Case "g" are higher than the ones of Case "e".

7.3.1 Injector BHPs Are Not Available

Probably the most important property we need to consider is related to the availability of the BHP data. If the injector BHP data are not available, the only source of the data to estimate the heterogeneity matrix is production rates and average reservoir pressure (if available). However, based on Eqs. 6.12 and 6.15, these are independent of the $[\mathbf{A}_{\mathbf{inj}}]$, and this matrix is important only in calculating injector BHPs. So, in this case we cannot estimate the $[\mathbf{\Delta}_{\mathbf{inj}}]$. If we have some producers converted to injectors we may be able to estimate the elements of this matrix associated with the converted wells.

7.3.2 No Need for Diagonal Elements for Small Delay

In case of the delay term is small and can be approximated by zero, Eq. 6.16 reduces into

$$\vec{q}=\left\{\left(\frac{1}{[\mathbf{1}]_{1xK}\left[\mathbf{A}_{\mathbf{prod}}\right]^{-1}[\mathbf{1}]_{Kx1}}\right)\left[\mathbf{A}_{\mathbf{prod}}\right]^{-1}\left([\mathbf{1}]_{KxK}\left[\mathbf{A}_{\mathbf{prod}}\right]^{-1}[\mathbf{A}_{\mathbf{con}}]^{T}-[\mathbf{1}]_{KxI}\right)-\left[\mathbf{A}_{\mathbf{prod}}\right]^{-1}[\mathbf{A}_{\mathbf{con}}]^{T}\right\}\vec{w} \quad \text{..... (7.5)}$$
$$+\kappa\left[\mathbf{A}_{\mathbf{prod}}\right]^{-1}\left\{\frac{[\mathbf{1}]_{1xK}\left[\mathbf{A}_{\mathbf{prod}}\right]^{-1}\vec{p}_{q^*}}{[\mathbf{1}]_{1xK}\left[\mathbf{A}_{\mathbf{prod}}\right]^{-1}[\mathbf{1}]_{Kx1}}[\mathbf{1}]_{Kx1}-\vec{p}_{q^*}\right\}$$

which has unique properties. The most important property of this case is in determining the heterogeneity matrix where we can set the diagonal elements to zero and just determine the off-diagonal elements. In fact, in this case we observed that modifying the off-diagonal elements using Eq.7.3 is equivalent to updating the off-diagonal elements. In other words, using the heterogeneity matrix $[\mathbf{\Delta}']$ (as defined in Eq. 7.4), we will have the same injector BHPs and production rates as using the heterogeneity matrix $[\mathbf{\Delta}]$. This property is the basis of the modified heterogeneity matrix definition. At this point, there is no mathematical proof for this property. However, we observed it in several cases (as we will see in the examples later), and also we confirmed it parametrically for different numbers of injectors and producers using calculations in Mathematica.

7.3.3 Adding a Constant Number to Each Row of $[\mathbf{A}_{\mathbf{con}}]$ for Small Delay

For a small delay term, we can show that when an arbitrary number is added to each row of the $[\mathbf{A}_{\mathbf{con}}]$ matrix, the production rate stays constant. In other words, adding matrix [**E**], defined as

$$[\mathbf{E}]=\begin{bmatrix}e_1 & \cdots & e_I\end{bmatrix}^{T}[\mathbf{1}]_{1xK} \quad \text{..... (7.6)}$$

(where e_i is an arbitrary number) into the $[\mathbf{A}_{\mathbf{con}}]$ will hold production rate constant. In this case, we see that the difference between the columns is constant. Also, the $[\mathbf{A}_{\mathbf{prod}}]$ is constant too, so, by normalizing each row of the $[\mathbf{\Delta}'_{\mathbf{con}}]$ matrix we can get another kind of connectivity index called *normalized connectivity index*. The normalized connectivity index is less robust than the modified connectivity index because its

value changes with the number of wells. However, it still has the relative connectivity information for each injector. This property is not valid for injector BHPs. We show the proof of this property in Appendix D.

7.3.4 Inconsistency of the [Δ] in Case of Constant Producer BHPs

If we have the same pressure at all producers, the weighted average of the BHPs will decrease to

$$\frac{[1]_{1xK}\left[\mathbf{A}_{\mathbf{prod}}\right]^{-1}\vec{p}_{q^*}}{[1]_{1xK}\left[\mathbf{A}_{\mathbf{prod}}\right]^{-1}[1]_{Kx1}} = p_q \,. \quad \text{..... (7.7)}$$

Replacing Eq. 7.7 into Eq. 6.15 we obtain

$$\vec{q} = \left\{ \left(\frac{1-\exp\left(-\frac{[\mathbf{1}]_{1xK}\left[\mathbf{A}_{\mathbf{prod}}\right]^{-1}[\mathbf{1}]_{Kx1}\,\kappa t}{c_t V_p} \right)}{[\mathbf{1}]_{1xK}\left[\mathbf{A}_{\mathbf{prod}}\right]^{-1}[\mathbf{1}]_{Kx1}} \right) \left[\mathbf{A}_{\mathbf{prod}}\right]^{-1} \left([\mathbf{1}]_{KxK}\left[\mathbf{A}_{\mathbf{prod}}\right]^{-1}\left[\mathbf{A}_{\mathbf{con}}\right]^{T} - [\mathbf{1}]_{KxI} \right) \right. \quad \text{..... (7.8)}$$

$$\left. -\left[\mathbf{A}_{\mathbf{prod}}\right]^{-1}\left[\mathbf{A}_{\mathbf{con}}\right]^{T} \right\} \vec{w} + \kappa\left(\bar{p}_i - p_q\right) \exp\left(-\frac{[\mathbf{1}]_{1xK}\left[\mathbf{A}_{\mathbf{prod}}\right]^{-1}[\mathbf{1}]_{Kx1}\,\kappa t}{c_t V_p} \right) \left[\mathbf{A}_{\mathbf{prod}}\right]^{-1}[\mathbf{1}]_{Kx1}$$

In this case, we have some difficulty in calculating the heterogeneity matrix, where several sets of [**A**] may give the same production rate. This is the well-known problem of "insufficient excitation". So we may obtain misleading results in estimating [**A**]. If we change [$\mathbf{A}_{\mathbf{prod}}$] with any [$\mathbf{A}_{\mathbf{prod\_new}}$], that satisfies

$$[\mathbf{A}_{\mathbf{prod\_new}}]^{-1}[1]_{Kx1} = [\mathbf{A}_{\mathbf{prod}}]^{-1}[1]_{Kx1} \quad \text{..... (7.9)}$$

and [$\mathbf{A}_{\mathbf{con}}$] with [$\mathbf{A}_{\mathbf{con\_new}}$], defined as

$$\left[\mathbf{A}_{\mathbf{con\_new}}{}^{T}\right] = \left[\left(\frac{1-\exp\left(-\frac{[\mathbf{1}]_{1xK}\left[\mathbf{A}_{\mathbf{prod}}\right]^{-1}[\mathbf{1}]_{Kx1}\,t}{c_t V_p} \right)}{[\mathbf{1}]_{1xK}\left[\mathbf{A}_{\mathbf{prod}}\right]^{-1}[\mathbf{1}]_{Kx1}} \right) \left[\mathbf{A}_{\mathbf{prod}}\right]^{-1}[\mathbf{1}]_{KxK}\left[\mathbf{A}_{\mathbf{prod}}\right]^{-1} - \left[\mathbf{A}_{\mathbf{prod\_new}}\right]^{-1} \right]^{-1}, \quad \text{..... (7.10)}$$

$$\cdot \left[\left(\frac{1-\exp\left(-\frac{[\mathbf{1}]_{1xK}\left[\mathbf{A}_{\mathbf{prod}}\right]^{-1}[\mathbf{1}]_{Kx1}\,t}{c_t V_p} \right)}{[\mathbf{1}]_{1xK}\left[\mathbf{A}_{\mathbf{prod}}\right]^{-1}[\mathbf{1}]_{Kx1}} \right) \left[\mathbf{A}_{\mathbf{prod}}\right]^{-1}[\mathbf{1}]_{KxK}\left[\mathbf{A}_{\mathbf{prod}}\right]^{-1} - \left[\mathbf{A}_{\mathbf{prod}}\right]^{-1} \right] \left[\mathbf{A}_{\mathbf{con}}{}^{T}\right]$$

the production rate and injector BHPs stay constant (Appendix D). In case of having small delay, we can show (Appendix D) that, by changing [$\mathbf{A}_{\mathbf{prod}}$] to any arbitrary [$\mathbf{A}_{\mathbf{prod\_new}}$] and replacing [$\mathbf{A}_{\mathbf{con}}$] with [$\mathbf{A}_{\mathbf{con\_new}}$], defined as

$$\left[\mathbf{A}_{\mathbf{con\_new}}{}^{T}\right]=\left[\left(\frac{1-\exp\left(-\frac{[1]_{1xK}\left[\mathbf{A}_{\mathbf{prod}}\right]^{-1}[1]_{Kx1}\,t}{c_tV_p}\right)}{[1]_{1xK}\left[\mathbf{A}_{\mathbf{prod}}\right]^{-1}[1]_{Kx1}}\right)\left[\mathbf{A}_{\mathbf{prod\_new}}\right]^{-1}[1]_{KxK}\left[\mathbf{A}_{\mathbf{prod\_new}}\right]^{-1}-\left[\mathbf{A}_{\mathbf{prod\_new}}\right]^{-1}\right]^{-1}\cdot$$

$$\left\{\left[\left(\frac{1-\exp\left(-\frac{[1]_{1xK}\left[\mathbf{A}_{\mathbf{prod}}\right]^{-1}[1]_{Kx1}\,t}{c_tV_p}\right)}{[1]_{1xK}\left[\mathbf{A}_{\mathbf{prod}}\right]^{-1}[1]_{Kx1}}\right)\left[\mathbf{A}_{\mathbf{prod}}\right]^{-1}[1]_{KxK}\left[\mathbf{A}_{\mathbf{prod}}\right]^{-1}-\left[\mathbf{A}_{\mathbf{prod}}\right]^{-1}\right]\left[\mathbf{A}_{\mathbf{con}}{}^{T}\right]-\right.$$

$$\left.\left(\frac{1-\exp\left(-\frac{[1]_{1xK}\left[\mathbf{A}_{\mathbf{prod}}\right]^{-1}[1]_{Kx1}\,t}{c_tV_p}\right)}{[1]_{1xK}\left[\mathbf{A}_{\mathbf{prod}}\right]^{-1}[1]_{Kx1}}\right)\left[\mathbf{A}_{\mathbf{prod}}\right]^{-1}[1]_{KxI}+\left(\frac{1-\exp\left(-\frac{[1]_{1xK}\left[\mathbf{A}_{\mathbf{prod}}\right]^{-1}[1]_{Kx1}\,t}{c_tV_p}\right)}{[1]_{1xK}\left[\mathbf{A}_{\mathbf{prod}}\right]^{-1}[1]_{Kx1}}\right)\left[\mathbf{A}_{\mathbf{prod\_new}}\right]^{-1}[1]_{KxI}\right\}\quad(7.11)$$

we will have the same production rate (but not the same injector BHPs). The reason for the delay term in the equation is to avoid the singularity problem (see Appendix D). In case of limited changes in producer BHPs (and not only constant ones), we observed several cases nonuniqueness of optimum MPI matrix that we did not discuss here. The point is that if more changes exist in production conditions, more accurate estimation of the heterogeneity matrix is possible.

Now, we show the described properties using a simple example.

Example 7-1. We have a 2x2 system with all reservoir properties similar to Case 6-1. However, to have an ideal situation, in this case we assumed only water exists in the reservoir. The influence matrix for this case is

$$[\mathbf{A}]=\begin{bmatrix}7.7832 & -0.7278 & -0.4375 & -0.0414\\ -0.7278 & 8.9155 & 0.1224 & 0.0900\\ -0.4375 & 0.1224 & 8.2208 & -0.4519\\ -0.0414 & 0.0900 & -0.4519 & 7.8256\end{bmatrix}$$

The delay term for this case for t=1 month is 9.56 x 10^{-6}. This is small enough to use properties 7.3.2 and 7.3.3. By changing the diagonal to [8.3, 7.2, 8.1, 6.5] and using Property 7.3.2, the updated influence function will be

$$\left[\mathbf{A}_{\mathbf{new\_1}}\right]=\begin{bmatrix}8.3 & -1.3272 & -0.2396 & -0.4458\\ -1.3272 & 7.2 & -0.7957 & -1.4305\\ -0.2396 & -0.7957 & 8.1 & -1.1751\\ -0.4458 & -1.4305 & -1.1751 & 6.5\end{bmatrix}$$

Applying this matrix to 118 months of data, the SSE [in $(rb/day)^2$] of the production rate calculated using [$\mathbf{A}_{new\_1}$] comparing to the production rate calculated using [**A**] was 0.0019, and the SSE (in psi^2) of injector BHPs was 0.0001.

Using Property 7.3.3 by replacing [**A**] with

$$\left[\mathbf{A}_{new\_2}\right]=\begin{bmatrix} 7.7832 & -0.7278 & -1.4375 & -1.0414 \\ -0.7278 & 8.9155 & 2.1224 & 2.0900 \\ -1.4375 & 2.1224 & 8.2208 & -0.4519 \\ -1.0414 & 2.0900 & -0.4519 & 7.8256 \end{bmatrix}$$

and applying [$\mathbf{A}_{new\_2}$], the SSE of the production rate was 0.00025 $(rb/day)^2$ and that of the injector BHPs was 5.987×10^6 psi^2 because this property is only valid for production rate and not for injector BHPs.

Using Property 7.3.4 (Eq. 7.11), if the producer BHPs are the same, for an arbitrary [$\mathbf{A}_{prod\_new\_1}$] that meets the criteria in Eq. 9, we can calculate the equivalent [$\mathbf{A}_{prod\_con\_1}$]. For example, having

$$\left[\mathbf{A}_{prod\_new\_1}\right]=\begin{bmatrix} 9.1803 & 0.3403 \\ 0.3403 & 8.4813 \end{bmatrix}$$

and computing [$\mathbf{A}_{con\_new\_1}$] based on Eq. 7.11 as

$$\left[\mathbf{A}_{con\_new\_1}\right]=\begin{bmatrix} -0.4119 & -0.1666 \\ 0.2238 & 0.0399 \end{bmatrix},$$

the SSE of the production rate will be 0.0625 $(rb/day)^2$. As we mentioned, this is not valid for injector BHPs, and the SSE of injector BHPs is 1.0983×10^6 psi^2. If we define the [$\mathbf{A}_{prod\_new\_1}$] in a way that meets the criteria in Eq. 7.9, for example as

$$\left[\mathbf{A}_{prod\_new\_1}\right]=\begin{bmatrix} 6.1852 & 1.4910 \\ 1.4910 & 5.9713 \end{bmatrix}$$

and define [$\mathbf{A}_{con\_new\_1}$] based on Eq. 7.10 as

$$\left[\mathbf{A}_{con\_new\_1}\right]=\begin{bmatrix} -0.3446 & -0.1302 \\ 0.1148 & 0.0973 \end{bmatrix},$$

the SSE of the production rate will be 3.11×10^{-17} $(rb/day)^2$ and for injector BHPs it is 2.3763 psi^2. To test this property for a longer delay time, we decreased the permeability to 4 md, and the SSE of production rate rose to 7.52×10^{-24} $(rb/day)^2$ and the injector BHPs to 237.63 psi^2 (the absolute error percentage is still less than 0.0155%).

To see the effect of the delay term on the properties, we ran cases with different permeabilities from 40 md (the base case with a small enough delay term) to 1 md. We observed that the percentage error in both production rate and injector BHPs is negligible for Property 7.3.2 for permeabilities higher than 5 md (**Fig.**

7.2). Using property 7.3.3, this error is negligible for permeabilities higher than 9 md (**Fig. 7.3**). For Property 7.3.4, Eq. 7.10 is valid for all permeabilities (**Fig. 7.4**) and Eq. 7.11 is valid only for small delay terms (**Fig. 7.5**).

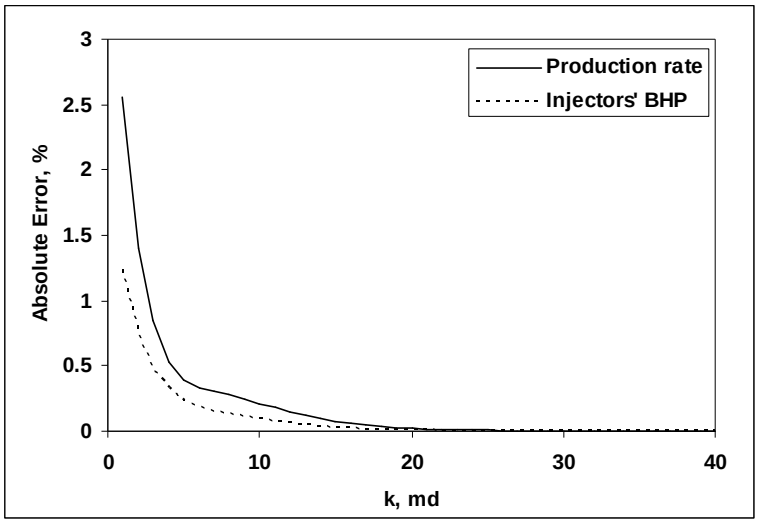

Fig. 7.2—The difference between the correct MPI predictor and the estimated one using property 7.3.2 increases with decreasing the permeability. This property is valid for both injector BHPs and production rate.

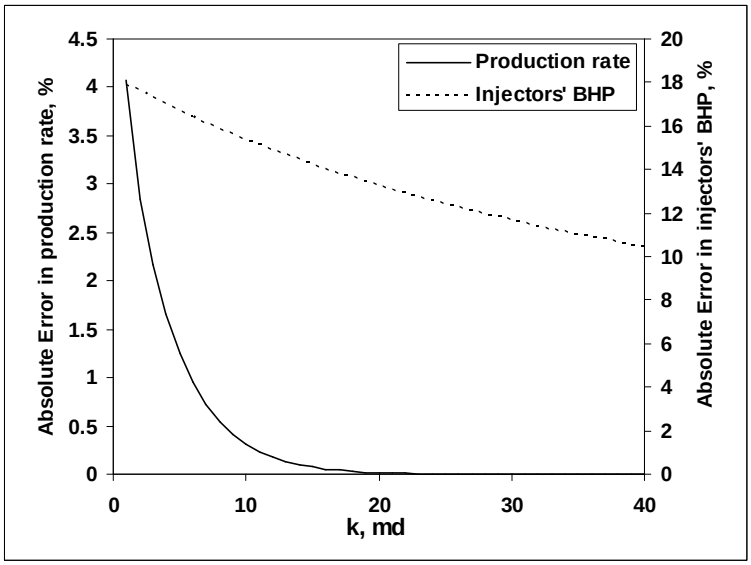

Fig. 7.3—The difference between the correct MPI predictor and the estimated one using property 7.3.3 increases with decreasing permeability. As expected, this property is valid only for the production rate, and it does not work for the injector BHPs.

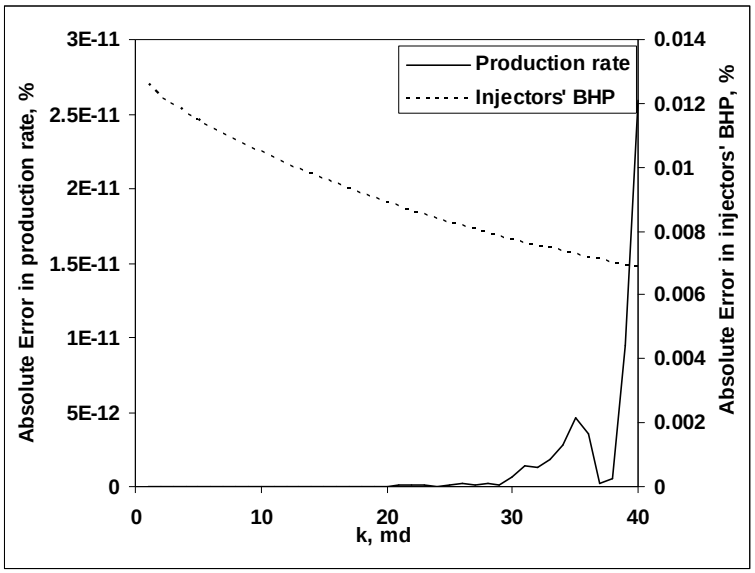

Fig. 7.4—Property 7.3.4 (Eq. 7.10) is valid for all permeabilities, and the difference between the correct MPI predictor and the estimated one using this property is small enough for all permeabilities. This property is valid for both injector BHPs and production rate. The negligible oscillation in the production error change is because of computational errors.

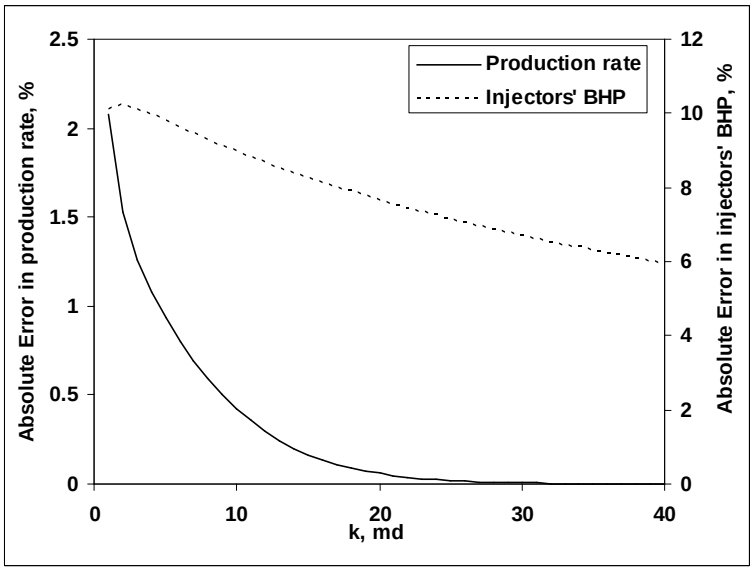

Fig. 7.5—The difference between the correct MPI predictor and the estimated one using property 7.3.4 (Eq. 7.11) increases with decreasing the permeability. As expected, this property is valid only for the production rate, and it does not work for the injector BHPs.

At this point, we need to emphasize that these ranges for permeability are just valid for this case, and by changing the other properties of the system as well as locations and number of the wells, these ranges

can change. In fact, the main reason to show this example and these properties was to discuss the nonuniqueness of the estimated heterogeneity matrix that allows us to interpret the MPI results more reasonably.

7.4 Heterogeneity Matrix Estimation

Having at least three of our elements-injection rates, production rates, producer BHPs and injector BHPs- we can estimate the heterogeneity matrix. As we discussed in Section 7.3, having more diverse and "excited" data can give us better estimations of [**Δ**]. Since estimating the heterogeneity matrix involves optimization of a nonconvex objective function, according to our numerical experiences, it may have several local minima. Thus, setting a proper initial point is vital. If we have no information about the reservoir and possible heterogeneity of the system, the best guess is initializing the heterogeneity matrix randomly. We just need to set a proper range for each connectivity index. To have a simpler model, it is better to start with a narrow range and increase the ranges if required at the next steps. In addition, we need to set the ranges in a way that the [$\mathbf{A_{prod}}$] stays nonsingular and have the summation of the elements of its inverse positive. If the summation of the elements of this matrix is negative (that is equivalent to having a negative productivity index for a single-well system), the delay term becomes more than 1, and that leads to an infinite average reservoir pressure, which is physically impossible. To avoid this problem, we need to add a modification to the MPI predictor in a way that it produces a relatively large error (instead of infinite) when this problem happens. In the foregoing examples, this simple modification worked efficiently.

Here we show some examples of heterogeneity matrix evaluation.

Case 7-1. This is a 2x2 system with well location and reservoir heterogeneity similar to the example shown in Fig. 7.1a with only water in the reservoir. Because of the small delay term, we expect to have a nonunique answer if we estimate the full heterogeneity matrix. Thus, using these data we will be only able to estimate the modified heterogeneity matrix. By setting the diagonal elements of the heterogeneity matrix to zero, we can obtain the modified heterogeneity matrix as

$$[\Delta_1'] = \begin{bmatrix} 0 & -0.8829 & -0.3834 & -1.3871 \\ -0.8829 & 0 & -0.2278 & -0.0892 \\ -0.3834 & -0.2278 & 0 & -0.5287 \\ -1.3971 & -0.0892 & -0.5287 & 0 \end{bmatrix}$$

The interpretation of this matrix is explained earlier (See Figs. 7.1a and b). By running the same case with reservoir permeability of 10 md and barrier permeability of 0.25 md, we calculated the heterogeneity matrix as

$$[\boldsymbol{\Delta}_2]=\begin{bmatrix}1.3593 & 0.3312 & 0.8263 & 0.0762\\ 0.3312 & 1.0264 & 0.8135 & 1.2171\\ 0.8263 & 0.8135 & 1.0544 & 0.7749\\ 0.0762 & 1.2171 & 0.7749 & 1.5832\end{bmatrix}$$

Hence the modified heterogeneity matrix is

$$[\boldsymbol{\Delta}'_2]=\begin{bmatrix}0 & -0.8617 & -0.3806 & -1.3950\\ -0.8617 & 0 & -0.2268 & -0.0877\\ -0.3806 & -0.2268 & 0 & -0.5439\\ -1.3950 & -0.0877 & -0.5439 & 0\end{bmatrix}$$

For a case with average permeability of 4 md with barrier permeability of 0.1 md, we estimated the heterogeneity matrix as

$$[\boldsymbol{\Delta}_3]=\begin{bmatrix}0.7067 & -0.2894 & 0.2132 & -0.5509\\ -0.2894 & 0.3290 & 0.1757 & 0.5625\\ 0.2132 & 0.1757 & 0.4846 & 0.1197\\ -0.5509 & 0.5625 & 0.1197 & 0.9824\end{bmatrix}$$

hence the modified heterogeneity matrix is

$$[\boldsymbol{\Delta}'_3]=\begin{bmatrix}0 & -0.8072 & -0.3824 & -1.3955\\ -0.8072 & 0 & -0.2311 & -0.0932\\ -0.3824 & -0.2311 & 0 & -0.6138\\ -1.3955 & -0.0932 & -0.6138 & 0\end{bmatrix}$$

Comparing the connectivity matrices obtained for these three permeabilities, we see that although the heterogeneity matrices are different, the modified heterogeneity matrices are very similar to each other and we can easily acquire the connectivity information of the reservoir from these matrices. In addition, this matrix is almost insensitive to the average permeability of the system, and its elements represent the interwell heterogeneity clearer.

For the case of high permeability, if we have no BHP data we will obtain

$$[\boldsymbol{\Delta}'_4]=\begin{bmatrix}0 & 0 & 1.5 & 0.4689\\ 0 & 0 & 1.3618 & 1.5\\ 1.5 & 1.3618 & 0 & -0.5324\\ 0.4689 & 1.5 & -0.5324 & 0\end{bmatrix}$$

that is equivalent to the main heterogeneity matrix for this case ($[\boldsymbol{\Delta}'_1]$), based on property 7.3.3. For the case with k=10 md we will have

$$[\Delta'_5]=\begin{bmatrix} 0 & 0 & 1.6152 & 0.5998 \\ 0 & 0 & 1.5239 & 1.6639 \\ 1.6152 & 1.5239 & 0 & -0.5384 \\ 0.5998 & 1.6639 & -0.5384 & 0 \end{bmatrix}$$

and for k=4 md

$$[\Delta'_6]=\begin{bmatrix} 0 & 0 & -0.1358 & -1.1469 \\ 0 & 0 & -0.1437 & -0.0075 \\ -0.1358 & -0.1437 & 0 & -0.6226 \\ -1.1469 & -0.0075 & -0.6226 & 0 \end{bmatrix}$$

Although the obtained [Δ'] for k=10 md is far from the original one ([Δ'_2]), it can be interpreted using property 7.3.3 and will be equivalent to [Δ'_2]. However, the one for k=4 md ([Δ'_6]) is closer to the correct one ([Δ'_3]). In fact, as we discussed in Example 7.1, Property 7.3.3 disturbs the results for k=10 md; however, for k=4 md, it has a smaller effect.

If we do not have any change in the BHP data, as discussed earlier, the heterogeneity matrix will be nonunique. For example, for the high permeability case we obtained

$$[\Delta'_7]=\begin{bmatrix} 0 & -0.8819 & 0.0771 & -0.8421 \\ -0.8819 & 0 & 0.3134 & 0.3837 \\ 0.0771 & 0.3134 & 0 & 1.5 \\ -0.8421 & 0.3837 & 1.5 & 0 \end{bmatrix},$$

and by setting different [$\mathbf{\Delta_{prod}}$], based on Property 7.3.4 we will obtain several other heterogeneity matrices. In this case, one possible solution to obtain a unique answer is to set the [$\mathbf{\Delta_{prod}}$] zero. Thus, for this case we will have:

$$[\Delta'_8]=\begin{bmatrix} 0 & -0.8843 & -0.2638 & -1.2529 \\ -0.8843 & 0 & -0.0873 & 0.0336 \\ -0.2638 & -0.0873 & 0 & 0 \\ -1.2529 & 0.0336 & 0 & 0 \end{bmatrix},$$

which is equivalent to the previous one based on Properties 7.3.3 and 7.3.4. Although this matrix is slightly different from the original modified heterogeneity matrix for this case, it still has most of the connectivity information between the injector/producer well pairs (**Fig. 7.6**).

Case 7-2. Similar to Case 6-2, this case represents a 5x4 system. Some barriers and a channel exist in the reservoir (**Fig. 7.7**) but the general reservoir properties are similar to Case 7-1. The analysis period is 15 years. In this case, the numbers of injectors and producers change during the production period and some of the producers are converted into injectors. The producers are stimulated a couple of times during the production period (**Fig. 7.8**). The producer BHPs change every 15 months. To consider the effect of

variable total compressibility on the data, we used the oil production data to update the total compressibility at each time step. In fact, we can calculate the total compressibility simply based on average oil saturation obtained from cumulative oil production. Based on these data, we estimated the connectivity indices (**Fig. 7.9**). Similar to what we had in Fig. 7.1, we can see how the connectivity indices are related to the geological features. For example, for well P01, we have negative modified connectivity indices with all the other wells. These negative values are higher between this well and I01, I04, I05, P02, and P03. Since the only large negative values of I01, I04, I05, and P02 are between these wells and P01 and P03, we expect to have barriers in the interwell region of these wells. Because both P01 and P03 have negative connectivity indices in several other directions, the moderate negative connectivity index between them could be interpreted as the effect of the diagonal elements of the heterogeneity matrix on their modified connectivity index. In other words, the large negative modified connectivity index between these two wells is due to their small productivity index and not because of a possible barrier between them. We also see a slightly small negative value between I03 and P01 and P03. Since all the other connectivity indices of I03 are positive, we expect to have a channel around this well and also barriers between I03 and P01 and P03. The reason for this slightly small negative connectivity index despite the barrier between them is the large productivity index of I03 due to the channel.

We also obtained the correct skin factor from the data. To get a more accurate estimation of the connectivity indices, we ran a case when only water is present (and hence we do not have the problem of variable compressibility and also we have a higher effective permeability that eliminates the effect of transients). The modified connectivity coefficients of both cases are very similar (**Fig. 7.10**).

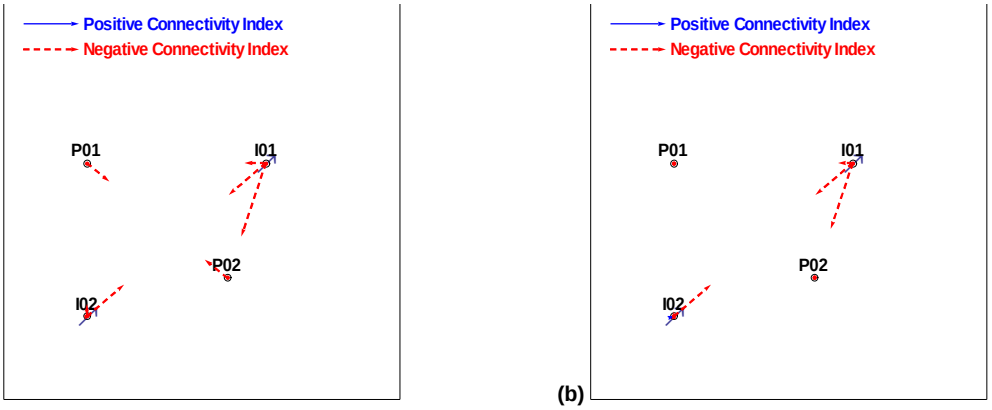

Fig. 7.6—Connectivity map of Case 7-1 (at *k*=40 md) for fluctuating (a) and constant (b) BHP. When the BHP is constant, the estimated [Δ'_{prod}] is not valid and we set it to zero. In this case, although [Δ'_{con}] is different from the true one, it has the relative connectivity information.

Assuming the injectors' BHP data are not available, we recalculated the connectivity coefficients for the oil case. Comparing the connectivity coefficients of the producers and injectors/producers ($[\mathbf{\Delta'_{con}}]$ and $[\mathbf{\Delta'_{prod}}]$) with the one of the base case (**Fig. 7.11**), we can see that for each injector the connectivity coefficients follow a 45^o straight line, and for some of them the line has a nonzero intercept. There are two reasons for this intercept. First of all, since we do not have the injector BHP data, the $[\mathbf{\Delta'_{inj}}]$ cannot be calculated. So in the calculation of the modified connectivity coefficients, we have a systematic shift because of ignoring the δ_{ii} of the injectors. Since for a short period, injectors 2, 4, and 5 were producers, we have some estimation of the $[\mathbf{\Delta'_{inj}}]$ for these wells; however, for the other two injectors, we have no estimation of this matrix. Thus we have less error in the calculation of the connectivity indices for these three injectors. The second reason for this shift is Property 7.3.3, where all the coefficients of an injector may be shifted by the same amount. Again, for three of the injectors we do not have this problem.

We also tested a case where no producer was converted to injector. As expected, in the crossplot of the connectivity indices between the cases with injector's BHP data included and not included (**Fig. 7.12**), we have large intercepts. **Fig. 7.13** shows the normalized connectivity index map of Case 7-2. As we discussed earlier, this map has the relative connectivity information. For example, no specific high permeability zone exists between or around I01 and P02; however, since the connectivity between (I01, P01) and (I01, P03) is small because of the barriers, the normalized connectivity index between I01 and P02 becomes positive.

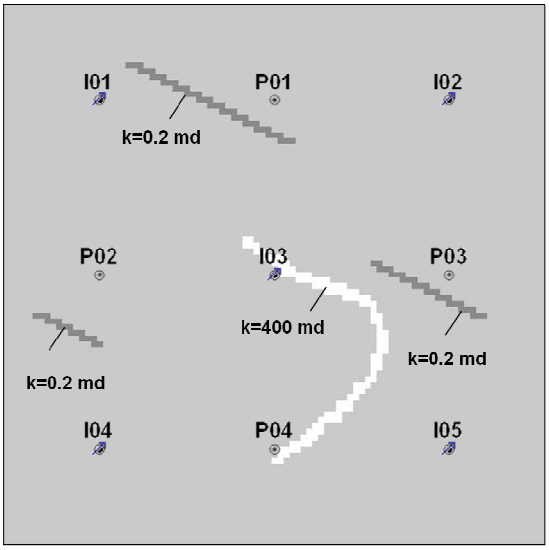

Fig. 7.7—Permeability map of Case 7-2. The permeability of the reservoir is 40 md and there are three barriers with permeability of 0.2 md and a channel with permeability of 400 md.

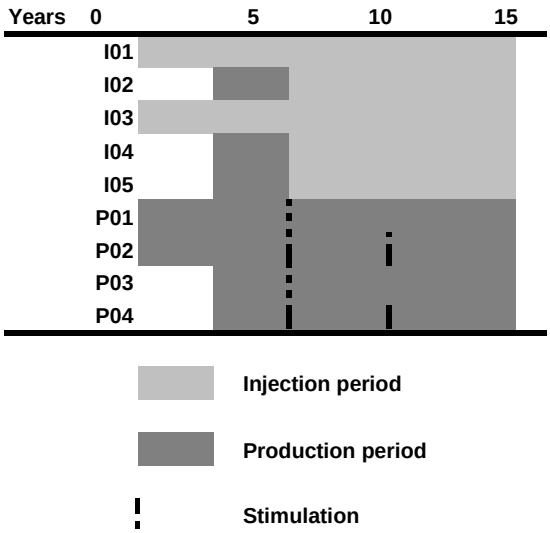

Fig. 7.8—Injection and production periods in Case 7-2. Dashed line shows time of stimulation.

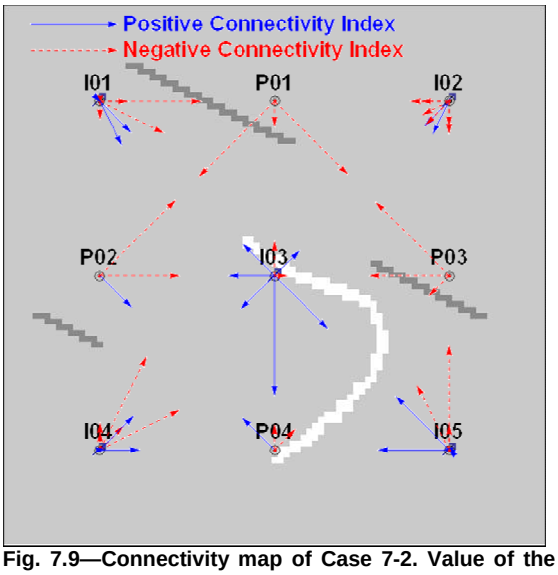

Fig. 7.9—Connectivity map of Case 7-2. Value of the modified connectivity index is related to the geological features in the interwell region and around the wells.

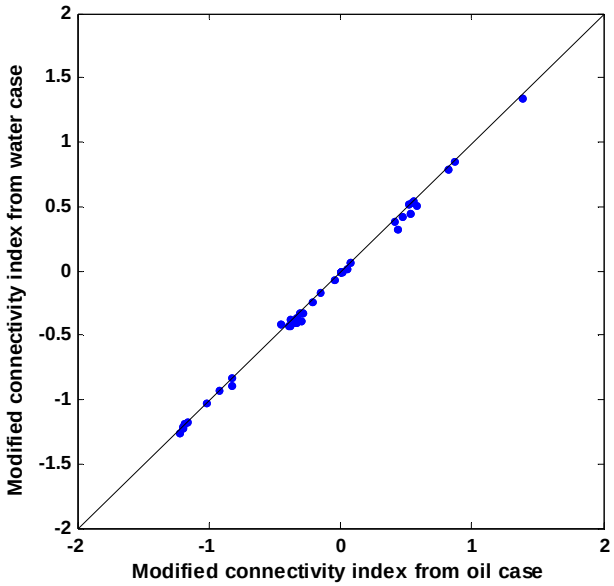

Fig. 7.10—Modified connectivity indices from the oil case and the ones from the water case are in good agreement for Case 7-2.

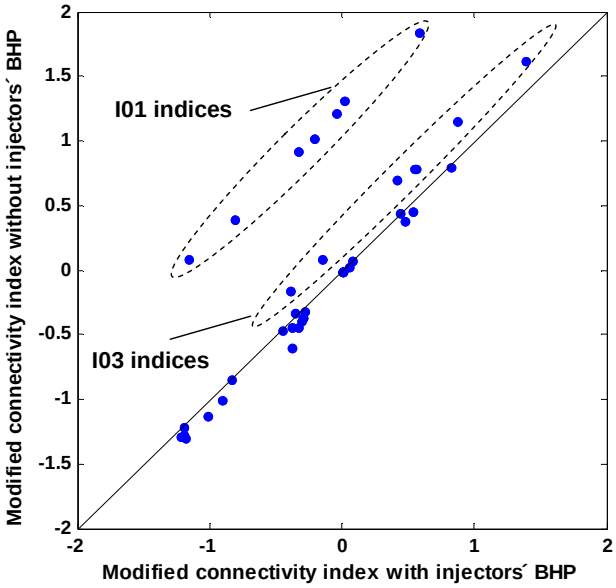

Fig. 7.11—If an injector is converted from producer (I01, I04 and I05 for Case 7-2), we can estimate the true modified connectivity indices for this well even in case the injector BHPs are not available. However, if they are not converted from a producer in case of no injector BHPs data the estimated modified connectivity indices will be shifted (I01 and I03 for Case 7-2).

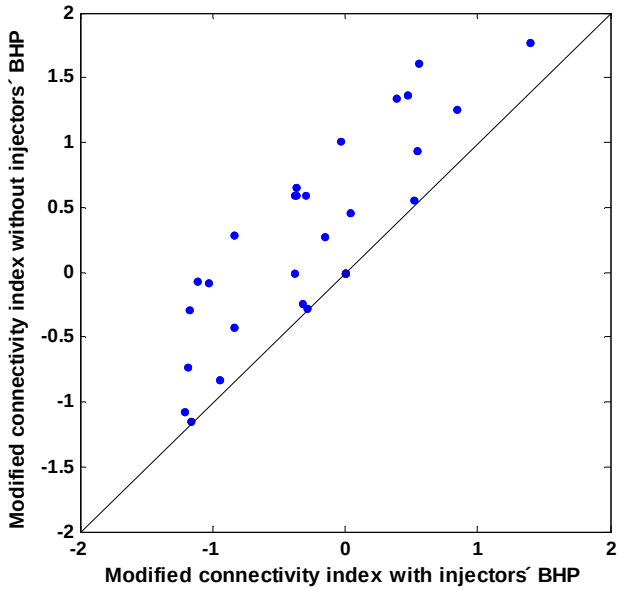

Fig. 7.12—In case no producer converts to injector, we have a shift for most of the connectivity indices.

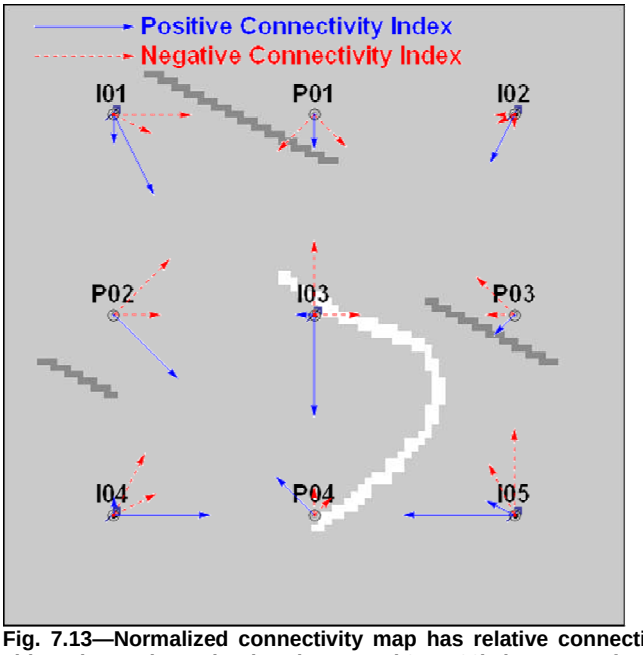

Fig. 7.13—Normalized connectivity map has relative connectivity information for each injector. For example, although no channel exists between (I01, P02), because of normalization of the connectivity indices and two very large negative connectivity indices between (I01, P01) and (I01, P03), the normalized connectivity index between (I01, P02) becomes positive.

7.5 Conclusions

In general, for a heterogeneous system, no theoretical formula exists to determine the influence matrix. We can estimate this matrix from the injection and production data. The difference between the optimized influence matrix from the actual production data and the theoretical influence matrix calculated for the homogeneous case provides the heterogeneity matrix. By a simple modification of this matrix, each nondiagonal element of this matrix (the modified connectivity index) indicates the connectivity between the well pairs independent of the total number of wells, the distances between them, or the operating conditions. Studying the properties of the heterogeneity matrix provides the key to the interpretation of the connectivity indices. Having more diverse data allows us to estimate the heterogeneity matrix more accurately.

8. ADOPTING THE MPI-BASED METHOD TO REALISTIC CONDITIONS

8.1 Introduction

In Section 7.4, we showed how to estimate the heterogeneity matrix for simple cases where we had a volumetric rectangular reservoir and a limited number of wells. If the reservoir is not volumetric, because of the material balance assumption in the MPI solution, we cannot predict the reservoir performance using the equations we derived in Section 6.3. Also, if the reservoir is not rectangular, we cannot obtain the exact MPI matrix analytically. On the other hand, if we have large number of wells, estimation of the heterogeneity matrix becomes very time-consuming and the number of the required data increases. In the following we address these difficulties one by one. Here, we first show a modification of the original MPI formula to evaluate nonvolumetric systems. Then we discuss the possible issues in reservoirs with nonrectangular geometry. At the end we show and discuss a possible solution strategy for a large number of wells. All the approaches discussed in the following sections are preliminary, and more investigation is needed to solve the problems more efficiently.

8.2 MPI for Nonvolumetric Systems

One of the main assumptions in deriving the prediction of reservoir performance with MPI is material balance of the system based on a volumetric reservoir. Based on Eq. 6.11, we assume that the total injection rate over time is close to the total production rate. However, in field applications we may have cases with the total injection rate considerably different from the total production rate. If we have a strong aquifer, we may have a larger production rate than injection rate. On the other hand, if we inject into a zone that is not connected to the producers, the injection rate may be much higher than the production rate. Here, we focus on the second case.

It is possible to have perforation in a zone that is isolated from the target zones. In this case, a portion of the injected water fills the isolated zone. Depending on the size and pressure of this zone, this portion may decrease in time. To model this using the MPI, we defined a coefficient, l_p, for each injector that represents the fraction of lost injected liquid over time. Increasing the pressure of the isolated zone decreases the fraction of the lost water from each injectors. Assuming exponential decrease in lost fraction, the effective injection rate of a well (that leads to production) at each time step will be

$$w_{eff\_i}(t)=\left[l_{p\_i}+\left(1-l_{p\_i}\right)\cdot\exp\left(\frac{t-t_n}{\zeta_i}\right)\right]w_i(t)\ , \quad \text{..... (8.1)}$$

where $w_{eff\_i}(t)$ is the effective injection rate of injector i, l_{p_i} is the lost fraction of this well, and ζ_i is the decrease in the lost fraction of this well. Applying this formula, in the connectivity evaluation we need to estimate two new parameters for each injector: l_p and ζ_i. In general, to estimate these parameters we need to have the pressure at the isolated layer(s), and based on that and considering the injection rate

fluctuations, we estimate the effective injection rate. However, in practice this kind of information is rarely available and we need to estimate these parameters by fitting the model to the data.

Case 8-1. Similar to Case 3-1, this is a 5x4 homogeneous system. A layer that is not connected to the other layers and has a large pore volume exists at the bottom of the system. All the injectors have perforations in this layer; however, producers are not perforated at this zone. So a portion of injected water enters this layer. Applying the MPI predictor to predict the reservoir performance without considering this fact, we have a large error in rate prediction with R^2=0.645 (**Fig. 8.1a**) and R^2=0.761 for injector BHPs. However, if we determine the lost fraction from Eq. 8.1, the average R^2 of production rate becomes 0.990 (**Fig. 8.1b**) and the one for injector BHP becomes R^2=0.993.

Case 8-2. Reservoir properties and well locations are similar to Case 6-2. However, an isolated layer exists under the reservoir, and the injectors and producers are perforated similarly to Case 8-1. Considering Eq. 8.1, we calculated the modified connectivity indices. We found that they are in a good agreement with Case 6-2 (**Fig. 8.2a**). The problem for this case was the inconsistency of the results, where using different starting estimates obtained different answers (In fact, similar to the CM, when the assumptions of the model were violated the estimated parameters become nonunique.). However, almost all of the obtained answers can show the relative connectivity in the system. For example, although the results of one of the runs were a little bit far from Case 7-2 (**Fig. 8.2b**), its connectivity map can still reveal the features of the system (**Fig. 8.3**). If we do not apply Eq.8.1, we may still get a good estimate of the modified connectivity indices (**Fig. 8.4)**; however, the prediction of the production rate will be very poor (R^2=0.665).

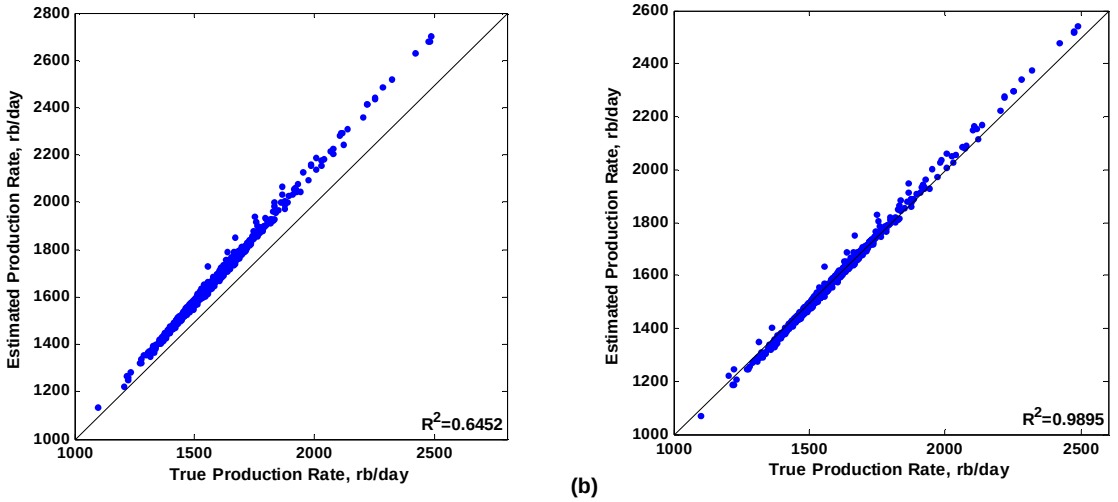

(a) (b)

Fig. 8.1—In nonvolumetric reservoirs, the MPI cannot calculate the production rate accurately (a). Applying Eq. 8.1, however, we could calculate the production rate more accurately (b).

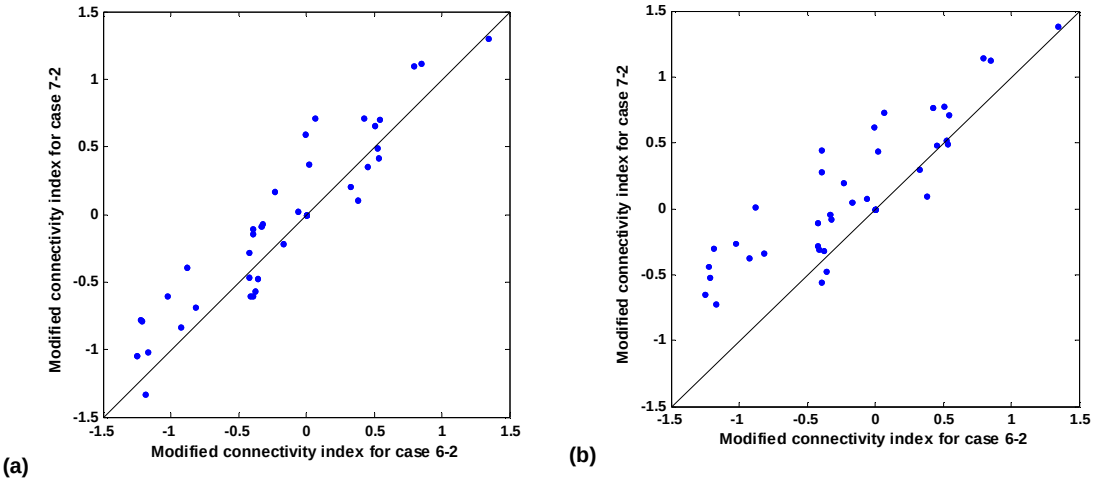

Fig. 8.2—In nonvolumetric cases applying Eq. 8.1, the estimated modified connectivity indices may varied by different initialization of the model parameters. However, the estimated parameters may still have the relative connectivity information. Modified connectivity indices in a and b are based on two different initializations.

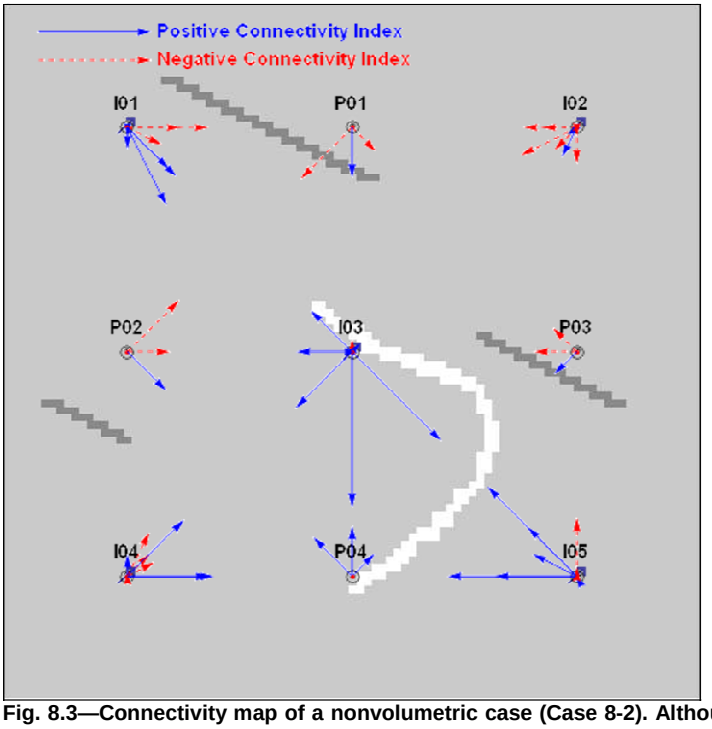

Fig. 8.3—Connectivity map of a nonvolumetric case (Case 8-2). Although the modified connectivity indices may be different from the true ones (Fig. 8.2b), the connectivity map still has most of the connectivity information, and the channel and barrier locations can be inferred from the map.

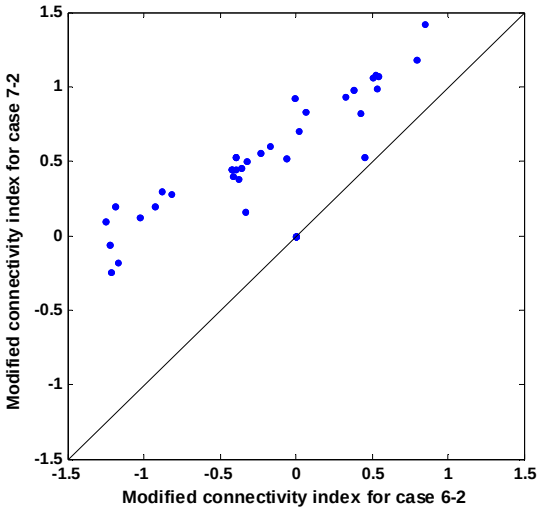

Fig. 8.4—With no use of Eq. 8.1, the estimated connectivity indices are in relatively good agreement with those from the nonvolumetric case. However, the production rate prediction is very poor.

In the example above, we observed that Eq. 8.1 effectively helps us to predict the reservoir performance in nonvolumetric cases. As we observed, in evaluating connectivity, the results are not exactly the same as the volumetric case; however, they are in good agreement. In the field cases, depending on how far the data are from the volumetric case, we may need to use this equation or a new one in a way that considers the reservoir conditions. For example, if we know there is a leaking zone in the reservoir that acts at high pressure, by adding a condition based on average reservoir pressure to the model, and estimating its parameters based on reservoir performance, we may model it.

8.3 MPI for Nonrectangular Systems

The influence function that we used is developed only for rectangular systems. For specific nonrectangular cases, we can use symmetrical properties to determine the influence function analytically. In general, however, no analytical formula exists to calculate the influence function for nonrectangular shapes. Here using some simple example we investigate how valid the rectangular influence function is in cases of nonrectangular geometry.

Case 8-3. Similar to Case 6-1, this case is a homogenous 2x2; however, the geometry of the reservoir is not a perfect rectangle and the locations of the wells are different (**Fig. 8.5**). Calculating the modified connectivity indices, we observed very small changes in the influence matrix. The modified connectivity indices of the wells closer to the cut boundary are more distorted than the other ones because of the smaller productivity index of the wells close to the boundary. For this case it seems that neglecting the actual drainage shape does not lead to misleading results.

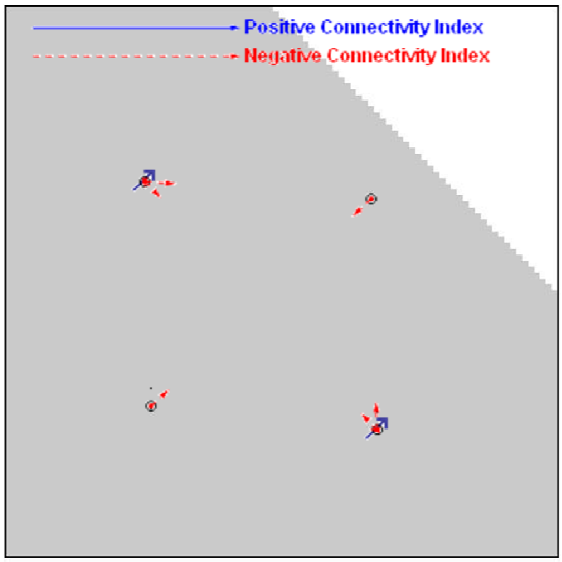

Fig. 8.5—In a homogenous nonrectangular case (Case 8-3), we may have small distortion from the analytical modified connectivity indices. The gray area shows the reservoir. The arrows in the legend show the unit modified connectivity index.

Case 8-4. Similar to Case 8-3, this is a homogenous 2x2; however, the reservoir geometry is more complicated (**Fig. 8.6a**). If we use the same influence matrix as the one we used for the previous case based on the full square, the connectivity map implies several barriers in the reservoir (Fig. 8.6a). If we calculate the influence matrix based on a smaller box (by "box" here we mean the base rectangle that we use to calculate the influence matrix analytically), the connectivity maps show some channels (**Fig. 8.6b**). However, we know both of them are incorrect since the system is homogeneous. By selecting the box somewhere between these two (**Fig. 8.6c**), we observed a very small distortion from the true connectivity map. In fact, selecting a proper position and size for the box is the key point to get the best result.

Case 8-5. This case is very similar to Case 7-2. However, the geometry of the reservoir is different (**Fig. 8.7**). By selecting the box as Fig. 8.10, we calculated the modified heterogeneity matrix and we observed that the calculated one is very close to the one for the rectangular case (**Fig. 8.8**).

In Cases 8-3 and 8-4, as expected, we observed that when the reservoir geometry is different than a rectangle, the analytical influence matrix is not valid to predict the reservoir performance even in the homogeneous cases. In fact, the shape of the reservoir leads to a nonzero modified heterogeneity matrix. If we select a proper box to calculate the influence matrix, the distortion from the analytical influence matrix decreases. However, at this point we cannot provide a procedure to determine this box. If the system has both heterogeneity and nonrectangular shape together, they affect the heterogeneity matrix. In fact, their effect depends on how and how much they change the modified connectivity indices; that is, both of them may increase or decrease it or they may act in different directions. For example, in Case 8-5, the effect of

nonrectangularity was negligible compared to the reservoir heterogeneity. So the modified connectivity indices were very close to the one for the rectangular case.

Future works should focus on estimating the location of the box and better understanding and interpretation of the effect of shape on the obtained connectivity indices.

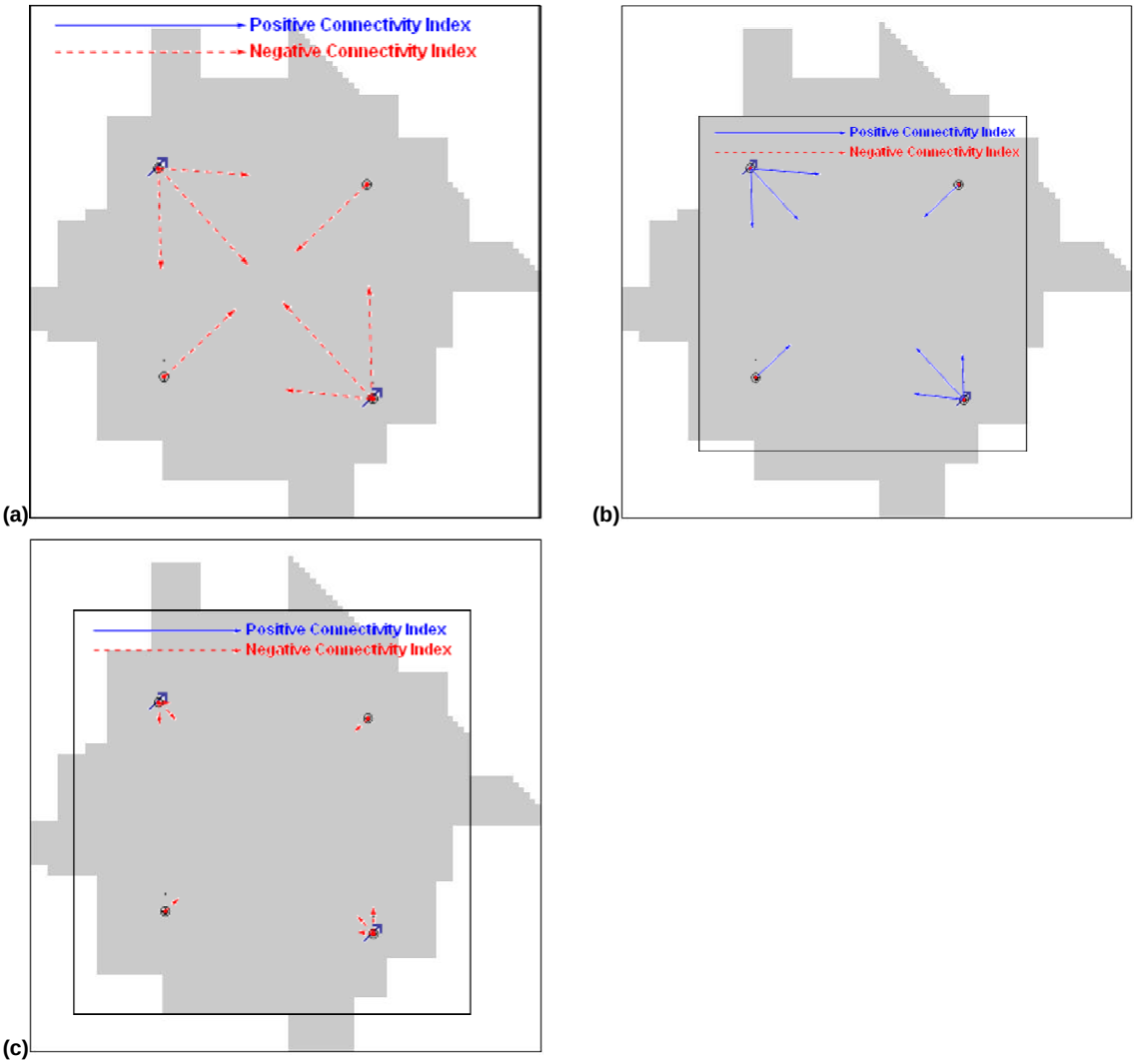

Fig. 8.6—Depending on the selected base "box" for the reservoir, we may obtain a different connectivity map for the nonrectangular case. Assuming a large area (a), the connectivity map indicates some barriers in the system. Considering a small box (b), the estimated connectivity indices show some channels. Selecting a proper box (c) will give the minimum distortion from the analytical rectangular model.

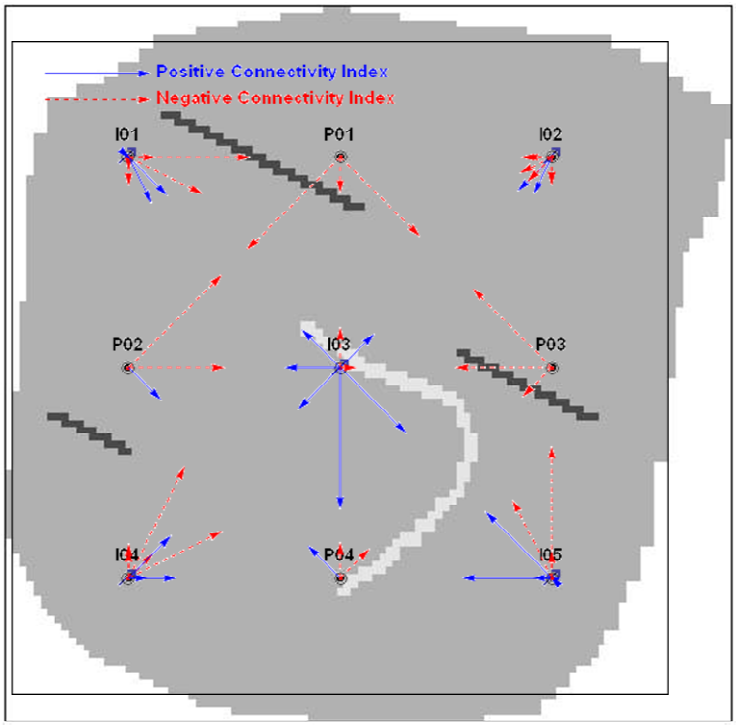

Fig. 8.7—Connectivity map for a nonrectangular case (Case 8-5) represents the reservoir heterogeneity properly. In fact, if the effect of nonrectangular geometry is less than the effect of reservoir heterogeneity and a proper box is selected for the system, the heterogeneity information will be dominant in the modified connectivity indices.

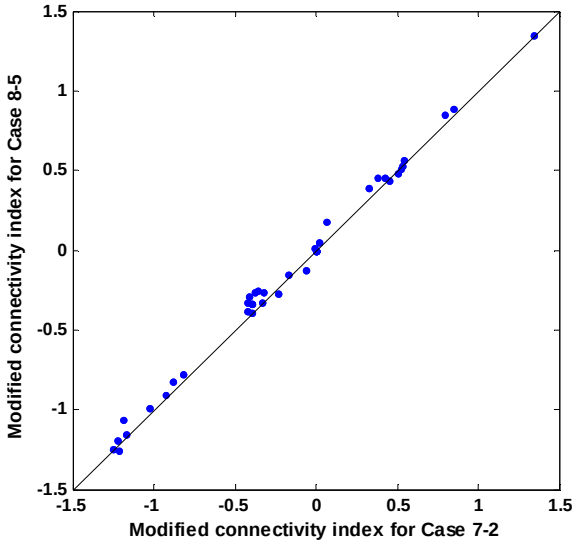

Fig. 8.8—Modified connectivity indices of the nonrectangular case (Case 8-5) are in excellent agreement with the similar rectangular case (Case 7-2).

8.4 MPI for Large Number of Wells

Independently of the number of the wells in a homogeneous rectangular reservoir, the MPI can predict the reservoir performance accurately under the pseudosteady-state regime. In heterogeneous cases, we need to evaluate the heterogeneity matrix that has $(I+K).(I+K+1)/2$ elements, where I is the number of injectors and K is the number of producers. If the number of the wells in the system is small, we can evaluate this matrix quickly. However, with an increasing number of wells, the required computational effort grows dramatically. For example, evaluating the heterogeneity matrix for a 25x16 well system may take almost three orders of magnitude more time than a 8x8 case and four orders of magnitude more time than a 5x4 case. An effective way to overcome this problem is to decrease the number of model parameters by eliminating the parameters that have smaller effect on the reservoir performance. In this project, we suggest a model reduction strategy called *windowing*.

In windowing, we define a window for each well based on the well distances and geological data (if available). We evaluate all the connectivity indices for the wells inside the window. For the wells outside the window we may assign only one value, representing their connectivity index to the corresponding well (**Fig. 8.9**). In case we have a large number of wells, we can define several windows for each well, where besides the first one (where a connectivity index exists between each well pair) a single value is assigned to all the connectivity indices in each pair (**Fig. 8.10**). In this method, we assume that having a large number of wells, the reservoir performance is less sensitive to connectivity indices between distant wells. If we have some information about the anisotropy of the reservoir, we may use an ellipse instead of a circle to define the windows. In addition, if we have some geological information about the reservoir, we can use it to change the shape of the window. For example, if we know a set of wells are poorly connected to some wells compared to the other wells, we can assign different values inside a window (**Fig. 8.11**). Depending on the number and size of the windows, this approach can decrease the number of the parameters efficiently. For example, for a 25x16 case (Fig. 8.10), defining three windows at radius 3,520, 4,620, and 5,720 ft decreases the number of estimated connectivity indices from 861 to 425.

Here, we show the application of windowing for some heterogeneous cases.

Case 8-5. Similar to Case 6-5, this case is an 8x8 system. However, a couple of channels and barriers exist in the reservoir (**Fig. 8.12**). First, using the data for 400 months, we calculated the modified connectivity indices of the system. Then we applied a window at 2,750 ft for the system (similar to the one depicted in Fig. 8.9) that reduced the number of unknown parameters from 136 to 88. By calculating the connectivity indices for this case, we observed that the results are in good agreement with the results of the full model (**Fig. 8.13**). In addition, the R^2 values obtained with the window are 0.9996 and 0.9998 for production rate and injector BHPs, respectively. This shows the number of parameters was sufficient to fit the data.

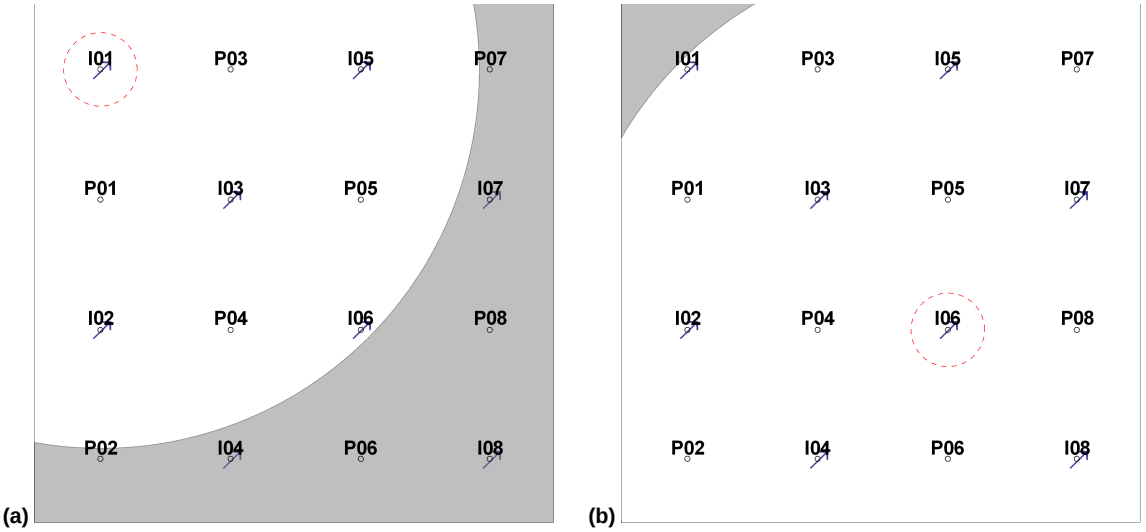

Fig. 8.9—A single window system for 8x8 Case. For Well I01 (a), 8 wells (I04, I07, I08, P02, P06, P07 and P08) will have the same connectivity index. For Well I06 (b), none of the wells are outside the window, so a different connectivity index will be assigned between this well and all the other wells.

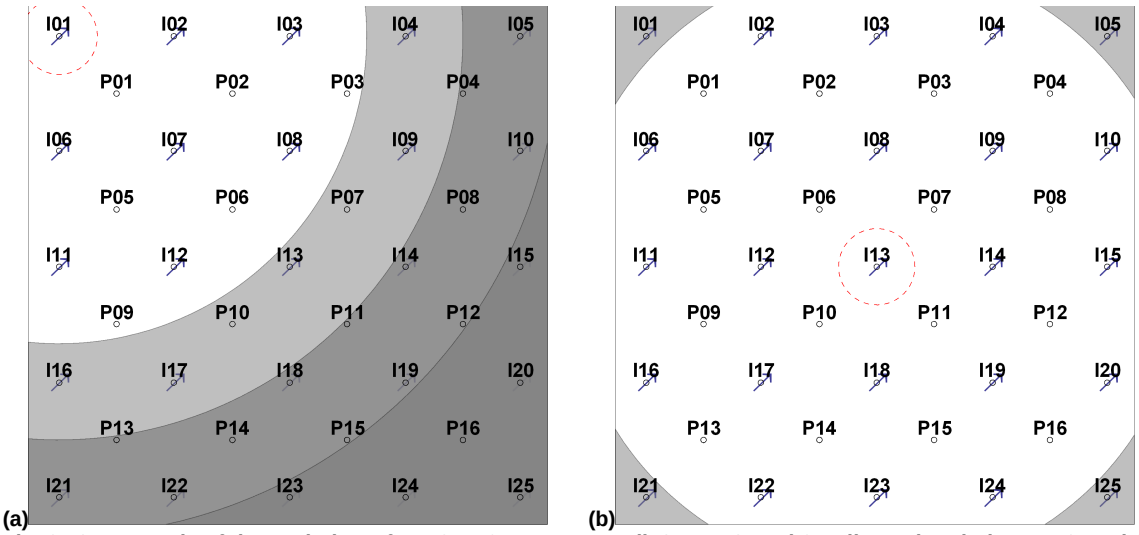

Fig. 8.10—Example of three windows for a 25x16 case. For Well I01, 7, 13, and 6 wells are in Windows 1, 2, and 3 respectively. For Well I13, only 4 wells exist in Window 1.

Case 8-6. This case is a 25x16 heterogeneous reservoir (**Fig. 8.14**), with similar rock and fluid properties as Case 3-1. Without windowing, 861 parameters were required for this case. Applying one window at 2,750 ft, the number of parameters decreased to 254 and the R^2 values obtained with this window were 0.9987 and 0.9926 for production rate and injector BHP, respectively. Applying a different window (this time at 3,520 feet) we obtained slightly better prediction (R^2 was 0.9993 for injector BHP

and 0.9964 for production rate). Running the full model (with no window) for this case the prediction became more accurate (R^2 was 0.9996 for injector BHP and 0.9987 for production rate). By comparing the modified connectivity indices obtained from two window sizes and the ones obtained from the full case, as expected, we observed that the results of the larger window are in a better agreement with the full case (**Fig. 8.15**). Thus for this case, although the smaller window size could predict the reservoir performance properly, its estimated modified connectivity indices was relatively less accurate than the ones of large window. In addition, we applied a three-window pattern (similar to Fig. 8.10) and the results were very close to the large window.

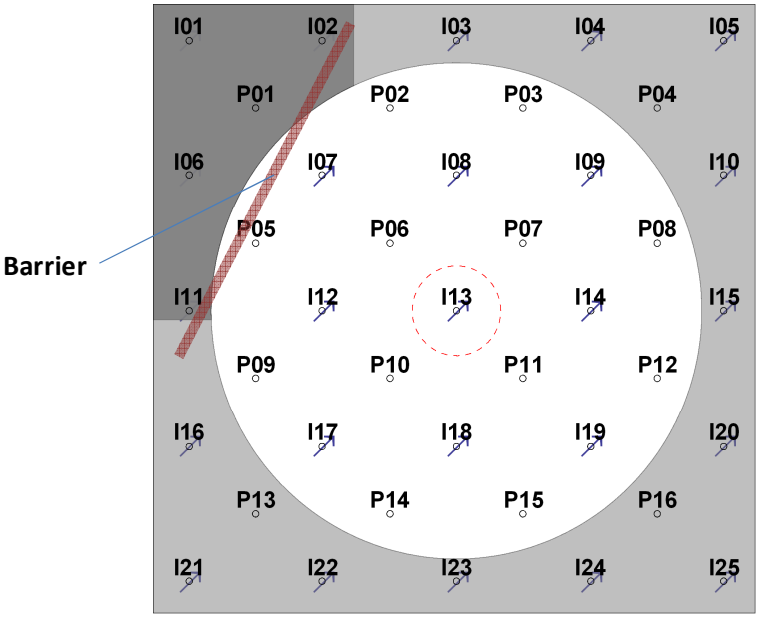

Fig. 8.11—If we know a major feature exists in the reservoir, we can change the windows. For example, in this case, we used a different window for wells behind the barrier.

The windowing technique can effectively reduce the number of required parameters in modeling the data. In the two presented cases, it could accurately predict the reservoir performance and provide the proper connectivity indices if the window size was selected carefully. One further development in this technique could be the recommendation on the proper size, shape, and number of windows, based on information available on heterogeneity, anisotropy, and the number and location of the wells. In addition, investigating the possible effects of operating conditions–including shut-ins, large injection rate changes and injector/producer conversions–could improve the practical aspects of this technique.

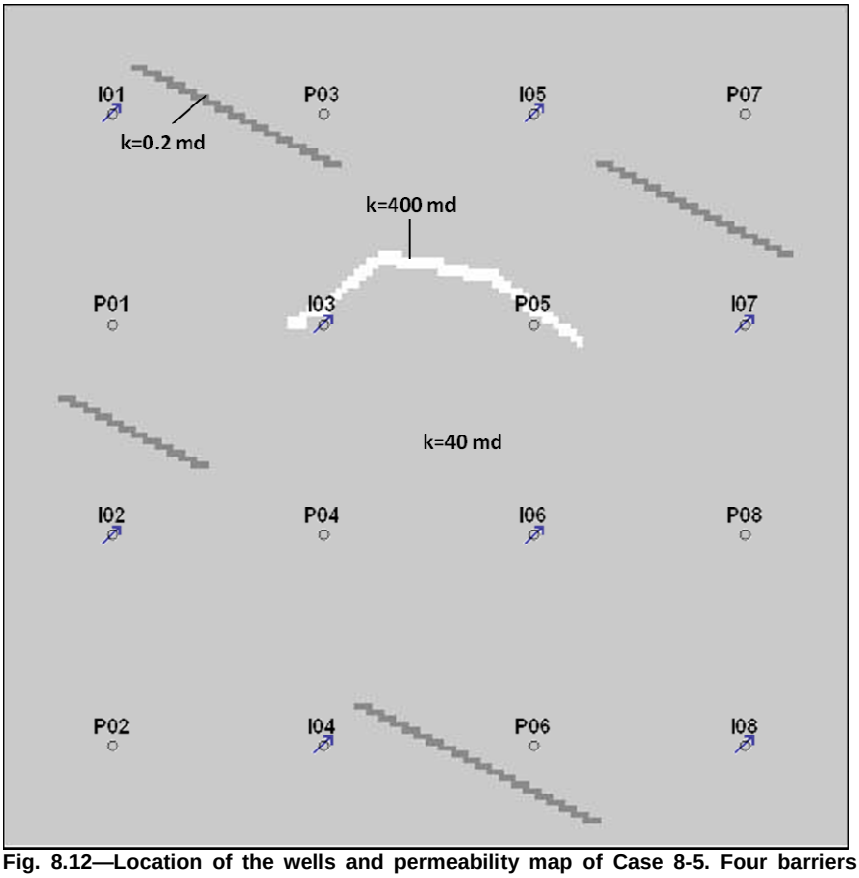

Fig. 8.12—Location of the wells and permeability map of Case 8-5. Four barriers and a channel exist in the system.

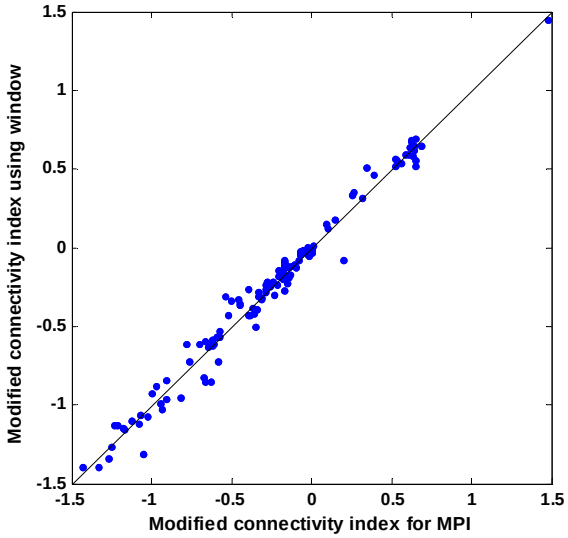

Fig. 8.13—Applying a window (as we have in Fig. 8.9), the estimated modified connectivity coefficients are in good agreement with the case with no window.

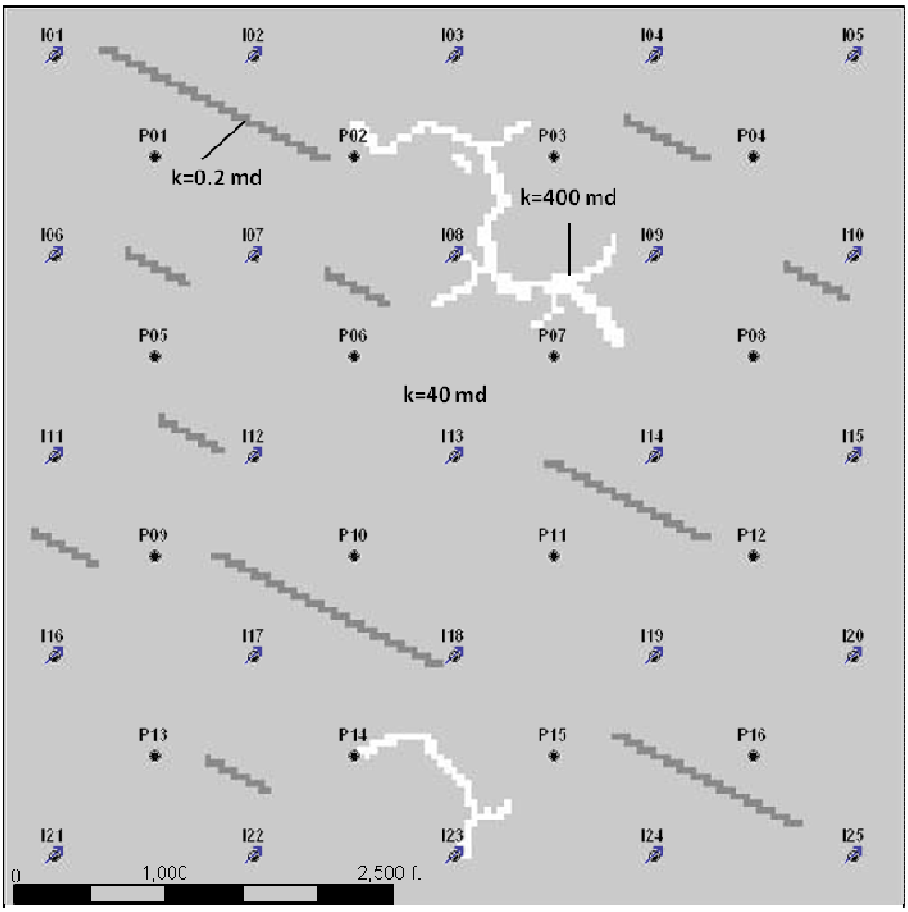

Fig. 8.14—Location of the wells and permeability map of Case 8-6. Eleven barriers and two channels exist in the system.

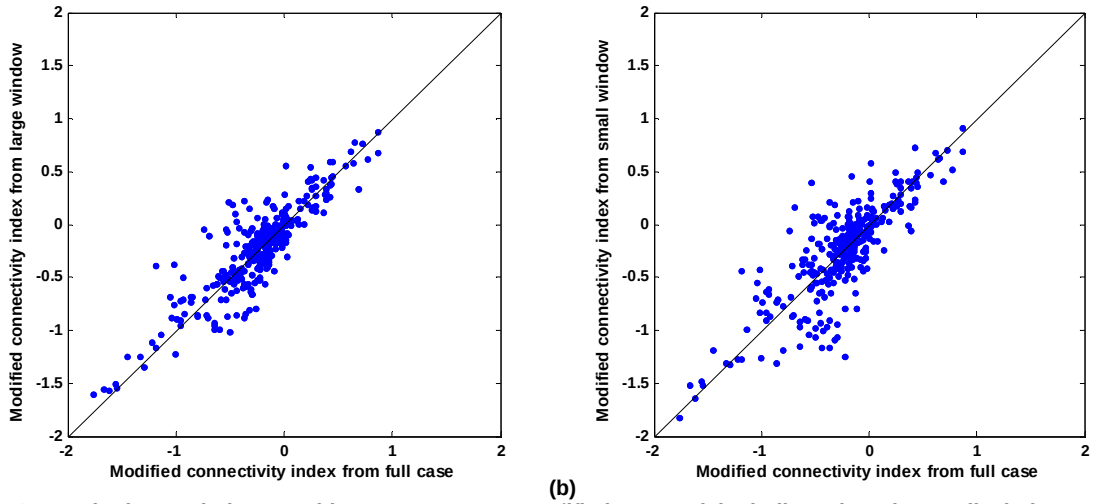

a) **(b)**

Fig. 8.15—The large window provides more accurate modified connectivity indices than the small window. For Case 8-6, using large window the R^2 between the modified connectivity indices obtained from large window and the ones from full case is 0.78; however, this value for the results of small window is 0.63.

8.5 Conclusions

In the nonvolumetric reservoirs, the material balance assumption of the MPI-based method is violated. The modification developed here is able to overcome this problem for specific cases; however, in general we may need to conduct different proper modifications to model the data with respect to the reservoir properties and leaking mechanism. In the nonrectangular systems, the homogeneous influence function is different from the one for the rectangular case. By selecting a proper box for defining the influence matrix we can decrease this distortion. If the effect of interwell heterogeneity on the heterogeneity matrix is larger than the effect of the reservoir shape, this distortion may be negligible. However, in general, we need to take into account this distortion in interpreting the connectivity indices. If we increase the number of wells, the number of model parameters increases, which leads to a dramatic growth in the required computational effort. We suggest the windowing technique to decrease the number of model parameters. In two heterogeneous hypothetical cases, this technique could determine the major connectivity indices and predict the reservoir performance accurately with a significantly reduced computational effort.

9. RELATIONSHIP AND COMPARISON OF THE CM AND MPI-BASED METHOD

9.1 Introduction

In this dissertation we described two methods to evaluate interwell connectivity using injection and production data. Both these methods are based on the pseudosteady-state productivity index and material balance. However, because of dissimilar assumptions the methods are different in some aspects. In the following sections, after describing the similarities and differences between these methods, we derive some of the CM properties using MPI. Then we discuss the possible advantages of each method.

9.2 Comparison of the Models for a 1x1 Case

The main difference between the CM and MPI approaches arises from the definition of productivity index. In the MPI we use the analytical formula of the influence matrix to describe the multiwell system. In the CM, however, we approximate the effect of this matrix in the pore volume between the well pairs using a single number. To investigate this issue better we consider the 1x1 case, where the full analytical form of the CM is derived. Recalling Eq. 3.1, and assuming step changes in injection rate and producer BHPs we have

$$\hat{q}(t)=q(t_0)\exp\left[-\frac{(t-t_0)}{\tau}\right]+\sum_{m=1}^{n}\left\{\exp\left[\frac{(t_m-t)}{\tau}\right]-\exp\left[\frac{(t_{m-1}-t)}{\tau}\right]\right\}w(t_m)+ \\ J\left[p_{wf}(t_0)\exp\left[-\frac{(t-t_0)}{\tau}\right]-p_{wf}(t)+\sum_{m=1}^{n}\left\{\exp\left[\frac{(t_m-t)}{\tau}\right]-\exp\left[\frac{(t_{m-1}-t)}{\tau}\right]\right\}p_{wf}(t_m)\right] \quad \text{. ..... (9.1)}$$

Considering the productivity index definition at time zero for $\hat{q}(t_0)$ we have

$$\hat{q}(t_0)=J\left[\bar{p}(0)-p_{wf}(t_0)\right]\exp\left[-\frac{(t-t_0)}{\tau}\right] \quad \text{..... (9.2)}$$

Replacing Eq. 9.2 in Eq. 9.1 we obtain

$$\hat{q}(t)=\sum_{m=1}^{n}\left\{\exp\left[\frac{(t_m-t)}{\tau}\right]-\exp\left[\frac{(t_{m-1}-t)}{\tau}\right]\right\}w(t_m)+ \\ J\left[-p_{wf}(t)+\sum_{m=1}^{n}\left\{\exp\left[\frac{(t_m-t)}{\tau}\right]-\exp\left[\frac{(t_{m-1}-t)}{\tau}\right]\right\}p_{wf}(t_m)\right]+J\bar{p}(0)\exp\left[-\frac{(t-t_0)}{\tau}\right] \quad \text{..... (9.3)}$$

On the other hand, for a 1x1 case, the influence matrix is

$$[\mathbf{A}]=\begin{bmatrix}a_{inj} & a_{con}\\ a_{con} & a_{prod}\end{bmatrix} \quad \text{..... (9.4)}$$

Rewriting Eq. 6.19 (to have the same notation as the CM, here we assume the injection rates positive) for a 1x1 case using MPI we have (see Appendix E)

$$q(t)=\frac{a_{con}}{a_{prod}}w(t)+\sum_{m=1}^{n}w(t_m)\left(1-\frac{a_{con}}{a_{prod}}\right)\left\{\exp\left[-\frac{\kappa(t-t_m)}{a_{prod}c_tV_p}\right]-\exp\left[-\frac{\kappa(t-t_{m-1})}{a_{prod}c_tV_p}\right]\right\}$$
$$+\frac{\kappa}{a_{prod}}\sum_{m=1}^{n}p_{wf}(t_m)\left\{\exp\left[-\frac{\kappa(t-t_m)}{a_{prod}c_tV_p}\right]-\exp\left[-\frac{\kappa(t-t_{m-1})}{a_{prod}c_tV_p}\right]\right\} \quad \text{. ..... (9.5)}$$
$$+\frac{\kappa}{a_{prod}}\overline{p}_i\exp\left[\frac{-c_1}{c_tV_p}(t-t_0)\right]$$

Eqs. 9.3 and 9.5 have some similarities and differences. First of all, as expected, in both equations the coefficient of the producers' BHPs are the same. In fact, *J* in the CM (where it is defined as the single producer productivity index) is equivalent to κ/a_{prod} in Eq. 9.5. We also observe that the exponential coefficients in the second term of both equations are equivalent. Based on that, τ in the CM will be

$$\tau=\frac{a_{prod}c_tV_p}{\kappa}, \quad \text{..... (9.6)}$$

which is equivalent to the original definition of the τ in the CM (see Section 3.2). The coefficients of the injection rates in the equations are slightly different from each other. For the coefficient of the injection rate, the solutions are equivalent to each other in the specific case when a_{con}=0. However, in general, there is no equivalent for τ for injection rates in the MPI solution.

9.3 Comparison of the Models for Multiwell Cases

For the case of several injectors and producers, the comparison becomes complicated. In fact, as we observed in Appendix A, a couple of intuitive approximations and generalizations in the CM extension for the cases of several injectors and producers make the comparison difficult.

Similar to Eq. 9.3. rewriting Eq. 3.2 based on initial pressure, yields

$$\hat{q}_j(t)=\lambda_{pj}J_j\overline{p}_j(t_0)\exp\left[-\frac{(t_0-t)}{\tau_{pj}}\right]+\sum_{i=1}^{i=I}\lambda_{ij}\sum_{m=1}^{n}\left\{\exp\left[\frac{(t_m-t)}{\tau_{ij}}\right]-\exp\left[\frac{(t_{m-1}-t)}{\tau_{ij}}\right]\right\}w_j(t_m)$$
$$+\sum_{k=1}^{k=K}\nu_{kj}\left\{p_{wf_j}(t_0)\exp\left[-\frac{(t_0-t)}{\tau_{kj}}\right]-\frac{\lambda_{pj}J_j}{\nu_{kj}}p_{wf_j}(t_0)\exp\left[-\frac{(t_0-t)}{\tau_{pj}}\right]-p_{wf_k}(t)\right. \quad \text{. ..... (9.7)}$$
$$\left.+\sum_{m=1}^{n}\left\{\exp\left[\frac{(t_m-t)}{\tau_{kj}}\right]-\exp\left[\frac{(t_{m-1}-t)}{\tau_{kj}}\right]\right\}p_{wf_k}(t_m)\right\}$$

In terms of the MPI solution (considering injection rates as positive numbers), in Eq. 6.19 the coefficient of injection rate is

Injection rate coefficient=

$$-\left(\frac{1-\exp\left(-\frac{[\mathbf{1}]_{1xK}\left[\mathbf{A_{prod}}\right]^{-1}[\mathbf{1}]_{Kx1}\,\kappa t}{c_t V_p}\right)}{[\mathbf{1}]_{1xK}\left[\mathbf{A_{prod}}\right]^{-1}[\mathbf{1}]_{Kx1}}\right)\left[\mathbf{A_{prod}}\right]^{-1}\left([\mathbf{1}]_{KxK}\left[\mathbf{A_{prod}}\right]^{-1}\left[\mathbf{A_{con}}\right]^{T}-[\mathbf{1}]_{KxI}\right)+\left[\mathbf{A_{prod}}\right]^{-1}\left[\mathbf{A_{con}}\right]^{T}, \quad (9.8)$$

which consists of two parts: the first part contains the delay term, and the second part is independent of the delay term. Assuming a small delay term, [**Λ**] (the *I*x*J* matrix of λs) is equivalent to

$$[\mathbf{\Lambda}]=-\frac{1}{[\mathbf{1}]_{1xK}\left[\mathbf{A_{prod}}\right]^{-1}[\mathbf{1}]_{Kx1}}\left[\mathbf{A_{prod}}\right]^{-1}\left([\mathbf{1}]_{KxK}\left[\mathbf{A_{prod}}\right]^{-1}\left[\mathbf{A_{con}}\right]^{T}-[\mathbf{1}]_{KxI}\right)+\left[\mathbf{A_{prod}}\right]^{-1}\left[\mathbf{A_{con}}\right]^{T} \quad (9.9)$$

that defines the share of each injector in each producer. This confirms that the λs are independent from the injection rates. Interestingly, for several sets of influence matrices, the summation of these λs for each injector is exactly one and its values between the well pairs is between 0 and 1.

Similar to the 1x1 case, we could not determine the interpretation of τ in terms of the MPI solution.

To determine ν_{ij}, we can rewrite Eq. 6.19 as (see Appendix E)

$$\vec{q}(t)=\kappa\left[\mathbf{A_{prod}}\right]^{-1}\bar{p}(t_0)\exp\left[\frac{-c_1}{c_t V_p}(t-t_0)\right][\mathbf{1}]_{Kx1}-\left[\mathbf{A_{prod}}\right]^{-1}\left[\mathbf{A_{con}}\right]^{T}\vec{w}(t)+$$

$$\kappa\left[\mathbf{A_{prod}}\right]^{-1}\sum_{m=1}^{n}\left\{\exp\left[\frac{-c_1(t-t_m)}{c_t V_p}\right]-\exp\left[\frac{-c_1(t-t_{m-1})}{c_t V_p}\right]\right\}\frac{-\sum\vec{w}(t_m)+\sum\left[\mathbf{A_{prod}}\right]^{-1}\left[\mathbf{A_{con}}\right]^{T}\vec{w}(t_m)}{c_1}[\mathbf{1}]_{Kx1} \quad (9.10)$$

$$+\kappa\left[\mathbf{A_{prod}}\right]^{-1}\left\{\sum_{m=1}^{n}\left\{\exp\left[\frac{-c_1(t-t_m)}{c_t V_p}\right]-\exp\left[\frac{-c_1(t-t_{m-1})}{c_t V_p}\right]\right\}\frac{\kappa[\mathbf{1}]_{1xK}\left[\mathbf{A_{prod}}\right]^{-1}\vec{p}_{q^*}(t_m)}{c_1}[\mathbf{1}]_{Kx1}-\vec{p}_{q^*}(t)\right\}$$

We can rewrite the producers' BHP term as

BHP term=

$$\kappa\left[\mathbf{A_{prod}}\right]^{-1}\left\{\sum_{m=1}^{n}\left\{\exp\left[\frac{-c_1(t-t_m)}{c_t V_p}\right]-\exp\left[\frac{-c_1(t-t_{m-1})}{c_t V_p}\right]\right\}\frac{\kappa[\mathbf{1}]_{1xK}\left[\mathbf{A_{prod}}\right]^{-1}\vec{p}_{q^*}(t_m)}{c_1}[\mathbf{1}]_{Kx1}-\vec{p}_{q^*}(t)\right\}. \quad (9.11)$$

The producers' BHP term is not exactly the same as the one we have for the CM. In fact, besides the influence matrix it includes two parts: the first term is the summation of convolution of the weighted average of the producers' BHP from previous time steps up to the current one (this part is constant for all the wells at each time step), and the second term is the vector of producers' BHP at the current time step. The inverse of the [**A**$_{\mathbf{prod}}$] is mainly dominated by its diagonal. So for each producer, the main portion of the BHP term is caused by the difference between its own BHP and the convolution term. In the CM (Eq. 9.7) the BHP term consists of the initial producers' BHP and the convolution of the producers' BHP (and

not their average). Thus we cannot determine the equivalent ν (producers' connectivity in the CM) using MPI.

Because of the differences between the initial pressure term in the CM (initial average reservoir pressure for each well) and MPI (initial average reservoir pressure for the reservoir) the coefficient of initial pressure of the CM cannot be approximated using MPI.

9.4 Segmented and Compensated CM from MPI

In Section 3.2, we showed that using CM, if the producer BHPs are the same at one time step, we can ignore the BHP term at that time step. We also showed that if the producers' BHPs are constant during an interval, we can estimate the BHP term using a constant number at that interval. Here, we investigate this property using the MPI-derived formula.

If the producers' BHPs are equal to each other as we showed in Section 7.3.4, we have

$$\frac{\kappa[\mathbf{1}]_{1xK}\left[\mathbf{A}_{\mathbf{prod}}\right]^{-1}\vec{p}_{q^*}(t)}{c_1}=p_{q^*}(t)\cdot \quad \text{..... (9.12)}$$

Thus the BHP term as defined in Eq. 9.11 will be

$$\text{BHP term}=\kappa\left[\mathbf{A}_{\mathbf{prod}}\right]^{-1}\left\{-\exp\left[\frac{-c_1(t-t_{n-1})}{c_t V_p}\right]p_{q^*}(t)[\mathbf{1}]_{Kx1}+\sum_{m=1}^{n-1}\left\{\exp\left[\frac{-c_1(t-t_m)}{c_t V_p}\right]-\exp\left[\frac{-c_1(t-t_{m-1})}{c_t V_p}\right]\right\}\frac{\kappa[\mathbf{1}]_{1xK}\left[\mathbf{A}_{\mathbf{prod}}\right]^{-1}\vec{p}_{q^*}(t_m)}{c_1}[\mathbf{1}]_{Kx1}\right\} \quad \text{. ..... (9.13)}$$

We can easily see that if the producers' BHPs are constant for a few months, this term decays to zero. However, if the BHPs are different from each other and then become equal and constant depending on the delay term, it may take a few months for this term to reach zero. In a similar way, we can see that for the case of unequal BHPs, if BHP remains constant for a few time steps, the BHP term will become constant in time until we disturb the producer BHPs. We will illustrate these properties later using a synthetic example.

In Section 4.4, we discussed that the effect of changing the skin factor of a well on the well performance is different from the BHP changes. We observed that changing the skin factor affects the λs; so we could not use the segmented CM for these cases. We tried to show these using Eq. 9.9. Since we need to change one of the elements of the $[\mathbf{A}_{\mathbf{prod}}]$ matrix and this matrix is inverted in λ calculation, we could not prove the λ change analytically. However, using Eq. 9.9 we tested it for simple 5x4 and 2x2 cases and we found that having even small changes in skin factor of one producer affects all the λs.

In Section 5.2, we discussed that changing the number of injectors has no effect on the CM parameters. In Appendix F, we show this analytically based on the definition of λ using MPI. In Section 5.2, we also

showed that we can approximate the λs after shutting in a producer based on the λs before shut-in (Eq. 5.10). We tried to derive this property using the definition of λ from Eq. 9.9. Since this definition contains the inverse of a matrix, and since removing one row and column of the matrix complicates analytical calculation of the matrix inverse in terms of the original one, we could not derive the formula. However, for the 2x2 and 5x4 cases we tested Eq. 5.10 parametrically using calculations in Mathematica based on Eq. 9.9, and we observed that Eq. 5.10 exactly reproduces the λ of the shut-in case.

Here we show our findings using a simple example.

Example 9-1. For Case 3-1, we calculated λ using Eq. 9.9 based on the influence matrix obtained analytically. We observed that the λs are in excellent agreement with the ones obtained from CM (**Fig. 9.1**). To compare the BHP terms from both methods, we calculated the BHP effect using MPI (Eq. 9.11). By plotting this term for P01 with the BHP term from the segmented and full CM, we observed that they are generally in good agreement (**Fig. 9.2**). Looking more precisely at this figure, we see a small difference between the solutions where the BHP changes. At the first few months after changing the BHP, we have a sharp change for all methods. In the MPI this sharp change is followed by a smaller sharp change and then approaches smoothly to a constant value. For both the segmented and full CM, however, after the sharp change the BHP term becomes a constant value instantly (or changes slightly and linearly). As discussed earlier in this section, this transition in the MPI is because of the effect of the previous average producers' BHP on the BHP term. However, in the segmented CM we cannot consider it. In addition, this transition is not observed in the full CM because the τ between the producers is generally high (see Section 4.2) that makes the BHP term changes slightly. To investigate this, we ran a case with constant injection rate, where the only source of the production rate changes is the BHP changes. As we observed in this case, this smooth change in production rate exists after every BHP change and MPI can describe it better than the CM (**Fig. 9.3**).

Example 9-2. In Case 4-2 we observed that the estimated λs before and after stimulation are different from each other. We calculated the λs for this case using Eq. 9.9. As we expected, λs for periods before and after stimulation were different from each other and they were very close to those obtained using the CM when we run the CM separately on the data (**Fig. 9.4**).

Example 9-3. For Case 7-2, which is a 5x4 case with several barriers and a channel (Fig. 7.7), we calculate the λs using Eq. 9.2, and they are in good agreement with the ones obtained using the CM (**Fig. 9.5**). In addition, we calculated the λs based on the heterogeneity matrix obtained for the case with constant BHP (as we discussed in Section 7.3.4, the heterogeneity matrix is different from the true one). As expected, we observed that the calculated λs for this case are similar to the ones obtained from the heterogeneity matrix estimated from data with BHP changes.

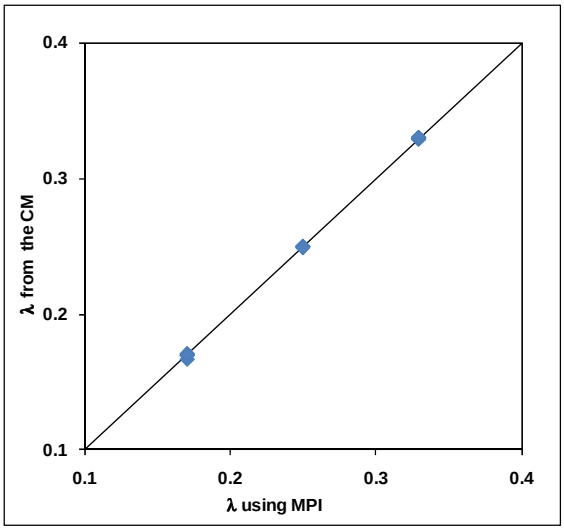

Fig. 9.1—Estiamted λs based on the analytical formula (Eq. 9.9) are in an excellent agreement with the ones obtained from the CM for a homogeneous case (Case 3-1).

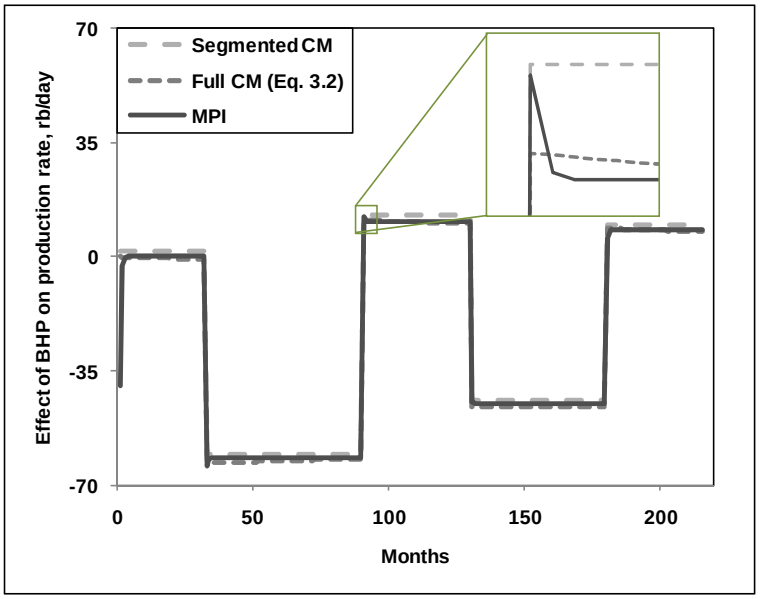

Fig. 9.2—The BHP term in the full CM and the segmented CM are different from the MPI. When the BHP changes, λ_0 instantly changes and then stays constant until the next segmentation time. In the full CM, after a sudden change, the BHP term changes slightly linearly until the next segmentation point. In the MPI, after a sudden change at the time of BHP change, at the first few time steps the BHP term changes exponentially and then stays constant until the next segmentation point.

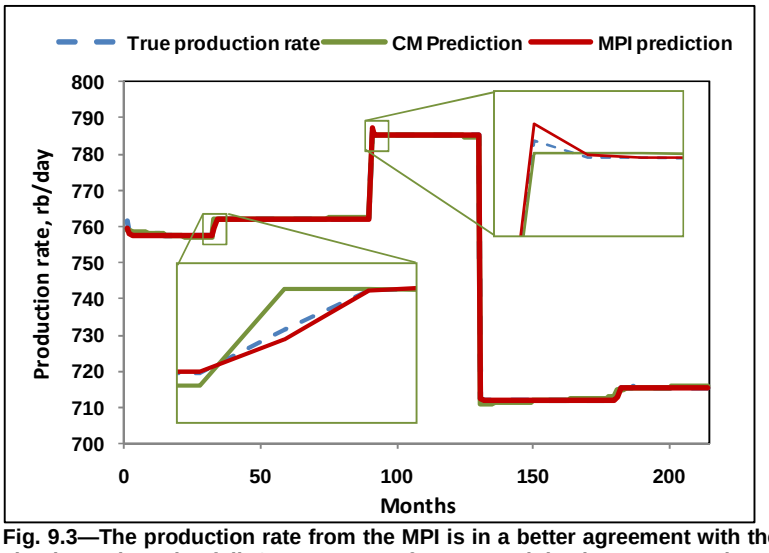

Fig. 9.3—The production rate from the MPI is in a better agreement with the production rate from the numerical simulator than the full CM. In case of constant injection rate, producer BHP is the only controller of the production rate fluctuations.

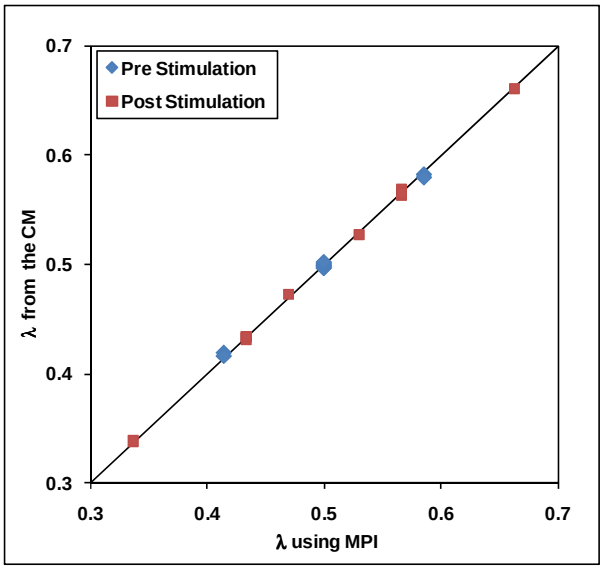

Fig. 9.4—The estimated λs based on analytical formula (Eq. 9.9) are in a good agreement with the ones using the CM for a stimulated case (Case 4-2) for both pre- and post-stimulation periods.

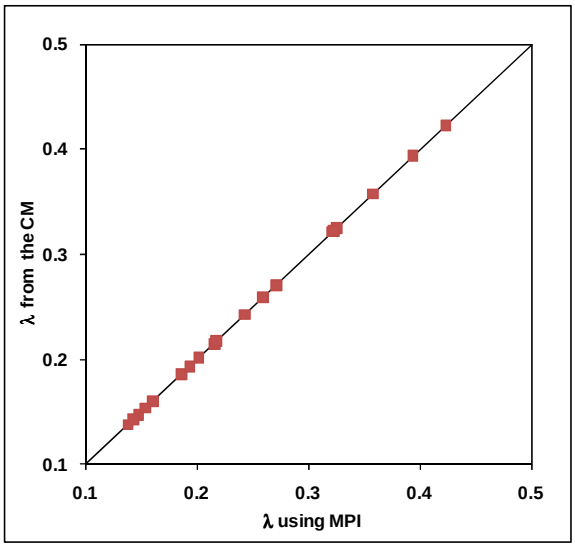

Fig. 9.5—The estimated λs using MPI are in a good agreement with the ones using the CM for a heterogeneous case (Case 7-2). The estimated λs using MPI were constant even for the case of constant BHP and ignoring the injectors' BHP.

9.5 Comparison of the Methods

We can analyze the injection and production data using both the CM and MPI-based methods. However, the type of connectivity information provided using each method is different. In the CM, we get two sets of connectivity information. The first one is the connectivity coefficient between the wells. For injector/producer well pairs, this coefficient (λ) is dimensionless and indicates the effect of injection rate of an injector on the production rate of a specific producer. For producer/producer pairs, this coefficient (ν) has the dimension of the productivity index and simply shows how changing the BHP of a producer affects the production rate of this well and the other producers. The second set of information obtained from the CM is the time constant (τ) that tells us how the injection rate (or the producers' BHP) will be shifted. In the MPI-based method all the connectivity information of the system is summarized in the modified heterogeneity matrix, and the connectivity indices between the wells (independent of their role as an injector or producer) are the same type. We can directly calculate λs from the heterogeneity matrix.

We can summarize the relative advantages of the information obtained from the CM and the MPI as:

- The heterogeneity matrix obtained using the MPI-based method represents a first-type connectivity parameter. Since the homogeneous influence matrix includes the geometry related component of the connectivity, the heterogeneity matrix merely shows the reservoir heterogeneity. In the CM, the distance of the wells is a key parameter in λ.
- Depending on existence of a barrier or a channel in the interwell region and the surrounding areas (that affects the productivity index of the well and so the modified connectivity indices),

the modified connectivity indices may have negative or positive values. The main advantage of having this type of information is that we can interpret the results easily: for example, for an adjacent well pair, a large negative or positive connectivity index can tell us the geological features in (or around) the interwell region. However, in the CM, the λs represent relative connectivity (for example, the summation of λ in the CM approach cannot exceed 1 for each injector) and are always positive. Interpretation of the results of this kind of connectivity is not as straightforward as in the MPI-based method. On the other hand, the advantage of λs is that they quickly tell us which injector/producer well pairs are better connected in general. For example, a very small λ between a relatively far well pair (that may even have a positive connectivity index) tells us that, practically, injection from this injector has negligible effect on the production rate of the producer.

- Comparison of πs and λs can reveal some information about the connectivity of the system that is not available at this point from the MPI-based method.
- Since the gradient of the parameters is available for the CM, the process of estimating model parameters is much faster than the MPI-based method.
- An option of oil prediction of the producers is available for the CM (Sayarpour 2008). Such an option does not exist for the MPI-based method at this point. In the MPI-based method we only use the injection rate, liquid production rate, and wellbore BHPs. In fact, by converting the rate data into pressure information, we evaluate the connectivity based on the pressure-dependent components of the data. However, another source of data that we did not consider in the MPI-based method (for the CM this is developed in Sayarpour 2008; but we did not cover it in this work) is the reservoir and interwell saturation-dependent data (e.g. water cut). These data have valuable information about the connectivity. By adopting these to our models we can also provide a more powerful model to predict the oil and water rates.
- In the CM, we can run the model for one well independent from the other wells. Although as we explained in Section 3.3 this may lead to incorrect results, in cases of large numbers of wells this could be the best option. Such an option is not available for the MPI-based method at this point.
- The MPI-based method is able to decouple the effect of skin factor from the interwell heterogeneity component. As we discussed in Case 7-2, by updating the diagonal elements we are able to consider the effect of the skin factor, while the other elements of the matrix stay effectively constant during the whole production period. This property of the MPI-based method will also help us to optimize reservoir performance under variable well conditions. In contrast, in the CM, if we change the skin of a well we need to update the λs of all the other (at least surrounding) wells, and for this we need new data.

- The MPI-based method provides flexibility to include more data in our model and also extract more connectivity information. For example, if we have the injectors' BHP we can obtain the connectivity indices between the injectors. If producers are converted to injectors, the connectivity matrix will not change. We can also define the producers' connectivity using the $[\mathbf{\Delta'_{prod}}]$ matrix. In the CM we cannot obtain information about the injectors' connectivity (except for those that are converted from a producer). We can get information of producers' connectivity information from the full CM; however, the results are different from the λs.
- If the producers' BHP data are not available, applying the segmented CM is the best choice to evaluate the connectivity. The results of the MPI-based method are strongly dependent on the presence of the BHP data.
- Having limited data or only small variability in the operating conditions may lead to nonunique results in the estimation of the MPI heterogeneity matrix. In these cases, we may only get some relative information from the $[\mathbf{\Delta'_{con}}]$ and the heterogeneity matrix may be not suitable for performance prediction. In fact, the more frequent and more substantial the changes are in the operational conditions, the more accurate is the estimation of the heterogeneity matrix. In particular, the heterogeneity matrix obtained using the MPI-based method is not sensitive to the producers' shut-in. In contrast, CM works better in cases where we have fewer changes in the production conditions (besides the injection rates). Applying the compensated CM can help to use the data in the case of a limited number of changes in the number of the active producers.
- Since both methods are based on single phase liquid pseudosteady-state regime, their performance decreases in case of a long transient regime, considerable gas production, and existence of the fluids with different mobility ratios.

9.6 Conclusions

The main difference between the CM and the MPI-based method stems from the definition of the productivity index in the two models. We rearranged the MPI formula in a way to be comparable with the CM. We were unable to determine an equivalent for τ and ν using the MPI. However, we found an analytical form of λ using MPI, which is in excellent agreement with the results obtained using the CM. We also compared the application and results of both methods. In general, the connectivity indices obtained using the MPI-based method may give clearer information on the reservoir heterogeneity. However, the results of the CM provide straightforward information for decision making in waterflood management. In cases of available and frequent fluctuating BHP and numerous shut-ins, the MPI may be more reliable; however, in cases that lack BHP data, the CM results are more consistent.

10. SUMMARY AND CONCLUSIONS

10.1 Summary

In this dissertation we described two approaches to evaluate connectivity: the CM and the MPI-based method.

Yousef et al. (2006) developed the CM. In this dissertation:

- By determining the analytical derivation of the CM over the model parameters, we represented a more effective and faster algorithm to estimate the model parameters.
- We investigated some of the limitations of the CM.
- We developed the segmented CM to estimate the model parameters in cases of unavailable fluctuating BHP data.
- We derived the compensated CM to model the injection and production data in case the number of producers changes.
- We showed the application of the developed method in several hypothetical cases and a field case.

We developed the MPI-based method to evaluate the connectivity:

- We derived the analytical formula to predict the liquid production rate and injectors' BHP under a pseudosteady-state regime in a rectangular homogeneous reservoir.
- We defined a robust connectivity parameter to evaluate connectivity in a heterogeneous system based on the estimated influence function of the system
- We discussed the possible issues in interpreting the estimated connectivity indices under different conditions
- We discussed the application of the method in practical cases where the system is nonvolumetric or nonrectangular or contains a large number of wells.
- We showed several hypothetical examples of the application of the method on homogeneous and heterogeneous cases.

We discussed the relationship and differences between the methods and compared their applicability in different cases.

10.2 Conclusions

Based on our modifications on the CM we found:

- If the producers' BHP changes and the BHP data are unavailable, the segmented CM can approximate the effect of BHP changes from the injection and production rates. On the basis of hypothetical cases, we observed that this model is able to approximate the effect of BHP changes with no use of BHP data and can estimate the true connectivity coefficients. In

addition, comparing to the simple CM, the segmented CM estimates the production rate more accurately.

- If the segmentation times are unknown, our new algorithm is able to determine the correct segmentation times.
- Stimulating the producers will change the connectivity coefficients, so we need to estimate the connectivity coefficients before and after the stimulation separately. However, if these intervals are not long enough, the segmented CM can provide a good estimation of connectivity coefficients in a single model.
- The compensated CM reveals the relationship between the connectivity coefficients before and after changes in the number of producers. By applying this method, we can evaluate the connectivity before and after this change using a single model. The producer/producer connectivity term defined using this method provides more information on the reservoir connectivity. In a hypothetical case the compensated CM estimated the true connectivity coefficients for before and after change shut-in accurately.
- If the producers' BHPs change and are unmeasured and the number of producers changes, applying the segmented and compensated CM simultaneously enables us to evaluate connectivity of the system. We applied the CMs in a hypothetical case and obtained the correct connectivity coefficients. In a field case the estimated connectivity coefficients, obtained from applying both the segmented and compensated CM, were in good agreement with the seismic impedance map.

Based on the MPI-based approach:

- In a rectangular homogeneous reservoir, under pseudosteady-state regime we can analytically predict the producers' liquid rate and injectors' BHP using the MPI. The MPI has the connectivity information of the wells. This model considers the effect of changing the number of the wells and stimulation. However, the nonunique mobility ratio and dramatic change in total compressibility decreases the performance of the method. We tested this model on several hypothetical cases and the results were in excellent agreement with the reservoir simulator results.
- We can estimate the influence matrix for the heterogeneous cases from the injection and production data. The difference between the estimated influence matrix and the theoretical one from the homogeneous case provides the heterogeneity matrix. A simple modification of this matrix provides a robust connectivity parameter that is independent of the location and distance of the wells, total number of the wells, and operating conditions.

- We need to consider the properties of the heterogeneity matrix in interpreting the connectivity indices. Having more diverse data and longer intervals of data allows us to estimate the heterogeneity matrix more accurately.
- Applying the developed model for the nonvolumetric reservoirs, we are able to predict the reservoir performance more accurately. However, in general, considering the reservoir properties and leaking mechanism, we require a different proper modification to model the data.
- In reservoirs with nonrectangular shapes, the homogeneous influence matrix is different from the rectangular case. The effect of the reservoir shape on the heterogeneity matrix depends on both the shape of the reservoir and interwell heterogeneity. Selecting a proper box to determine the theoretical influence matrix can decrease this effect.
- Increasing the number of the wells increases the number of model parameters dramatically. By applying the windowing technique, we can decrease the number of model parameters and predict the reservoir performance with acceptable accuracy.

Comparing the CM and the MPI-based method:

- The calculated λs from the analytical formula based on the MPI are in excellent agreement with the CM results. We could not determine an analytical equivalent for the other CM connectivity parameters.
- The accuracy of both the CM and MPI-based method decreases by increasing the length of the transient region.
- The modified connectivity indices from the MPI-based method can give clearer information on reservoir heterogeneity. The CM parameters, however, provide better information for decision making in waterflood management.
- In the case of available and frequent fluctuating BHP and numerous shut-ins, the MPI-based method may be more reliable; however, if the producers' BHPs are unmeasured, the CM results are more consistent.

NOMENCLATURE

Variables

$a[]$	=	influence function, dimensionless
B	=	formation volume factor, dimensionless
c_1	=	arbitrary constant, L^4t/m
c_2	=	arbitrary constant, L^3/t
c_t	=	total compressibility, Lt^2/m
e	=	arbitrary constant, dimensionless
h	=	formation thickness, L
I	=	total number of injection wells
J	=	single well productivity index, L^4t/m
k	=	permeability, L^2
K	=	total number of production wells
l_p	=	lost percentage of the injector, dimensionless
L	=	objective function of the production rate prediction in the CM, $(L^3/t)^2$
m	=	time step number in the CM
n	=	number of time steps in the CM, dimensionless
p_{wf}	=	producer's BHP, $m/(Lt^2)$
p'_{wf}	=	shifted producer's BHP, $m/(Lt^2)$
$\overline{p}$	=	average reservoir pressure, $m/(Lt^2)$
$\overline{p}_i$	=	initial average reservoir pressure, $m/(Lt^2)$
q	=	total liquid production rate, L^3/t
q_{0j}	=	the unbalanced term, reservoir L3/t
q'	=	shifted production rate in the compensated CM, L^3/t
$\hat{q}$	=	total estimated liquid production rate, L^3/t
s	=	skin factor, dimensionless
S	=	number of the segmentation times in the segmented CM
t	=	time, t
V_P	=	pore volume, L^3
w	=	injection rate, L^3/t
w'	=	shifted injection rate, L^3/t
w_{eff}	=	effective injection rate, L^3/t
x_e	=	size of study area in x direction, L

y_e = size of study area in y direction, L

x_w = individual well x coordinate, L

y_w = individual well y coordinate, L

x_D = x/x_e, dimensionless x-coordinate well location

y_D = y/x_e, dimensionless y-coordinate well location

α = impulse response for injection rate, dimensionless

β = impulse response for pressure, dimensionless

δ = element of the heterogeneity matrix, dimensionless

κ = rock-fluid factor, L^4t/m

λ_{ij} = interwell connectivity index between an injector/producer pair using the CM, dimensionless

λ_{pj} = coefficient of the primary production term, dimensionless

$\lambda'_{0j}(s)$ = segmentation time constant of producer *j* between segmentation times *s*-1 and *s*, L^3/t

μ = fluid viscosity, m/(Lt)

ν = interwell connectivity index between a producer/producer pair using the CM, L^4t/m

τ_{ij} = time constant between injector/producer well pair, t

τ_{pj} = time constant of the primary production term,t

ξ = variable of integration in the CM

ζ = decrease in the lost percentage, dimensionless

Matrices and vectors

$[\mathbf{A}]$ = influence matrix, dimensionless

$[\mathbf{A^{(H)}}]$ = estimated influence matrix for the heterogeneous case, dimensionless

$[\mathbf{D_s}]$ = diagonal matrix of skin factors, dimensionless

$[\mathbf{E}]$ = arbitrary matrix with the same element in each row, dimensionless

$[\mathbf{J}]$ = productivity index, L^4t/m

$[\mathbf{\Delta}]$ = heterogeneity matrix, dimensionless

$[\mathbf{\Delta'}]$ = modified heterogeneity matrix, dimensionless

$[\mathbf{\Lambda}]$ = matrix of λs between the injectors and producers

$\vec{w}$ = vector of injection rates, L^3/t

$\vec{q}$ = vector of production rates, L^3/t

$\vec{p}_{i*}$ = vector of injectors' BHP, $m/(Lt^2)$

$\vec{p}_{q^*}$ = vector of producers' BHP, m/(Lt^2)

Subscript

con = index of the interaction of injector/producer well pairs in the influence and heterogeneity matrix

i = injector index

inj = injector index in the influence and heterogeneity matrix

j = producer index

k = Producer-BHP index

prod = producer index in the influence and heterogeneity matrix

q = producer index

s = segmentation time index

Superscript

x = shut-in well index

T = transposed

REFERENCES

Abbaszadeh, M., Takahashi, I., and Suzuki, K. 2004. Integrated Seismic-Guided Characterization of a Carbonate Reservoir in Abu Dhabi, U.A.E. Paper SPE 90533 presented at the SPE Annual Technical Conference and Exhibition, Houston, 25-29 Sept. doi: 10.2118/90533-MS.

Albertoni, A. 2002. Inferring Interwell Connectivity From Well-Rate Fluctuations in Waterfloods. MS Thesis, The University of Texas at Austin, Texas.

Albertoni, A. and Lake, L.W. 2003. Inferring Interwell Connectivity Only From Well-Rate Fluctuations in Waterfloods. *SPEREE* **6** (1): 6-16. SPE-83381-PA. doi: 10.2118/83381-PA.

Demiroren, A.N. 2007. Inferring Interwell Connectivity from Injection and Production Data Using Frequency Domain Analysis. MS Thesis, Texas A&M University, College Station, Texas.

Demiryurek, U., Banaei-Kashani, F., Shahabi, C., and Wilkinson, F. 2008. Neural-Network based Sensitivity Analysis for Injector-Producer Relationship Identification. Paper SPE 112124 presented at the SPE Intelligent Energy Conference and Exhibition Amsterdam, 25–27 February. doi: 10.2118/112124-MS.

Dinh, A and Tiab, D. 2008a. Inferring Interwell Connectivity From Well Bottomhole-Pressure Fluctuations in Waterfloods. *SPEREE* **11** (5): 874-881. SPE-106881-PA. doi: 10.2118/106681-MS.

Dinh, A and Tiab, D. 2008b. Interpretation of Interwell Connectivity Tests in a Waterflood System. Paper SPE 116144 presented at the SPE Annual Technical Conference and Exhibition, Denver, 21-24 November. doi: 10.2118/116144-MS.

Du, Y. and Guan, L. 2005. Interwell Tracer Tests: Lessons Learned from Past Field Studies. Paper SPE 93140 presented at the SPE Asia Pacific Oil and Gas Conference and Exhibition, Jakarta, 5-7 April. doi: 10.2118/103188-MS.

Gentil, P. 2005. The Use of Multilinear Regression Models in Patterned Waterfloods: Physical Meaning of the Regression Coefficients. MS Thesis, The University of Texas at Austin, Texas.

Heffer, K.J., Fox, R.J., McGill, C.A., and Koutsabeloulis, N.C. 1997. Novel Techniques Show Links between Reservoir Flow Directionality, Earth Stress, Fault Structure and Geomechanical Changes in Mature Waterfloods. *SPEJ* **2** (2): 91-98. SPE-30711-PA. doi: 10.2118/30711-PA.

Hird, K.B. and Dubrule, O. 1998. Quantification of Reservoir Connectivity for Reservoir Description Applications. *SPEREE* **1** (1): 12-17. SPE-30571-PA. doi: 10.2118/30571-PA.

Honarpour, M.M. and Tomutsa, L. 1990. Injection/Production Monitoring: An Effective, Method for Reservoir Characterization. Paper SPE 20262 presented at the SPE/DOE Enhanced Oil Recovery Symposium, Tulsa, Oklahoma, 22-25 April. doi: 10.2118/20262-MS.

Jansen, F.E. and Kelkar, M.G. 1996. Exploratory Data Analysis of Production Data. Paper SPE 35184 presented at the Permian Basin Oil and Gas Recovery Conference, Midland, Texas, 27-29 March. doi: 10.2118/35184-MS.

Jansen, F.E. and Kelkar, M.G. 1997a. Application of Wavelets to Production Data in Describing Inter-Well Relationships. Paper SPE 38876 presented at the SPE Annual Technical Conference and Exhibition, San Antonio, Texas, 5-8 October. doi: 10.2118/38876-MS.

Jansen, F.E. and Kelkar, M.G. 1997b. Non-Stationary Estimation of Reservoir Properties Using Production Data. Paper SPE 38729 presented at the SPE Annual Technical Conference and Exhibition, San Antonio, Texas, 5-8 October. doi: 10.2118/38729-MS.

Jensen, J.L., Lake, L. W., Bui, T.D., Yousef, A. A., and Gentil, P. 2004. Interwell Connectivity and Diagnosis Using Correlation of Production and Injection Rate Data in Hydrocarbon Production. Annual report, Contract No. DE-FC26-03NT15397, U.S. DOE, Washington, DC (August 2004).

Jensen, J.L., Lake, L.W., Corbett, P.W.M., and Goggin, D.J. 2003. *Statistics for Petroleum Engineers and Geoscientists*. Amsterdam, The Netherlands: Elsevier.

Jensen, J.L., Lake, L. W., Yousef, A. A., et al. 2007. Interwell Connectivity and Diagnosis Using Correlation of Production and Injection Rate Data in Hydrocarbon Production. Final report, Contract No. DE-FC26-03NT15397, U.S. DOE, Washington, DC (March 2007).

Kaviani, D., Jensen, J.L., Lake, L.W., and Fahes, M. 2008. Estimation of Interwell Connectivity in the Case of Fluctuating Bottomhole Pressures. Paper SPE 117856 presented at the International Petroleum Exhibition and Conference, Abu Dhabi, 3-6 November. doi: 10.2118/117856-MS.

Lake, L.W. and Jensen, J. L. 1991. A review of heterogeneity measures used in reservoir characterization. *In Situ* **15** (4): 409-439.

Li, W., Jensen, J.L., Ayers, W.B., Hubbard, S.M., and Heidari, M.R. 2009. Comparison of Interwell Connectivity Predictions Using Percolation, Geometrical, and Monte Carlo Models. *Journal of Petroleum Science and Engineering*, **68** (3): 180-186. doi:10.1016/j.petrol.2009.06.013

Liang, X., Weber, D.B., Edgar, T.F., Lake, L.W., Sayarpour, M., and Al-Yousef, A. 2007. Optimization of Oil Production Based on a Capacitance Model of Production and Injection Rates. Paper SPE 107713 presented at the Hydrocarbon Economics and Evaluation Symposium, Dallas, 1-3 April. doi: 10.2118/107713-MS.

Liu, F. and Mendel, J.M. 2007. Forecasting Injector-Producer Relationships From Production and Injection Rates Using an Extended Kalman Filter. Paper SPE 110520 presented at the SPE Annual Technical Conference and Exhibition, Anaheim, California, 11-14 November. doi: 10.2118/110520-MS.

Lee, W.J., Rollins, J.B., and Spivey, J. P. 2003. *Pressure Transient Testing*. Textbook Series, SPE, Richardson, Texas **9**:190-201.

Ozkan, E., 1988. Performance of Horizontal Wells. PhD dissertation, University of Tulsa, Tulsa, Oklahoma.

Panda, M.N. and Chopra, A.K. 1998. An Integrated Approach to Estimate Well Interactions. Paper SPE 39563 presented at the SPE India Oil and Gas Conference and Exhibition, New Delhi, India, 17-19 February. doi: 10.2118/39563-MS.

Raghavan, R. 1993. *Well Test Analysis*. Englewood Cliffs, New Jersey: Prentice-Hall Inc.

Refunjol. B.T. and Lake, L.W. 1999. Reservoir Characterization Based on Tracer Response and Rank Analysis of Production and Injection Rates. In *Reservoir Characterization-Recent Advances*, ed. R. Schatzinger and J. Jordan. Chap 15, 209–218. AAPG Memoir 71.

Sayarpour, M., Zuluaga, E., Kabir, C.S., and Lake, L.W. 2007. The Use of Capacitance-Resistive Models for Rapid Estimation of Waterflood Performance. Paper SPE 110081 presented at the SPE Annual Technical Conference and Exhibition, Anaheim, California, 11-14 November. doi: 10.2118/110081-MS.

Sayarpour, M., Kabir, C.S., and Lake, L.W. 2008. Field Applications of Capacitance-Resistive Models in Waterfloods. Paper SPE 114983 presented at the SPE Annual Technical Conference and Exhibition, Denver, 21-24 November. doi: 10.2118/114983-MS.

Sayarpour, M. 2008. Development and Application of Capaciatnce/Resistive Models to Water/CO_2 Floods. PhD dissertation, The University of Texas at Austin, Texas.

Soeriawinata, T. and Kelkar, M. 1999. Reservoir Management Using Production Data. Paper SPE 52224 presented at the SPE Mid-Continent Operations Symposium, Oklahoma City, Oklahoma, 28-31 March. doi: 10.2118/52224-MS.

Umnuayponwiwat, S. and Ozkan, E. 2000. Pressure Transient Behavior and Inflow Performance of Multiple Wells in Closed Systems. Paper SPE 62988 presented at the SPE Annual Technical Conference and Exhibition, Dallas, 1-4 October. doi: 10.2118/62988-MS.

Valkó, P. P., Doublet, L.E., and Blasingame, T.A. 2000. Development and Application of the Multiwell Productivity Index (MPI). *SPEJ* **5** (1): 21-31. doi: 10.2118/51793-PA.

Wang. J., Abiaze, J., McVay, D., and Ayers, W. 2008. Evaluation of Reservoir Connectivity and Development Recovery Strategies in Monument Butte Field, Utah. SPE paper 116695 presented at the SPE Annual Technical Conference and Exhibition, Denver, 21-24 November. doi: 10.2118/116695-MS.

Weber, D., Edgar, T.F., Lake, L.W., Lasdon, L., Kawas, S., and Sayarpour, M. 2009. Improvements in Capacitance-Resistive Modeling and Optimization of Large Scale Reservoirs. Paper SPE 121299 presented at the SPE Western Regional Meeting, San Jose, California, 24-26 March. doi: 10.2118/121299-MS.

Yousef, A.A, Jensen, J.L., and Lake, L.W. 2009. Integrated Interpretation of Interwell Connectivity Using Injection and Production Fluctuations. *Mathematical Geosciences*, **41** (1): 81 - 102. doi: 10.1007/s11004-008-9189-x.

Yousef, A.A., Gentil, P., Jensen, J.L., and Lake, L.W. 2006. A Capacitance Model To Infer Interwell Connectivity From Production and Injection Rate Fluctuations. *SPEREE* **9** (5): 630-646. SPE-95322-PA. doi: 10.2118/95322-PA.

Yousef, A.A. 2006. Investigating Statistical Techniques to Infer Interwell Connectivity From Production and Injection Fluctuations. PhD dissertation, The University of Texas at Austin, Texas.

Zhai, D., Mendel, J.M. and Liu, F. 2009. A New Method for Continual Forecasting of Interwell Connectivity in Waterfloods Using an Extended Kalman Filter. Paper SPE 121393 presented at the SPE Western Regional Meeting, San Jose, California, 24-26 March. doi: 10.2118/121393-MS.

APPENDIX A. DERIVATION OF THE CM

Here we describe the derivation of the CM based on Yousef (2006), and explain the cases where our solution is different from the original one.

The starting point of the CM is the simple material balance of the reservoir fluid(s)

$$c_t V_P \frac{d\bar{p}}{dt} = w(t) - q(t). \quad \text{(A.1)}$$

Also based on the definition of the productivity index we have

$$q = J\left(\bar{p} - p_{wf}\right). \quad \text{(A.2)}$$

In Section 6.2 we will see that for a multiwell system we need to use the matrix of *J*, instead of a single number. At this point we continue with the current solution and we will discuss it in detail in Sections 9.2 and 9.3. Solving Eq. A.2 for the average pressure and differentiating over time we have

$$\frac{d\bar{p}}{dt} = \frac{d\left(\frac{q}{J} + p_{wf}\right)}{dt}. \quad \text{(A.3)}$$

Substituting Eq. A.3 into A.1 we obtain

$$c_t V_P \cdot \frac{1}{J} \cdot \frac{dq}{dt} + q(t) = w(t) - c_t V_P \frac{dp_{wf}}{dt}. \quad \text{(A.4)}$$

Defining $\tau = \frac{c_t V_P}{J}$ we have

$$\frac{dq}{dt} + \frac{1}{\tau} q(t) = \frac{1}{\tau} w(t) - J \frac{dp_{wf}}{dt}, \quad \text{(A.5)}$$

which is a first order differential equation. To solve this equation we can use the integrating factor technique. Multiplying both sides of Eq. A.5 by $e^{\frac{t}{\tau}}$ we obtain:

$$e^{\frac{t}{\tau}}\left[\frac{dq}{dt} + \frac{1}{\tau} q(t)\right] = e^{\frac{t}{\tau}}\left[\frac{1}{\tau} w(t) - J \frac{dp_{wf}}{dt}\right] \quad \text{(A.6)}$$

or:

$$\frac{d}{dt}\left[e^{\frac{t}{\tau}} q(t)\right] = e^{\frac{t}{\tau}}\left[\frac{1}{\tau} w(t) - J \frac{dp_{wf}}{dt}\right]. \quad \text{(A.7)}$$

Integrating and rearranging we have

$$q(t) = ce^{-\frac{t}{\tau}} + e^{-\frac{t}{\tau}} \int e^{\frac{t}{\tau}}\left[\frac{1}{\tau} w(t) - J \frac{dp_{wf}}{dt}\right] dt. \quad \text{(A.8)}$$

Finding c at $t=t_0$ [which will be the production rate at time 0: $q(t_0)$] and substituting t with ξ as the integration variable, we obtain

$$q(t)=q(t_0)e^{-\frac{(t-t_0)}{\tau}}+e^{-\frac{t}{\tau}}\int_{\xi=t_0}^{\xi=t}e^{\frac{\xi}{\tau}}\left[\frac{1}{\tau}w(\xi)-J\frac{dp_{wf}}{d\xi}\right]d\xi\,. \quad \text{(A.9)}$$

And by integration by parts and simplifying

$$q(t)=q(t_0)e^{-\frac{(t-t_0)}{\tau}}+\frac{e^{-\frac{t}{\tau}}}{\tau}\int_{\xi=t_0}^{\xi=t}e^{\frac{\xi}{\tau}}w(\xi)d\xi+J\left[p_{wf}(t_0)e^{\frac{-(t-t_0)}{\tau}}-p_{wf}(t)+\frac{e^{\frac{-t}{\tau}}}{\tau}\int_{\xi=t_0}^{\xi=t}e^{\frac{\xi}{\tau}}p_{wf}(\xi)d\xi\right]. \quad \text{(A.10)}$$

Since we generally do not have an analytical form for the injection rates and BHP changes, we need to discretize these integrals. Based on Yousef (2006) for the case of constant BHP we have

$$q(n)=q(t_0)e^{-\frac{(n-n_0)}{\tau}}+\sum_{m=n_0}^{n}\alpha_m w(m)\,, \quad \text{(A.11)}$$

where

$$\alpha_m=\frac{\Delta n}{\tau}e^{\frac{(m-n)}{\tau}}\,. \quad \text{(A.12)}$$

In fact, the total term $\int_{\xi=t_0}^{\xi=t}e^{\frac{\xi}{\tau}}w(\xi)d\xi$ is descretized. The problem we have in this case is that the summation of the impulse response is not one. Because

$$\sum_{m=1}^{n}\alpha_m=\frac{\Delta n}{\tau}\left[\frac{1-e^{\frac{-n\Delta n}{\tau}}}{1-e^{\frac{-\Delta n}{\tau}}}\right], \quad \text{(A.13)}$$

which is generally different from 1, we need to do a normalization to apply the CM correctly. If we assume constant injection rate at each interval (in other words a step function for injection signal), the integral term of the injection signal in Eq. A.10 can be written as:

$$\frac{e^{-\frac{t}{\tau}}}{\tau}\int_{\xi=t_0}^{\xi=t}e^{\frac{\xi}{\tau}}w(\xi)d\xi=\frac{e^{-\frac{t}{\tau}}}{\tau}\int_{\xi=t_0}^{\xi=t_1}e^{\frac{\xi}{\tau}}w(t_1)d\xi+\frac{e^{-\frac{t}{\tau}}}{\tau}\int_{\xi=t_1}^{\xi=t_2}e^{\frac{\xi}{\tau}}w(t_2)d\xi+\ldots+\frac{e^{-\frac{t}{\tau}}}{\tau}\int_{\xi=t_{n-1}}^{\xi=t}e^{\frac{\xi}{\tau}}w(t)d\xi \quad \text{(A.14)}$$

and at each time step we have

$$\frac{e^{-\frac{t}{\tau}}}{\tau}\int_{\xi=t_m-1}^{\xi=t_m}e^{\frac{\xi}{\tau}}w(t_m)d\xi=w(t_m)\cdot e^{-\frac{t}{\tau}}\cdot e^{w}\Big|_{w=t_{m-1}/\tau}^{w=t_m/\tau}=w(t_m)\left[e^{\frac{(t_m-t)}{\tau}}-e^{\frac{(t_{m-1}-t)}{\tau}}\right]. \quad \text{(A.15)}$$

Recalling Eq. A.11, based on Eq. A.15, we can redefine the αs as

$$\alpha_m = \left[e^{\frac{(t_m - t)}{\tau}} - e^{\frac{(t_{m-1} - t)}{\tau}} \right] . \quad \text{(A.16)}$$

It can be easily shown that the summation of αs in Eq. A.16 is 1. So in this research, instead of the definition of α from Eq. A.12, we use Eq. A.16. We use the same discretization for the BHP term. Sayarpour (2008) showed the solution for linear change (instead of step function) in injection signal and producer BHPs that we do not repeat here.

Extension of the CM to multiple producers and injectors is not as clear as the CM for single injector and producer, and more assumptions are involved. For this purpose, where we have *I* injectors for producer *j* we can replace Eq. A.1 with

$$c_t V_P \frac{d\overline{p}}{dt} = \sum_{i=1}^{I} \lambda_{ij} w_i(t) - q(t), \quad \text{(A.17)}$$

where λ_{ij} is the interwell connectivity coefficient between an injector/producer well pair, *I* is the number of injectors. In this case we will have only one τ for each producer pair (similar to the approach of Liang et al. 2007). However, if we want to have different attenuation for each well pair, the definition will be different, and for each injector/producer pair we obtain

$$c_{t_{ij}} V_{p_{ij}} \frac{d\overline{p}_{ij}}{dt} = \lambda_{ij} w_i(t) - q_{ij}(t), \quad \text{(A.18)}$$

where c_{tij}, V_{pij} and $\overline{p}_{ij}$ are properties of the volume drained by producer *j* when only injector *i* is being injected and q_{ij} is the production rate at well *j* that corresponds to the effect of injector *i*. Applying superposition law and also eliminating the $\overline{p}_{ij}$ term using the productivity index, we obtain

$$\sum_{i=1}^{I} \tau_{ij} \frac{dq_{ij}}{dt} + \sum_{i=1}^{I} q_{ij}(t) = \sum_{i=1}^{I} \lambda_{ij} w_i(t) - \frac{dp_{wf_j}}{dt} \sum_{i=1}^{I} \tau_{ij} J_{ij} \quad \text{(A.19)}$$

where $\tau_{ij} = \frac{c_{t_{ij}} V_{p_{ij}}}{J_{ij}}$. By solving this equation, we obtain the general form of the CM for multiple producers and injectors. In this solution the primary production term will be

$$\text{Primary production term} = q_{1j}(t_0) e^{\frac{-(t-t_0)}{\tau_{1p}}} + q_{2j}(t_0) e^{\frac{-(t-t_0)}{\tau_{2p}}} + \ldots + q_{Kj}(t_0) e^{\frac{-(t-t_0)}{\tau_{Kp}}} \quad \text{(A.20)}$$

and by imposing the same time constant (τ_p) in all terms we obtain (as assumed by Yousef, 2006)

$$\text{Primary production term} = q_j(t_0) e^{\frac{-(t-t_0)}{\tau_p}} . \quad \text{(A.21)}$$

Combining Eqs. A.20 and A.21 and solving for τ_p, we have (this is not from Yousef, 2006)

$$\tau_p = \frac{-(t-t_0)}{\ln\left[q_{1j}(t_0)e^{\frac{-(t-t_0)}{\tau_{1p}}} + q_{2j}(t_0)e^{\frac{-(t-t_0)}{\tau_{2p}}} + \ldots + q_{Kj}(t_0)e^{\frac{-(t-t_0)}{\tau_{Kp}}}\right] - \ln\left[q_j(t_0)\right]}. \quad \text{(A.22)}$$

Since we do not have the fraction of primary production term of each injector (q_{ij}), we cannot estimate τ_p using this formula. Also, τ_p depends on time; in other words, it is not a model parameter in the strict sense of the word. We checked this for a few cases, and we found out that for small to moderate τs (τ less than 50 time units)−since the primary production term is only important for the first few months−the change of τ_p could be neglected; however, for larger values of τ (or low diffusivity or permeability), this assumption is not valid. However, intuitively considering Eq. A.21 as the primary production term is reasonable.

For the producer's BHP term, based on Eq. A.16 we will have

$$\text{BHP term} = \sum_{k=1}^{K} J_{kj}\left[p_{wf_j}(t_0)e^{\frac{-(t-t_0)}{\tau_{kj}}} - p_{wf_j}(t) + \frac{e^{\frac{-t}{\tau_{kj}}}}{\tau_{kj}}\int_{\xi=t_0}^{\xi=t} e^{\frac{\xi}{\tau_{kj}}} p_{wf_j}(\xi)\,d\xi\right] \quad \text{(A.23)}$$

and since in the CM the J_{kj} is not known, in a similar way as for the primary production term, for the BHP term we will have

$$\text{BHP term} = \nu_j\left[p_{wf_j}(t_0)e^{\frac{-(t-t_0)}{\tau_j}} - p_{wf_j}(t) + \frac{e^{\frac{-t}{\tau_j}}}{\tau_j}\int_{\xi=t_0}^{\xi=t} e^{\frac{\xi}{\tau_j}} p_{wf_j}(\xi)\,d\xi\right] \quad \text{(A.24)}$$

where ν_j is equivalent to the summation of partial productivity indices (J_{ij}) for each producer. The problem with this formulation of the BHP term is that we do not have the interaction of the producer BHPs. In other words, we cannot see the effect of changing BHP in one well on the production rate of the other wells. Thus, Yousef (2006) modified Eq. A.24 into

$$\text{BHP term} = \sum_{k=1}^{K} \nu_{kj}\left[p_{wf_k}(t_0)e^{\frac{-(t-t_0)}{\tau_{kj}}} - p_{wf_k}(t) + \frac{e^{\frac{-t}{\tau_{kj}}}}{\tau_{kj}}\int_{\xi=t_0}^{\xi=t} e^{\frac{\xi}{\tau_{kj}}} p_{wf_{kj}}(\xi)\,d\xi\right]. \quad \text{(A.25)}$$

Eq. A.25 is the final form of the BHP term derived by Yousef (2006). We have more discussion on it in Section 9.3. Solving Eq. A.19 and combining with Eqs. A.21 and A.22 we obtain

$$q_j(t) = \lambda_{pj} q_j(t_0)e^{\frac{-(t-t_0)}{\tau_{pj}}} + \sum_{i=1}^{i=I} \lambda_{ij} w'_{ij}(t) + \sum_{k=1}^{k=K} \nu_{kj}\left[p_{wf_k}(t_0)e^{\frac{-(t-t_0)}{\tau_j}} - p_{wf_k}(t) + p'_{wf_{kj}}(t)\right]. \quad \text{(A.26)}$$

w'_{ij} is the shifted (convolved) injection rate of injector i with respect to producer j. Based on Eq. A.16 w'_{ij} is:

$$w'_{ij}(t) = \sum_{m=1}^{n} \left[e^{\frac{(t_m - t)}{\tau_{ij}}} - e^{\frac{(t_{m-1} - t)}{\tau_{ij}}} \right] w_j(t_m) \quad \text{..... (A.27)}$$

and p'_{wfkj} is the shifted BHP of producer k with respect to producer j

$$p'_{wf_{kj}}(t) = \sum_{m=1}^{n} \left[e^{\frac{(t_m - t)}{\tau_{kj}}} - e^{\frac{(t_{m-1} - t)}{\tau_{kj}}} \right] p_{wf_{kj}}(t_m) \cdot \text{..... (A.28)}$$

APPENDIX B. DEVELOPMENT OF MPI CONCEPT

In a rectangular homogeneous reservoir with constant reservoir properties, representing the well as a line source, the pressure distribution in the reservoir during the pseudosteady state is (Ozkan, 1988)

$$\bar{p} - p(x,y) = \frac{1}{\kappa} \times a\left[x_D, y_D, x_{wD}, y_{wD}, y_{eD}\right] q \quad \text{.....(B.1)}$$

where q is the production rate of the well. κ is the rock-fluid factor defined as

$$\kappa = \frac{2\pi kh}{\mu B} \quad \text{.....(B.2)}$$

where μ is the single-phase viscosity, B is the formation volume factor, k is the permeability, and h is the reservoir thickness (all units are in SI). $a[\ ]$, the dimensionless drop in pressure, is

$$a\left[x_D, y_D, x_{wD}, y_{wD}, y_{eD}\right] = 2\pi y_{eD}\left(\frac{1}{3} - \frac{y_D}{y_{eD}} + \frac{y_D^2 + y_{wD}^2}{2y_{eD}^2}\right) + 2\pi \sum_{m=1}^{\infty} \frac{t_m}{m} \cos\left(m\pi x_D\right) \times \cos\left(m\pi x_{wD}\right) \quad \text{.....(B.3)}$$

and

$$t_m = \frac{\cosh\left[m\pi\left(y_{eD} - \left|y_D - y_{wD}\right|\right)\right] + \cosh\left\{m\pi\left[y_{eD} - \left(y_D + y_{wD}\right)\right]\right\}}{\sinh\left(m\pi y_{eD}\right)}, \quad \text{.....(B.4)}$$

where x_D, y_D and y_{eD} are defined as x/x_e, y/x_e and y_e/x_e respectively, and x_{wD} and y_{wD} are dimensionless location of the well. x_e and y_e are size of the reservoir in the x and y directions, respectively.

Based on symmetry properties, we need to rewrite influence function as

$$a\left[x_D, y_D, x_{wD}, y_{wD}, y_{eD}\right] = a^1\left[\max\left(x_D, x_{wD}\right), \max\left(y_D, y_{wD}\right), \min\left(x_D, x_{wD}\right), \min\left(y_D, y_{wD}\right), y_{eD}\right]$$

where

$$a^1\left[x_D, y_D, x_{wD}, y_{wD}, y_{eD}\right] = \begin{cases} a\left[x_D, y_D, x_{wD}, y_{wD}, y_{eD}\right] & \text{if } \left(x_D - x_{wD}\right) > \left(y_D - y_{wD}\right) \\ a\left[y_D, x_D, y_{wD}, x_{wD}, 1/y_{eD}\right] & \text{otherwise} \end{cases}$$

Valkó et al. (2000) presented a fast algorithm to calculate the influence function.

Using superposition for K wells Eq. B.1 becomes (Valkó et al., 2000)

$$\bar{p} - p(x,y) = \frac{1}{\kappa} \times \sum_{k=1}^{K} a\left[x_D, y_D, x_{wDk}, y_{wDk}, y_{eD}\right] q_k \ . \quad \text{.....(B.5)}$$

At the well locations, considering the skin factor effect, Eq. B.5 becomes

$$\bar{p} - p_j = \frac{1}{\kappa} \times \left(\sum_{k=1}^{K} a\left[x_D, y_D, x_{wDk}, y_{wDk}, y_{eD}\right] q_k + s_j q_j \right), \quad \text{.....(B.6)}$$

where p_j is the flowing BHP at well j. Writing Eq. B.6 in matrix from, we obtain

$$\Delta\vec{p} = \frac{1}{\kappa} \times \left([\mathbf{A}] + [\mathbf{D_s}] \right) \vec{q} \ , \quad \text{.....(B.7)}$$

where $\Delta\vec{p}$ is the vector of drawdown, $\vec{q}$ is the vector of well rates. [**A**] is the influence matrix with elements a_{ij},

$$[\mathbf{A}] = \begin{bmatrix} a_{11} & a_{12} & \cdots & a_{1K} \\ a_{21} & a_{22} & \cdots & a_{2K} \\ \vdots & \cdots & \ddots & \vdots \\ a_{K1} & a_{K2} & \cdots & a_{KK} \end{bmatrix} \quad \text{.....(B.8)}$$

and

$$[\mathbf{D_s}] = \begin{bmatrix} s_1 & 0 & \cdots & 0 \\ 0 & s_2 & \cdots & 0 \\ \vdots & \cdots & \ddots & \vdots \\ 0 & 0 & \cdots & s_K \end{bmatrix} . \quad \text{.....(B.9)}$$

Solving Eq. B.7 for $\vec{q}$ we obtain

$$\vec{q} = \kappa \times \left([\mathbf{A}] + [\mathbf{D_s}] \right)^{-1} \Delta\vec{p} \ . \quad \text{.....(B.10)}$$

Here, for simplicity, we use [**A**], as the summation of [**A**] and [$\mathbf{D_s}$] for the initial set of skin factor of the wells.

The productivity index describes the relationship between production rate and drawdown:

$$\vec{q} = [\mathbf{J}] \Delta\vec{p} \quad \text{.....(B.11)}$$

Comparing B.10 and B.11 we obtain:

$$[\mathbf{J}] = \kappa \times [\mathbf{A}]^{-1} \quad \text{.....(B.12)}$$

APPENDIX C. DERIVATION OF MPI SOLUTION FOR A SET OF INJECTORS AND PRODUCERS

First we show how to calculate the average reservoir pressure if producer BHP and injection rates are available. Recalling Eq. 6.10 we have

$$\begin{bmatrix} \bar{p}-\vec{p}_{i^*} \\ \bar{p}-\vec{p}_{q^*} \end{bmatrix} = \frac{1}{\kappa}\begin{bmatrix} \mathbf{A}_{\mathbf{inj}} & \mathbf{A}_{\mathbf{con}} \\ \mathbf{A}_{\mathbf{con}}^{T} & \mathbf{A}_{\mathbf{prod}} \end{bmatrix}\begin{bmatrix} \vec{w} \\ \vec{q} \end{bmatrix}. \quad \text{.....(C.1)}$$

Splitting the matrix, we obtain

$$\left[\bar{p}-\vec{p}_{i^*}\right] = \frac{1}{\kappa}\left[\mathbf{A}_{\mathbf{inj}} \quad \mathbf{A}_{\mathbf{con}}\right]\begin{bmatrix} \vec{w} \\ \vec{q} \end{bmatrix}. \quad \text{.....(C.2)}$$

Solving Eq. C.2 for $\left[\vec{p}_{i^*}\right]$ gives us

$$\left[\vec{p}_{i^*}\right] = \bar{p}\cdot[\mathbf{1}]_{I\mathrm{x}1} - \frac{1}{\kappa}\left[\mathbf{A}_{\mathbf{inj}} \quad \mathbf{A}_{\mathbf{con}}\right]\begin{bmatrix} \vec{w} \\ \vec{q} \end{bmatrix}. \quad \text{.....(C.3)}$$

where $[\mathbf{1}]_{I\mathrm{x}1}$ is a Ix1 matrix where elements are the average reservoir pressure. Similarly, from Eq. C.3 we have

$$\left[\bar{p}-\vec{p}_{q^*}\right] = \frac{1}{\kappa}\left[\mathbf{A}_{\mathbf{con}}^{T} \quad \mathbf{A}_{\mathbf{prod}}\right]\begin{bmatrix} \vec{w} \\ \vec{q} \end{bmatrix} \quad \text{.....(C.4)}$$

or

$$\left[\bar{p}-\vec{p}_{q^*}\right] = \frac{1}{\kappa}\left[\mathbf{A}_{\mathbf{con}}^{T}\right]\vec{w} + \frac{1}{\kappa}\left[\mathbf{A}_{\mathbf{prod}}\right]\vec{q}\cdot \quad \text{.....(C.5)}$$

Solving for $\vec{q}$ we obtain

$$\vec{q} = \kappa\left[\mathbf{A}_{\mathbf{prod}}\right]^{-1}\left[\bar{p}-\vec{p}_{q^*}\right] - \left[\mathbf{A}_{\mathbf{prod}}\right]^{-1}\left[\mathbf{A}_{\mathbf{con}}\right]^{T}\vec{w}. \quad \text{.....(C.6)}$$

Replacing Eq. C.6 in the general material balance equation (Eq. 6.11) we have

$$c_t V_p \frac{d\bar{p}}{dt} = -\sum \vec{w} - \sum \vec{q} = -\sum \vec{w} - \sum\left\{\kappa\left[\mathbf{A}_{\mathbf{prod}}\right]^{-1}\left[\bar{p}-\vec{p}_{q^*}\right] - \left[\mathbf{A}_{\mathbf{prod}}\right]^{-1}\left[\mathbf{A}_{\mathbf{con}}^{\mathbf{T}}\right]\vec{w}\right\} \quad \text{.....(C.7)}$$

or

$$c_t V_p \frac{d\bar{p}}{dt} = -\sum \vec{w} + \sum\left[\mathbf{A}_{\mathbf{prod}}\right]^{-1}\left[\mathbf{A}_{\mathbf{con}}^{\mathbf{T}}\right]\vec{w} + \kappa\sum\left[\mathbf{A}_{\mathbf{prod}}\right]^{-1}\left[\vec{p}_{q^*}\right] - \kappa\bar{p}\sum\sum\left[\mathbf{A}_{\mathbf{prod}}\right]^{-1}\cdot \quad \text{.....(C.8)}$$

Solving for $\bar{p}$ give us

$$\bar{p} = \frac{c_2}{c_1} + \left(\bar{p}_i - \frac{c_2}{c_1} \right) \exp\left(\frac{-c_1}{c_t V_p} t \right) \quad \text{.....(C.9)}$$

where $\bar{p}_i$ is the initial average pressure (at the start of the pseudosteady-state condition)

$$c_1 = \kappa \sum \sum \left[\mathbf{A}_{\mathbf{prod}} \right]^{-1} \quad \text{.....(C.10)}$$

and

$$c_2 = -\sum \vec{w} + \sum \left[\mathbf{A}_{\mathbf{prod}} \right]^{-1} \left[\mathbf{A}_{\mathbf{con}} \right]^T \vec{w} + \sum \kappa \left[\mathbf{A}_{\mathbf{prod}} \right]^{-1} \vec{p}_{q^*} \cdot \quad \text{.....(C.11)}$$

If instead of injection rate the injector BHPs ($\vec{p}_{i^*}$) are available by rearranging Eq. C.2 we obtain

$$\begin{bmatrix} \vec{w} \\ \vec{q} \end{bmatrix} = \kappa \left[\mathbf{A} \right]^{-1} \begin{bmatrix} \bar{p} - \vec{p}_{i^*} \\ \bar{p} - \vec{p}_{q^*} \end{bmatrix} \quad \text{.....(C.12)}$$

and

$$\sum \left(-\vec{w} - \vec{q} \right) = \bar{p} \kappa \sum \sum \left[\mathbf{A} \right]^{-1} - \kappa \sum \left[\mathbf{A} \right]^{-1} \begin{bmatrix} \vec{p}_{i^*} \\ \vec{p}_{q^*} \end{bmatrix} \quad \text{.....(C.13)}$$

Replacing Eq. C.13 into Eq. 6.11 and solving for $\bar{p}$, we obtain

$$\bar{p} = \frac{\sum \left[\mathbf{A} \right]^{-1} \begin{bmatrix} \vec{p}_{i^*} & \vec{p}_{q^*} \end{bmatrix}^T}{\sum \sum \left[\mathbf{A} \right]^{-1}} + \left(\bar{p}_i - \frac{\sum \left[\mathbf{A} \right]^{-1} \begin{bmatrix} \vec{p}_{i^*} & \vec{p}_{q^*} \end{bmatrix}^T}{\sum \sum \left[\mathbf{A} \right]^{-1}} \right) \exp\left(\frac{\kappa \sum \sum \left[\mathbf{A} \right]^{-1}}{c_t V_p} t \right) \cdot \quad \text{.....(C.14)}$$

To obtain an explicit form of the production rate in terms of injection rates, producer BHPs, and influence matrix, we start by rewriting Eq. C.11in matrix form

$$c_2 = \left(\left[\mathbf{1} \right]_{1xK} \left[\mathbf{A}_{\mathbf{prod}} \right]^{-1} \left[\mathbf{A}_{\mathbf{con}} \right]^T - \left[\mathbf{1} \right]_{1xI} \right) \vec{w} + \kappa \left[\mathbf{1} \right]_{1xK} \left[\mathbf{A}_{\mathbf{prod}} \right]^{-1} \vec{p}_{q^*} \cdot \quad \text{.....(C.15)}$$

Substituting Eq. C.15 in Eq. C.9 we obtain

$$\bar{p} = \frac{\left(\left[1 \right]_{1xK} \left[\mathbf{A}_{\mathbf{prod}} \right]^{-1} \left[\mathbf{A}_{\mathbf{con}} \right]^T - \left[1 \right]_{1xI} \right) \vec{w} + \kappa \left[1 \right]_{1xK} \left[\mathbf{A}_{\mathbf{prod}} \right]^{-1} \vec{p}_{q^*}}{\kappa \left[1 \right]_{1xK} \left[\mathbf{A}_{\mathbf{prod}} \right]^{-1} \left[1 \right]_{Kx1}} +$$

$$\left(\bar{p}_i - \frac{\left(\left[1 \right]_{1xK} \left[\mathbf{A}_{\mathbf{prod}} \right]^{-1} \left[\mathbf{A}_{\mathbf{con}} \right]^T - \left[1 \right]_{1xI} \right) \vec{w} + \kappa \left[1 \right]_{1xK} \left[\mathbf{A}_{\mathbf{prod}} \right]^{-1} \vec{p}_{q^*}}{\kappa \left[1 \right]_{1xK} \left[\mathbf{A}_{\mathbf{prod}} \right]^{-1} \left[1 \right]_{Kx1}} \right) \exp\left(- \frac{\left[1 \right]_{1xK} \left[\mathbf{A}_{\mathbf{prod}} \right]^{-1} \left[1 \right]_{Kx1} \kappa t}{c_t V_p} \right) \quad \text{. ....(C.16)}$$

And substituting Eq. C.16 in Eq. C.6 we have

$$\vec{q} = \left[\mathbf{A_{prod}}\right]^{-1}\left[\frac{\left(\left[\mathbf{1}\right]_{1xK}\left[\mathbf{A_{prod}}\right]^{-1}\left[\mathbf{A_{con}}\right]^{T} - \left[\mathbf{1}\right]_{1xI}\right)\vec{w} + \kappa\left[\mathbf{1}\right]_{1xK}\left[\mathbf{A_{prod}}\right]^{-1}\vec{p}_{q^*}}{\kappa\left[\mathbf{1}\right]_{1xK}\left[\mathbf{A_{prod}}\right]^{-1}\left[\mathbf{1}\right]_{Kx1}}\left[\mathbf{1}\right]_{Kx1} + \right.$$

$$\left(\overline{p}_i - \frac{\left(\left[\mathbf{1}\right]_{1xK}\left[\mathbf{A_{prod}}\right]^{-1}\left[\mathbf{A_{con}}\right]^{T} - \left[\mathbf{1}\right]_{1xI}\right)\vec{w} + \kappa\left[\mathbf{1}\right]_{1xK}\left[\mathbf{A_{prod}}\right]^{-1}\vec{p}_{q^*}}{\kappa\left[\mathbf{1}\right]_{1xK}\left[\mathbf{A_{prod}}\right]^{-1}\left[\mathbf{1}\right]_{Kx1}}\right)\exp\left(-\frac{\left[\mathbf{1}\right]_{1xK}\left[\mathbf{A_{prod}}\right]^{-1}\left[\mathbf{1}\right]_{Kx1}\kappa t}{c_t V_p}\right)\left[\mathbf{1}\right]_{Kx1} \quad \text{(C.17)}$$

$$\left. - \vec{p}_{q^*}\right] - \left[\mathbf{A_{prod}}\right]^{-1}\left[\mathbf{A_{con}}\right]^{T}\vec{w}$$

or

$$\vec{q} = \left(\frac{1-\exp\left(-\frac{\left[\mathbf{1}\right]_{1xK}\left[\mathbf{A_{prod}}\right]^{-1}\left[\mathbf{1}\right]_{Kx1}\kappa t}{c_t V_p}\right)}{\left[\mathbf{1}\right]_{1xK}\left[\mathbf{A_{prod}}\right]^{-1}\left[\mathbf{1}\right]_{Kx1}}\right)\left[\mathbf{A_{prod}}\right]^{-1}\left(\left[\mathbf{1}\right]_{1xK}\left[\mathbf{A_{prod}}\right]^{-1}\left[\mathbf{A_{con}}\right]^{T} - \left[\mathbf{1}\right]_{1xI}\right)\vec{w}\left[\mathbf{1}\right]_{Kx1}$$

$$-\left[\mathbf{A_{prod}}\right]^{-1}\left[\mathbf{A_{con}}\right]^{T}\vec{w} +$$

$$\left[\mathbf{A_{prod}}\right]^{-1}\left\{\left[\frac{\left[\mathbf{1}\right]_{1xK}\left[\mathbf{A_{prod}}\right]^{-1}\vec{p}_{q^*}}{\left[\mathbf{1}\right]_{1xK}\left[\mathbf{A_{prod}}\right]^{-1}\left[\mathbf{1}\right]_{Kx1}} + \left(\overline{p}_i - \frac{\left[\mathbf{1}\right]_{1xK}\left[\mathbf{A_{prod}}\right]^{-1}\vec{p}_{q^*}}{\left[\mathbf{1}\right]_{1xK}\left[\mathbf{A_{prod}}\right]^{-1}\left[\mathbf{1}\right]_{Kx1}}\right)\exp\left(-\frac{\left[\mathbf{1}\right]_{1xK}\left[\mathbf{A_{prod}}\right]^{-1}\left[\mathbf{1}\right]_{Kx1}\kappa t}{c_t V_p}\right)\right]\left[\mathbf{1}\right]_{Kx1} - \vec{p}_{q^*}\right\}$$

. .....(C.18)

And finally

$$\vec{q} = \left(\frac{1-\exp\left(-\frac{\left[\mathbf{1}\right]_{1xK}\left[\mathbf{A_{prod}}\right]^{-1}\left[\mathbf{1}\right]_{Kx1}\kappa t}{c_t V_p}\right)}{\left[\mathbf{1}\right]_{1xK}\left[\mathbf{A_{prod}}\right]^{-1}\left[\mathbf{1}\right]_{Kx1}}\right)\left[\mathbf{A_{prod}}\right]^{-1}\left(\left[\mathbf{1}\right]_{KxK}\left[\mathbf{A_{prod}}\right]^{-1}\left[\mathbf{A_{con}}\right]^{T} - \left[\mathbf{1}\right]_{KxI}\right)\vec{w}$$

$$-\left[\mathbf{A_{prod}}\right]^{-1}\left[\mathbf{A_{con}}\right]^{T}\vec{w} +$$

$$\left[\mathbf{A_{prod}}\right]^{-1}\left\{\left[\frac{\left[\mathbf{1}\right]_{1xK}\left[\mathbf{A_{prod}}\right]^{-1}\vec{p}_{q^*}}{\left[\mathbf{1}\right]_{1xK}\left[\mathbf{A_{prod}}\right]^{-1}\left[\mathbf{1}\right]_{Kx1}} + \left(\overline{p}_i - \frac{\left[\mathbf{1}\right]_{1xK}\left[\mathbf{A_{prod}}\right]^{-1}\vec{p}_{q^*}}{\left[\mathbf{1}\right]_{1xK}\left[\mathbf{A_{prod}}\right]^{-1}\left[\mathbf{1}\right]_{Kx1}}\right)\exp\left(-\frac{\left[\mathbf{1}\right]_{1xK}\left[\mathbf{A_{prod}}\right]^{-1}\left[\mathbf{1}\right]_{Kx1}\kappa t}{c_t V_p}\right)\right]\left[\mathbf{1}\right]_{Kx1} - \vec{p}_{q^*}\right\}$$

. .....(C.19)

APPENDIX D. PROOF OF THE HETEROGENEITY MATRIX PROPERTIES

D.1 Adding a Constant Number to Each Row of [A_{con}] for Small Delay.

In case of small delay, if we approximate the delay term with zero, Eq. 6.19 reduces into

$$\vec{q}=\left\{\left(\frac{1}{[\mathbf{1}]_{1xK}\left[\mathbf{A_{prod}}\right]^{-1}[\mathbf{1}]_{Kx1}}\right)\left[\mathbf{A_{prod}}\right]^{-1}\left([\mathbf{1}]_{KxK}\left[\mathbf{A_{prod}}\right]^{-1}\left[\mathbf{A_{con}}\right]^{T}-[\mathbf{1}]_{KxI}\right)-\left[\mathbf{A_{prod}}\right]^{-1}\left[\mathbf{A_{con}}\right]^{T}\right\}\vec{w} \quad \text{..... (D.1)}$$
$$+\kappa\left[\mathbf{A_{prod}}\right]^{-1}\left[\frac{[\mathbf{1}]_{1xK}\left[\mathbf{A_{prod}}\right]^{-1}\vec{p}_{q^*}}{[\mathbf{1}]_{1xK}\left[\mathbf{A_{prod}}\right]^{-1}[\mathbf{1}]_{Kx1}}[\mathbf{1}]_{Kx1}-\vec{p}_{q^*}\right]$$

If we replace the [A_{con}] with [A_{con}]+ [**E**], where [**E**] is $[\mathbf{E}]=\left[e_1 \quad \cdots \quad e_I\right]^T[\mathbf{1}]_{1xK}$, we will have

$$\vec{q}_{new}=\left\{\left(\frac{1}{[\mathbf{1}]_{1xK}\left[\mathbf{A_{prod}}\right]^{-1}[\mathbf{1}]_{Kx1}}\right)\left[\mathbf{A_{prod}}\right]^{-1}\left([\mathbf{1}]_{KxK}\left[\mathbf{A_{prod}}\right]^{-1}\left[\mathbf{A_{con}}+\mathbf{E}\right]^{T}-[\mathbf{1}]_{KxI}\right)-\left[\mathbf{A_{prod}}\right]^{-1}\left[\mathbf{A_{con}}+\mathbf{E}\right]^{T}\right\}\vec{w} \quad \text{(D.2)}$$
$$+\kappa\left[\mathbf{A_{prod}}\right]^{-1}\left[\frac{[\mathbf{1}]_{1xK}\left[\mathbf{A_{prod}}\right]^{-1}\vec{p}_{q^*}}{[\mathbf{1}]_{1xK}\left[\mathbf{A_{prod}}\right]^{-1}[\mathbf{1}]_{Kx1}}[\mathbf{1}]_{Kx1}-\vec{p}_{q^*}\right]$$

By subtracting Eq. D.2 from 1 we obtain

$$\vec{q}_{new}-\vec{q}=\left\{\left[\mathbf{A_{prod}}\right]^{-1}\mathbf{E}^T-\left(\frac{1}{[\mathbf{1}]_{1xK}\left[\mathbf{A_{prod}}\right]^{-1}[\mathbf{1}]_{Kx1}}\right)\left[\mathbf{A_{prod}}\right]^{-1}\left([\mathbf{1}]_{KxK}\left[\mathbf{A_{prod}}\right]^{-1}\mathbf{E}^T\right)\right\}\vec{w}\cdot \quad \text{..... (D.3)}$$

On the other hand for an arbitrary matrix [X] defined as

$$[\mathbf{X}]=\begin{bmatrix} x_{11} & x_{12} & \cdots & x_{1K} \\ x_{21} & x_{22} & \cdots & x_{2K} \\ \vdots & \vdots & \ddots & \vdots \\ x_{K1} & x_{K2} & \cdots & x_{KK} \end{bmatrix}$$

we have

$$\mathbf{[X]}\cdot[\mathbf{1}]_{KxK}\cdot\mathbf{[X]}=\begin{bmatrix} \sum_{i=1}^{K}x_{1i}\sum_{i=1}^{K}b_{i1} & \sum_{i=1}^{K}x_{1i}\sum_{i=1}^{K}x_{i2} & \cdots & \sum_{i=1}^{K}x_{1i}\sum_{i=1}^{K}x_{iK} \\ \sum_{i=1}^{K}x_{2i}\sum_{i=1}^{K}x_{i1} & \sum_{i=1}^{K}x_{2i}\sum_{i=1}^{K}x_{i2} & \cdots & \sum_{i=1}^{K}x_{2i}\sum_{i=1}^{K}x_{iK} \\ \vdots & \vdots & \ddots & \vdots \\ \sum_{i=1}^{K}x_{Ki}\sum_{i=1}^{K}x_{i1} & \sum_{i=1}^{K}x_{Ki}\sum_{i=1}^{K}x_{i2} & \cdots & \sum_{i=1}^{K}x_{Ki}\sum_{i=1}^{K}x_{iK} \end{bmatrix}\cdot \quad \text{..... (D.4)}$$

Multiplying by [**E**] we obtain

$$[\mathbf{X}][\mathbf{1}]_{KxK}[\mathbf{X}][\mathbf{E}]^T = \begin{bmatrix} \sum_{i=1}^{K} x_{1i} \sum_{i=1}^{K} x_{i1} & \sum_{i=1}^{K} x_{1i} \sum_{i=1}^{K} x_{i2} & \cdots & \sum_{i=1}^{K} x_{1i} \sum_{i=1}^{K} x_{iK} \\ \sum_{i=1}^{K} x_{2i} \sum_{i=1}^{K} x_{i1} & \sum_{i=1}^{K} x_{2i} \sum_{i=1}^{K} x_{i2} & \cdots & \sum_{i=1}^{K} x_{2i} \sum_{i=1}^{K} x_{iK} \\ \vdots & \vdots & \ddots & \vdots \\ \sum_{i=1}^{K} x_{Ki} \sum_{i=1}^{K} x_{i1} & \sum_{i=1}^{K} x_{Ki} \sum_{i=1}^{K} x_{i2} & \cdots & \sum_{i=1}^{K} x_{Ki} \sum_{i=1}^{K} x_{iK} \end{bmatrix} \begin{bmatrix} e_1 & e_2 & \cdots & e_K \\ e_1 & e_2 & \cdots & e_K \\ \vdots & \vdots & \ddots & \vdots \\ e_1 & e_2 & \cdots & e_K \end{bmatrix}$$

$$= \begin{bmatrix} e_1 \sum_{i=1}^{K} x_{1i} \left[\sum_{i=1}^{K} x_{i1} + \sum_{i=1}^{K} x_{i2} + \ldots + \sum_{i=1}^{K} x_{iK} \right] & e_2 \sum_{i=1}^{K} x_{1i} \left[\sum_{i=1}^{K} x_{i1} + \sum_{i=1}^{K} x_{i2} + \ldots + \sum_{i=1}^{K} x_{iK} \right] & \cdots & e_K \sum_{i=1}^{K} x_{1i} \left[\sum_{i=1}^{K} x_{i1} + \sum_{i=1}^{K} x_{i2} + \ldots + \sum_{i=1}^{K} x_{iK} \right] \\ e_1 \sum_{i=1}^{K} x_{2i} \left[\sum_{i=1}^{K} x_{i1} + \sum_{i=1}^{K} x_{i2} + \ldots + \sum_{i=1}^{K} x_{iK} \right] & e_2 \sum_{i=1}^{K} x_{2i} \left[\sum_{i=1}^{K} x_{i1} + \sum_{i=1}^{K} x_{i2} + \ldots + \sum_{i=1}^{K} x_{iK} \right] & \cdots & e_K \sum_{i=1}^{K} x_{2i} \left[\sum_{i=1}^{K} x_{1i} + \sum_{i=1}^{K} x_{2i} + \ldots + \sum_{i=1}^{K} x_{Ki} \right] \\ \vdots & \vdots & \ddots & \vdots \\ e_1 \sum_{i=1}^{K} x_{Ki} \left[\sum_{i=1}^{K} x_{i1} + \sum_{i=1}^{K} x_{i2} + \ldots + \sum_{i=1}^{K} x_{iK} \right] & e_2 \sum_{i=1}^{K} x_{Ki} \left[\sum_{i=1}^{K} x_{i1} + \sum_{i=1}^{K} x_{i2} + \ldots + \sum_{i=1}^{K} x_{iK} \right] & \cdots & e_K \sum_{i=1}^{K} x_{Ki} \left[\sum_{i=1}^{K} x_{i1} + \sum_{i=1}^{K} x_{i2} + \ldots + \sum_{i=1}^{K} x_{iK} \right] \end{bmatrix}$$

. ..... (D.5)

So

$$\frac{1}{[\mathbf{1}]_{1xK}[\mathbf{X}][\mathbf{1}]_{Kx1}}[\mathbf{X}][\mathbf{1}]_{KxK}[\mathbf{X}][\mathbf{E}]^T = \frac{1}{\left[\sum_{i=1}^{K} x_{1i} + \sum_{i=1}^{K} x_{2i} + \ldots + \sum_{i=1}^{K} x_{Ki} \right]}[\mathbf{X}][\mathbf{1}]_{KxK}[\mathbf{X}][\mathbf{E}]^T$$

$$= \begin{bmatrix} e_1 \sum_{i=1}^{K} x_{1i} & e_2 \sum_{i=1}^{K} x_{1i} & \cdots & e_K \sum_{i=1}^{K} x_{1i} \\ e_1 \sum_{i=1}^{K} x_{2i} & e_2 \sum_{i=1}^{K} x_{2i} & \cdots & e_K \sum_{i=1}^{K} x_{2i} \\ \vdots & \vdots & \ddots & \vdots \\ e_1 \sum_{i=1}^{K} x_{Ki} & e_2 \sum_{i=1}^{K} x_{Ki} & \cdots & e_K \sum_{i=1}^{K} x_{Ki} \end{bmatrix} \quad \text{. ..... (D.6)}$$

On the other hand we have

$$[\mathbf{X}][\mathbf{E}]^T = \begin{bmatrix} e_1 \sum_{i=1}^{K} x_{1i} & e_2 \sum_{i=1}^{K} x_{1i} & \cdots & e_K \sum_{i=1}^{K} x_{1i} \\ e_1 \sum_{i=1}^{K} x_{2i} & e_2 \sum_{i=1}^{K} x_{2i} & \cdots & e_K \sum_{i=1}^{K} x_{2i} \\ \vdots & \vdots & \ddots & \vdots \\ e_1 \sum_{i=1}^{K} x_{Ki} & e_2 \sum_{i=1}^{K} x_{Ki} & \cdots & e_K \sum_{i=1}^{K} x_{Ki} \end{bmatrix} \text{. ..... (D.7)}$$

So

$$\frac{1}{[\mathbf{1}]_{1xK}[\mathbf{X}][\mathbf{1}]_{Kx1}}[\mathbf{X}][\mathbf{1}]_{KxK}[\mathbf{X}][\mathbf{E}]^T = [\mathbf{X}][\mathbf{E}]^T \text{ . ..... (D.8)}$$

Replacing [**X**] with $[\mathbf{A}_{\mathbf{prod}}]^{-1}$ and substituting Eq. D.8 in Eq. D.2 we obtain

$$\vec{q}_{new} = \vec{q}\ . \quad \text{(D.9)}$$

D.2 Inconsistency of the [Δ] in Case of Having Constant Producer BHPs

By rearranging Eq. 6.19 and factoring out [$\mathbf{A_{con}}$] we have

$$\vec{q} = \left\{ \left(\frac{1 - \exp\left(-\frac{[\mathbf{1}]_{1xK} \left[\mathbf{A_{prod}}\right]^{-1} [\mathbf{1}]_{Kx1}\, \kappa t}{c_t V_p} \right)}{[\mathbf{1}]_{1xK} \left[\mathbf{A_{prod}}\right]^{-1} [\mathbf{1}]_{Kx1}} \right) \left[\mathbf{A_{prod}}\right]^{-1} [\mathbf{1}]_{KxK} \left[\mathbf{A_{prod}}\right]^{-1} - \left[\mathbf{A_{prod}}\right]^{-1} \right\} [\mathbf{A_{con}}]^T\, \vec{w} +$$

$$- \left(\frac{1 - \exp\left(-\frac{[\mathbf{1}]_{1xK} \left[\mathbf{A_{prod}}\right]^{-1} [\mathbf{1}]_{Kx1}\, \kappa t}{c_t V_p} \right)}{[\mathbf{1}]_{1xK} \left[\mathbf{A_{prod}}\right]^{-1} [\mathbf{1}]_{Kx1}} \right) \left[\mathbf{A_{prod}}\right]^{-1} [\mathbf{1}]_{KxI}\, \vec{w} +$$

$$\kappa \left[\mathbf{A_{prod}}\right]^{-1} \left\{ \left[\frac{[\mathbf{1}]_{1xK} \left[\mathbf{A_{prod}}\right]^{-1} \vec{p}_{q^*}}{[\mathbf{1}]_{1xK} \left[\mathbf{A_{prod}}\right]^{-1} [\mathbf{1}]_{Kx1}} + \left(\overline{p}_i - \frac{[\mathbf{1}]_{1xK} \left[\mathbf{A_{prod}}\right]^{-1} \vec{p}_{q^*}}{[\mathbf{1}]_{1xK} \left[\mathbf{A_{prod}}\right]^{-1} [\mathbf{1}]_{Kx1}} \right) \exp\left(-\frac{[\mathbf{1}]_{1xK} \left[\mathbf{A_{prod}}\right]^{-1} [\mathbf{1}]_{Kx1}\, \kappa t}{c_t V_p} \right) \right] [\mathbf{1}]_{Kx1} - \vec{p}_{q^*} \right\}$$

. (D.10)

In general if we replace [$\mathbf{A_{prod}}$] with [$\mathbf{A_{prod\_new}}$] and [$\mathbf{A_{con}}$] with [$\mathbf{A_{con\_new}}$], the difference between the original production rate and the new one will be

$$\vec{q}-\vec{q}_{new}=\left\{\left(\frac{1-\exp\left(-\frac{[\mathbf{1}]_{1xK}\left[\mathbf{A_{prod}}\right]^{-1}[\mathbf{1}]_{Kx1}\,\kappa t}{c_t V_p}\right)}{[\mathbf{1}]_{1xK}\left[\mathbf{A_{prod}}\right]^{-1}[\mathbf{1}]_{Kx1}}\right)\left[\mathbf{A_{prod}}\right]^{-1}[\mathbf{1}]_{Kx1}[\mathbf{1}]_{1xK}\left[\mathbf{A_{prod}}\right]^{-1}-\left[\mathbf{A_{prod}}\right]^{-1}\right\}[\mathbf{A_{con}}]^{T}\,\vec{w}$$

$$-\left(\frac{1-\exp\left(-\frac{[\mathbf{1}]_{1xK}\left[\mathbf{A_{prod}}\right]^{-1}[\mathbf{1}]_{Kx1}\,\kappa t}{c_t V_p}\right)}{[\mathbf{1}]_{1xK}\left[\mathbf{A_{prod}}\right]^{-1}[\mathbf{1}]_{Kx1}}\right)\left[\mathbf{A_{prod}}\right]^{-1}[\mathbf{1}]_{KxI}\,\vec{w}$$

$$+\kappa\left\{\frac{[\mathbf{1}]_{1xK}\left[\mathbf{A_{prod}}\right]^{-1}\vec{p}_{q^*}}{[\mathbf{1}]_{1xK}\left[\mathbf{A_{prod}}\right]^{-1}[\mathbf{1}]_{Kx1}}+\left(\overline{p}_i-\frac{[\mathbf{1}]_{1xK}\left[\mathbf{A_{prod}}\right]^{-1}\vec{p}_{q^*}}{[\mathbf{1}]_{1xK}\left[\mathbf{A_{prod}}\right]^{-1}[\mathbf{1}]_{Kx1}}\right)\exp\left(-\frac{[\mathbf{1}]_{1xK}\left[\mathbf{A_{prod}}\right]^{-1}[\mathbf{1}]_{Kx1}\,\kappa t}{c_t V_p}\right)\right\}\left[\mathbf{A_{prod}}\right]^{-1}[\mathbf{1}]_{Kx1}$$

$$-\kappa\left[\mathbf{A_{prod}}\right]^{-1}\vec{p}_{q^*}$$

$$-\left\{\left(\frac{1-\exp\left(-\frac{[\mathbf{1}]_{1xK}\left[\mathbf{A_{prod\_new}}\right]^{-1}[\mathbf{1}]_{Kx1}\,\kappa t}{c_t V_p}\right)}{[\mathbf{1}]_{1xK}\left[\mathbf{A_{prod\_new}}\right]^{-1}[\mathbf{1}]_{Kx1}}\right)\left[\mathbf{A_{prod\_new}}\right]^{-1}[\mathbf{1}]_{Kx1}[\mathbf{1}]_{1xK}\left[\mathbf{A_{prod\_new}}\right]^{-1}-\left[\mathbf{A_{prod\_new}}\right]^{-1}\right\}\left[\mathbf{A_{con\_new}}\right]^{T}\vec{w}$$

$$+\left(\frac{1-\exp\left(-\frac{[\mathbf{1}]_{1xK}\left[\mathbf{A_{prod\_new}}\right]^{-1}[\mathbf{1}]_{Kx1}\,\kappa t}{c_t V_p}\right)}{[\mathbf{1}]_{1xK}\left[\mathbf{A_{prod\_new}}\right]^{-1}[\mathbf{1}]_{Kx1}}\right)\left[\mathbf{A_{prod\_new}}\right]^{-1}[\mathbf{1}]_{KxI}\,\vec{w}$$

$$-\kappa\left\{\frac{[\mathbf{1}]_{1xK}\left[\mathbf{A_{prod\_new}}\right]^{-1}\vec{p}_{q^*}}{[\mathbf{1}]_{1xK}\left[\mathbf{A_{prod\_new}}\right]^{-1}[\mathbf{1}]_{Kx1}}+\left(\overline{p}_i-\frac{[\mathbf{1}]_{1xK}\left[\mathbf{A_{prod\_new}}\right]^{-1}\vec{p}_{q^*}}{[\mathbf{1}]_{1xK}\left[\mathbf{A_{prod\_new}}\right]^{-1}[\mathbf{1}]_{Kx1}}\right)\exp\left(-\frac{[\mathbf{1}]_{1xK}\left[\mathbf{A_{prod\_new}}\right]^{-1}[\mathbf{1}]_{Kx1}\,\kappa t}{c_t V_p}\right)\right\}\left[\mathbf{A_{prod\_new}}\right]^{-1}[\mathbf{1}]_{Kx1}$$

$$+\kappa\left[\mathbf{A_{prod\_new}}\right]^{-1}\vec{p}_{q^*} \qquad \text{. (D.11)}$$

If $[\mathbf{A_{prod}}][\mathbf{1}]_{Kx1}=[\mathbf{A_{prod\_new}}][\mathbf{1}]_{Kx1}$, (since these matrices are symmetric, we also have $[\mathbf{1}]_{Kx1}.[\mathbf{A_{prod}}]=[\mathbf{1}]_{Kx1}.[\mathbf{A_{prod\_new}}]$), we can rewrite Eq. D.11 as

$$\vec{q}-\vec{q}_{new}=\left\{\left(\frac{1-\exp\left(-\frac{[\mathbf{1}]_{1xK}\left[\mathbf{A_{prod}}\right]^{-1}[\mathbf{1}]_{Kx1}\,\kappa t}{c_t V_p}\right)}{[\mathbf{1}]_{1xK}\left[\mathbf{A_{prod}}\right]^{-1}[\mathbf{1}]_{Kx1}}\right)\left[\mathbf{A_{prod}}\right]^{-1}[\mathbf{1}]_{Kx1}[\mathbf{1}]_{1xK}\left[\mathbf{A_{prod}}\right]^{-1}-\left[\mathbf{A_{prod}}\right]^{-1}\right\}\left[\mathbf{A_{con}}\right]^{T}\vec{w}$$

$$-\left(\frac{1-\exp\left(-\frac{[\mathbf{1}]_{1xK}\left[\mathbf{A_{prod}}\right]^{-1}[\mathbf{1}]_{Kx1}\,\kappa t}{c_t V_p}\right)}{[\mathbf{1}]_{1xK}\left[\mathbf{A_{prod}}\right]^{-1}[\mathbf{1}]_{Kx1}}\right)\left[\mathbf{A_{prod}}\right]^{-1}[\mathbf{1}]_{KxI}\,\vec{w}$$

$$+\kappa\left\{\frac{[\mathbf{1}]_{1xK}\left[\mathbf{A_{prod}}\right]^{-1}\vec{p}_{q^*}}{[\mathbf{1}]_{1xK}\left[\mathbf{A_{prod}}\right]^{-1}[\mathbf{1}]_{Kx1}}+\left(\overline{p}_i-\frac{[\mathbf{1}]_{1xK}\left[\mathbf{A_{prod}}\right]^{-1}\vec{p}_{q^*}}{[\mathbf{1}]_{1xK}\left[\mathbf{A_{prod}}\right]^{-1}[\mathbf{1}]_{Kx1}}\right)\exp\left(-\frac{[\mathbf{1}]_{1xK}\left[\mathbf{A_{prod}}\right]^{-1}[\mathbf{1}]_{Kx1}\,\kappa t}{c_t V_p}\right)\right\}\left[\mathbf{A_{prod}}\right]^{-1}[\mathbf{1}]_{Kx1}$$

$$-\kappa\left[\mathbf{A_{prod}}\right]^{-1}\vec{p}_{q^*}$$

$$-\left\{\left(\frac{1-\exp\left(-\frac{[\mathbf{1}]_{1xK}\left[\mathbf{A_{prod}}\right]^{-1}[\mathbf{1}]_{Kx1}\,\kappa t}{c_t V_p}\right)}{[\mathbf{1}]_{1xK}\left[\mathbf{A_{prod}}\right]^{-1}[\mathbf{1}]_{Kx1}}\right)\left[\mathbf{A_{prod}}\right]^{-1}[\mathbf{1}]_{Kx1}[\mathbf{1}]_{1xK}\left[\mathbf{A_{prod}}\right]^{-1}-\left[\mathbf{A_{prod\_new}}\right]^{-1}\right\}\left[\mathbf{A_{con\_new}}\right]^{T}\vec{w}$$

$$+\left(\frac{1-\exp\left(-\frac{[\mathbf{1}]_{1xK}\left[\mathbf{A_{prod}}\right]^{-1}[\mathbf{1}]_{Kx1}\,\kappa t}{c_t V_p}\right)}{[\mathbf{1}]_{1xK}\left[\mathbf{A_{prod}}\right]^{-1}[\mathbf{1}]_{Kx1}}\right)\left[\mathbf{A_{prod}}\right]^{-1}[\mathbf{1}]_{KxI}\,\vec{w}$$

$$-\kappa\left\{\frac{[\mathbf{1}]_{1xK}\left[\mathbf{A_{prod}}\right]^{-1}\vec{p}_{q^*}}{[\mathbf{1}]_{1xK}\left[\mathbf{A_{prod}}\right]^{-1}[\mathbf{1}]_{Kx1}}+\left(\overline{p}_i-\frac{[\mathbf{1}]_{1xK}\left[\mathbf{A_{prod}}\right]^{-1}\vec{p}_{q^*}}{[\mathbf{1}]_{1xK}\left[\mathbf{A_{prod}}\right]^{-1}[\mathbf{1}]_{Kx1}}\right)\exp\left(-\frac{[\mathbf{1}]_{1xK}\left[\mathbf{A_{prod}}\right]^{-1}[\mathbf{1}]_{Kx1}\,\kappa t}{c_t V_p}\right)\right\}\left[\mathbf{A_{prod}}\right]^{-1}[\mathbf{1}]_{Kx1}$$

$$+\kappa\left[\mathbf{A_{prod\_new}}\right]^{-1}\vec{p}_{q^*} \qquad \text{. (D.12)}$$

Cancelling the similar terms we obtain

$$\vec{q}-\vec{q}_{new}=\left\{\left(\frac{1-\exp\left(-\frac{[\mathbf{1}]_{1xK}\left[\mathbf{A_{prod}}\right]^{-1}[\mathbf{1}]_{Kx1}\,\kappa t}{c_t V_p}\right)}{[\mathbf{1}]_{1xK}\left[\mathbf{A_{prod}}\right]^{-1}[\mathbf{1}]_{Kx1}}\right)\left[\mathbf{A_{prod}}\right]^{-1}[\mathbf{1}]_{Kx1}[\mathbf{1}]_{1xK}\left[\mathbf{A_{prod}}\right]^{-1}-\left[\mathbf{A_{prod}}\right]^{-1}\right\}\left[\mathbf{A_{con}}\right]^{T}\vec{w}$$

$$-\left\{\left(\frac{1-\exp\left(-\frac{[\mathbf{1}]_{1xK}\left[\mathbf{A_{prod}}\right]^{-1}[\mathbf{1}]_{Kx1}\,\kappa t}{c_t V_p}\right)}{[\mathbf{1}]_{1xK}\left[\mathbf{A_{prod}}\right]^{-1}[\mathbf{1}]_{Kx1}}\right)\left[\mathbf{A_{prod}}\right]^{-1}[\mathbf{1}]_{Kx1}[\mathbf{1}]_{1xK}\left[\mathbf{A_{prod}}\right]^{-1}-\left[\mathbf{A_{prod\_new}}\right]^{-1}\right\}\left[\mathbf{A_{con\_new}}\right]^{T}\vec{w} \quad \text{. (D.13)}$$

$$+\kappa\left(\left[\mathbf{A_{prod\_new}}\right]^{-1}-\left[\mathbf{A_{prod}}\right]^{-1}\right)\vec{p}_{q^*}$$

If the BHPs of the producers are equal, we have

$$\left(\left[\mathbf{A_{prod\_new}}\right]^{-1}-\left[\mathbf{A_{prod}}\right]^{-1}\right)\vec{p}_{q^*}=p_q\left(\left[\mathbf{A_{prod\_new}}\right]^{-1}-\left[\mathbf{A_{prod}}\right]^{-1}\right)[\mathbf{1}]_{Kx1}=0\,. \quad \text{..... (D.14)}$$

In this case, if

$$\left[\mathbf{A_{con\_new}}^{T}\right]=\left[\left(\frac{1-\exp\left(-\frac{[1]_{1xK}\left[\mathbf{A_{prod}}\right]^{-1}[1]_{Kx1}\,t}{c_t V_p}\right)}{[1]_{1xK}\left[\mathbf{A_{prod}}\right]^{-1}[1]_{Kx1}}\right)\left[\mathbf{A_{prod}}\right]^{-1}[1]_{KxK}\left[\mathbf{A_{prod}}\right]^{-1}-\left[\mathbf{A_{prod\_new}}\right]^{-1}\right]^{-1} \quad \text{, ... (D.15)}$$

$$\cdot\left[\left(\frac{1-\exp\left(-\frac{[1]_{1xK}\left[\mathbf{A_{prod}}\right]^{-1}[1]_{Kx1}\,t}{c_t V_p}\right)}{[1]_{1xK}\left[\mathbf{A_{prod}}\right]^{-1}[1]_{Kx1}}\right)\left[\mathbf{A_{prod}}\right]^{-1}[1]_{KxK}\left[\mathbf{A_{prod}}\right]^{-1}-\left[\mathbf{A_{prod}}\right]^{-1}\right]\left[\mathbf{A_{con}}^{T}\right]$$

the production rate using the new [**A**] will be the same as the production rate for the original [**A**].

In case of small BHP, Eq. D.11 becomes:

$$\vec{q}-\vec{q}_{new}=\left\{\left(\frac{1}{[\mathbf{1}]_{1xK}\left[\mathbf{A}_{\mathbf{prod}}\right]^{-1}[\mathbf{1}]_{Kx1}}\right)\left[\mathbf{A}_{\mathbf{prod}}\right]^{-1}[\mathbf{1}]_{Kx1}[\mathbf{1}]_{1xK}\left[\mathbf{A}_{\mathbf{prod}}\right]^{-1}-\left[\mathbf{A}_{\mathbf{prod}}\right]^{-1}\right\}\left[\mathbf{A}_{\mathbf{con}}\right]^{T}\vec{w}$$
$$-\left(\frac{1}{[\mathbf{1}]_{1xK}\left[\mathbf{A}_{\mathbf{prod}}\right]^{-1}[\mathbf{1}]_{Kx1}}\right)\left[\mathbf{A}_{\mathbf{prod}}\right]^{-1}[\mathbf{1}]_{KxI}\vec{w}$$
$$+\kappa\left\{\frac{[\mathbf{1}]_{1xK}\left[\mathbf{A}_{\mathbf{prod}}\right]^{-1}\vec{p}_{q^*}}{[\mathbf{1}]_{1xK}\left[\mathbf{A}_{\mathbf{prod}}\right]^{-1}[\mathbf{1}]_{Kx1}}\right\}\left[\mathbf{A}_{\mathbf{prod}}\right]^{-1}[\mathbf{1}]_{Kx1}-\kappa\left[\mathbf{A}_{\mathbf{prod}}\right]^{-1}\vec{p}_{q^*}$$
$$-\left\{\left(\frac{1}{[\mathbf{1}]_{1xK}\left[\mathbf{A}_{\mathbf{prod\_new}}\right]^{-1}[\mathbf{1}]_{Kx1}}\right)\left[\mathbf{A}_{\mathbf{prod\_new}}\right]^{-1}[\mathbf{1}]_{Kx1}[\mathbf{1}]_{1xK}\left[\mathbf{A}_{\mathbf{prod\_new}}\right]^{-1}-\left[\mathbf{A}_{\mathbf{prod\_new}}\right]^{-1}\right\}\left[\mathbf{A}_{\mathbf{con\_new}}\right]^{T}\vec{w}$$
$$+\left(\frac{1}{[\mathbf{1}]_{1xK}\left[\mathbf{A}_{\mathbf{prod\_new}}\right]^{-1}[\mathbf{1}]_{Kx1}}\right)\left[\mathbf{A}_{\mathbf{prod\_new}}\right]^{-1}[\mathbf{1}]_{KxI}\vec{w}$$
$$-\kappa\left\{\frac{[\mathbf{1}]_{1xK}\left[\mathbf{A}_{\mathbf{prod\_new}}\right]^{-1}\vec{p}_{q^*}}{[\mathbf{1}]_{1xK}\left[\mathbf{A}_{\mathbf{prod\_new}}\right]^{-1}[\mathbf{1}]_{Kx1}}\right\}\left[\mathbf{A}_{\mathbf{prod\_new}}\right]^{-1}[\mathbf{1}]_{Kx1}+\kappa\left[\mathbf{A}_{\mathbf{prod\_new}}\right]^{-1}\vec{p}_{q^*} \quad \text{. (D.16)}$$

If the BHPs of the producers are equal, based on Eq. D.7 we can rewrite Eq. D.16 as

$$\vec{q}-\vec{q}_{new}=\left\{\left(\frac{1}{[\mathbf{1}]_{1xK}\left[\mathbf{A}_{\mathbf{prod}}\right]^{-1}[\mathbf{1}]_{Kx1}}\right)\left[\mathbf{A}_{\mathbf{prod}}\right]^{-1}[\mathbf{1}]_{Kx1}[\mathbf{1}]_{1xK}\left[\mathbf{A}_{\mathbf{prod}}\right]^{-1}-\left[\mathbf{A}_{\mathbf{prod}}\right]^{-1}\right\}\left[\mathbf{A}_{\mathbf{con}}\right]^{T}\vec{w}$$
$$-\left(\frac{1}{[\mathbf{1}]_{1xK}\left[\mathbf{A}_{\mathbf{prod}}\right]^{-1}[\mathbf{1}]_{Kx1}}\right)\left[\mathbf{A}_{\mathbf{prod}}\right]^{-1}[\mathbf{1}]_{KxI}\vec{w}$$
$$+\kappa p_q\left[\mathbf{A}_{\mathbf{prod}}\right]^{-1}[\mathbf{1}]_{Kx1}-\kappa p_q\left[\mathbf{A}_{\mathbf{prod}}\right]^{-1}[\mathbf{1}]_{Kx1} \quad \text{(D.17)}$$
$$-\left\{\left(\frac{1}{[\mathbf{1}]_{1xK}\left[\mathbf{A}_{\mathbf{prod\_new}}\right]^{-1}[\mathbf{1}]_{Kx1}}\right)\left[\mathbf{A}_{\mathbf{prod\_new}}\right]^{-1}[\mathbf{1}]_{Kx1}[\mathbf{1}]_{1xK}\left[\mathbf{A}_{\mathbf{prod\_new}}\right]^{-1}-\left[\mathbf{A}_{\mathbf{prod\_new}}\right]^{-1}\right\}\left[\mathbf{A}_{\mathbf{con\_new}}\right]^{T}\vec{w}$$
$$+\left(\frac{1}{[\mathbf{1}]_{1xK}\left[\mathbf{A}_{\mathbf{prod\_new}}\right]^{-1}[\mathbf{1}]_{Kx1}}\right)\left[\mathbf{A}_{\mathbf{prod\_new}}\right]^{-1}[\mathbf{1}]_{KxI}\vec{w}$$
$$-\kappa p_q\left[\mathbf{A}_{\mathbf{prod\_new}}\right]^{-1}[\mathbf{1}]_{Kx1}+\kappa p_q\left[\mathbf{A}_{\mathbf{prod\_new}}\right]^{-1}[\mathbf{1}]_{Kx1}$$

or

$$\vec{q}-\vec{q}_{new}=\left\{\left(\frac{1}{[\mathbf{1}]_{1xK}\left[\mathbf{A}_{\mathbf{prod}}\right]^{-1}[\mathbf{1}]_{Kx1}}\right)\left[\mathbf{A}_{\mathbf{prod}}\right]^{-1}[\mathbf{1}]_{Kx1}[\mathbf{1}]_{1xK}\left[\mathbf{A}_{\mathbf{prod}}\right]^{-1}-\left[\mathbf{A}_{\mathbf{prod}}\right]^{-1}\right\}\left[\mathbf{A}_{\mathbf{con}}\right]^{T}\vec{w}$$
$$-\left(\frac{1}{[\mathbf{1}]_{1xK}\left[\mathbf{A}_{\mathbf{prod}}\right]^{-1}[\mathbf{1}]_{Kx1}}\right)\left[\mathbf{A}_{\mathbf{prod}}\right]^{-1}[\mathbf{1}]_{KxI}\vec{w} \qquad \text{. (D.18)}$$
$$-\left\{\left(\frac{1}{[\mathbf{1}]_{1xK}\left[\mathbf{A}_{\mathbf{prod\_new}}\right]^{-1}[\mathbf{1}]_{Kx1}}\right)\left[\mathbf{A}_{\mathbf{prod\_new}}\right]^{-1}[\mathbf{1}]_{Kx1}[\mathbf{1}]_{1xK}\left[\mathbf{A}_{\mathbf{prod\_new}}\right]^{-1}-\left[\mathbf{A}_{\mathbf{prod\_new}}\right]^{-1}\right\}\left[\mathbf{A}_{\mathbf{con\_new}}\right]^{T}\vec{w}$$
$$+\left(\frac{1}{[\mathbf{1}]_{1xK}\left[\mathbf{A}_{\mathbf{prod\_new}}\right]^{-1}[\mathbf{1}]_{Kx1}}\right)\left[\mathbf{A}_{\mathbf{prod\_new}}\right]^{-1}[\mathbf{1}]_{KxI}\vec{w}$$

Therefore, to have constant production rate we just need to have

$$\left[\mathbf{A}_{\mathbf{con\_new}}\right]^{T}=\left\{\left(\frac{1}{[\mathbf{1}]_{1xK}\left[\mathbf{A}_{\mathbf{prod\_new}}\right]^{-1}[\mathbf{1}]_{Kx1}}\right)\left[\mathbf{A}_{\mathbf{prod\_new}}\right]^{-1}[\mathbf{1}]_{KxK}\left[\mathbf{A}_{\mathbf{prod\_new}}\right]^{-1}-\left[\mathbf{A}_{\mathbf{prod\_new}}\right]^{-1}\right\}^{-1}\cdot$$
$$\left(\left\{\left(\frac{1}{[\mathbf{1}]_{1xK}\left[\mathbf{A}_{\mathbf{prod}}\right]^{-1}[\mathbf{1}]_{Kx1}}\right)\left[\mathbf{A}_{\mathbf{prod}}\right]^{-1}[\mathbf{1}]_{KxK}\left[\mathbf{A}_{\mathbf{prod}}\right]^{-1}-\left[\mathbf{A}_{\mathbf{prod}}\right]^{-1}\right\}\left[\mathbf{A}_{\mathbf{con}}\right]^{T}\right. \qquad \text{. ..... (D.19)}$$
$$\left.-\left(\frac{1}{[\mathbf{1}]_{1xK}\left[\mathbf{A}_{\mathbf{prod}}\right]^{-1}[\mathbf{1}]_{Kx1}}\right)\left[\mathbf{A}_{\mathbf{prod}}\right]^{-1}[\mathbf{1}]_{KxI}+\left(\frac{1}{[\mathbf{1}]_{1xK}\left[\mathbf{A}_{\mathbf{prod\_new}}\right]^{-1}[\mathbf{1}]_{Kx1}}\right)\left[\mathbf{A}_{\mathbf{prod\_new}}\right]^{-1}[\mathbf{1}]_{KxI}\right)$$

Since $\left\{\left(\frac{1}{[\mathbf{1}]_{1xK}\left[\mathbf{A}_{\mathbf{prod\_new}}\right]^{-1}[\mathbf{1}]_{Kx1}}\right)\left[\mathbf{A}_{\mathbf{prod\_new}}\right]^{-1}[\mathbf{1}]_{KxK}\left[\mathbf{A}_{\mathbf{prod\_new}}\right]^{-1}-\left[\mathbf{A}_{\mathbf{prod\_new}}\right]^{-1}\right\}$ is singular, we add the delay term to overcome this problem and Eq. D.19 becomes

$$\left[\mathbf{A}_{\mathbf{con\_new}}{}^{T}\right]=\left[\left(\frac{1-\exp\left(-\frac{[1]_{1xK}\left[\mathbf{A}_{\mathbf{prod}}\right]^{-1}[1]_{Kx1}\,t}{c_t V_p}\right)}{[1]_{1xK}\left[\mathbf{A}_{\mathbf{prod}}\right]^{-1}[1]_{Kx1}}\right)\left[\mathbf{A}_{\mathbf{prod\_new}}\right]^{-1}[1]_{KxK}\left[\mathbf{A}_{\mathbf{prod\_new}}\right]^{-1}-\left[\mathbf{A}_{\mathbf{prod\_new}}\right]^{-1}\right]^{-1}\cdot$$

$$\left\{\left[\left(\frac{1-\exp\left(-\frac{[1]_{1xK}\left[\mathbf{A}_{\mathbf{prod}}\right]^{-1}[1]_{Kx1}\,t}{c_t V_p}\right)}{[1]_{1xK}\left[\mathbf{A}_{\mathbf{prod}}\right]^{-1}[1]_{Kx1}}\right)\left[\mathbf{A}_{\mathbf{prod}}\right]^{-1}[1]_{KxK}\left[\mathbf{A}_{\mathbf{prod}}\right]^{-1}-\left[\mathbf{A}_{\mathbf{prod}}\right]^{-1}\right]\left[\mathbf{A}_{\mathbf{con}}{}^{T}\right]-\right.$$

$$\left.\left(\frac{1-\exp\left(-\frac{[1]_{1xK}\left[\mathbf{A}_{\mathbf{prod}}\right]^{-1}[1]_{Kx1}\,t}{c_t V_p}\right)}{[1]_{1xK}\left[\mathbf{A}_{\mathbf{prod}}\right]^{-1}[1]_{Kx1}}\right)\left[\mathbf{A}_{\mathbf{prod}}\right]^{-1}[1]_{KxI}+\left(\frac{1-\exp\left(-\frac{[1]_{1xK}\left[\mathbf{A}_{\mathbf{prod}}\right]^{-1}[1]_{Kx1}\,t}{c_t V_p}\right)}{[1]_{1xK}\left[\mathbf{A}_{\mathbf{prod}}\right]^{-1}[1]_{Kx1}}\right)\left[\mathbf{A}_{\mathbf{prod\_new}}\right]^{-1}[1]_{KxI}\right\} \quad \text{(D.20)}$$

APPENDIX E. DERIVATION OF EQUIVALENT CM SOLUTION USING MPI

At time step *n*, recalling Eq. 6.19 the production rate is

$$q(t_n)=\left\{1-\exp\left[-\frac{\kappa(t_n-t_{n-1})}{a_{prod}c_tV_p}\right]\left(1-\frac{a_{con}}{a_{prod}}\right)\right\}w(t_n)+\frac{\kappa}{a_{prod}}\left[\bar{p}_{n-1}-p_{wf}(t_n)\right]\exp\left[-\frac{\kappa(t_n-t_{n-1})}{a_{prod}c_tV_p}\right]. \quad \text{.....(E.1)}$$

We have the effect of previous time steps in the production rate from the average reservoir pressure at the end of the previous time step. Based on Eq. 6.12 at time step *n*-1, the average reservoir pressure is

$$\bar{p}_{n-1}=\frac{c_2(n-1)}{c_1}+\left[\bar{p}_{n-2}-\frac{c_2(n-1)}{c_1}\right]\exp\left[\frac{-c_1}{c_tV_p}(t_{n-1}-t_{n-2})\right] \quad \text{.....(E.2)}$$

where $c_2(n\text{-}1)$ is c_2 (form Eq. 6.14) at time $t_{n\text{-}1}$. Similarly, at time *n*-2, we have

$$\bar{p}_{n-2}=\frac{c_2(n-2)}{c_1}+\left[\bar{p}_{n-3}-\frac{c_2(n-2)}{c_1}\right]\exp\left[\frac{-c_1}{c_tV_p}(t_{n-2}-t_{n-3})\right]. \quad \text{.....(E.3)}$$

In a similar way for *n*-*m* at the other time steps we have

$$\bar{p}_{n-m}=\frac{c_2(n-m)}{c_1}+\left[\bar{p}_{n-m}-\frac{c_2(n-m)}{c_1}\right]\exp\left[\frac{-c_1}{c_tV_p}(t_{n-m}-t_{n-m-1})\right] \quad \text{.....(E.4)}$$

and at the first time step we have

$$\bar{p}_1=\frac{c_2(1)}{c_1}+\left[\bar{p}_i-\frac{c_2(1)}{c_1}\right]\exp\left[\frac{-c_1}{c_tV_p}(t_1-t_0)\right]. \quad \text{.....(E.5)}$$

Substituting Eqs. E.3 to E.5 in Eq. E.2 we obtain

$$\begin{aligned}
\bar{p}_{n-1}=&\frac{c_2(n-1)}{c_1}-\frac{c_2(n-1)}{c_1}\exp\left[\frac{-c_1}{c_tV_p}(t_{n-1}-t_{n-2})\right]\\
&+\frac{c_2(n-2)}{c_1}\exp\left[\frac{-c_1}{c_tV_p}(t_{n-1}-t_{n-2})\right]-\frac{c_2(n-2)}{c_1}\exp\left[\frac{-c_1}{c_tV_p}(t_{n-2}-t_{n-3})\right]\exp\left[\frac{-c_1}{c_tV_p}(t_{n-1}-t_{n-2})\right]\\
&+...\\
&+\frac{c_2(n-m)}{c_1}\exp\left[\frac{-c_1}{c_tV_p}(t_{n-m+1}-t_{n-m})\right]...\exp\left[\frac{-c_1}{c_tV_p}(t_{n-1}-t_{n-2})\right]\\
&-\frac{c_2(n-m)}{c_1}\exp\left[\frac{-c_1}{c_tV_p}(t_{n-m}-t_{n-m-1})\right]...\exp\left[\frac{-c_1}{c_tV_p}(t_{n-1}-t_{n-2})\right]\\
&+...\\
&+\frac{c_2(1)}{c_1}\exp\left[\frac{-c_1}{c_tV_p}(t_2-t_1)\right]...\exp\left[\frac{-c_1}{c_tV_p}(t_{n-1}-t_{n-2})\right]+\left(\bar{p}_i-\frac{c_2(1)}{c_1}\right)\exp\left[\frac{-c_1}{c_tV_p}(t_1-t_0)\right]...\exp\left[\frac{-c_1}{c_tV_p}(t_{n-1}-t_{n-2})\right]
\end{aligned} \quad \text{(E.6)}$$

or

$$\bar{p}_{n-1} = \frac{c_2(n-1)}{c_1}\left\{1-\exp\left[\frac{-c_1}{c_t V_p}\left(t_{n-1}-t_{n-2}\right)\right]\right\}$$
$$+\frac{c_2(n-2)}{c_1}\left\{\exp\left[\frac{-c_1}{c_t V_p}\left(t_{n-1}-t_{n-2}\right)\right]-\exp\left[\frac{-c_1}{c_t V_p}\left(t_{n-1}-t_{n-3}\right)\right]\right\}$$
$$+...$$
$$+\frac{c_2(n-m)}{c_1}\left\{\exp\left[\frac{-c_1}{c_t V_p}\left(t_{n-1}-t_{n-m}\right)\right]-\exp\left[\frac{-c_1}{c_t V_p}\left(t_{n-1}-t_{n-m-1}\right)\right]\right\} \quad \text{.....(E.7)}$$
$$+...$$
$$+\frac{c_2(1)}{c_1}\left\{\left[\frac{-c_1}{c_t V_p}\left(t_{n-1}-t_1\right)\right]-\exp\left[\frac{-c_1}{c_t V_p}\left(t_{n-1}-t_0\right)\right]\right\}$$
$$+\bar{p}_i \exp\left[\frac{-c_1}{c_t V_p}\left(t_{n-1}-t_0\right)\right]$$

and finally

$$\bar{p}_{n-1} = \sum_{m=1}^{n-1}\frac{c_2(m)}{c_1}\left\{\exp\left[\frac{-c_1}{c_t V_p}\left(t_{n-1}-t_m\right)\right]-\exp\left[\frac{-c_1}{c_t V_p}\left(t_{n-1}-t_{m-1}\right)\right]\right\}+\bar{p}_i \exp\left[\frac{-c_1}{c_t V_p}\left(t_{n-1}-t_0\right)\right]. \quad \text{.....(E.8)}$$

Substituting Eq. E.8 into Eq. E.1 we obtain

$$q(t_n) = \left\{1-\exp\left[-\frac{\kappa\left(t_n-t_{n-1}\right)}{a_{prod}c_t V_p}\right]\left(1-\frac{a_{con}}{a_{prod}}\right)\right\}w(t_n)-\frac{\kappa}{a_{prod}}p_{wf}(t_n)\exp\left[-\frac{\kappa\left(t_n-t_{n-1}\right)}{a_{prod}c_t V_p}\right]$$
$$+\sum_{m=1}^{n-1}\left[w(t_m)\left(1-\frac{a_{con}}{a_{prod}}\right)+\frac{\kappa}{a_{prod}}p_{wf}(t_m)\right]\left\{\exp\left[-\frac{\kappa\left(t_n-t_m\right)}{a_{prod}c_t V_p}\right]-\exp\left[-\frac{\kappa\left(t_n-t_{m-1}\right)}{a_{prod}c_t V_p}\right]\right\} \quad \text{.....(E.9)}$$
$$+\frac{\kappa}{a_{prod}}\bar{p}_i \exp\left[\frac{-c_1}{c_t V_p}\left(t_n-t_0\right)\right]$$

or

$$q(t_n) = \frac{a_{con}}{a_{prod}}w(t_n)+\sum_{m=1}^{n}w(t_m)\left(1-\frac{a_{con}}{a_{prod}}\right)\left\{\exp\left[-\frac{\kappa\left(t_n-t_m\right)}{a_{prod}c_t V_p}\right]-\exp\left[-\frac{\kappa\left(t_n-t_{m-1}\right)}{a_{prod}c_t V_p}\right]\right\}$$
$$+\frac{\kappa}{a_{prod}}\sum_{m=1}^{n}p_{wf}(t_m)\left\{\exp\left[-\frac{\kappa\left(t_n-t_m\right)}{a_{prod}c_t V_p}\right]-\exp\left[-\frac{\kappa\left(t_n-t_{m-1}\right)}{a_{prod}c_t V_p}\right]\right\} \quad \text{. .....(E.10)}$$
$$+\frac{\kappa}{a_{prod}}\bar{p}_i \exp\left[\frac{-c_1}{c_t V_p}\left(t_n-t_0\right)\right]$$

To estimate the production rate for the multiwell case, substituting Eq. E.8 into Eq. 6.12 we obtain

$$\bar{p}_n = \frac{c_2(n)}{c_1} + \left(\sum_{m=1}^{n-1} \frac{c_2(m)}{c_1} \left\{ \exp\left[\frac{-c_1}{c_t V_p} (t_{n-1} - t_m) \right] - \exp\left[\frac{-c_1}{c_t V_p} (t_{n-1} - t_{m-1}) \right] \right\} \right. \quad \text{.....(E.11)}$$
$$\left. + \bar{p}_i \exp\left[\frac{-c_1}{c_t V_p} (t_{n-1} - t_0) \right] - \frac{c_2(n)}{c_1} \right) \exp\left(\frac{-c_1}{c_t V_p} (t_n - t_{n-1}) \right)$$

or

$$\bar{p}_n = \sum_{m=1}^{n} \frac{c_2(m)}{c_1} \left\{ \exp\left[\frac{-c_1}{c_t V_p} (t_n - t_m) \right] - \exp\left[\frac{-c_1}{c_t V_p} (t_n - t_{m-1}) \right] \right\} + \bar{p}_i \exp\left[\frac{-c_1}{c_t V_p} (t_n - t_0) \right] . \quad \text{.....(E.12)}$$

Substituting Eq. E.12 into Eq. 6.15 we obtain

$$\vec{q}(t_n) = -\left[\mathbf{A}_{\mathbf{prod}} \right]^{-1} \left[\mathbf{A}_{\mathbf{con}} \right]^T \vec{w}(t_n)$$
$$+ \kappa \left[\mathbf{A}_{\mathbf{prod}} \right]^{-1} \left[\sum_{m=1}^{n} \frac{c_2(m)}{c_1} \left\{ \exp\left[\frac{-c_1}{c_t V_p} (t_n - t_m) \right] - \exp\left[\frac{-c_1}{c_t V_p} (t_n - t_{m-1}) \right] \right\} [\mathbf{1}]_{Kx1} + \bar{p}_i \exp\left[\frac{-c_1}{c_t V_p} (t_n - t_0) \right] [\mathbf{1}]_{Kx1} - \vec{p}_{q^*}(t_n) \right]$$
. .....(E.13)

Substituting Eqs. 6.14 into Eq. E.13 we have

$$\vec{q}(t_n) = \kappa \left[\mathbf{A}_{\mathbf{prod}} \right]^{-1} \sum_{m=1}^{n} \frac{-\sum \vec{w}(t_m) + \sum \left[\mathbf{A}_{\mathbf{prod}} \right]^{-1} \left[\mathbf{A}_{\mathbf{con}} \right]^T \vec{w}(t_m) + \kappa \sum \left[\mathbf{A}_{\mathbf{prod}} \right]^{-1} \vec{p}_{q^*}(t_m)}{c_1}$$
$$\left\{ \exp\left[\frac{-c_1 (t_n - t_m)}{c_t V_p} \right] - \exp\left[\frac{-c_1 (t_n - t_{m-1})}{c_t V_p} \right] \right\} [\mathbf{1}]_{Kx1} \quad \text{. .....(E.14)}$$
$$- \left[\mathbf{A}_{\mathbf{prod}} \right]^{-1} \left[\mathbf{A}_{\mathbf{con}} \right]^T \vec{w}(t_n) - \kappa \left[\mathbf{A}_{\mathbf{prod}} \right]^{-1} \vec{p}_{q^*}(t_n) + \kappa \left[\mathbf{A}_{\mathbf{prod}} \right]^{-1} \bar{p}_i \exp\left[\frac{-c_1}{c_t V_p} (t_n - t_0) \right] [\mathbf{1}]_{Kx1}$$

By factoring out the terms containing producer BHPs we get

$$\vec{q}(t_n) = \kappa \left[\mathbf{A}_{\mathbf{prod}} \right]^{-1} \bar{p}_i \exp\left[\frac{-c_1}{c_t V_p} (t_n - t_0) \right] [\mathbf{1}]_{Kx1} - \left[\mathbf{A}_{\mathbf{prod}} \right]^{-1} \left[\mathbf{A}_{\mathbf{con}} \right]^T \vec{w}(t_n) +$$
$$\kappa \left[\mathbf{A}_{\mathbf{prod}} \right]^{-1} \sum_{m=1}^{n} \left\{ \exp\left[\frac{-c_1 (t_n - t_m)}{c_t V_p} \right] - \exp\left[\frac{-c_1 (t_n - t_{m-1})}{c_t V_p} \right] \right\} \frac{-\sum \vec{w}(t_m) + \sum \left[\mathbf{A}_{\mathbf{prod}} \right]^{-1} \left[\mathbf{A}_{\mathbf{con}} \right]^T \vec{w}(t_m)}{c_1} [\mathbf{1}]_{Kx1} \quad \text{(E.15)}$$
$$+ \kappa \left[\mathbf{A}_{\mathbf{prod}} \right]^{-1} \left\{ \sum_{m=1}^{n} \left\{ \exp\left[\frac{-c_1 (t_n - t_m)}{c_t V_p} \right] - \exp\left[\frac{-c_1 (t_n - t_{m-1})}{c_t V_p} \right] \right\} \frac{\kappa [\mathbf{1}]_{1xK} \left[\mathbf{A}_{\mathbf{prod}} \right]^{-1} \vec{p}_{q^*}(t_m)}{c_1} [\mathbf{1}]_{Kx1} - \vec{p}_{q^*}(t_n) \right\}$$

APPENDIX F. INDEPENDENCY OF λ FROM INJECTOR NUMBER CHANGES

If we add an injector to a system of *I* injectors and *K* producers, we can write the matrix of interaction of injectors and producers, [$\mathbf{A}_{\mathbf{con\_updated}}$], as

$$\left[\mathbf{A}_{\mathbf{con\_updated}}\right]=\begin{bmatrix}\mathbf{A}_{\mathbf{con\_x}}\\ \mathbf{A}_{\mathbf{con}}\end{bmatrix} \quad \text{.....(F.1)}$$

where [$\mathbf{A}_{\mathbf{con\_x}}$] is the matrix of interaction of the new injector and the producers. Based on Eq. 9.9 the [$\mathbf{\Lambda}_{\mathbf{updated}}$] of the system is

$$\left[\mathbf{\Lambda}_{\mathbf{updated}}\right]=-\frac{1}{\left[\mathbf{1}\right]_{1xK}\left[\mathbf{A}_{\mathbf{prod}}\right]^{-1}\left[\mathbf{1}\right]_{Kx1}}\left[\mathbf{A}_{\mathbf{prod}}\right]^{-1}\left(\left[\mathbf{1}\right]_{KxK}\left[\mathbf{A}_{\mathbf{prod}}\right]^{-1}\begin{bmatrix}\mathbf{A}_{\mathbf{con\_x}}\\ \mathbf{A}_{\mathbf{con}}\end{bmatrix}^{T}-\left[\mathbf{1}\right]_{Kx(I+1)}\right)+\left[\mathbf{A}_{\mathbf{prod}}\right]^{-1}\begin{bmatrix}\mathbf{A}_{\mathbf{con\_x}}\\ \mathbf{A}_{\mathbf{con}}\end{bmatrix}^{T} \quad \text{(F.2)}$$

or

$$\left[\mathbf{\Lambda}_{\mathbf{updated}}\right]=-\frac{1}{\left[\mathbf{1}\right]_{1xK}\left[\mathbf{A}_{\mathbf{prod}}\right]^{-1}\left[\mathbf{1}\right]_{Kx1}}\left[\mathbf{A}_{\mathbf{prod}}\right]^{-1}\begin{bmatrix}\left[\mathbf{1}\right]_{KxK}\left[\mathbf{A}_{\mathbf{prod}}\right]^{-1}\left[\mathbf{A}_{\mathbf{con\_x}}\right]^{T}-\left[\mathbf{1}\right]_{Kx1}\\ \left[\mathbf{1}\right]_{KxK}\left[\mathbf{A}_{\mathbf{prod}}\right]^{-1}\left[\mathbf{A}_{\mathbf{con}}\right]^{T}-\left[\mathbf{1}\right]_{KxI}\end{bmatrix}^{T}+\left[\mathbf{A}_{\mathbf{prod}}\right]^{-1}\begin{bmatrix}\mathbf{A}_{\mathbf{con\_x}}\\ \mathbf{A}_{\mathbf{con}}\end{bmatrix}^{T} \quad \text{(F.3)}$$

and finally

$$\left[\mathbf{\Lambda}_{\mathbf{updated}}\right]=\begin{bmatrix}-\frac{1}{\left[\mathbf{1}\right]_{1xK}\left[\mathbf{A}_{\mathbf{prod}}\right]^{-1}\left[\mathbf{1}\right]_{Kx1}}\left[\mathbf{A}_{\mathbf{prod}}\right]^{-1}\left(\left[\mathbf{1}\right]_{KxK}\left[\mathbf{A}_{\mathbf{prod}}\right]^{-1}\left[\mathbf{A}_{\mathbf{con\_x}}\right]^{T}-\left[\mathbf{1}\right]_{Kx1}\right)+\left[\mathbf{A}_{\mathbf{prod}}\right]^{-1}\left[\mathbf{A}_{\mathbf{con\_x}}\right]^{T}\\ -\frac{1}{\left[\mathbf{1}\right]_{1xK}\left[\mathbf{A}_{\mathbf{prod}}\right]^{-1}\left[\mathbf{1}\right]_{Kx1}}\left[\mathbf{A}_{\mathbf{prod}}\right]^{-1}\left(\left[\mathbf{1}\right]_{KxK}\left[\mathbf{A}_{\mathbf{prod}}\right]^{-1}\left[\mathbf{A}_{\mathbf{con}}\right]^{T}-\left[\mathbf{1}\right]_{KxI}\right)+\left[\mathbf{A}_{\mathbf{prod}}\right]^{-1}\left[\mathbf{A}_{\mathbf{con}}\right]^{T}\end{bmatrix}^{T} \quad \text{(F.4)}$$

or

$$\left[\mathbf{\Lambda}_{\mathbf{updated}}\right]=\left[\mathbf{\Lambda}_{\mathbf{x}}\quad\mathbf{\Lambda}\right] \quad \text{.....(F.5)}$$

where [$\mathbf{\Lambda}_{\mathbf{x}}$] is the matrix of λs for the new injector. According to Eq. F.5, if we add an injector to the system, the λs of the other injectors remains constant and we just need to add a column to the [$\mathbf{\Lambda}$] to include the λs of the new injector. If an injector is shut in, in similar way, we just need to eliminate the correspondence column from the [$\mathbf{\Lambda}$].

VITA

Name:	Danial Kaviani
Address:	Dr. Peter Valkó Department of Petroleum Engineering Texas A&M University College Station, TX 77843-3116
Email Address:	danialkaviani@gmail.com
Education:	B.S., Mining Engineering, Amirkabir University of Technology (Tehran Polytechnic), August 1998 M.S., Mining Engineering, Amirkabir University of Technology (Tehran Polytechnic), March 2001 Ph.D., Petroleum Engineering, Texas A&M University, TX, USA, December 2009